SPECTROSCOPIC STUDIES OF THE STOICHIOMETRIC AND NONSTOICHIOMETRIC SODIUM SALTS OF TCNQ AND TCNE

By

MURLIDHAR SADASHIV KHATKALE

Bachelor of Science
University of Poona
Poona, India
1965

Master of Science
University of Poona
Poona, India
1972

Master of Science
University of Rochester
Rochester, New York
1974

Submitted to the Faculty of the Graduate College
of the Oklahoma State University
in partial fulfillment of the requirements
for the Degree of
DOCTOR OF PHILOSOPHY
July, 1978

SPECTROSCOPIC STUDIES OF THE STOICHIOMETRIC AND NONSTOICHIOMETRIC SODIUM SALTS OF TCNQ AND TCNE

Thesis Approved:

J Paul Devlin
Thesis Adviser

Leonel M. Raff

Neil Purdie

N. V. V. J. Swamy

Norman N. Durham
Dean of Graduate College

DEDICATION

To my Father, the late Mr. Sadashiv Abasahib Khatkale and my Mother Mrs. Yashoda S. Khatkale.

ACKNOWLEDGMENTS

I wish to express my deep and heartfelt gratitude to Dr. J. Paul Devlin, Research Adviser, for his kind understanding and patient guidance during the course of this study.

Sacrifice and love of my parents are gratefully acknowledged. This Thesis is dedicated to my late father Sadashiv Abasahib Khatkale and mother Mrs. Yashoda S. Khatkale with great pleasure. Sacrifice and patience of Kum. Swapnil is greatly appreciated.

I would like to thank Dr. N. V. V. J. Swamy, Dr. Lionel M. Raff and Dr. Neil P. Purdie for serving as members of my advisory committee.

Financial assistance from Oklahoma State University, Chemistry Department and the National Science Foundation in support of this study is gratefully appreciated.

Thanks are also due to Mr. Wayne Adkins and Mr. Heinz Hall for their competent and willing assistance in making the vacuum cell, its accessories and their modifications.

I would also like to thank Mr. Gary Ritzaupt and fellow graduate students for their cooperation and comradeship.

It is a pleasure to thank Mrs. Terri Lager for typing this thesis.

TABLE OF CONTENTS

LIST OF TABLES

LIST OF FIGURES

CHAPTER I

INTRODUCTION

Strong Lewis π-acids like ethenetetracarbonitrile (Tetracyanoethylene-TCNE), 2,5-cyclohexadiene-$\Delta^{1,\alpha:4,\alpha'}$-dimalonitrile (7,7,8,8-Tetracyanoquinodimethane-TCNQ) and their charge transfer (CT) complexes are being investigated with increasing interest for their unusual electrical, optical and magnetic properties (1). Both compounds, with their high electron affinities (TCNE:2.9 eV and TCNQ:2.88 eV) (2) (3), readily form stable CT complexes with the organic and inorganic electron donors (1) (4) (5). The extent and energy of CT interactions depend on the nature of an electron donor (1), the crystal structure (6) and the relative energies and symmetries of the highest occupied molecular orbital (HOMO) of the donor and the lowest empty molecular orbital (LEMO) of the acceptor (7). TCNQ and TCNE, with their low energy LEMO's of the order of 2.8 eV (8) (9), form CT complexes with organic electron donors like tetrathiofulvalene (TTF), triethylammonium (TEA), N-methylphenazine (NMP) etc., and with metals of low ionization potentials (IP), like alkali metals and transition metals like Cu, Mn, Ca, Zn, Ag etc., where an electron is almost completely transferred from donor to acceptor (10) (11) (12). There is a similarity in the physical and chemical properties of TCNQ and TCNE, like high electron affinity (EA), low activation energy (2 K.cal/mole) and a high rate of electron exchange (12) (13) (14) ($\sim 10^{-9}$ mol.-sec^{-1}) between the neutral

molecule and the monoanion radical. Little change was observed in the molecular symmetry when the neutral TCNQ and TCNE molecules were converted into the monoanion radicals (11-14). The monoanion radicals of TCNQ and TCNE contain a negative charge and an unpaired electron, the resultant coulombic interaction is one of the important factors contributing to the stability of their CT complexes.

In the study of CT complex spectra, in addition to the conventional factors like symmetry, selection rules, intensity, band width, etc. (15-17), allowance must be made for the interactions arising out of the mobile nature of electrons involved in the charge transfer e.g., Van der Waals, dipole-dipole, dipole-induced dipole and those due to London dispersion type forces (7). Because of the low energy of CT electronic bands and the mobility of the radical electrons, the interaction between the electronic and vibrational states, 'vibronic interaction', assumes a more important role in CT complexes than in ordinary chemical compounds. Such interactions are considered to play an important role in the unusual electrical, magnetic and optical properties of the organic CT complexes (1) (4). Quantitative considerations of such interactions, however, need quite reliable and accurate structural data for the CT complexes.

Crystal Structure, Electrical and Magnetic Properties of TCNQ Salts

The CT complexes (or 'salts') of TCNQ prepared by the solution methods (18) (19) were observed to be of two types. The $M_n^+ TCNQ_m^{\cdot -}$(1:1) simple salts and $M_n^+ (TCNQ^{\cdot -})_m TCNQ^{o}{}_{m'}$, complex salts where m is equal to n and m' is usually equal to m or $m/_2$ were observed (11) (20). X-ray crystallographic study of the simple 1:1 alkali metal salts of TCNQ revealed two types of crystal structures (11) (21-25). Monoclinic crystals

of space group contain $P2_1/n$ (C_{2h}^5) with eight monoanion radicals of TCNQ per unit cell, stacked along the needle axis. The needle axis of the crystal is nearly perpendicular to the TCNQ molecular plane (x-axis in Figure 1). Each $TCNQ^{\cdot-}$ stacks in such a way that the long axes in the molecular planes (z-axis, Figure 1) of the neighboring stacks are perpendicular to each other (21) (22). Alkali metal cations are placed between these $TCNQ^{\cdot-}$ stacks so that each cation is octahedrally surrounded by the C≡N groups of different TCNQ anion radicals. The interplanar distance between the neighboring $TCNQ^{\cdot-}$ within the stack, along the needle axis of a NaTCNQ crystal, alternates between 3·223 and 3·505°A (21). Such a difference in distances between molecular planes of $TCNQ^{\cdot-}$ gives some credence to the idea of dimerization in crystals. The distance between Na^+ and the nitrogen atoms of different C≡N groups varies between 3·384 and 3·686°A (21), which means that different C≡N groups are not affected equally by the neighboring cations. The other crystallographic structure, which is predominant above 65-75°C for Na-TCNQ, is triclinic with space group $p\bar{1}$ (C_i) (25), and one $TCNQ^{\cdot-}$ molecule per unit cell. Eight N atoms of the C≡N groups from four neighboring TCNQ radical anions surrounding sodium cation occupy corners of a cube (25). Since the present spectroscopic investigation was done at room temperature (∿25°C) and liquid nitrogen temperature, the NaTCNQ crystal structure is presumed to be monoclinic, i.e. the dimerized form. For the di- and trianion salts of TCNQ, crystallographic data are not available. Interpretation of the di- and trianion vibrational spectra will be based on the assumption that there is no significant change in the molecular symmetry of TCNQ when two or three electrons are added to it.

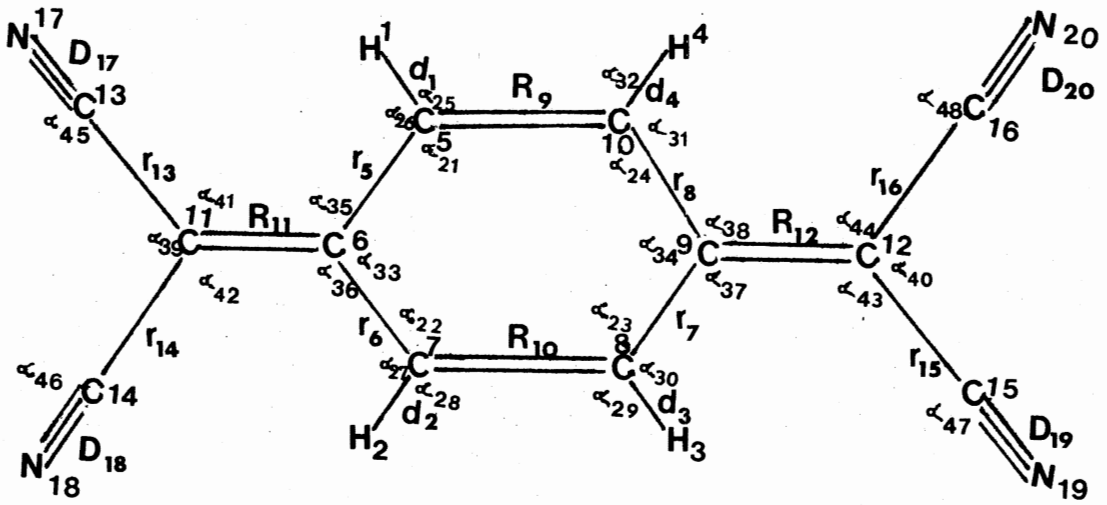

a) TCNQ

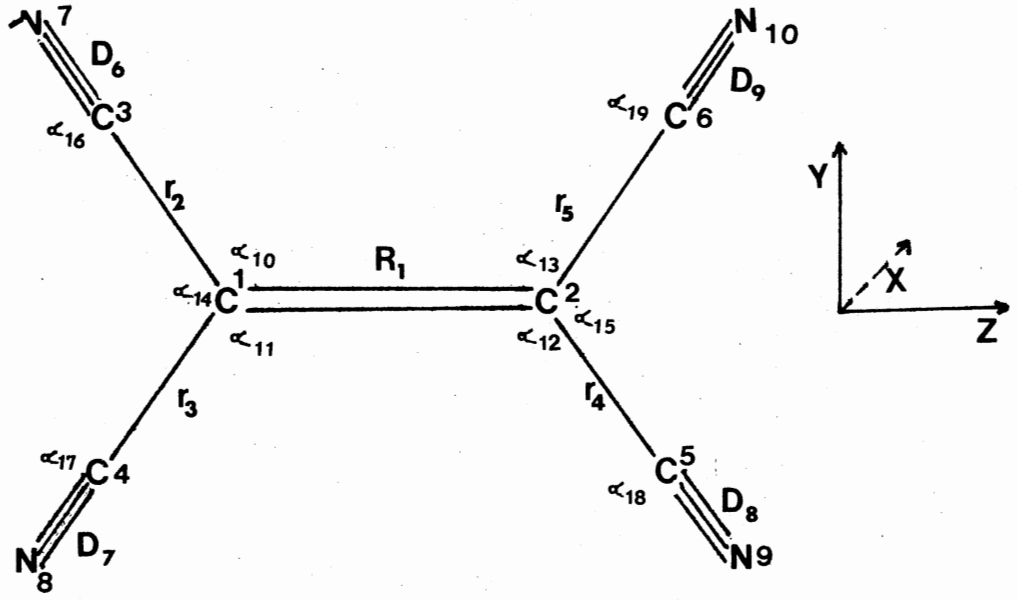

b) TCNE

Figure 1. Molecular Structure Numbering of Atoms and Definations of the Internal Coordinates Used in Normal Coordinate Analysis of a) TCNQ and b) TCNE

Complex salt crystals of TCNQ, like $Cs_2(TCNQ)_3$, were observed to be of the monoclinic type (26). In these salts, also, $TCNQ^-$ dimerization is quite extensive (26).

A correlation between various physical properties like electrical conductivity and magnetic behavior of TCNQ radical anions and their spectroscopic properties has been suggested (11) (27). Electrical (11) (20) (25) (28) (29) and magnetic (10) (30-32) properties of TCNQ salts depend on the nature of the cation (11) (28), the crystal structure (11) (25) and the character (composition) (25) of the salt. Electrical conductivity of TCNQ salts for example, varies from 10^{-10} ohm^{-1}-cm^{-1} (with diethylthiacyanine as a donor (23)) to 10^{3} ohm^{-1}-cm^{-1} (for TTF donor) (30). Alkali metal salts of TCNQ have electrical conductivity that hovers in the border range of the insulator and semiconductor (10^{-3}-10^{-5} ohm^{-1}-cm^{-1}) (11) (20) (25). Electrical conductivity of NaTCNQ along the needle axis of the crystal is 10^{-4} ohm^{-1}-cm^{-1} and the activation energy (i.e., energy required for an electron to jump from valence state to conduction state, (Ea)) is about 0·23 eV (20) (25) (28). Electrical conductivities in directions perpendicular to the needle axis are less by an order of a magnitude ($\sim 10^{-5}$ ohm^{-1}-cm^{-1}). The electrical conductivity decreases with increase in temperature and pressure (25). At a certain temperature (65-75°C) (25) (32), the conductivity along the needle axis decreases suddenly due to a phase transition from the monoclinic to the triclinic crystal structure (21). A similar phase transition was observed at a certain pressure ($\sim$6 K·Bar) (25) (30). Alkali metal salts of TCNQ are considered to be extrinsic semiconductors in the low temperature region (20). TCNQ monoanion radical salts are paramagnetic due to the unpaired electron (11) (32).

For TCNE salts extensive crystallographic structural, electrical or magnetic investigation, such as for TCNQ salts has not been done. However, limited studies (14) indicate paramagnetic behavior of the TCNE monoanion radical salts. Phillips et al. (14), from the electron exchange reaction between $TCNE^{\cdot-}$ and TCNQ, showed that no significant structural deviation from D_{2h} symmetry occurs when the TCNE radical anion is formed.

Information about the crystal structure, electrical and magnetic properties of TCNQ and TCNE salts is helpful in understanding the spectroscopic properties and the interactions involved.

Observed and Calculated Electronic States of TCNQ, TCNE and Their Anions

The optical properties, like other physical properties of TCNQ and TCNE salts, depend on the nature of the cation and the composition (27). The electronic bands for the TCNQ molecule were observed at 420 mμ (3·15 eV) and 288 mμ (5·44 eV) (33-37) and with addition of one electron to TCNQ, the monoanion radical formed shows electronic absorption bands in the visible and uv region (27) (36) (43-55). The electronic bands of $TCNQ^{\cdot-}$ salts can be classified as of two types: delocalized excitation (DE) electronic bands which originate from the electronic transitions of electrons involved in the charge transfer interactions (27) (37) (43) (53) and localized excitation (LE) bands. The DE bands are characterized by their low energy of excitation (0·04-11 kk) (27) (36-43), a polarization parallel to the crystal needle axis (27) (37) (53) and a good correlation between their excitation energy and the electrical conductivity of the salt (20) (25) (31) (51). Usually highly conductive

TCNQ salts show low energy DE bands. For the alkali metal simple salts like NaTCNQ, with the electrical conductivity in a 10^{-4}-10^{-5} ohm^{-1}-cm^{-1} range ($0.25 \leq E \leq 0.35$ eV), a DE band was observed at 9.3 kk (1.15) (27) (37) (46) (47). For the comples alkali metal salts of higher conductivity ($\sim 10^{-3}$ ohm^{-1}-cm^{-1}), like a $Cs_2CTcNQ)_3$, two bands in the 4-6 kk and the 10.1 kk ranges were observed (25) (53). TCNQ salts with very high electrical conductivity (10^{2}-10^{3} ohm^{-1} cm^{-1}) like TTF (TCNQ), NMP $(TCNQ)_2$, TEA $(TCNQ)_2$ etc., show very low energy DE bands (0·04-6kk) (38-42). Though there is a strong correlation between the energy of an excited change transfer state and the conducting state, they are not the same, as illustrated in the case of hexamethylbenzene (HMB) and pentamethylbenzene (PMB) CT complexes of TCNE. A difference of about 0.5 eV between the two states was observed (4). DE bands of the simple and complex alkali metal salts of TCNQ in the range 8-12 kk (0.65-0.97 eV) were attributed to the electron exchange between two TCNQ radical monoanions of the dimer within the stack (27). The energy of the electron exchange reaction

$$TCNQ^{\bar{\cdot}} + TCNQ^{\bar{\cdot}} \rightleftharpoons TCNQ^{o} + TCNQ^{-2}$$

calculated from MO theory (32) (36) (56) (57) was in the range 0.7 - 1.04 eV. DE bands observed in the range 4-6 kk, observed only for the complex TCNQ salts, were attributed to the electron exchange between TCNQ monanion radical and neutral TCNQ . The other type of electronic bands of TCNQ salts in the range 15-43 kk (1.5-5.6 eV), which originate from the electronic transitions of electrons localized on $TCNQ^{\bar{\cdot}}$, are termed as local excitation (LE) electronic bands (27) (37) (43) (44) (51) (53). The LE bands can be distinguished from the DE bands by their polarization in the molecular plane of TCNQ and perpendicular to the needle

axis, as well as the higher transition energy and less obvious correlation with the physical properties like electrical conductivity (25) (31) (37). For the complex TCNQ salts like $Cs_2(TCNQ)_3$, LE bands were observed at 16.3 and 27.5 kk and for the simple salts like NaTCNQ at 16.5 and 27.5 kk. LE bands at 16.5 kk are polarized along the long molecular axis (z-axis, Figure 1) (27) (53) (36), and the 27.5 kk LE bands along both the z- and y-axis (27).

A number of MO calculations for TCNQ and its anions have been published in the literature (37) (37) (48-50) (56-61). There is fairly good agreement between the calculated and observed energy states of $TCNQ^o$ and its anions (36) (37) (58-61). Polarizations of LE electronic bands from MO calculation and their assignments have been given as follows. The 5.44 and 3.15 eV electronic bands of $TCNQ^o$ were assigned to $^1B_{1u} \leftarrow {}^1A_g$ (z-axis) and $^1B_{2u} \leftarrow {}^1A_g$ (y-axis) electronic transitions respectively (60). The LE electronic bands of TCNQ monoanion radical at 1.49, 2.91, 3.15, 4.43, 4.71 and 5.33 eV were assigned to the electronic transitions $^2B_{3u}(1) \leftarrow {}^2B_{2g}$ (z-axis), $^2A_u(1) \leftarrow {}^2B_{2g}$ (y-axis), $^2B_{3u}(2) \leftarrow {}^2B_{2g}$ (z-axis), $^2A_u(2) \leftarrow {}^2B_{2g}$ (y-axis), $^2B_{2u}(3) \leftarrow {}^2B_{2g}$ (z-axis), and $^2B_{3g} \leftarrow {}^2B_{2g}$ (z-axis) respectively. Polarizations of electronic transitions given in brackets indicate their axis orientations. The z-axis is a long molecular axis and the y-axis is a short molecular axis of TCNQ (Figure 1). Three electronic transitions at 1.49, 2.91 and 3.15 eV are of particular importance in the study of resonance Raman spectra of (1:1) NaTCNQ stoichiometric salts (62) and the nonstoichiometric salts in the composition range $1.0 < Na/_{TCNQ} < 2.0$.

Another important factor that affects the spectroscopic properties of the monoanion radicals is dimerization. Electronic spectra of TCNQ

monoanion radical salts in solution indicate that in highly polar solvents like water, the dimerized form is dominant (63). $TCNQ^{\cdot-}$ in less polar solvents like acetonitrile, methanol, ethanol, and N-methylformamide is present in the monomeric form (63-67). Electronic bands of the monomer $TCNQ^{\cdot-}$ were observed at 395.3 mμ ($^2B_{3u}(2) \leftarrow {}^2B_{2g}$ and $^2A_u(1) \leftarrow {}^2B_{2g}$), 737, and 848.3 mμ ($^2B_{3u}(1) \leftarrow {}^2B_{2g}$) which shifted to 370, 643, and 870 mμ after dimerization (63) (64). The extent of dimerization in solution increases with increase in polarity of the solvent (63) (65), presence of ionic salts (64), and decrease in temperature (63). X-ray crystallography, as mentioned earlier, shows extensive dimerization in monoclinic crystals of $TCNQ^{\cdot-}$ salt (21) (22) (26). This is confirmed by electronic spectra of these crystals (27) (43) (47) (53). The extent of dimerization in monoclinic crystals increases with increase in pressure as indicated by blue shifts of the 370 and 643 mμ electronic bands (27). Decrease in the temperature of solid crystals increases an extent of dimerization. This was indicated by the increase in the intensity of the dimer vibronic IR bands when MTCNQ (M = Li, Na, K etc.) salts were cooled to the liquid nitrogen temperature (68). Similarity, Anderson and McNeely (66) observed splitting of 16.7 kk electronic band ($^2B_{3u}(1) \leftarrow {}^2B_{2g}$) into two 16.5 and 18.1 kk bands when KTCNQ crystals were cooled to liquid nitrogen temperature. These two components are separated by about 1600 cm^{-1}, a frequency of one of the a_g modes of $TCNQ^{\cdot-}$ (68). Thus, the 18.1 kk was assigned to the vibronic band of $TCNQ^{\cdot-}$ dimer in the salt (66). MO calculation on relative orientations of $TCNQ^-$ in the dimer indicated that the most favorable position is one monoanion radical on top of the other (53) (67). This was confirmed by the x-ray crystallographic studies (21) (22). Thus, dimerization

significantly affects electronic (63-66) and vibrational spectra (68) of TCNQ salts due to the increase in extent of vibronic interaction. Such vibronic interactions acquire much importance in interpretation of the vibrational spectra, particularly for the monoanion radical salts of TCNQ.

The aromatic electron acceptors act like a sink for electrons and can accommodate one or more electrons (69-73). Thus, the 'stoichiometric' CT complexes can be prepared where each acceptor molecule interacts with one or several donor molecules. Thus, the 'dianion' salts of aromatic hydrocarbons like 9.9'-Bianthranyl (70), napthalene (71) (72), anthracene (72) (73), tetracene (72), pyrene (72), perylene (72), etc. have been reported. For the 2:1 complexes of HMB and PMB with TCNE, the 1295 cm^{-1} $C-CH_3$ vibronic bands were observed (which were absent in the 1:1 comples (74)). Also the dianion and trianion alkali metal salts of TCNE were observed by Moore, et al. (75). The first report for the electronic spectrum of the dianion of TCNQ was published by Jonkman and Kommandeur (36). The electronic bands were observed at 2.56, 3.36 and 3.69 eV, for the electrochemically prepared $TCNQ^{-2}$. However, subsequent observation by Suchanski and VanDuyne (76) showed that the above mentioned spectrum was not due to $TCNQ^{-2}$ but that of α,α -dicyano-p-toluoylcyanide anion (α,α-$DCTC^-$), formed due to reaction with oxygen. Electrochemically prepared $TCNQ^{-2}$ in oxygen free atmosphere and in an acetonitrile solution, shows electronic absorption bands at 3.75, 5.16 and 5.90 eV in the uv region. The electron affinity for $TCNQ^{\cdot-}$ has been calculated to be in the range of 0.76-1.07 eV (36) (56-68) (77) (78). The apparent stability of $TCNQ^{-2}$ may be attributed to a large separation of two electrons at the two extreme C≡N ends of the

molecule so as to reduce Heitler-London repulsion interaction (79). The excess negative charge of $TCNQ^{-2}$ is partially located on N and C_{11} (or C_{12}) sites (see Figure 1). The best geometry of $TCNQ^{-2}$ obtained from the MO calculation does not show very significant deviation from the D_{2h} symmetry (78). The 3.75, 5.16, and 5.90 eV electronic bands of the dianion were assigned to $^1B_{2u} \leftarrow {}^1A_g$ (y-axis), $^1B_{1u} \leftarrow {}^1A_g$ (z-axis), and $^1A_g(1) \leftarrow {}^1A_g$ (y-axis) electronic transitions, respectively (36) (58) (77). Axes in the parenthesis show polarizations of the electronic transitions (Figure 1). An agreement between calculated and observed electronic states of $TCNQ^{-2}$ is good (58) (77).

Since the dianions of the conjugated molecules are very susceptible to reaction with moisture and oxygen (71) (76), such compounds should be studied under conditions where such reaction can be prevented as much as possible. Published spectroscopic results (36) (80-83) for $TCNQ^{-2}$ obtained without such precautions should be accepted with caution. Recently, electronic and vibrational spectra of $(perylene)_3$ TCNQ have been reported. The 470 (2.8 eV) electronic band and the 833 and 1635 cm^{-1} IR bands assigned to the CT complex have also been reported for α,α-$DCTC^-$ (19) (76). Apparently, the above mentioned CT complex was prepared in open atmosphere and with the possibility of its reaction with moisture and oxygen, the results should be accepted with due qualifications.

Neutral TCNE molecule has a monoclinic $P2_1/n(C_{2h}^5)$ crystal structure (34). The D_{2h} molecular symmetry of neutral TCNE will be presumed not altered significantly, with addition of one, two or three electrons. The 5.05 eV electronic absorption band of neutral TCNE (85) was assigned to the $^1B_{1u} \leftarrow {}^1A_g$ electronic transition, polarized

along the long molecular axis (9) (z-axis, Figure 1). NaTCNE in acetonitrile and tetrahydrofuran (THF) shows an electronic absorption band at 23.6 kk (2.93 eV) (86). This monomer $TCNE^{-}$ band (86) was assigned to the $^2B_{3g} \leftarrow {}^2B_{1u}$ electronic transition, polarized along the short molecular axis (y-axis, Figure 1). The $Na^{+}(TCNE)_2^{-}$ dimer electronic bands in 2-methyltetrahydrofuran (MTHF) solution were observed at 18.7 kk (2.32 eV) and 30.3 kk (3.76 eV) (86), similar to the $TCNQ^{-}$ dimer (63). The 450 mμ monomer (87) and 536 mμ dimer electronic bands are important in the study of the intensity pattern of the resonance Raman spectrum of NaTCNE.

Formation of $TCNE^{-2}$ and $TCNE^{-3}$ alkali metal salts was observed by Moore et al. (75). The C≡N stretching IR bands for $TCNE^{-2}$ and $TCNE^{-3}$ were observed at 2090 and 1980 cm^{-1}, respectively (75). More detailed study of the di- and trianions of TCNE is intended in the present investigation.

Vibronic Interactions

Interactions of the mobile charge transfer electrons with the vibrational modes of conjugated π-electronic systems, like alkali metal salts of TCNQ and TCNE, have pronounced effects on the intensity and frequency of their electronic (9) (38) (39) (88) and vibrational bands (9) (75) (89) (90). Vibronic interactions, as manifested in the IR (75) (89) (90) and Raman (9) (62) (91) vibrational spectra of the monoanion salts of TCNQ and TCNE, assume more importance than is usual for chemical compounds. Herzberg and Teller (92) first proposed a scheme of interaction between the electronic and vibrational states to explain certain weak symmetry forbidden electronic bands of formaldehyde. Considerable progress since then has been made in the understand-

ing of vibronic interactions involved in conventional chemical compounds (93-96) and CT complexes (97-100). In the CT complexes interaction between vibrational states of electron acceptor (or donor) with low energy CT electronic states, as well as local electronic states, activates certain otherwise symmetry forbidden electronic and vibrational transitions (97-99). For TCNQ salts in particular, induced vibronic interactions by electron exchange between $TCNQ^{\cdot-}$ dimers along the stack activate certain intense and broad IR vibrational bands (68) (89) (101) polarized along the needle axis of the crystal (66) (89). Fulton and Gouterman (100) gave a general mathematical treatment for vibronic interaction in dimers. Vibronic coupling in dimers was described in terms of two dimensionless paramers ε and λ, where ε represents energy separation between the two electronic states involved in vibronic interaction, and λ a nuclear displacement during the vibration. For a weak coupling, i.e., $\varepsilon << \lambda$, vibronic interaction can be described as a pseudo-Jahn-Teller effect. In case of Jahn-Teller effect (102) the excition coupling parameter ε is vanishingly small. The strong coupling ($\varepsilon >> \lambda$), results in vibrational intensity borrowing (92) (93). The $\varepsilon \sim \lambda$ is an intermediate case in between the above two cases. Vibronic interactions in dimers formed in CT complexes are special cases of strong ($\varepsilon >> \lambda$) and intermediate $\varepsilon \sim \lambda$ vibronic coupling. Different schemes of vibronic interactions have been proposed to explain the appearance of symmetry forbidden IR bands of CT complexes: a) charge oscillation or electronic vibration theory (103), b) charge density wave (CDW) theory (104), and c) resonance Raman effect (105).

FMFP Charge Oscillation Theory

Based on Mulliken's theory of CT complexes (7), Ferguson and Matsen (103) proposed the mechanism of oscillations of electronic charge between the donor and aceptor induced by vibronic interaction, to explain the anomalous intensity patterns of the vibrational spectra of helogen-benzene complexes. Since electronic potential curves (^{E}electronic vs ^{Q}vibrational) are generally not parallel for the neutral molecule and its ion, EA (or IP) of the electron acceptor (or donor) are functions of the normal coordinate (Q) of its stretching vibrations. The dipole moment of the CT complex is a function of EA of the electron acceptor (or IP of the donor), the coulombic interactions between dative structures of the CT complex, and the overlap between wave functions of the donor and acceptor molecules (7). Changes in EA (or IP) during the stretching vibration of the acceptor (or donor) result in oscillations in the dipole moment of the CT complex with a frequency of the stretching vibration. This is caused by mixing of low energy excited electronic states of appropriate symmetry with the ground electronic state through the normal mode of the acceptor (or donor). An appropriate symmetry in group theoretical language means the direct product of the irreducible representations of the ground state, excited state and the normal vibrational mode must contain at least once the total symmetric irreducible representation. Since for the TCNQ monoanion the ground electronic and the first excited states are of B_{2g} and B_{3u} symmetry respectively (60) (61) (77), the only nonvanishing triple direct product is with totally symmetric a_g vibrational normal modes. Thus, the case of $TCNQ^{\cdot-}$ is similar to the CT complexes of centrosymmetric molecules like benzene (103) (166), TCNE (9) (75) and other aromatic compounds (71) (73) (74).

The oscillations in dipole moment induced by electronic vibrations activate the totally symmetric vibrational modes (which are inactive as required by the "mutual exclusion principle" (15-17)), in the IR spectrum. Thus, any IR activation of forbidden a_g modes of a centrosymmetric electron acceptor (or donor) molecule can be attributed to changes in EA or (IP). Charge oscillation vibronic (COV) activation of other non-totally symmetric modes, forbidden by the mutual exclusion principle, can be attributed to the electrostatic interaction arising from the changes in overlap of the acceptor and donor wave functions during the vibration (106) (107). This electrostatic interaction, induced by the mechanical motion of the donor and acceptor, depends on the geometry of the CT complex. Vibrational modes activated by this mechanism are usually of out-of-plane rotational character (106). In short, the totally symmetric modes $a_{1g}(D_{6h})$, $a_1'(D_{3h})$ and $a_g(D_{2h})$ become IR active due to the COV interaction induced by changes in EA or IP. Other modes symmetric to inversion containing non-planar rotations like $e_{1g}(D_{6h})$, $e'(D_{3h})$, and b_{1g} and $b_{2g}(D_{2h})$ become IR active by the electrostatic COV interactions (103). Since COV interactions resulting from changes in EA or IP are very large compared with other electrostatic or coulombic COV interactions, the intensities of the totally symmetric modes usually dominate the IR spectra of CT complexes.

Friedrich and Person (108) derived expressions for the intensity enhancement of COV activated vibrational bands by using Liehr (93) and Jones (96) vibronic formalism. They derived an explicit expression for EA (or IP) in terms of Q, to calculate the intensity enhancement of COV bands. On the basis of their calculation for halogen-benzene complexes, substantial contribution to COV IR intensity comes from an electronic reorientation during the stretching vibration of the electron acceptor (or donor).

This Ferguson-Matsen-Friedrich-Person (FMFP) charge oscillation theory was successfully applied to interpret unusual vibrational spectra of various CT complexes. A reasonable explanation was provided for the dichroic behavior of the oriented crystals of HMB-TCNE and PMB-TCNE (74). IR activation of the totally symmetric C-CH_3 stretching vibrational mode of the donor at 1295 cm^{-1}, and the acceptor at 1560 cm^{-1}, in HMB_2-TCNE was attributed to COV interaction. The donor molecules in the 2:1 complex are sitting at the asymmetric site in the chain of CT complexes and crystal symmetry about the HMB molecule is reduced. Symmetry cancellation of vibronic charge oscillation is thus not possible, as in the case of 1:1 HMB-TCNE (74) (109). IR activation of the totally symmetric modes in such situations were explained in terms of FMFP theory. Drastic effects of COV interaction on the vibrational spectrum of radical anion were dramatically demonstrated for the alkali metal salts of TCNE (75,110). $TCNE^{\cdot-}$, with its presumed D_{2h} molecular symmetry, shows most intense IR bands of a_g symmetry (75) (110), normally forbidden by symmetry. Thus, most intense and broad IR bands of NaTCNE at 2222, 2188, 1385, 530, 521, 463, and 455 cm^{-1} were attributed to charge oscillation activated a_g modes, as a result of changes in EA of $TCNE^{\cdot-}$ (75). These assignments of $TCNE^{\cdot-}$ IR bands were further supported by the nearly coincident Raman vibrational bands (9) (110) (111) and the results of a normal coordinate analysis (9) (110). Unusually large (~50 cm^{-1}) splitting between the vibrational bands assigned to the same a_g mode was attributed to factor group or transverse/longitudinal (T/L) (112) coupling associated with COV interactions. Normally IR active b_{1u} and b_{2u} vibrational bands were apparently 'washed out'. Similar results were observed for other alkali metal salts of TCNE (9) (10) (75).

For TCNQ monoanion radical salts, substantial contribution of the COV interaction had to be taken into account to explain the observed IR spectra satisfactorily (89). Initially, some doubts were raised as to the the importance of vibronic interactions in $TCNQ^{\cdot-}$ salts, on the ground that IR bands coincident or nearly coincident with the a_g Raman bands were not observed (113) (114). In the polarization study of reflectance IR spectra of the KTCNQ salt, the vibrational bands at 719, 825, 1183, 1343, 1583 and 2175 cm^{-1} were observed to be polarized, in a direction parallel to the crystal needle axis and perpendicular to $TCNQ^{\cdot-}$ molecular plane (x-axis, Figure 1). IR bands at 988, 1221 and 1369 cm^{-1} were polarized along the molecular plane as well as perpendicular to it. The 1512 and 2200 cm^{-1} bands were polarized only along the molecular plane of $TCNQ^{\cdot-}$. Since the IR active fundamental modes of neutral TCNQ in the 900-4000 cm^{-1} region are planar in character (115-117), in the absence of any significant vibronic interaction the transition dipole moment for the $TCNQ^{\cdot-}$ IR bands in this region should be aligned along the molecular plane. As a result, all IR bands of $TCNQ^{\cdot-}$ in the 900-4000 cm^{-1} region should be polarized along the molecular plane and perpendicular to the needle axis. Presence of IR bands polarized perpendicular to the $TCNQ^{\cdot-}$ molecular plane shows substantial contribution of the vibronic interaction to the vibrational spectrum. In view of significant electron exchange between near neighbor $TCNQ^{\cdot-}$ in the dimer along the needle axis (27) (56), the change in their EA's with the stretching vibration, through charge oscillation, should induce a transition dipole moment along the stack direction. The polarization of the vibrational bands, activated by vibronic interaction, must be along the needle axis as observed by Anderson and Devlin (89). According to FMFP theory most IR bands

activated by COV interaction should belong to the totally symmetric modes. Hence, the out-of-plane polarized IR bands of $TCNQ^{\cdot-}$ except one at 825 cm^{-1}, were assigned to the modes of a_g symmetry (89). The 825 cm^{-1} out-of-plane IR band can be assigned to a b_{3u} symmetry mode (corresponding to the neutral band at 859 cm^{-1}, ν_{50} b_{3u} mode (116) (117)). The discrepancy between the frequencies of IR bands and the Raman bands assigned to the same a_g symmetry mode was observed to be less than 40 cm^{-1} (91), which can be attributed to factor group or T/L splittings. Since each monoclinic crystal unit cell has eight TCNQ anions, each fundamental mode can split into eight factor group components. Abnormally high intensity and line width of these vibronic bands can be attributed to charge density fluctuations of the unpaired electron (99). Similar intense and broad vibronic bands, polarized out of the TCNQ molecular plane, were observed for quinoline $(TCNQ)_2$ and TEA $(TCNQ)_2$ salts (101).

These charge oscillation bands of $TCNQ^{\cdot-}$ can be described in terms of mixing of $^2B_{2g}$ ground electronic state and the first excited $^2B_{3u}{}^{(1)}$ state through the normal vibrational modes of a_g symmetry. Splitting of the 643 mμ electronic band of KTCNQ (66) into two components at liquid nitrogen temperature may be due to mixing of $^2B_{2g}$ and $^2B_{3u}{}^{(1)}$ electronic state through the 1583 cm^{-1} normal mode of a_g symmetry. Also splitting of the 1100 mμ DE band at liquid nitrogen temperature may be due to vibronic mixing of an electronic state and the first excited charge transfer state through the 1369 and 1583 cm^{-1} a_g vibrational modes.

The intensity of COV IR bands increases with decreasing temperature of $TCNQ^{\cdot-}$ salts (90). Such intensity enhancement has been attributed to an increase in vibronic interaction due to the increased extent of dimerization and the extent of monoclinic crystal structure. The

transition temperature (87°C) for NaTCNQ was observed from abrupt intensity changes of vibronic bands. This result compares favorably with the temperature of the phase transition between triclinic to monoclinic crystal structures observed from x-ray crystallographic studies (65-75°C) (21) and conductivity measurements (25). In triclinic crystals the extent of vibronic interaction is reduced since $TCNQ^{\cdot-}$ is predominantly in the monomeric form (21). The intensity of the COV IR bands was reduced considerably when $TCNQ^{\cdot-}$ salts were dissolved in less polar solvents (66) (68) like dimethyl formamide where the monomeric form of TCNQ is present. The effects of vibronic interaction on electronic spectra, like intensity borrowing and appearance of fine structure, were observed in some TCNQ salts (88).

Low energy electronic states of highly conductive TCNQ salts (38) (39) and the polarization of DE (27) and COV IR bands (66) along the highest conductivity axis (30) have raised the question of a connection between the vibronic interaction and electrical conductivity. Kaplunov et al. (101) suggested formation of small polarons through such vibronic interactions. Alternatively, a charge density wave (CDW) mechanism has been suggested (104).

Charge Density Wave (CDW) Theory

The temperature and frequency dependence of electrical dark and photoconductivity have been demonstrated for various CT complexes (30) (42). The highest electrical conductivity for TTF-TCNQ at 65°C was observed at about 1050 cm^{-1} ($\sim 1.2 \times 10^{-3}$ ohm^{-1}-cm^{-1}) (30). Brau et al. (56) observed photoconductive absorption peaks for $Cs_2(TCNQ)_3$ and $TEA(TCNQ)_2$ at the frequencies of a_g symmetry modes of $TCNQ^{\cdot-}$ polarized

along the needle axis. These results were interpreted in terms of the interaction between the charge transfer electron in the conduction state and phonons (104) (118).

The semi-conducting state at low temperature arises from the action of a periodic potential inducing the conduction electrons to condense into charge density waves (CDW) (104). The phase of CDW is fixed by the phase of the periodic potential. The frequency dependence of the conductivity is a result of single electronic transitions between two subbands contained in the electronic energy states (104). Stabilization of CDW states in organic conductors is caused by intermolecular (superlattice) distortions and distortions due to intramolecular vibronic coupling (119). When a set of phonons interacts with underlying conduction electronic bands, an induced CDW leads to the periodic distortions of the molecular lattice. This gives rise to collective contributions associated with oscillations in the phases of combined lattice (104) (119), and charge distortions about their equalibrium values. These oscillations involve a bodily displacement of an appropriate component of condensed charge and give rise to the optical activity along the chain direction for psuedo-linear conductors (118), like organic salts of TCNQ. Presuming no significant contribution to conductivity from oscillations in the amplitudes of collective modes, changes in dipole moment due to phase oscillation distortions are mostly caused by the restoring forces. These forces are intrinsic and depend on the strength of electron-phonon coupling (104) (118-120). Though phase oscillations of individual phonons are harmonically coupled, it is still possible to associate each of them with a particular electron-phonon coupling constant (118). The frequency of collective phase oscillations

depend on the nature of electron and phonon wave propagators. Vibronic coupling constants between the a_g vibrational modes of $TCNQ^{\cdot-}$ and its ground electronic state $^2B_{2g}$, were estimated to be of the order of 50 meV (118) which contribute to the stabilization of distortions in CDW state. As a result of extensive delocalization of conduction molecular orbital over a large molecule, distortions are stabilized by a large number of phase phonons of small amplitude. Intramolecular distortions, i.e. the value of the band gap parameter, is largely determined by intramolecular electron-phonon interactions. For a frequency of collective phonon modes well below twice the band gap parameter value, lead electron-phonon coupling to a series of vibronic absorption bands. Band widths of these vibronic bands are limited by the natural widths of original (uncoupled) phonon states (118) (119). Thus, low frequency IR inactive phase oscillations become active due to the electron phonon coupling. These phonon vibronic bands are polarized in a direction perpendicular to the $TCNQ^{\cdot-}$ molecular plane. Symmetry, frequency, and polarization of phonon bands (56) (118) thus are same as those of the COV bands (92). The nature and symmetry of these phonon bands, as for the COV bands, is determined by molecular symmetry and electronic structure. Collective phase phonons of frequency above twice the band gap parameter are damped via excitation of electron-hole pairs (104).

Distinction has been made between the CDW and COV modes of vibronic interactions (121). The predominance of the CDW vibronic mechanism over the FMFP COV mechanism depends on the nature of the cation and the crystal structure (121). For alkali metal salts of TCNQ where the dimerized form of $TCNQ^{\cdot-}$ is present to a significant extent, COV interaction over short range is more important. The molecular vibrations

couple with the unpaired electrons of the TCNQ monoanion radical and drive long wavelength plasma-like electron oscillations in the range of vibrational frequencies. For the highly conductive organic salts like TTF-TCNQ or $TEA(TCNQ)_2$ with long linear chain structure, the long range CDW mechanism is more prevalent. Despite separate underlying mechanisms, both types of vibronic IR bands belong to the totally symmetric a_g modes and are polarized along the stack-axis, and their intensity increases (54) (89) with decreasing temperature. Consideration of another type of vibronic interaction is essential in the interpretation of the vibrational spectra of TCNQ and TCNE salts, particularly for the colored salts. The Resonance Raman (RR) effect, in contrast with the other two vibronic effects mentioned above, is not confined to the CT complexes only but can be observed for any colored chemical compounds.

Resonance Raman Effect

When the excitation frequency of a source light approaches the frequency of the electronic absorption band of the scattering sample, the intensity of the Raman vibrational bands is resonantly enhanced through the interaction between the electronic states and the vibrational states (105). Intensity patterns of the resonantly enhanced Raman vibrational bands depend on the relative position of the excitation line with respect to the electronic absorption band, the overlap of electronic bands and the symmetry of the vibrational modes (105) (122-129). When the excitation frequency lies within absorption band profile of a strongly allowed electronic transition, the resulting vibronic interactions involved in intensity enhancement of the Raman vibration band can adequately be described in terms of the adiabatic

approximation (105) (125). This type of resonance intensity enhancement is similar to resonance fluorescence effect or the A-type RR effect (125). When the excitation light frequency lies in the region of overlap of two or more electronic absorption bands, or a weakly allowed band (e.g. symmetry forbidden transition) which may borrow intensity from the other excited electronic state (or states), then nonadiabalic terms of the Herzberg-Teller expansion must also be included (105) (122-126). Intensity borrowing by a weakly allowed transition is accomplished by mixing symmetry modes other than totally symmetric modes. In such a case the intensity of the non-totally symmetric vibrational bands is also enhanced. This type of resonance intensity enhancement is termed as nonadiabatic or non-A-type RR effect (122) (123). The relative position of laser excitation line with respect to an electronic absorption bands of the sample and the nature of the intensity enhancement pattern are helpful in the vibrational band assignments. Since the largest contribution to the polarizability tensor and hence Raman intensity comes from adiabatic terms, RR intensity enhancement of the totally symmetric modes is higher than other symmetry modes (125).

RR spectra of neutral TCNQ molecule (115-117) (130), its monoanion radical salts (62) (91) (113) (114) (130) (131) and TCNE monoanion radical salts (9) (87) (110) (111) (132) (133) have been investigated quite extensively. $MTCNQ^{\cdot-}$ (1:1) salts show changing intensity patterns of Raman vibrational bands with a change in the laser excitation wave length (91) (131). Intensities of the 1208, 1396, 1610 and 2220 cm^{-1} Raman bands were highly enhanced for the 5145^{o}A, 5682^{o}A and 6471^{o}A laser excitation lines (91) (131). Intensities of other Raman vibrational bands at 1633, 1407, 1370, 1326, 1295, 1186, 1012, 986, 730 and 348

cm^{-1}, were resonantly enhanced for shorter wavelength laser excitation lines such as at 4880°A and 4579°A (91). Such variation of intensity patterns of $TCNQ^{\cdot-}$ RR spectra, as the laser excitation line moves across the electronic absorption bands from higher to lower wavelength, can be explained in terms of a change from A-type to non-A-type RR spectrum (91). Alkali metal salts of $TCNQ^{\cdot-}$ show electronic absorption bands at 620 mμ ($^2B_{3u}{}^{(1)} \leftarrow {}^2B_{2g}$) and 420 mμ ($^2B_{3u}{}^{(2)} \leftarrow {}^2B_{2g}$ and $^2A_u{}^{(1)} \leftarrow {}^2B_{2g}$), in the region of the laser lines used (91). The higher wavelength laser lines like 6471°A, 5682°A and 5145°A lie in the absorption region of the $^2B_{3u}{}^{(1)} \leftarrow {}^2B_{2g}$ band which is an allowed electronic transition (60) (61). The A-type RR intensity enhancement of the 2220, 1610, 1396 and 1208 cm^{-1} a_g bands is due to the contribution to the polarizability tensor from the adiabatic terms (91). The 4880°A and 4579°A laser excitation lines lie in the overlap region of the 420 and 620 mμ electronic bands and the Raman vibrational bands of b_g type symmetry modes become more intense in this region due to the contribution from non-adiabatic terms (91). A question has been raised about this scheme of interactions for $TCNQ^{\cdot-}$. Are the Raman bands whose intensities are enhanced at 4880°A and 4579°A due to the non-A-type RR effect or the presence of α,α-$DCTC^-$, in the sample, as a result of a reaction of oxygen with TCNQ salts (130). The 1635, 1295, 1136, 1010, 980 and 350 cm^{-1} bands were shown to be the Raman vibrational bands of α,α-$DCTC^-$ (76) and some reaction of oxygen with $M^+TCNQ^{\cdot-}$ (1:1) salts prepared by a solution method is possible (130). The question of non-A-type bands will be discussed in more detail in a later part of this study. However, here it can be said that except for the 1295, 1635 and 1012 cm^{-1} bands, other Raman bands belong to the $TCNQ^{\cdot-}$ monoanion as well as α,α-$DCTC^-$.

The intensity enhancement of Raman lines of $TCNQ^{\cdot-}$ in acetonitrile solution, at different excitation wavelengths has also been studied (62) (130). In case of solution Raman spectra only the 2192, 1613, 1389, 1195, 976, 724, 612 and 336 cm^{-1} bands of a_g symmetry were observed (130). The RR intensity enhancement of these bands was observed when the laser lines, in the 6300-6500^{o}A wavelength range were used, as the excitation source. However, intensity enhancement of other nontotally symmetric lines for laser lines of lower wavelengths (4500-5000^{o}A) was not observed. One possible explanation is that since $TCNQ^{\cdot-}$ in acetonitrile solution is largely in a monomeric form (63-65) which has different electronic absorption spectrum than the dimeric salts. In the solid state, $TCNQ^{\cdot-}$ salts are to a large extent in the dimer form (27) (43) (46); hence, display of the different intensity patterns of RR spectra in a solution and in the crystal may be attributed to the dimerization and solid state effects. Jeannaire and VanDuyne (130) plotted intensity ratios of the resonant $TCNQ^{\cdot-}$ Raman line and a nearby nonresonant CH_3CN Raman line versus laser excitation frequency. Resonance Raman excitation curves, as these plots were called revealed a substantial vibronic structure in the electronic bands. A possibility of experimentally resolving electronic spectrum into fine vibronic structure by using RR excitation curves was demonstrated.

Unlike $TCNQ^{\cdot-}$ salts, TCNE CT complexes do not show distinctly different RR intensity patterns with a change of excitation wavelength (9) (110) (111). For the alkali metal salts of TCNE (110) the 523 cm^{-1} band is resonant for the 4880^{o}A and 5145^{o}A laser excitation lines. The 2222 and 1430 cm^{-1} Raman bands were also resonantly enhanced at 4579^{o}A and 4880^{o}A laser excitation wavelengths (9). Like TCNQ salts, resonance excitation profiles (intensity of Raman band vs. wavelength of the

laser excitation line) for TCNE and $TCNE^{\cdot-}$ have been constructed using Raman band intensities for the 4579^{o}A excitation line as a reference (132) (133). Usually, the peak of the laser excitation profile is at a lower energy than the peak of the electronic absorption band (133).

The vibronic interaction in CT complexes where more than one electron is transferred to the electron acceptor has not been studied as extensively as for the monoanion radical salts. However, some vibronic interaction due to additional electron density may be possible in the di- and tri-anions of TCNQ and TCNE.

A cursory survey of the available vibrational data of TCNQ, TCNE and their monoanion radicals will now be made before describing the details of this study.

Vibrational Spectra

Stoichiometric Salts

Vibrational spectra of neutral TCNQ (18) (115-117) (134) and its monoanion radical salts (62) (66) (88-91) (101) (113) (114) (130-136) have been reported in the literature. The vibrational spectra of single crystals (115-117), coupled with normal coordinate analysis (115) (116) (134) has established reasonably reliable assignments for thirty-two planar and eleven out-of-plane vibrational bands of neutral TCNQ (115-117). As mentioned earlier, all the fundamental vibrational modes of neutral TCNQ for the out-of-plane vibrational modes were assigned to the vibrational bands observed in the 80-1000 cm^{-1} range (115) (116). For its monoanion radical salts, however, the vibrational band assignments had been a subject of discussion. Normal coordinate analyses (114) (134), published so far, have neglected vibronic interactions

involved in the $TCNQ^{\cdot-}$ salts. Anderson and Devlin (89) established the importance of COV interactions in the TCNQ salts and assigned strong IR bands at 719, 1183, 1343, 1583 and 2175 cm^{-1} to the totally symmetric a_g modes. These assignments were confirmed by other vibrational studies (68) (90) (135). Additional IR bands at 620 and 325 cm^{-1} were also assigned to the COV a_g modes of $TCNQ^{\cdot-}$ (90). Assignments (114) of the Raman bands at 2220, 1580, 1409, 1368, 963, 800, 752, 590, 456 and 482 cm^{-1} need to be reexamined. Similarly, some IR bands at 3038, 3020, 2197, 1475, 1226, 967, 954, 902, 521, 496 and 484 cm^{-1} should be examined for better assignments.

Despite negative electron affinity of the dianion with respect to the monoanion of TCNQ (-1.87 ev (77), -3.34 (57), -1.79 ev (56)), it is fairly stable in an oxygen free atmosphere (76). Apparently, TCNQ acts as a sink for electrons (77) and seems to accommodate electron density in the same manner whether one, two or three electrons are added. Besides the total energy of $TCNQ^{-2}$ is less than TCNQ neutral (plus two electrons at infinite separation) (0.76 - 1.04 ev) (56) (57) (78). However, the dianion in the presence of even a weak electron acceptor like oxygen, acts as an electron donor and undergoes chemical reaction to produce α,α-$DCTC^{-}$ (76), so it must be studied in an atmosphere free of such reactants. The C≡N stretching vibrational IR bands of the dianion, in brown colored N,N'-ethylene-bis (acetyl-acetoniminato) $cobalt^{2+}$ $TCNQ^{-2}$ salt (80) at 2102 and 2151 cm^{-1} and in purple Cr^{3+} $(CH_3CN)_2$ $TCNQ^{\cdot-}$ $TCNQ^{2-}$ (81) at 2090 and 2190 cm^{-1}, have been reported. It is not clear from the report whether these dianion salts were prevented from interaction with oxygen, so these values should be accepted with due caution.

The vibrational IR spectrum of supposedly trianionic TCNQ CT

complex of perylene has recently been reported (83). However, the 833, 1635, and 2230 cm^{-1} IR bands as well as its electronic band at 470 mμ are similar to the α,α-$DCTC^{-}$ bands (19) (76). Also some of the neutral TCNQ and perylene electronic and IR bands appear in the published spectra. This again raises a question of oxygen reaction with $perylene_3(TCNQ)$ CT complex. In this study, electronic and vibrational spectra of the alkali metal salts of $TCNQ^{-2}$ and $TCNQ^{-3}$ and their oxygen reaction products will be presented.

The vibrational spectra of the neutral TCNE (137) and $TCNE^{\cdot-}$ with vibrational band assignments (9) (137) have been reported in the literature. For TCNE monoanion radical vibrational spectra are completely dominated by the COV bands (9) (110). Thus, the intense IR bands at 2222, 2188, 1385, 530, 521, 463 and 455 cm^{-1} and the Raman bands at 2225, 2188, 1430, 1380, 536 and 523 cm^{-1} were assigned to the a_g symmetry modes of NaTCNE (75) (110). Normal coordinate calculation confirmed the above vibrational band assignments (9) (110).

The C≡N stretching IR vibrational bands for the dianion and trianion sodium salts of TCNE were observed at 2090 and 1980 cm^{-1} respectively (75). In this investigation vibration spectra of $TCNE^{-2}$ and $TCNE^{-3}$ will be studied in more detail.

Nonstoichiometric Salts

The CT complexes of anamalous composition exhibit many interesting physical properties (69). The 3:2 and 2:1 CT complexes of dibenzo-(c,d) phenothiazine and 2,3-dihalogeno-5,6-dicyano-p-benzoquinone show the absorption edges (the point at which absorption is reduced by 50%) at 6μ (1.7 kk), not observed in the 1:1 complex (69). $Cs_2(TCNQ)_3$ is a

better electrical conductor than 1:1 alkali metal salts of TCNQ (20) (25). TCNQ and TCNE can accommodate one, two, three electrons (or fractions in between) to form stoichiometric as well as nonstoichiometric salts. The readiness to accept additional electrons and the stability of the CT complex depend on the electron affinity, LEMO of the electron acceptor and ionization potential of the donor. The reactivity of the di- and trianions as well as nonstoichiometric salts, formed from their mixtures, towards oxygen and moisture, depend on energy of their HOMO's and ionization potentials. The observed or calculated values of EA, IP, LEMO, HOMO, etc., for TCNQ, TCNE, their anions, oxygen, etc., are given in Table I.

Physical properties like electrical conductivity of CT complexes depend on their composition. However, electrical conductivity characteristics show erratic behavior for reasons not clearly understood. The electron acceptors like TCNE (9), napthalene (71), anthracene (73) and a large number of aromatic compounds (69) (70) readily form nonstoichiometric CT complexes over a wide range of composition with alkali metals under vaccum.

The intensity pattern of RR spectra of nonstoichiometric CT complexes were observed to be more sensitive to the change in their composition (9) (71) (73) than the vibrational and electronic band frequencies. The usefulness of the RR effect to measure the sample characteristics for possible correlation with electrical conductivity and other physical properties seems worth exploring.

Figure 2 shows the RR spectra of KTCNQ (1:1) of fixed composition, prepared by a solution method, for different laser excitation lines (91). The changing RR intensity patterns of $TCNQ^{\cdot-}$ were correlated to the

TABLE I

ELECTRON AFFINITIES, IONIZATION POTENTIALS OF TCNQ, TCNE, THEIR ANIONS, SODIUM AND OXYGEN MOLECULE

Chemical Species	Electron Affinity (EA) eV	Ionization Potential (IP) eV	Highest Occupied Molecular (HOMO) Orbital eV	Lowest Empty Molecular Orbital LEMO eV
Sodium[b]	0.54 or 0.47	5.138		
TCNQ	2.83[c]	8.01[e]	-9.256[a]	-2.659[a]
$TCNQ^{-}$	0.76 - 1.07[d,e]	0.09[e]	-2.702[a](α)	7.967[a](α)
			-4.740[a](β)	4.090[a](β)
$TCNQ^{-2}$	-0.09[e]	-1.07[e]	2.623[a]	13.064[a]
$TCNQ^{-3}$				
TCNE	2.88[c]	8.832[a]	-10.87[g]	-2.85[g]
$TCNE^{-}$	0.4[f]	6.38[f]	0.0024[g]	3.47[g]
$TCNE^{-2}$	-6.38[f]		5.992[a]	18.129[a]
$TCNE^{-3}$				
Oxygen	0.43[h]			

[a] Reference 57

[b] M. Karplus and R. N. Porter, Atoms and Molecules, W. A. Benzamine Inc., Manlo Park, California, 1970, pp. 205.

[c] Reference 2

[d] Reference 56

[e] Reference 78

[f] $E_{ion} - E_{(mol + ne_{\infty})}$ $\because$ n = number of electrons involved in charge transfer; e_{∞}=electrons at infinite distance, Reference 57

[g] Reference 9

[h] Adiabatic electron affinity, Reference 140

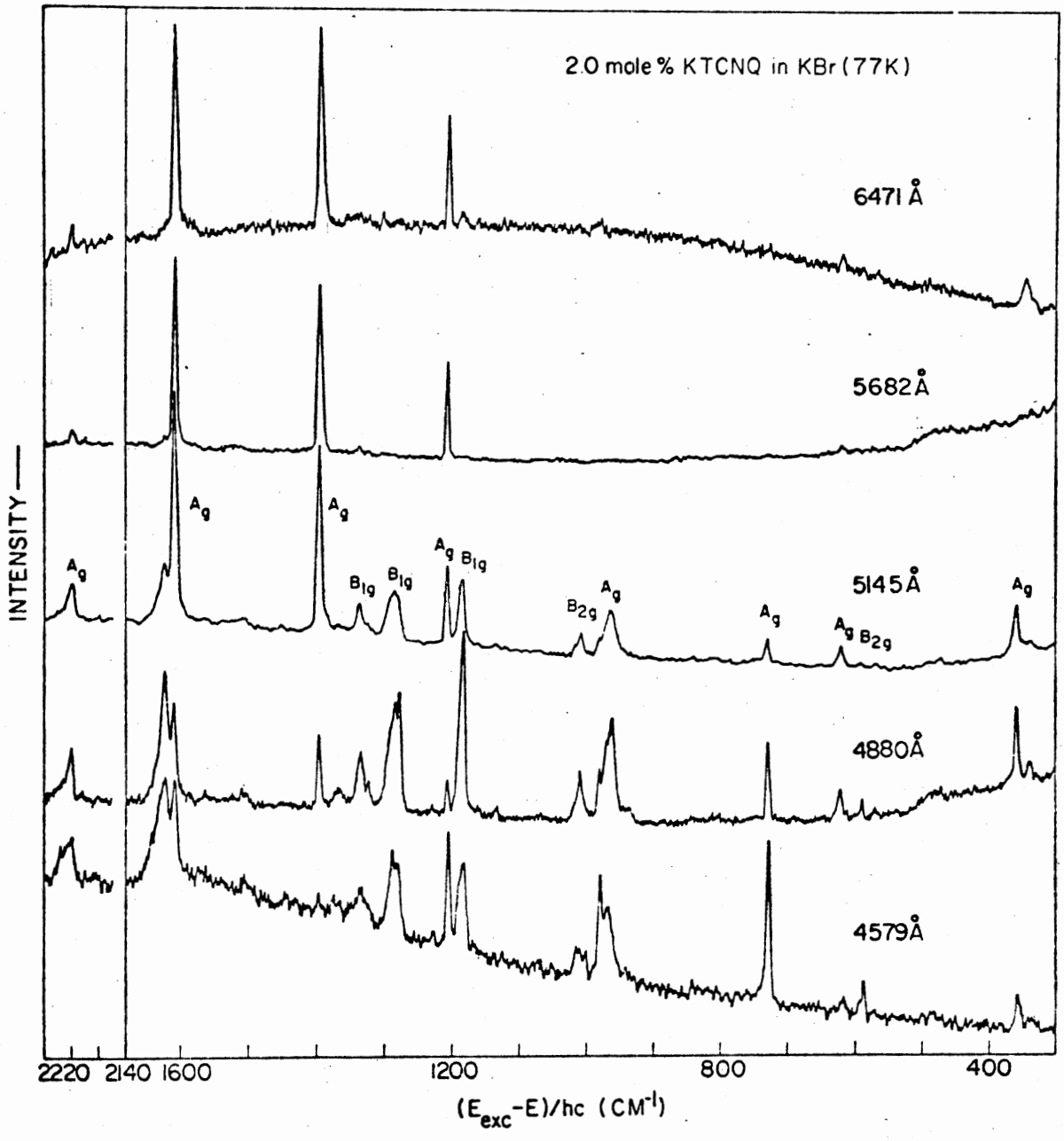

Figure 2. Resonance Raman Spectra of KTCNQ (1:1) for the Different Laser Excitation Lines (Chi and Nixon (76))

electronic spectrum of the sample (91) in terms of A and non-A-type resonance as described earlier. These RR spectra display changing intensity patterns as laser excitation lines were moved across the electronic spectrum. These RR intensity patterns will be used as reference points, for a correlation between RR spectra of the nonstoichiometric soidum salts of TCNQ and their composition. The intensity ratios with respect to one of the Raman bands for the TCNQ anion vs. composition will be plotted to construct the Resonance Raman composition curves, similar to the Jeanmaire and VanDuyne's (130) Resonance Raman excitation curves.

Interaction of the TCNQ and TCNE Anions with Oxygen

The interaction of oxygen with salts of TCNQ and TCNE changes their physical and chemical properties (19) (25) (76) (138) (139). Interaction of oxygen with the alkali metal salts of $TCNQ^{\cdot-}$, such as NaTCNQ, causes decrease in electrical conductivity (from 10^{-4} to 10^{-5} ohm $^{-1}$ cm^{-1}), increase in the activation energy and reversal of the sign of charge carrier from n- to p-type (25) (138). The oxygen molecule with its small electron affinity (0.43 ev) (140) acts as an electron acceptor and $TCNQ^{\cdot-}$ as a donor with IP = 0.09 ev (78). However, such changes in physical properties do not alter the electronic or vibrational spectra (138), except for a very slight shoulder at about 20 kk (500 mμ) (139). A similar band at 20 kk (1.7 ev) in the electronic spectrum of a TCNE salt (139) was observed when it reacted with oxygen.

The dianion of TCNQ reacts spontaneously with oxygen to form a red colored anion of α,α -DCTC$^{\sim}$ (76). The electronic absorption band at 477 mμ was assigned to $TCNQ^{-2}$ by Jonkman and Kommandeur (36). A similar

electronic absorption band was observed when $TCNQ^{-2}$, prepared in oxygen free atmosphere was allowed to react with oxygen (76). The reaction product was identified as α,α-$DCTC^{-}$ by superimposing its electronic and Raman spectra on the spectra of α,α-$DCTC^{-}$ prepared by reaction between TCNQ and $NaNO_2$ (19). α,α-$DCTC^{-}$ shows IR vibrational bands at 835, 1590, 1645, 2150 and 2200 cm^{-1} (19). The RR spectrum shows strong vibrational bands at 349, 963, 1000, 1174, 1281, 1327, 1638 and 2214 cm^{-1} (76). However, many α,α-$DCTC^{-}$ vibrational bands are at almost the same frequency as for $TCNQ^{\cdot-}$ in the solid state (113,131). Only the 838 and 1645 cm^{-1} IR and the 1281 and 1638 cm^{-1} Raman bands can exclusively be assigned to α,α-$DCTC^{-}$. The presence or absence of these vibrational bands as well as a 477 mμ electronic band should indicate whether there is any reaction of TCNQ anions with oxygen.

The study of TCNQ anionic reactions with oxygen is useful to distinguish the spectroscopic characteristics of pure anion salts from those contaminated with oxygen reaction products. Also oxygen derivatives of TCNQ salts show many interesting physical properties. Spectroscopic properties of various reaction products, when oxygen reacts with TCNQ or TCNE anions, will be discussed in this study.

Force Constants and π-Bond Orders

When electrons are transferred from an electron donor to TCNQ and TCNE, the C=C and C≡N bonds are weakened and the C-C bonds become stronger as reflected in their π-bond order changes (9) (36) (77) (78) (84). The mobile π-bond order for a bond between atoms p and q was defined as

$$\rho_{pq} = \sum_{\ell=1}^{N} n_{\ell} C_{\ell p} C_{\ell q} \qquad (1)$$

where n_ℓ, $C_{\ell p}$, $C_{\ell q}$ and N are the number of electrons in ℓth molecular orbital, coefficient of p atomic orbital in ℓth MO, coefficient of q atomic orbital in ℓth MO and number of occupied MOs, respectively.

Changes in bond orders have quite often been correlated with bond lengths (141) (143), force constants (9) (142), and vibrational frequencies (144). Gordy (142) developed an empirical relation between force constant and π-bond order which was written in the form

$$K = aN \left[\frac{X_p X_q}{d_{pq}^2} \right]^{3/4} + b \qquad (2)$$

where K is the force constant in mdyne/^{o}A. N is the π-bond order for a bond between atoms p and q, d_{pq} is a bond length of pq bond, X_p is the electronegativity of an atom p on Pauling scale and X_q is the electronegativity of an atom q. The constants a and b depend on the type of a bond between p and q. For the bonds involved in TCNQ, TCNE and their anions, values of a and b are given as 1.67 and 0.3 respectively. There is nearly linear relationship between force constants and π-bond orders of TCNE and some ketones (9)(142). Also, a linear relation between force constants and overlap population has been shown for the N-O bonds (145).

In this study, relations between the C=C, C-C and C≡N force constants and π-bond orders as well as overlap populations, for the different ionic states of TCNQ and TCNE will be examined.

CHAPTER II

EXPERIMENTAL PROCEDURES

In order to study, electronic and vibrational spectroscopic properties of the stoichiometric and nonstoichiometric sodium salts of TCNQ and TCNE, it was essential to take into consideration the following points: a) IR, Raman and electronic spectroscopic measurements must be made on the same sample, b) since the di- and trianions are susceptible to oxygen and moisture (9) (75) (76), precautions must be taken to prevent reactions with oxygen, water vapor, etc., c) it should be possible to vary alkali metal to organic ratio in the preparation of the stoichiometric and nonstoichiometric salts of desired composition and, d) reactions of the di- and trianions with dry oxygen should be carried out in atmosphere free of moisture and other reactive gases.

To fulfill the above requirements, the technique used to prepare TCNQ and TCNE salts was the co-condensation of alkali metal and organic vapors under vacuum, as developed by Stanley et al. (109) (146). The stoichiometric and nonstoichiometric salts thus prepared, were deposited on proper substrates, suitable for the IR, Raman and electronic spectroscopic sampling. The vacuum cell used for salt preparation was a modified version of a matrix isolation cell constructed by Stanley et al. (109) (146), so as to fit into the cell compartments of the IR, Raman and electronic spectrometers. The vacuum system was connected to a dry oxygen cylinder, in order to prevent any contamination and to control

the amount of oxygen to be introduced into the vacuum cell, for the preparation of oxygen reaction products of the anions of TCNQ and TCNE. Samples were prepared under high vacuum ($\sim 10^{-5}$ torr) to preserve their purity and prevent any disintegration due to reaction with oxygen, water vapor, etc. All the samples were prepared at room temperature ($\sim 25^{\circ}C$).

Preparation and Characterization

NaTCNQ Salts

TCNQ crystals available commercially (Aldrich Chemical Co., Inc., Lot No. 072347), were resublimed four to five times under vacuum. Pinkish orange crystals (m.p.$216^{\circ}C$), thus obtained were crushed into a fine powder and mounted into a kundsen oven. In another oven, freshly cut slices of sodium metal were mounted under n-heptane to avoid a formation of oxides and peroxides. Evacuation of the vacuum cell started immediately after mounting sodium and TCNQ. Each of the Knudsen ovens was surrounded by resistance heater. Resistance heaters were nichrome wire coils precalibrated, by plotting temperature vs. voltage under experimental conditions. These coils were connected to variacs to heat the ovens to desired temperatures. The sodium oven was heated for four to five hours, before starting the heating of TCNQ oven, to expedite the removal of n-heptane. When the presure in the vacuum cell was reduced to 10^{-4} torr or less, the temperatures of organic and sodium ovens were raised in small steps to the desired values. The temperatures required to prepare the salt of certain metal/organic ratio, depend on the hole sizes of Na and TCNQ ovens, presence of heptane, extent of oxide coating on the surface of sodium metal, etc. Because of some

uncertainity involved in these factors, the precise temperatures could not be determined a priori, but were determined by trial and error.

Molecular and atomic vapor beams of TCNQ and sodium were crossed at the appropriate substrates. The substrates used for the IR and electronic spectroscopic measurements were polished crystals of alkali halides, like sodium chloride or cesium iodide. Outer windows of the vacuum cell were also of the same material as the substrate. The substrate used for the Raman spectroscopic measurements was a freshly polished copper wedge. IR and Raman substrates were placed in a close proximity to obtain uniform sample deposition.

Both substrates were mounted on a cryotip so that spectroscopic sampling was routinely done at liquid nitrogen temperature ($-180^{o}C$). Outer windows were protected with appropriate shields, from possible contamination during deposition.

For the colored substances thin film samples have been shown to be appropriate for the Raman spectroscopic study (9) (71) (75). The time of preparation for a thin film a few microns (2-7 μ) thick varied depending on the salt to be prepared. For the 1:1 NaTCNQ salt it was 0.5-1 hour, for the dianion salt, 1.5-2 hours and the trianion salt, 4-6 hours. Since radical anions easily form nonstoichiometric salts, it was essential to control carefully, the rate of heating and temperatures of the metal and organic ovens, to release the exact amount of sodium and TCNQ vapors to obtain pure stoichiometric mono-, di- and trianion salts. Samples thus obtained were characterized by color, electronic spectrum, and the frequencies of the C≡N stretching IR vibrational bands (Table 2). On account of the instability of the salts in atmospheric condition, elemental analysis for the samples was not done. The

TABLE II

CHARACTERIZATION OF SODIUM SALTS OF TCNQ AND TCNE

Electron Acceptor	Composition of the Sample $X=C_{Na}/C_A^*$	Color of the Film	Electronic Bands (mμ)	IR Frequency of C≡N Stretching (cm^{-1})
	0.0	yellow	228,410[a]	2230[b]
	0.1-0.7	green		
	0.8-0.9	turquoise		
	1.0	blue	260,305,365,620[c]	2166,2197
	1.1-1.8	dark blue		
TCNQ	2.0	colorless	205,240,295	2096,2164
	2.1-2.9	golden yellow	190,230,246,285, 330,430	
	3.0	golden yellow	195,223,265,310, 370,427	1901,2035
	Na.α,α-DCTC	blood red	190,220,275,335, 420,470,760,842	2102,2188
	$Na_3TCNQ.O_2$	brown yellow	246,292,352	2096,2166
	0.0	colorless	265[d]	2230,2263[e]
	0.1-0.9	violet		
	1.0	violet		
	1.1-1.4	violet	350,580	2188,2222[f]
	1.5-1.8	blue		
TCNE	2.0	colorless	213,237	2086,2146
	2.1-2.8	yellow	195,230,370	
	3.0	yellow	210,236,265,365	1980,2236
	$Na_2TCNE.O_2$	pink	470	2186,2226
	$Na_3TCNE.O_2$	brown yellow	195,226	2086,2158

[a] Reference 27

[b] Reference 115,116

[c] Some of the electronic bands are reported in reference 43,46

* A = TCNQ; TCNE

[d] Reference 84,85

[e] Reference 137

[f] Reference 9, 75, 110

composition of TCNQ salts is expressed as a ratio of sodium to TCNQ. This ratio henceforth will be referred as X (= C_{Na}/C_{TCNQ}). The ratio was calculated from the intensities of the 2230, 2197, 2164 and 2035 cm^{-1} C≡N IR bands for the neutral mono-, di- and trianion salts of TCNQ respectively. The relative intensities of these 'nonvibronic' C≡N bands were presumed to be dependent only on the concentration of ionic species present in the sample. Within these uncertainties for composition measurements, all reported compositions of nonstoichiometric salts and their correlations with IR and Raman spectra should be taken as indicative of trends rather than accurate. For stoichiometric salts identification from our spectroscopic data was checked with published spectroscopic results (76) (89-91) (136), where available. All spectra and samples were checked for their reproducibility. Our results for $TCNQ^{-2}$ also confirm Suchansky and VanDuyne's (76) observation that the dianion is colorless and has electronic absorption bands in the uv region only and is not red colored with a 477 mμ electronic band in the visible region. This, and other results for $TCNQ^{-3}$, raise some questions about recently published $perylene_3(TCNQ)$ spectroscopic data (83). Because of earlier mentioned suspicions about this perylene complex, the reactions of oxygen with the different anions of TCNQ were studied.

Before exposing a well characterized dianion or trianion TCNQ salt to oxygen, the vacuum system, including the part connected to the oxygen cylinder, was evacuated and then the sample was exposed to dry oxygen. The amount of oxygen allowed in the vacuum cell was controlled by limiting its pressure. Time of exposure to the sample was also controlled. When very little oxygen was allowed in the cell for a

very short time (less than half a minute) and a cell was evacuated immediately, the color of the dianion TCNQ sample turned light red. The IR spectrum did not show much change except intensity of the 1194 cm^{-1} band was increased slightly. However, the Raman spectrum showed two broad bands (band widths more than 100 cm^{-1}), centered around 350 and 550 cm^{-1}. These bands did not change their positions with either a change of laser excitation wavelength or minor changes in the composition. These Raman bands were also observed for samples when there was a minute leak during preparation of the dianion salt. These bands usually arise when limited amount of O_2 was allowed to react with samples of metal/organic ratio in the vicinity of 2.0 (i.e., 1.9, 2.0, and 2.1). When the samples with these bands were further exposed to oxygen, these low frequency, broad Raman bands disappeared and the IR electronic and Raman bands of the blood red colored α,α-$DCTC^-$ were observed. For many $TCNQ^{-2}$ samples the 550 and 350 cm^{-1} broad Raman bands were not observed when exposed to a limited amount of oxygen but were converted directly into α,α-$DCTC^-$ for reasons not clearly understood. The 350 and 550 cm^{-1} broad Raman bands were reproduced only a few times when the dianion samples were exposed to O_2. When a red colored oxygen reaction product of $TCNQ^{-2}$ (which predominantly shows bands of α,α-$DCTC^-$) was further exposed to atmosphere the color of the sample turned to dark blue. The additional IR and Raman bands observed can be attributed to the neutral and the monoanion of TCNQ. When $TCNQ^{-2}.O_2$ reaction products were dissolved in acetone, the electronic spectrum resolved into additional component bands and some new bands appeared. The $Na_2TCNQ.O_2$ reaction product seems to be more soluble in water than in acetone. However, a detailed description of its solubility

in different solvents is beyond the scope of the present study. The reaction of $TCNQ^{-2}$ with oxygen was vigorous and the red color of α,α-$DCTC^{-}$ was developed within 5-10 minutes. However, for a complete disappearence of the dianion IR and electronic bands, it took about 5-10 hours and at times even longer.

A more interesting interaction of oxygen, however, was observed with the trianionic salt of TCNQ, alone or mixed with the dianion. $TCNQ^{-3}$, with three extra electrons, can reasonably be expected to be more reactive with oxygen than the dianion. However, Na_3TCNQ was observed to be more stable than the dianion salt, though less stable than the monoanion salt, in the presence of dry oxygen. When a golden yellow colored sample was exposed to dry oxygen (press. $\sim$1 atm) at room temperature, the rate of disappearance of the color was very slow. It required about 30-50 hours for complete disappearance of the trianion IR and electronic bands. This reaction was arrested at several stages to characterize the reaction products produced during the progress of the reaction, by spectroscopic measurements. At each stage, progressively decreasing intensities of the $TCNQ^{-3}$ IR and Raman bands were observed. The end product was a yellowish brown colored sample whose IR and Raman bands were similar to those of Na_2TCNQ. The Raman bands were broader than Na_2TCNQ vibrational bands. In the IR spectrum the intensities of the 1190, and 1589 cm^{-1} bands were increased and a new band at 1396 cm^{-1} appeared. Electronic absorption bands, though all in the uv region, were at different wavelengths than the Na_2TCNQ bands. Once the reaction of Na_3TCNQ and oxygen was complete, the end product was found to be very stable and no significant changes in color or the spectra were observed even when the sample was exposed to the atmosphere

for several days. However, when it was dissolved in acetone a deep orange-red colored solution was formed. Again like the $Na_2TCNQ.O_2$ reaction product, the $Na_3TCNQ.O_2$ reaction product was apparently more soluble in water than in acetone.

Before each run, the vacuum cell was dismounted and cleaned thoroughly. Substrates and outer windows were polished. Only silicone grease was used to avoid fluorescence interference in the Raman spectroscopic measurements.

For the preparation of nonstoichiometric salts no special precautions were necessary. TCNQ, like TCNE (9), anthracene (71) (73), etc., easily forms nonstoichiometric salts of composition in the $1.0 \leq x \leq 2.0$ range, as temperatures of the sodium and TCNQ ovens were set between those required for the preparation of NaTCNQ and Na_2TCNQ. Nonstoichiometric salts with, increasing value of x within this range, were prepared by setting the temperature of the TCNQ oven constant at a value fixed for NaTCNQ and increasing the temperature of the sodium oven in short steps. Similarly, nonstoichiometric salts of composition in the $2.0 \leq x \leq 3.0$ range were prepared by heating the TCNQ oven at a temperature required for Na_2TCNQ and increasing temperature of the sodium oven in steps. In fact, pure Na_3TCNQ could not be prepared. There was always some dianion contamination. At best, 90% pure Na_3TCNQ salts were obtained during this study.

NaTCNE Salts

The experimental procedure of the preparation of sodium salts of TCNE is the same as for TCNQ salts. However, TCNE is more volatile than TCNQ. In the preparation of the di- and trianions, because of the

proximity of metal and organic ovens, heat of radiation from the sodium oven releases more TCNE vapors than desired in preparation of these metal rich samples. A special Knudsen oven with three glass shields was made for TCNE. The heat of radiation was further reduced by using two glass shields over the sodium oven. Only the sodium oven was heated and by adjusting heat shields between the ovens, the TCNE salts of desired composition were obtained. Commercially available (Eastman Organic Chemicals) TCNE was sublimed five times in the vacuum. Colorless crystals thus obtained were placed in the specially shielded Knudsen oven. The 1:1 NaTCNE salts were obtained by using the special oven for TCNE and no shields for the sodium oven. For the Na_2TCNE salt one extra shield over the metal oven was used. Na_3TCNE was obtained by using two glass shields and aluminum foil over the sodium oven. In the preparation of these metal rich complexes of TCNE, the problem of an impurity, produced by the reaction of oxygen with the TCNE anions at times becomes a nuisance, even under high vacuum. This problem was solved by using a shield over the deposition substrates till the sample of desired composition was formed which was deduced from the color of the film on the shield. Characterization of TCNE salts was made in the same way as for the TCNQ salts. Na_2TCNE and Na_3TCNE, like their TCNQ counterparts, were colorless and yellow in color respectively. The oxygen reaction products of Na_2TCNE and Na_3TCNE were of pink and yellowish brown color respectively. Again as for TCNQ, Na_2TCNE was observed to be more reactive with oxygen than Na_3TCNE. The reaction product of Na_3TCNE and oxygen shows IR bands similar to Na_2TCNE and is apparently more stable than any of the TCNE anion salts. When

$Na_3TCNE.O_2$ reaction product was exposed to the atmosphere little change in appearance or the spectra was observed even after a long time (2-3 days).

Spectroscopic Measurements

Infra^red spectroscopic measurements were made by using a Beckman IR-7 instrument. IR spectra were taken both at room temperature and liquid nitrogen temperature for which no new features were observed except the expected band sharpening. Raman spectra were obtained by using a single reflection technique. A Coherent Radiation Model-52 argon ion laser was the Raman excitation source and a Jarrell-Ash 25-100 double monochromator, with Hamner photon counting accessories were used to detect the Raman signal. Slit widths were used in the range of 1.8-2.2 cm^{-1}. The 4880^{o}A (Blue) and 5145^{o}A (Green) Ar^{+} laser excitation lines (0.6-0.7 watt power) were used. All Raman spectra were taken at liquid nitrogen temperature. All the salts were stable under vacuum and no detectable detoriation of any sample was observed. Spectra for each sample were checked for their reproductibility. Electronic spectra were recorded using a Cary-14 Model uv-visible spectrometer, without any reference cell. Because of light scattering from the alkali halide crystals, particularly in the uv region and the uncertainty in the amount of sample in the thin films, the measurement of molar extinction coefficients was not possible.

The intensities of electronic and vibrational bands are expressed in arbitrary units for reasons mentioned above. Intensity increases or decreases with a change of composition, wavelength of laser excitation line in the Raman spectra or the orientation with respect to the source

light in IR spectra were noted relative to the intensities of other bands rather than in any absolute sense.

Normal Coordinate Analysis of TCNQ, TCNE and Their Anions

A normal coordinate analysis based on reasonable vibrational band assignments for neutral TCNQ have been reported in the literature (115) (116) (134). Force constant calculations using a Urey-Bradley force field (UBFF) (115) and modified valence force field (MVFF) (116) coupled with single crystal studies of the vibrational spectra provided a basis for reliable vibrational band assignments of $TCNQ^{o}$. In the normal coordinate analysis of monoanion radicals of TCNQ salts reported so far, the effects of vibronic interactions have been neglected completely (114) (134). The 325, 620, 723, 1183, 1340, 1580, and 2175 cm^{-1} IR COV bands which have been shown to be of a_g symmetry (89) (90), were assigned to either b_{1u} or b_{2u} modes of $TCNQ^{\cdot-}$ (114) (134). In order to provide satisfactory vibrational band assignments for the vibrational bands of $TCNQ^{\cdot-}$ with due allowance for vibronic interactions, the assignments of above mentioned IR bands and some other vibrational bands were changed. Force constants for $TCNQ^{\cdot-}$ with the new assignments were calculated. For the di- and trianions of TCNQ vibrational assignments were made and their force constants were calculated. Force constants thus calculated will be correlated with π-bond orders of TCNQ anions which may be helpful to understand the change in nature of the C-C, C=C and C≡N bonds with the addition of each electron.

Normal coordinate analyses for neutral TCNE, using UBFF and MVFF have been reported (9) (110) (137). In the vibrational band assignments

of TCNE monoanion radical, the dominant role played by COV interactions to determine its vibrational spectroscopic pattern was taken into account. The force constants thus calculated for $TCNE^{\cdot-}$ by using MVFF, by Hinkel and Devlin (110), were used as initial force constants to calculate the vibrational frequencies of $TCNE^{-2}$ and $TCNE^{-3}$. Then stretching force constants were adjusted to obtain the best fit between the observed and calculated frequencies of the di- and trianions of TCNE. Again an attempt will be made to correlate the calculated force constants of TCNE and its anions with their π-bond orders reported by Penfold and Lipscomb (84).

The vibrational band assignments for neutral TCNQ as published by Girlando and Pecile (116) were used as a reference in the vibrational band assignments of the TCNQ anions. The molecular structure and definitions of the internal coordinates used in the normal coordinate analyses of TCNE, TCNQ and their anions are given in Figure 1. A modified valence force field was used to calculate frequencies of the neutral molecules and their anions. The structural data for TCNQ neutral was taken from Long et al.'s (147) x-ray crystallographic study. For $TCNQ^{\cdot-}$ structural data published for NaTCNQ monoclinic crystals (21) was used except for the C≡N bond lengths which were taken from the refined x-ray crystallographic study of Fritchie and Arthur (26). For the dianion of TCNQ, bond lengths and bond angles from an MO calculation are available (78). From these calculations it seems that there is little change in the D_{2h} symmetry when two electrons are added to neutral TCNQ. However, the structural parameters used in the normal coordinate analysis of the dianion were the same as for NaTCNQ. Since the elements of the G-matrix are not very sensitive to small changes in bond lengths and bond angles, the force field thus calculated should not be much effected by this choice. Since the trianion of TCNQ is

prepared for the first time, structural data, crystallographic or otherwise, is not available. Again as in the case of $TCNQ^{-2}$, the values of the structural parameters of NaTCNQ were used in the calculation of the G-matrix for $TCNQ^{-3}$. The C-H bond length value was taken to be 1.08°A (116). For TCNE and its anions, the values of the bond lengths and bond angles used to calculate the G-matrix were taken from x-ray crystallographic study by Penfold and Lipscomb (84). All the bond angles for TCNQ and TCNE except C-C≡N (which was taken as 180°) were given a value of 120°. The bond lengths used were the average of values given by crystallographic study for the symmetrically identical bonds. The values of structural parameters used in normal coordinate analyses of TCNQ, TCNE and their anions are summarized in Table III.

To calculate the force constants and frequencies, a computer program developed by Overend and Scherer (148) was used. Initial force constants for $TCNQ^{o}$ were used from the MVFF reported by Girlando and Pecile (116) with some modifications for the interaction force constants like $F_{r_5}'(\alpha 24-\alpha 26)$ $F_{R_g}'(\alpha 25-\alpha 26)$ and $F_{r_5}'(\alpha 35-\alpha 36)$ which are associated with local redundancies. Scherer's (149) scheme was followed. Thus $F_{r_5}'\alpha 26 = -F_{r_5}'\alpha 25$, $F_{R_g}'\alpha 25 = F_{R_g}'\alpha 26$ and $F_{r_5}'\alpha 35 = -F_{r_5}'$, (for $\alpha 36$ were assumed for definitions of r_5, R_g, and α's see Figure 1). The force field of the neutral TCNQ which reproduces the observed vibrational frequencies as nearly as possible was used as a starting point to calculate force constants for $TCNQ^{-}$. The frequencies for the vibrational modes of a_g symmetry were taken to be the average of factor group component frequencies, observed in IR and Raman spectra of $TCNQ^{-}$. Initially only those observed frequencies for which vibrational band assignments were established, were used and the stretching force

TABLE III

MOLECULAR PARAMETERS FOR TCNQ, $TCNQ^{\cdot-}$ AND TCNE

Structural Parameters* / Ionic Species	Bond Lengths (^{o}A)						Bond Angles	
	d_1	r_5	R_9	R_{11}	r_{13}	D_{17}	$\alpha_{21}\cdots\alpha_{44}\alpha_{45}\cdots\alpha_{48}$	
$TCNQ^{o+}$	1.08	1.448	1.346	1.374	1.441	1.140	120°	180°
$TCNQ^{\cdot-}$ $TCNQ^{-2}$ ‡ $TCNQ^{-3}$	1.08	1.416	1.365	1.419	1.418	1.153¢	120°	180°
$TCNE^{o}$ $TCNE^{\cdot-}$ $TCNE^{-2}$ § $TCNE^{-3}$		R_1		r_2	D_6		$\alpha_{10}\cdots\alpha_{15}\alpha_{16}\cdots\alpha_{19}$	
		1.317		1.448	1.15		120°	180°

*Definition see Figure 1

+Reference 147

‡Reference 21

¢Reference 26

§Reference 84

constants were adjusted to fit those frequencies. Then remaining observed frequencies were fed to the computer and the force field was readjusted so as to reduce the difference between the observed and calculated frequencies as much as possible. Only the stretching force constants were allowed to change in the calculation of a force field for $TCNQ^{\cdot-}$, with the remainder the same as that of the neutral TCNQ. Thus, thirty-two frequencies of the neutral TCNQ were reproduced by using twenty-six force constants. Twenty frequencies of $TCNQ^{\cdot-}$ were reproduced by adjusting only six force constants. For the dianion initially, vibrational bands were assigned tentatively using the vibrational band assignment of the monoanion as a reference. Again the average frequencies of factor group components were used for the a_g symmetry modes. The $TCNQ^{\cdot-}$ force field was used and only the stretching force constants were adjusted to fit the observed frequencies of the dianion. Sixteen observed frequencies of $TCNQ^{-2}$ were reproduced by adjusting six force constants. The same procedure was followed for $TCNQ^{-3}$. Fourteen observed frequencies of the trianion were reproduced by adjusting six stretching force constants of the $TCNQ^{-2}$ force field. The average error between the observed and calculated frequencies was less than 7 cm^{-1}.

Consideration of vibronic interactions provides more reasonable vibrational band assignments. The agreement between calculated and observed frequencies for $TCNQ^{\cdot-}$ is better than published results when vibronic interaction was neglected (114) (134).

The MVFF used for the force constant calculations of $TCNE^{-2}$ and $TCNE^{-3}$ was taken from Hinkel and Devlin (110). Again the same procedure as outlined for TCNQ was followed. Five frequencies of $TCNE^{-2}$

were fit by adjusting three MVFF force constants of $TCNE^{\cdot -}$ (110). Five observed frequencies of $TCNE^{-3}$ were reproduced by adjusting three stretching force constants of the dianion force field. The average error was less than 5 cm^{-1}.

The observed spectra and the results of the force constant calculations will be presented in the next two chapters.

CHAPTER III

RESULTS FOR SODIUM SALTS OF TCNQ

Since the vibrational band assignments for neutral TCNQ have been established without much ambiquity (115-117), this study will focus attention on the anions. The monoanion spectra have been studied extensively (89) (91) (113) (114) (130) (134), however, for the sake of normal coordinate analysis as well as vibrational band assignments the observed spectra of thin films of NaTCNQ will be presented. First, spectroscopic results for stoichiometric salts of TCNQ will be presented. Then results for force constant calculations, nonstoichiometric salts, and the interaction of oxygen with anions of TCNQ will be discussed.

As mentioned earlier, electronic and vibrational spectra presented in this study are qualitative in nature. For the electronic spectra no attempt was made to calculate the molar extinction coefficients for the following reasons: a) scattering from alkali halide substrate surfaces and outer windows of the vacuum cell contribute to the intensity of electronic bands, particularly in the uv region, b) there is some uncertainty in the estimation of the quantity of sample in the path of light and no elemental analysis of thin films was done, c) quantitative measurements of optical dnesities were not feasible on account of very high optical intensities ($\varepsilon \sim 5\text{-}6$) of the electronic bands, i.e., light attenuators were used to bring the electronic peaks within scale, even for thin film samples. Thus, results for the electronic spectra will

be discussed with these limitations in mind. For similar reasons vibrational band intensities in the IR and Raman spectra are qualitative in nature.

NaTCNQ: Monoanion Salt

Electronic Spectrum

As mentioned earlier, $^1B_{1u} \leftarrow {}^1A_g$ and $^1B_{2u} \leftarrow {}^1A_g$ electronic transitions of neutral TCNQ were observed at 394 and 228 mμ (37) (60). The NaTCNQ blue thin films show electronic absorption bands at 620 (2.01 eV), 365 (3.40 eV), 305 (4.05 eV) and 260 mμ (4.77 eV) (Figure 3). This solid state spectrum appears different from that of the liquid solution of $TCNQ^-$ where six electronic absorption bands at 1.49, 3.15, 4.43, 4.71 and 5.33 eV have been reported (36) (37) (60). Such differences may be attributed to solid state effects. The 620 and 365 mμ electronic bands for $Na_x^{\wedge}TCNQ$ have also been reported by Vlasova et al. (46) (47). For the RR spectra of NaTCNQ (1:1) salt and nonstoichiometric ($1.0<x<2.0$) salts the electronic bands at 365 mμ ($^2B_{3u}(2) \leftarrow {}^2B_{2g}$ and $^2A_u(1) \leftarrow {}^2B_{2g}$) and 620 mμ ($^2B_{3u}(1) \leftarrow {}^2B_{2g}$) are of particular interest. Different electronic absorption patterns in the solid state and in solution should be taken into account when comparing the RR spectra of $TCNQ^-$ in these two states.

Vibrational Spectra: IR and Raman

Vibrational spectra of single crystals of $TCNQ^o$ have been published (115-117). Since TCNQ is a centrosymmetric molecule, according to the mutual exclusion principle (15-17) it follows that Raman active a_g and

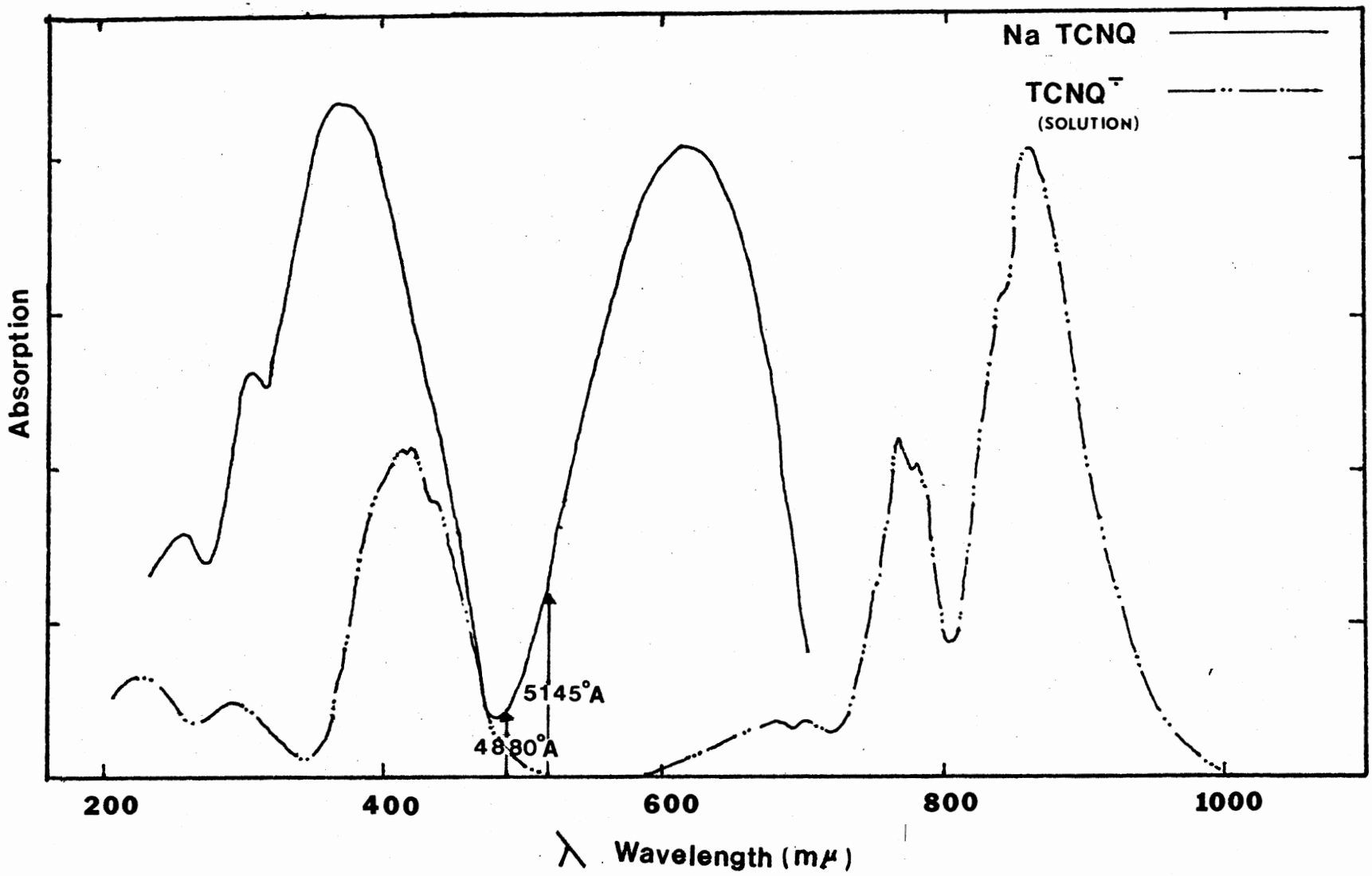

Figure 3. Electronic Spectra of NaRCNQ in the Solid State (——) and $TCNQ^{\cdot-}$ in Solution (36) (—··—)

b_g modes are IR inactive, and IR active b_u modes are Raman inactive. For $TCNQ^o$ this principle was observed to be strictly obeyed (115-117).

All except one of the fundamental IR bands of $TCNQ^o$ in the 800-4000 cm^{-1} range are polarized along the molecular plane (115) (116). The only exception is the out-of-plane b_{3u} mode at the frequency of 859 cm^{-1} (116). Similarly the fundamental Raman bands in the 900-4000 cm^{-1} range, except for a weak band at 1002 cm^{-1} (b_{2g} mode), are of planar character (116). All the vibrational bands of $TCNQ^o$ are narrow (band width $\sim$3-5 cm^{-1}) (115) (116).

The IR spectrum of NaTCNQ (Figure 4) shows broad and intense IR bands at 328, 618, 723, 1186, 1343, 1578 and 2166 cm^{-1}, identified to be of a_g symmetry modes activated by COV interaction (89) (90). In addition, the thin film IR spectrum of NaTCNQ shows COV bands of a_g symmetry at 719, 725, 967, 978, 987, 1167, 1178, 1219, and 1326 cm^{-1}. Some of these additional bands were observed when the sample was cooled to liquid nitrogen temperature. In the vibrational band assignments, several IR and Raman bands were assigned to the same a_g vibrational mode of $TCNQ^-$. Thus, the ν_4, ν_5, ν_6, and ν_7 a_g modes of $TCNQ^-$ split into two (1327, 1342 cm^{-1}), four (1167, 1178, 1186, 1219 cm^{-1}), three (967, 973, 987 cm^{-1}) and three (719, 723, 725 cm^{-1}) factor group components, respectively. The tentative assignments of IR and Raman factor group components of the a_g symmetry modes are shown in Table IV. The amount of factor group splittings between the components of COV bands varies from 2 cm^{-1} (618 and 620 cm^{-1}) to 83 cm^{-1}. The 83 cm^{-1} splitting is unusually large but considering that this mode is one engaged in the formation of small polarons (101) or electron-phonon interaction (119-121), the possibility of such a large value should not be ruled out.

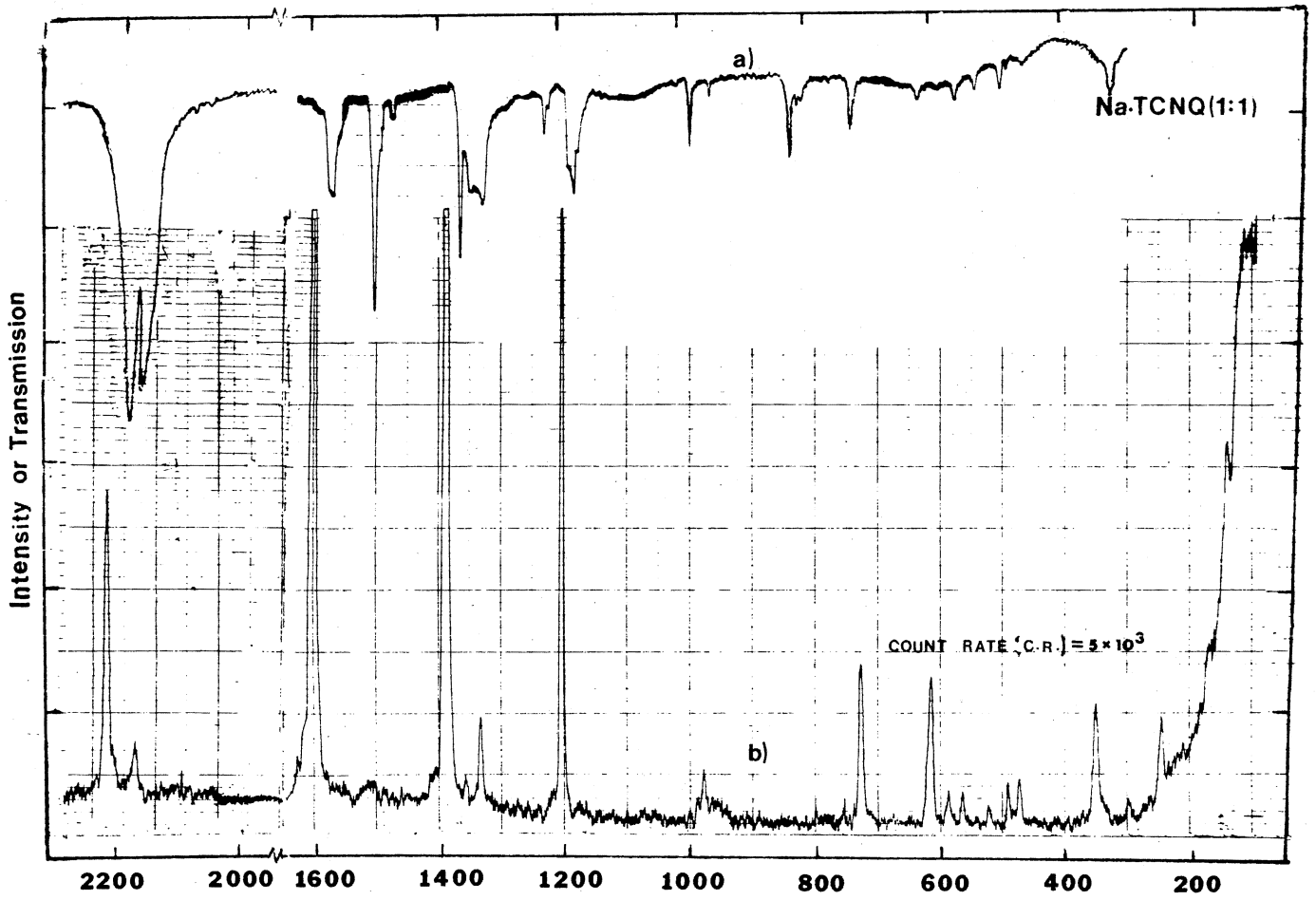

a) IR spectrum
b) Raman spectrum at 5145°A

Figure 4. IR and Raman Vibrational Spectra of NaTCNQ

TABLE IV

OBSERVED VIBRATIONAL FREQUENCIES OF
TCNQ AND ITS ANIONS

$TCNQ^{o+}$		NaTCNQ		Na_2TCNQ		Na_3TCNQ		
IR cm^{-1}	Raman cm^{-1}	IR cm^{-1}	Raman cm^{-1}	IR cm^{-1}	Raman cm^{-1}	IR cm^{-1}	Raman cm^{-1}	Assignment[$]
	97						91	
	105						102	
			117					
	144		143					$\nu_{10}\ a_g$
	169		180					$\nu_{17}\ b_{1g}$
							210	
220								$\nu_{53}\ b_{1u}$
			243				260	
	300		299				306	$\nu_{31}\ b_{2g}$
	334	328*	347		355		381	$\nu_{g}\ a_g$
	428		433	435	435		420	
							450	$\nu_{16}\ b_{1g}$
475		468						$\nu_{51}\ b_{3u}$
		486	482					
		496	494	500	500	483	479	$\nu_{30}\ b_{2g}$
519								
	519		519		526		523	$\nu_{47}\ b_{3g}$
549		521		514				$\nu_{25}\ b_{1u}$
	554	552	558	558			560	

TABLE IV (continued)

$TCNQ^{o+}$		NaTCNQ		Na_2TCNQ		Na_3TCNQ		Assignment[§]
IR cm^{-1}	Raman cm^{-1}	IR cm^{-1}	Raman cm^{-1}	IR cm^{-1}	Raman cm^{-1}	IR cm^{-1}	Raman cm^{-1}	
	593	578	590	578	578	582	580	$^{2g}\ ^{b}_{2g}$
600		608		606		604		$^{24}\ ^{b}_{1u}$
	602	618*	620	623	640	628*	598	
							642	$^{8}\ ^{a}_{g}$
	609							$^{46}\ ^{b}_{3g}$
		655					672	
	711	719					698	
		723*	729	715	745		722	
		725						$^{7}\ ^{a}_{g}$
	752		752					$^{28}\ ^{b}_{2g}$
	816	802	800			780*	780	$^{15}\ ^{b}_{1g}$
859		823*		822*		812*	812	
						819	820	
						822	840	$^{50}\ ^{b}_{3u}$
							848	
	948	967*	967	999	999	983*	989	
		978	974					$^{6}\ ^{a}_{g}$
		987						
962		948						
		954						$^{23}\ ^{b}_{1u}$
998		1008						$^{22}\ ^{b}_{1u}$
	1002		1012					$^{27}\ ^{b}_{2g}$
				1046	1052	1073	1071	
						1090	1088	

TABLE IV (continued)

$TCNQ^{o+}$		$NaTCNQ$		Na_2TCNQ		Na_3TCNQ		Assignment[$]
IR cm^{-1}	Raman cm^{-1}	IR cm^{-1}	Raman cm^{-1}	IR cm^{-1}	Raman cm^{-1}	IR cm^{-1}	Raman cm^{-1}	
1125				1127 1140		1136	1138	$\nu_{37}\ b_{2u}$
1207		1167* 1178 1186 1219	1184 1207	1195	1196	1183*	1186	$\nu_5\ a_g$
1223			1226		1238	1245	1247	$\nu_{36}\ b_{2u}$
	1323		1297		1295			$\nu_{44}\ b_{3g}$
1354		1363						$\nu_{35}\ b_{2u}$
	1451				1546		1599	$\nu_{43}\ b_{3g}$
	1454	1327* 1343*	1326 1339 1368 1396 1409	1303* 1353	1301 1326 1354	1284	1286 1318	$\nu_4\ a_g$
		1475		1435	1436	1408	1410	
1540		1505		1503				$\nu_{34}\ b_{2u}$
1545				1498		1476*	1478	$\nu_{20}\ b_{1u}$
	1602	1578*	1583	1598	1596	1577*	1579	$\nu_3\ a_g$
		1908						
2228		2197		2164		2035		$\nu_{19}\ b_{1u}$ or $\nu_{33}\ b_{2u}$

TABLE IV (continued)

$TCNQ^{o+}$		$NaTCNQ$		Na_2TCNQ		Na_3TCNQ		Assignment[$]
IR cm^{-1}	Raman cm^{-1}	IR cm^{-1}	Raman cm^{-1}	IR cm^{-1}	Raman xm^{-1}	IR cm^{-1}	Raman cm^{-1}	
	2229	2166*	2168 2220	2096	2096 2196	1901*	1943 2126 2163	$\nu_2\ a_g$
3053		3020		3010				$\nu_{32}\ b_{2u}$
3065		3038		3016		2996		$\nu_{18}\ b_{1u}$
							2276	$2 \times \nu_{37}\ b_{2u}$

[$] Symmetry species adopted from Reference 116

* IR bands with orientation out of substrate surface plane

+ From Reference 115 and 116

Other intense and narrow IR bands at 1226, 1363, 1505 and 2197 cm^{-1} can be assigned to the in-plane, non-vibronic b_u modes. It is noteworthy that the IR intensity, of the 1186, 1343 and 1578 cm^{-1} COV bands at room temperature is smaller than those of the nonvibronic planar 1363 or 1563 cm^{-1} bands. The band widths of the COV IR bands (∿10-30 cm^{-1}) are larger than those of nonvibronic bands (∿3-5 cm^{-1}), however, the C≡N stretching IR bands of both types are broader than other bands.

The Raman spectrum of $TCNQ^{\cdot-}$ shows vibrational bands of a_g symmetry modes, nearly coincident with the IR charge oscillation bands, as has previously been noted for the monoanion radical salts of TCNE (110). For example, the 618,(719, 723, 725 cm^{-1}), (967, 978 cm^{-1}), 1578 and 2166 cm^{-1} IR bands are nearly coincident with the 620, 729, (967, 974 cm^{-1}), 1184, (1327, 1339 cm^{-1}), 1583 and 2168 cm^{-1} Raman bands respectively as expected by Anderson and Devlin (89). The Raman bands at 347, 1207, 1396, 1409, 1610 and 2220 cm^{-1}, which are also produced by a_g modes, are separated from their IR counterparts by rather large values. Here it should be noted that these bands also appear for the monomeric $TCNQ^{\cdot-}$ dissolved in less polar solvents (130) and are resonantly enhanced by the laser excitation lines of wavelengths in a range of 550-640 mμ (91) (130) (131).

Nearly coincidental pairs of $TCNQ^{\cdot-}$ vibrational bands such as 484 (IR)/482 (Raman), 496 (IR)/494 (Raman), 578 (IR)/590 (Raman) and 802 (IR)/800 (Raman) cm^{-1} raise an interesting question as to whether these are also charge oscillation bands. All these pairs of bands may be assigned to b_{1g} and b_{2g} symmetry species which contain the out-of-plane rotational modes. Changes in the overlap of wave functions of the neighboring TCNQ monoanion radicals of the dimer (51) (66) (67), due

to the mechanical motion with respect to each other, may possibly activate such vibronic bands in the IR spectrum (103) (107). Vibronic interactions involved, may induce the changes in the dipole moment along the crystal needle axis so that the 484 (b_{2g}), 496 (b_{2g}), 578 (b_{2g}) and 802 (b_{1g}) cm^{-1} IR bands may be considered as COV interaction bands. The possible symmetries of modes responsible for such interaction are indicated in parantheses.

The orientation of $TCNQ^{\cdot-}$ IR bands in single crystals was observed to be different for the COV and nonvibronic modes (66) (89). For NaTCNQ thin films, when the incident light was perpendicular to the surface of the substrate (normal incidence), the planar nonvibronic IR bands, at 1226, 1363, 1505 and 2197 cm^{-1} were more intense than the COV bands at 1186, 1326, 1343 and 1578 cm^{-1}. When the orientation of the incident light with respect to the substrate surface was changed to 45^{o} (45^{o} incidence), the intensities of the COV IR bands with respect to nonvibronic bands were increased (Figure 5). Since the COV IR bands in single crystals were observed to be oriented along the crystal needle axis and nonvibronic bands along the molecular plane (89), the $TCNQ^{\cdot-}$ molecular plane for thin film deposits seems to be preferentially oriented parallel to the substrate surface. In such a case the induced dipole moment for the COV IR bands should be aligned in a perpendicular direction to the substrate surface so that they do not couple with light traveling perpendicularly to the surface.

Vibrational Band Assignments

The convention for the numbering of vibrational modes for TCNQ and its anions has been adopted from Girlando and Pecile (116). When the vibrational mode splits into the factor group components, their

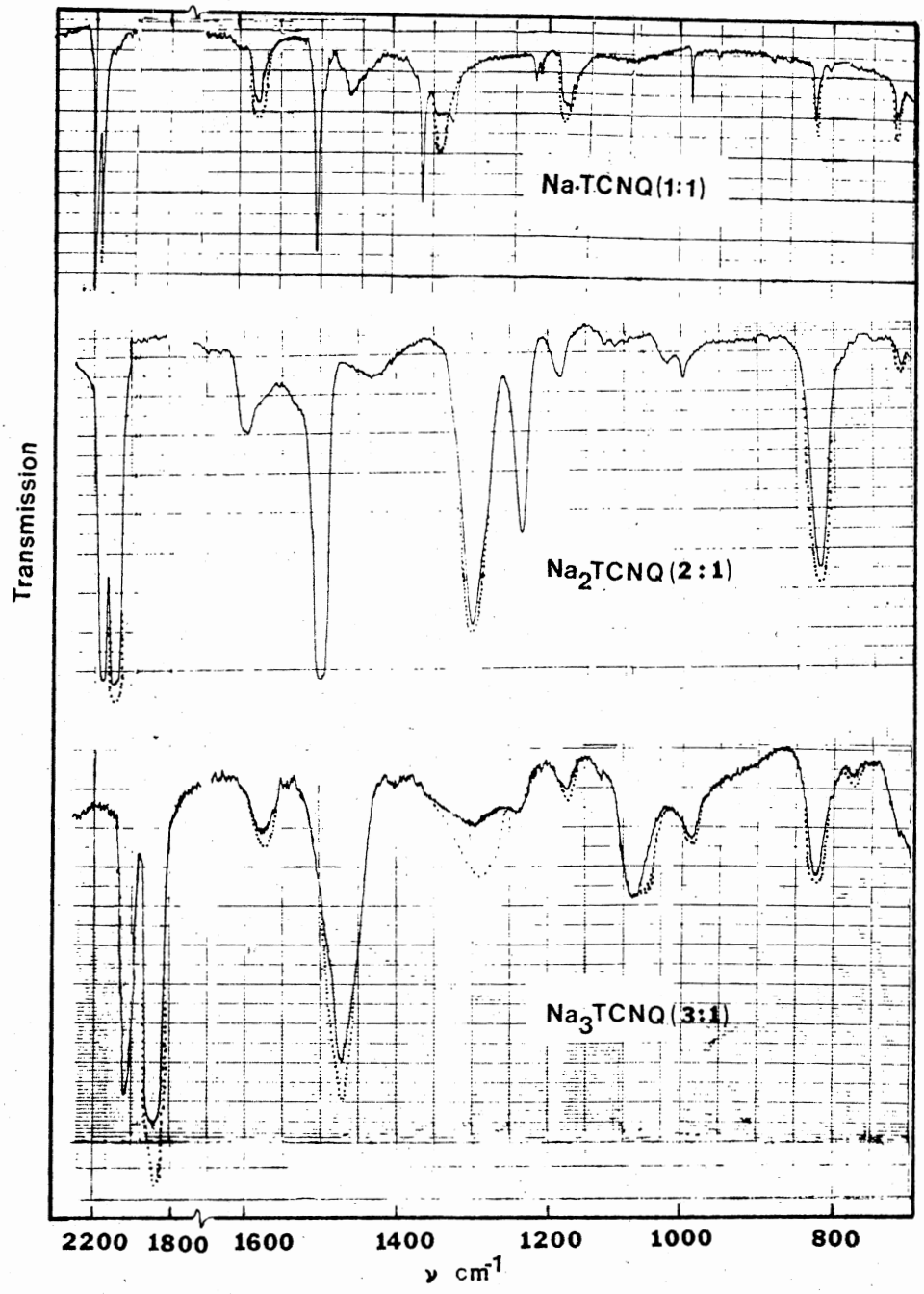

(——— Normal incidence) and (····· Incidence at 45°)

Figure 5. Orientation of the IR Vibrational Bands of the TCNQ Anions

frequency values lie on both sides of the unsplit band frequency. Hence, the average frequency of the factor group components should be a good approximation for the frequency of the unsplit vibrational mode. The frequencies of the $TCNQ^{\cdot-}$ a_g modes are taken as the average of the factor group component band frequencies. Thus, for the ν_2, ν_3, ν_4, ν_5, ν_6, ν_7, and ν_8 a_g modes the tabulated frequencies for the force constant calculations are the average of 3, 3, 7, 6, 5, 4 and 2 factor group components, respectively. Some of the vibrational bands, e.g., the 987 and 1167 cm^{-1} IR bands, which are listed as factor group components of a_g bands may alternatively be assigned to the nonvibronic planar b_u symmetry modes. However, because of the lack of any certain polarization evidence there is no basis for choosing either vibrational band assignment. Inclusion of these bands as a_g factor group components is only on a contingency basis. Similarly, the 1008 cm^{-1} IR band can alternatively be assigned to COV activated modes of out-of-plane rotational character of b_{2g} symmetry. The 967, 1178 cm^{-1} IR bands and the 965, 1012, 1297 and 1327 cm^{-1} Raman bands of a_g symmetry are very close to the vibrational bands observed for α,α-$DCTC^{-}$ (19) (76). Even with maximum possible precautions taken to prevent NaTCNQ reaction with oxygen, these bands appeared in the vibrational spectra. Hence they are assigned to the vibrational modes of $TCNQ^{\cdot-}$. For b_{1g} and b_{2g} symmetry modes of $TCNQ^{\cdot-}$ which were mentioned earlier as being involved in COV interaction, the average frequency for the 482, 484, 494 and 496 cm^{-1} components is 489 cm^{-1} which is assigned to the ν_{30} mode of b_{2g} symmetry. However, for the 496 cm^{-1} IR band and the 494 cm^{-1} Raman band, alternate assignments to $b_{2u}(\nu_{38})$ and b_{3g} (ν_{47}) are equally feasible. Average frequencies for other

nontotally symmetric modes involved in COV interaction are 584 cm^{-1} (ν_{29} b_{2g}) and 801 cm^{-1} (ν_{15} b_{1g}).

Vibrational assignments for the planar nonvibronic bands are more straighforward although, for some of the nonvibronic IR bands, there is ambiquity as to whether they belong to b_{1u} or b_{2u} mode, e.g., the 1505 cm^{-1} band can be assigned as either a $b_{1u}(\nu_{20})$ or b_{2u} (ν_{34}) mode. The 2197 cm^{-1} band also can be assigned to either a b_{1u} (ν_{19}) or b_{2u} (ν_{33}) mode. Similarly, assignment of the 1363 cm^{-1} band is ambiguious (ν_{21} b_{1u} and ν_{35} b_{2u}). In force constant calculations these bands were assigned to one of the possible modes.

There are still some additional vibrational bands which remain unassigned. In particular, the 552, 655, 1475 and 1908 cm^{-1} IR bands and the 243 and 554 cm^{-1} Raman bands could not be provided with any reasonable assignments. Since all these vibrational bands except the 243 cm^{-1} Raman and the 1475 cm^{-1} IR bands are very weak, they are considered to be combination, overtone or impurity bands.

Na_2TCNQ: Dianion Salt

Electronic Spectrum

Suchanski and VanDuyne (76) reported the electronic spectrum of electrochemically prepared dianionic TCNQ, in acetonitrile solution, in an oxygen free atmosphere. The electronic absorption bands at 330 (3.75 eV), 240 (5.16 eV) and 210 mμ (5.90 eV) were observed. An earlier electronic absorption spectrum reported for $TCNQ^{-2}$ prepared by a similar method turned out to be dominated by α,α-$DCTC^{-}$ due to interaction with oxygen (36). For the colorless Na_2TCNQ crystalline thin films an electronic spectrum similar to that of Suchanski and

VanDuyne was observed. Though the intensity pattern of the 295 (4.20 eV) 240 (5.16 eV) and 205 mμ (6.26 eV) is the same as for the solution spectrum, the position of one electronic band, at 330 mμ shifted to 295 mμ in the solid state (Figure 6) as compared with solution state. The blue shift from 330 to 295 mμ may be attributed to either the transition from a solution to solid state or change of cation. The observed values of energy states are in fair agreement with the calculated values (58) (77). Comparison between the experimental and calculated energies of electronic transitions for the anions of TCNQ and assignments are shown in Table V. The 295, 240 and 205 mμ electronic bands are assigned to transitions between the $^1A_g^{(1)}$ ground state and the $^1B_{2u}$, $^1B_{3u}$ and $^1A_g^{(2)}$ excited states, respectively (77). No charge transfer electronic transition in the visible or IR region for Na_2TCNQ was observed.

Vibrational Spectra: IR and Raman

The C≡N stretching vibrational frequencies of TCNQ dianion complexed with transition metals have been variously quoted as 2102, 2151 cm^{-1}, (80), 2100, 2205 cm^{-1} (81) and 2090, 2190 cm^{-1} (81). All these transition metal complexes were studied in an open atmosphere. In view of the reactive nature of $TCNQ^{-2}$ towards oxygen and water vapor (76), it is essential to reexamine the dianion vibrational spectra in an oxygen free atmosphere.

IR and Raman spectra of Na_2TCNQ prepared in vacuum are shown in Figure 7. In general all the dianion IR bands are broader (band width ∿10-40 cm^{-1}) than the monoanion bands. The planar 954 and 1363 cm^{-1} IR bands apparently disappeared with the addition of one more

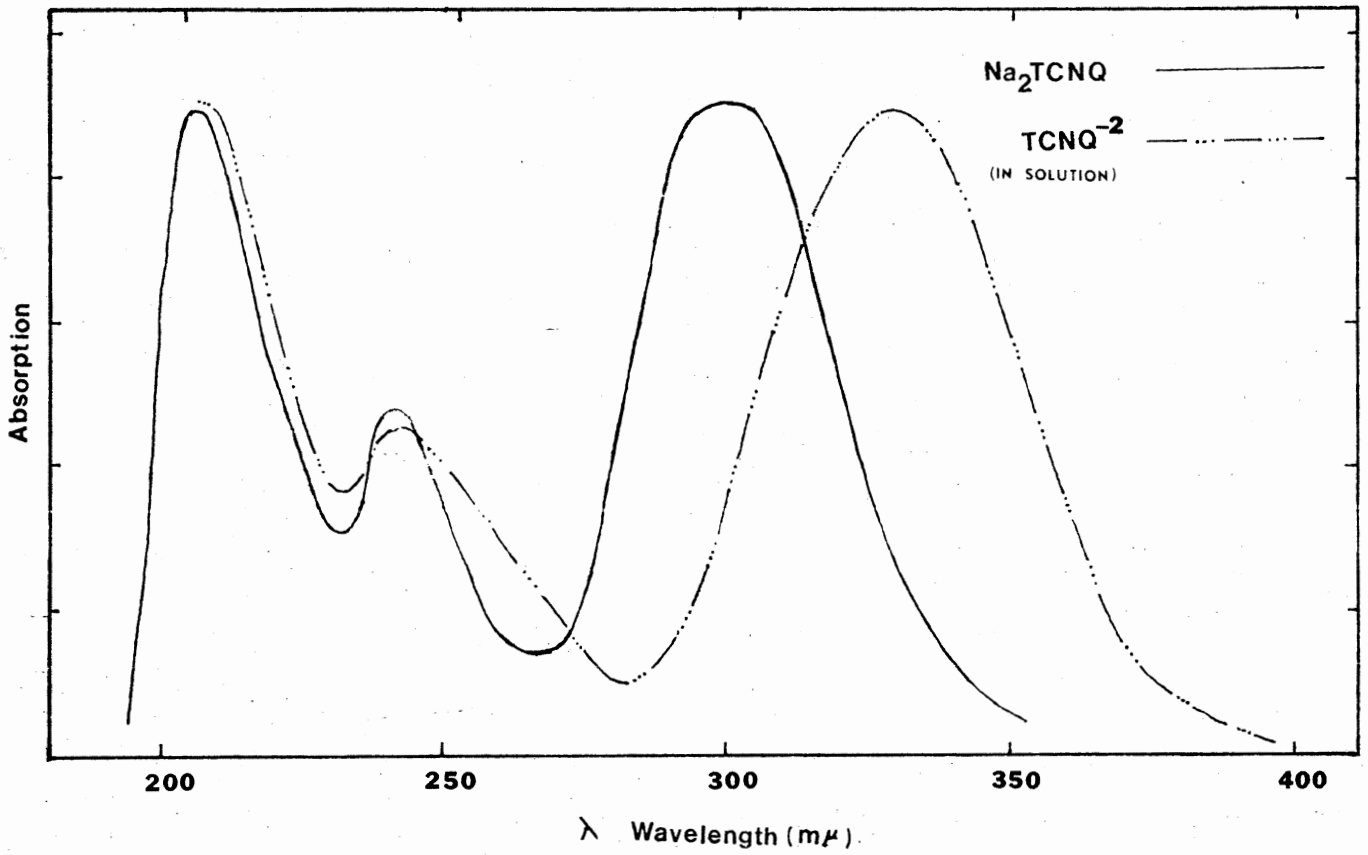

Figure 6. Electronic Spectra of Na_2TCNQ in the Solid State (———) and $TCNQ^{-2}$ in Solution (76) (—·—)

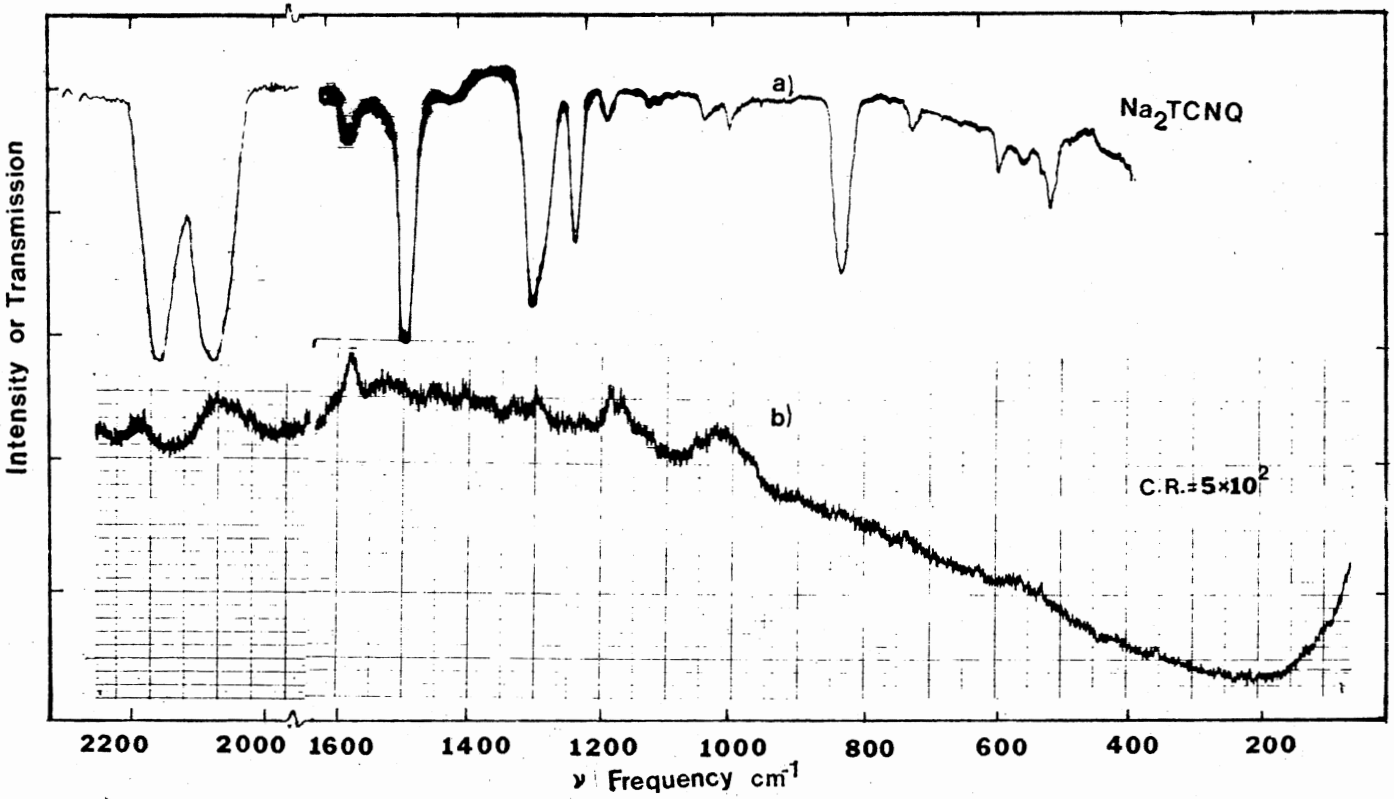

a) IR spectrum
b) Raman spectrum at 4880°A

Figure 7. IR and Raman Vibrational Spectra of Na_2TCNQ

TABLE V

THE OBSERVED AND CALCULATED ELECTRONIC BANDS OF TCNQ, ITS SODIUM SALTS AND THE OXYGEN REACTION PRODUCTS

Compound	Observed		Calculated		Polarization[f]	Assignment[b]
	Solid State eV	Solution eV	eV[a,b]	eV[c]		
$TCNQ^o$	3.15[a]	3.10[d]	2.83	2.994	z	$^1B_{2u} \leftarrow {}^1A_g$
	5.44		5.63		y	$^1B_{1u} \leftarrow {}^1A_g$
		1.48[a]	1.21	1.57	z	$^2B_{3u}(1) \leftarrow {}^2B_{2g}$
NaTCNQ or $TCNQ^-$		1.63[a] 1.67[a]				
	2.01	2.91[a]	2.91	2.92	z	$^2A_u(2) \leftarrow {}^2B_{2g}$
	3.40	3.15[a]	2.99	3.34	y	$^2B_{3u}(2) \leftarrow {}^2B_g$
	4.07	4.43[a]	3.44	3.80		$^2A_u(3) \leftarrow {}^2B_{2g}$
	4.77	4.74[a]	4.24	4.71	z	$^2B_{3u}(3) \leftarrow {}^2B_{2g}$
		5.33[a]	5.21	5.15	z	$^2B_{3g} \leftarrow {}^2B_{2g}$
	4.20	3.75[e]	4.14	3.466	z	$^1B_{2u} \leftarrow {}^1A_g(1)$
Na_2TCNQ or $TCNQ^{-2}$	5.16	5.16[e]	4.67	3.819	y	$^1B_{3u} \leftarrow {}^1A_g(1)$
	6.05	5.90[e]	8.15	4.464	y	$^1A_g(2) \leftarrow {}^1A_g(1)$
Na_3TCNQ	2.9 3.35 4.0 4.68 5.56 6.36					
Na^+ - α,α-DCTC$^-$	1.48 1.63 2.64 2.95 3.70 4.60 5.64 6.625					

TABLE V (continued)

Compound	Observed		Calculated		Polarization[f]	Assignment[b]
	Solid State eV	Solution eV	eV[a,b]	eV[c]		
$Na_3TCNQ.O_2$	3.52 4.246 5.04					

[a] Reference 27 and 47

[b] Reference 77

[c] Reference 58

[d] Reference 58

[e] Reference 76

[f] Axis as shown in Figure 1

electron to $TCNQ^{\cdot-}$. Even for fairly thick films (6-7 μ), these bands could not be detected. The out-of-plane, 822 cm^{-1} (b_{3u}) and the in-plane 1503 cm^{-1} (b_{1u} or b_{2u}) dianion bands do not show any significant shift with respect to the corresponding $TCNQ^{\cdot-}$ bands. Only their band widths are increased. Some of the dianion IR bands corresponding to the COV bands of $TCNQ^{\cdot-}$ shift to a higher frequency, e.g., the 978, 1186 and 1578 cm^{-1} bands shift to 999, 1195 and 1598 cm^{-1}, respectively in the dianion. Other COV IR bands of the monoanion undergo bathochromic shifts, e.g., the 723, 1343 and 2166 cm^{-1} bands shifted to 715, 1303 and 2096 cm^{-1}, respectively with the addition of a second electron. The relative intensity of the dianion IR bands corresponding to the $TCNQ^{\cdot-}$ COV bands appear to be decreased except for the 1303 and 2096 cm^{-1} bands. The relative intensity of the 1238 cm^{-1} dianion band seems to be higher than the corresponding 1226 cm^{-1} (b_{2u}) monoanion band. The changes in intensities of the IR bands described above are qualitative.

As electrons are added to TCNQ, the C≡N stretching frequencies shift to lower frequencies. When the first electron is added to the neutral TCNQ, the 2223 cm^{-1} (b_{1u}) and the 2229 cm^{-1} (a_g) bands shifted to 2197 and the 2166 cm^{-1}, thus showing shifts of 26 and 63 cm^{-1}, respectively. The same C≡N stretching bands, with the addition of a second electron increased their bathochromic shifts to 33 and 70 cm^{-1} for the b_{1u} and a_g modes, respectively. The C≡N stretching frequencies of the dianion bands are 2164 cm^{-1} (b_{1u}) and 2096 cm^{-1} (a_g).

The change in orientation of the $TCNQ^{-2}$ thin film with respect to the IR source light does not show very significant changes in intensities of the vibrational bands (Figure 5). Since the crystal

structure and the orientation of the dianion in thin films are not known, any conclusion from an orientation study is a matter of speculation.

The Raman spectra of Na_2TCNQ with the 4880°A and 5145°A laser excitation lines are of nonresonant type. The Na_2TCNQ Raman spectrum shown in Figure 7 was observed with the 4880°A laser excitation line. Since the TCNQ dianion does not have any electronic absorption band in the vicinity of the laser excitation lines used, intensity enhancement of the dianion vibrational bands due to the RR effect is not expected. The nonresonant Raman bands at 640, 745, 999, 1052, 1196, 1303, 1326, 1545, 1594, 2096 and 2196 cm^{-1} were observed in the dianion spectrum. Other very weak Raman bands are indicated in Table IV. It is noteworthy that Na_2TCNQ does not show Raman bands corresponding to the strong 1207, 1396 and 1610 cm^{-1} bands of $TCNQ^{\cdot-}$.

Another interesting featuer of the Na_2TCNQ vibrational spectra is that the factor group splitting between the IR and Raman bands corresponding to the $TCNQ^{\cdot-}$ COV bands is reduced. The dianion IR band frequencies at 500, 578, 999, 1195, 1303, 1598 and 2096 cm^{-1} differ very little from the corresponding Raman bands at 500, 578, 999, 1196, 1301, 1594 and 2096 cm^{-1}, respectively. IR and Raman bands of $TCNQ^{-2}$ at 623 and 620 cm^{-1} (ν_8 a_g) and 715 and 745 cm^{-1} (ν_7 a_g) show larger band separation than the corresponding monoanion bands.

In Na_2TCNQ no visible evidence for extensive charge interaction in the sense described by Mulliken's CT complex theory (7) was found. Neither color, nor low energy electronic absorption bands were observed for the dianion salt of TCNQ. In spite of no evidence for charge transfer vibronic interaction, the dianion infrared bands

corresponding to the monoanionic COV bands do not disappear completely, though apparently their intensity is reduced. Thus, the appearance of the 622, 715, 999, 1195, 1303, 1598 and 2096 cm^{-1} IR bands in the Na_2TCNQ spectrum suggest some vibronic interaction, though probably less extensive than in the monoanion salts. Cases of the coincident vibrational bands at 500 and 578 cm^{-1} in IR and Raman spectra are particularly interesting. Thought the extent of COV interactions due to oscillations in electron affinity of $TCNQ^{-2}$ with the stretching vibrational frequency might have been reduced, the vibronic interaction (107) through the change overlap of molecular orbitals of the neighboring molecules should not be completely ruled out. The 500 cm^{-1} IR and Raman bands of $TCNQ^{-2}$ may correspond to the COV bands of the monoanion at 484 cm^{-1} (IR), 482 cm^{-1} (Raman), 496 cm^{-1} (IR) and 494 cm^{-1} (Raman) of b_{2g} symmetry mode. Similarly, IR and Raman bands of 578 cm^{-1} of $TCNQ^{-2}$ may correspond to the 578 cm^{-1} (IR) and 590 cm^{-1} (Raman) $TCNQ^{\cdot-}$ bands.

Vibrational Band Assignments

Though the crystallographic and molecular structure for Na_2TCNQ is not known, there is some independent evidence from MO calculations (58) (77) (78) to indicate that no extensive deviation from D_{2h} symmetry occurs when two electrons are added to the neutral TCNQ. The vibrational band assignments of the dianion are thus based on the presumption of D_{2h} molecular symmetry. These assignments are made purely through analogy and nearness to the corresponding vibrational bands of the monoanion. In case of D_{2h} symmetry, the coincidence of IR and Raman vibrational bands at 500, 578, 999, 1195, 1303, 1598 and 2096 cm^{-1} should be attributed to some form of vibronic interaction.

In the absence of such interaction it is difficult to explain violation of the mutual exclusion principle. Thus, the 623, 715, 999, 1195, 1303, 1598 and 2096 cm^{-1} IR bands are assigned to the a_g symmetry modes. These bands are close to the corresponding 618, 723, 978, 1186, 1343, 1578 and 2166 cm^{-1} $TCNQ^{\cdot-}$ COV IR bands of a_g symmetry. The dianion Raman bands at 352, 640, 745, 999, 1196, 1301, 1594, 2096 and 2196 cm^{-1} are also assigned to the a_g symmetry for similar reasons. The frequency of a molecular mode, which is assigned to more than one vibrational band, is calculated from the average of the individual (factor group) band frequencies.

In this scheme some of the vibrational bands pose certain questions. For example, do the 1127 and 1140 cm^{-1} IR bands result from factor group components of the ν_5 (a_g) mode or are they produced by the ν_{37} (b_{2u}) mode? Are the 1046, 1353 and 1435 cm^{-1} IR bands and their Raman counterparts, factor group components of one of the a_g modes or is their near coincidence merely accidental? Answers to these and other questions depend on the availability of information about the molecular structure, orientation of the vibrational bands, and vibronic interaction.

The vibrational bands which have not been considered so far, like the 822, 1238, 1498, 1503, 2164, 3010 and 3014 cm^{-1} IR bands and the 1295 and 1546 cm^{-1} Raman bands were assigned to the vibrational modes of $TCNQ^{-2}$ by using the corresponding monoanion bands as a reference. These non vibronic bands were assigned to the b_u and b_g modes as shown in Table IV. Also a possibility that the 352, 1295, 1326 and 1353 cm^{-1} bands from α,α-$DCTC^{-}$ due to reaction with oxygen present in the vacuum cell at high vacuum ($\sim 10^{-5}$ torr) or through some minor leaks, should also be considered.

An alternate explanation for the near coincidence of the IR and Raman bands of the dianion may be that the molecular symmetry is changed to a noncentrosymetric molecule. This possibility will be further discussed in a later part of this study.

Na_3TCNQ: Trianion Salt

This is a new trianion salt of TCNQ prepared for the first time during this investigation. Possibility of formation of triply charged anion salts of cyanocarbon electron acceptor has been indicated by Moore et al. (75). As discussed earlier, results for $perlyne_3TCNQ$ complex (83) will also be examined against the spectroscopic data obtained in this study. Because of the reactive nature of metal rich TCNQ and TCNE salts (75) (76), all possible precautions were taken to avoid reaction with oxygen and water vapor as described in the experimental part. Also the reaction of Na_3TCNQ with oxygen was studied to compare the spectrum of the pure salt with that of the reaction products.

Electronic Spectrum

Since the best of the Na_3TCNQ samples were about 90% pure with some contamination by Na_2TCNQ, due allowance is made in the interpretation of the spectroscopic results. Only those electronic bands not previously observed for the dianion salt were assigned to Na_3TCNQ. The golden yellow colored trianion salt exhibits six absorption bands at 427 (2.9 eV), 370 (3.35 eV), 310 (4.0 eV), 265 (4.68 eV), 223 (5.56 eV) and 195 mμ (6.36 eV) in the electronic spectrum (Figure 9). The 427 mμ electronic absorption band is of particular interest in the

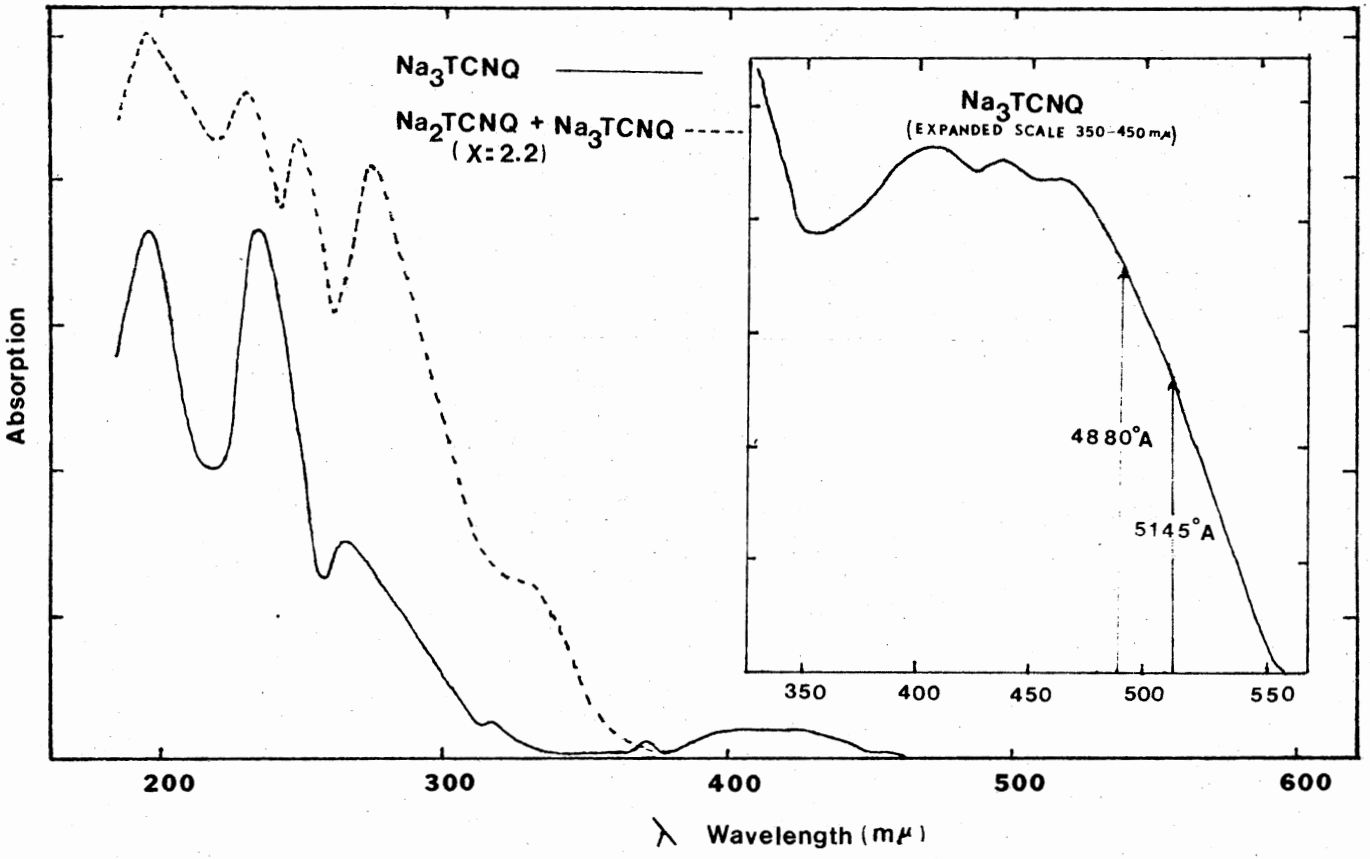

Figure 8. Electronic Spectrum of Na_3TCNQ (———) and a (1:4) Mixture of Na_3TCNQ and Na_2TCNQ (-----)

study of the RR spectra of Na_3TCNQ and the nonstoichiometric salts in the composition range $2.0 \leq x \leq 3.0$. The laser excitation lines at $4880^{o}A$ and $5145^{o}A$ are in the low energy tail of this electronic band (Figure 8, inset part). Thus, resonant intensity enhancement of Na_3TCNQ Raman vibrational bands is expected. The intensity pattern of the uv electronic bands, as in other salts, may have been affected to some extent by light scattering from the alkali halide substrate and outer windows. Since no MO calculation has been done, the assignments for the electronic bands is not shown in Table V.

The $perylene_3(TCNQ)$ salt shows electronic absorption bands at about 401, 438, 465, 475 and 930 mμ (83). The 401, 438, and 465 mμ electronic bands are similar to those observed for perylene in nonpolar solvents (150), indicating the presence of free perylene in the sample. The remaining two electronic bands at 475 and 930 mμ may have originated from α,α-$DCTC^-$ (76) as well as the 1:1 perylene-TCNQ complex. The electronic spectrum of α,α-$DCTC^-$, produced when the dianion reacts with oxygen, shows some presence of monoanion salt (Table V). The 475 mμ electronic band seems suspiciously close to the 470 mμ α,α-$DCTC^-$ band in the solid state (Table V) and 477 mμ in solution (76). When the electronic spectrum of $perylene_3(TCNQ)$ is compared with that of Na_3TCNQ, it is observed that none of the reported bands match in appearance or frequency. Only the 438 mμ electronic band of $perylene_3TCNQ$ is close to 427 mμ band of Na_3TCNQ. However, as mentioned above this band may have originated from free perylene. Thus, from the electronic spectrum of $perylene_3TCNQ$, it appears that free perylene, 1:1 perylene-TCNQ, and an oxygen reaction product may be present in the complex.

Vibrational Spectra: IR and Raman

The vibrational spectrum of perylene$_3$TCNQ again apparently shows the presence of free perylene, 1:1 perylene-TCNQ and α,α-DCTC$^-$. The vibrational IR bands at 833, 1350, 1537 and 1567 cm^{-1} which were exclusively attributed to the 3:1 complex (83) can also be assigned to α,α-DCTC$^-$ or TCNQ neutral. The C≡N stretching IR vibrational band for the 3:1 perylene$_3$TCNQ complex was observed nearly at the same position as for the neutral TCNQ or 1:1 perylene-TCNQ. Besides both the 1:1 and 3:1 perylene-TCNQ complexes show the 835 and 1638 cm^{-1} bands which have been assigned to the C-H bending vibration of α,α-DCTC$^-$ (19).

The vibrational IR and Raman spectra of Na_3TCNQ are shown in Figure 9. The C≡N stretching frequencies of $TCNQ^{-3}$ in the IR spectrum are observed at 1901 and 2035 cm^{-1}. Other IR bands appear at 483, 582, 604, 628, 780, 822, 983, 1073, 1090, 1183, 1245, 1284, 1476, 1577 and 2994 cm^{-1} (Table IV). None of these except the 822 cm^{-1} band (out-of-plane b_{3u} mode), are at the same frequency as those for Na_2TCNQ. Even the 1505 (b_{1u} or b_{2u}) cm^{-1} IR band, which was at same frequency for the mono- and dianions, shifted to 1476 cm^{-1} in the trianion salt. Some IR bands, involved in COV interaction in $TCNQ^{\cdot-}$, show consistant blue shifts when one or two electrons are added to $TCNQ^{o}$ but reverse this trend of blue shifts as a third electron is added. For example, the 948 cm^{-1} band of $TCNQ^{o}$ shifts to 978 cm^{-1} in the monoanion, 999 cm^{-1} in the dianion and 983 cm^{-1} in the trianion Similarly, the 1207 and 1602 cm^{-1} bands of neutral TCNQ shift to 1186 and 1578 cm^{-1} in the monoanion, 1195 and 1598 cm^{-1} in the dianion and 1183 and 1579 cm^{-1} in the trianion. Still other IR bands of a_g

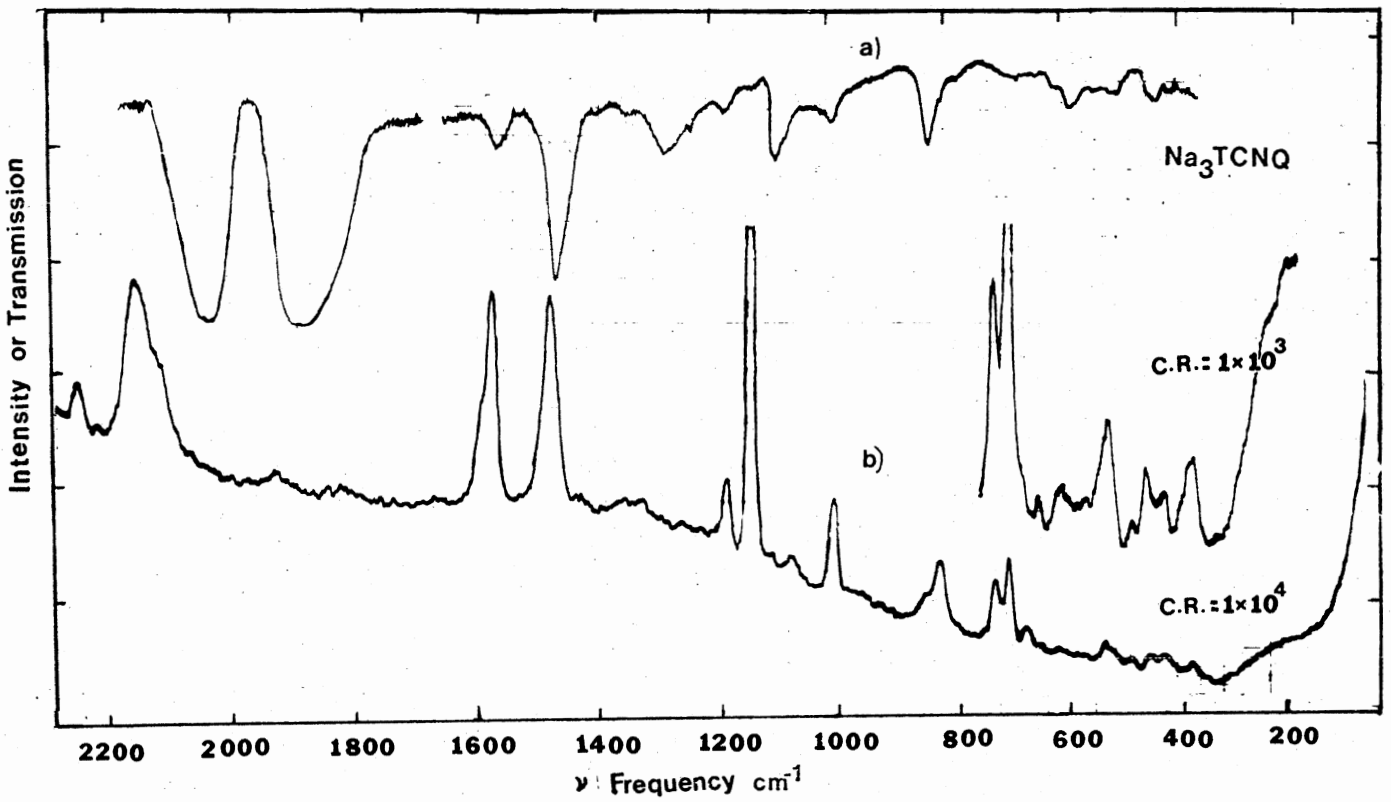

a) IR spectrum
b) Raman spectrum at 5145°A

Figure 9. IR and Raman Vibrational Spectra of Na_3TCNQ

symmetry show shifts to low frequency with addition of each electron, e.g., the 1454 and 2229 cm^{-1} bands of $TCNQ^{o}$ shift to 1343 and 2166 cm^{-1} with the addition of first electron, 1303 and 2096 cm^{-1} for the second electron and 1284 and 1901 cm^{-1} for the third electron respectively. For the C≡N stretching frequencies, the red shift per electron increases tremendously with the addition of a third electron as compared with the first and second electron. Thus, C≡N IR bands, as mentioned earlier, shift by 27 and 63 cm^{-1} for the first electron addition, 33 and 70 cm^{-1} for the second electron and 127 (b_{1u} or b_{2u}) and 195 (a_g) cm^{-1} for the third electron respectively. The intensities of COV IR bands of $TCNQ^{\bar{\cdot}}$ did not show very significant reduction as compared with the dianion bands when the third electron is added except for the 1284 and 1901 cm^{-1} bands. The relative intensity of the 1284 cm^{-1} band appears to be reduced as compared with the 1303 cm^{-1} band while for the 1901 cm^{-1} trianion band, the intensity seems to be increased as compared with the 2096 cm^{-1} band of the dianion. The 2035 and 2164 cm^{-1} IR bands of the tri- and dianion are used to compare the relative intensity changes when a third electronis added to TCNQ.

The trend of broadening of the IR bands with the addition of each electron also continued for the trianion. The IR bands of $TCNQ^{-3}$ are considerably broadened (band width 20-100 cm^{-1}). When the orientation of the thin film with respect to IR source light was changed from the normal incidence to the 45^{o} incidence, the intensity of the 780, 819, 983, 1073, 1090, 1136, 1183, 1284, 1476, 1577, and 1901 cm^{-1} bands was increased (Figure 5). The intensities of 1245 and 2035 cm^{-1} IR bands did not change significantly with the change of orientation. The conclusion can be drawn that the polarization of the

1245 and 2035 cm^{-1} absorptions may be different than the rest of the IR bands mentioned above.

The Raman vibrational bands of $TCNQ^{-3}$, as expected, are resonantly enhanced when the 4880°A and 5145°A laser excitation lines are used. The intensity pattern of the RR spectrum is entirely different than those observed for the neutral, nono- or dianion (Figure 9). Strong Raman lines appear at 1138 and 1478 cm^{-1} for which no corresponding bands were observed in the mono- or dianion. Again, as in case of the mono-and dianion, several nearly coincident $TCNQ^{-3}$ Raman lines at 479, 580, 983, 1071, 1088, 1138, 1186, 1247, 1286, 1478, 1579 and 1943 cm^{-1} with the IR bands corresponding to the COV interaction bands of the monoanion were observed. Interesting Raman bands at 820, 840 and 848 cm^{-1} can be attributed to the b_{3u} out-of-plane mode of $TCNQ^{-3}$. Similarly, the 1138 and 1478 cm^{-1} Raman bands seem to go with the 1136 and 1476 cm^{-1} IR modes respectively of b_{2u} symmetry. Such activation of b_u modes in the Raman spectra were not observed in the cases of the neutral, mono- or dianion.

The 483 and 582 cm^{-1} IR bands, corresponding to the 479 and 580 cm^{-1} Raman bands, can be assigned to the b_{2g} symmetry modes with out-of-plane rotational character. Several other vibrational bands of low frequency were observed in the RR spectrum of $TCNQ^{-3}$ (Figure 9).

Vibrational Band Assignments

As in the case of Na_2TCNQ, for the trianion also, D_{2h} molecular symmetry is presumed for the vibrational band assignments. With this presumption and based on an analogy with the mono- and dianion vibrational band assignments, the vibrational modes tentatively associated with the vibrational bands of $TCNQ^{-3}$ are shown in Table IV. Thus

the 628, 983, 1183, 1284, 1577 and 1901 cm^{-1} IR bands are assigned to a_g symmetry modes of $TCNQ^{-3}$. Similarly the 381, 968, 722, 989, 1186, 1286, 1318, 1579, 1943, 2126 and 2163 cm^{-1} Raman lines are assigned to the factor group components of a_g modes of $TCNQ^{-3}$. In these assignments the implied presumption is that a vibronic interaction, similar to the COV interaction in the monoanion salt makes an important contribution to the vibrational spectra. In addition to these assignments, the 812, 819, 822, 1136, 1245 and 1476 cm^{-1} IR bands and the corresponding 820, 840, 848, 1138, 1247 and 1478 cm^{-1} Raman bands are assigned to b_u modes purely by analogy to the mono- and dianion assignments. These assignments however, raise questions about the mechanism by which b_u modes of D_{2h} symmetry become Raman active in violation of the mutual exclusion principle. The Raman bands at 820, 1138 and 1478 cm^{-1} are very strong bands. In fact, the 1138 cm^{-1} band is the strongest in the Raman spectrum of $TCNQ^{-3}$. The only $TCNQ^{o}$ band in this region is at 1125 cm^{-1} (ν_{32} b_{2u} mode) (116). Also, the vibrational band assignments to ν_{29} and ν_{30}, b_{2g} and ν_{15} modes which have out-of-plane rotational character, presume charge oscillation type vibronic interactions in $TCNQ^{-3}$.

Several Raman bands of $TCNQ^{-3}$ in the 200-700 cm^{-1} frequency range are activated in the spectrum (Figure 9). Such bands may have originated from the structural distortions in the trianion. When three sodium cations are attached to the TCNQ molecule such a possibility should be considered.

The questions about alternate vibrational assignments, possible change in molecular symmetry and vibronic interactions will be discussed in Chapter V.

Based on a D_{2h} symmetry for the mono-, di- and trianions, a normal coordinate analysis was done. Instead of correlating shifts in vibrational band frequencies of TCNQ with anionic charge, it may be more informative to correlate the force constants with the number of electrons added to the electron acceptor. The π-bond orders of TCNQ and its anions calculated from MO calculations can also be correlated with the force constants obtained from the normal coordinate analyses.

Force Constant Calculations for TCNQ and Its Anions

For the normal coordinate analysis of TCNQ and its anions a modified valence force field similar to one of Girlando and Pecile (116) is used as outlined in Chapter II. For the neutral TCNQ, the MVFF is somewhat modified though the same vibrational band assignments as published (116) were used. For the anions of TCNQ only the stretching force constants were readjusted to reproduce the observed frequencies. Results of force constant calculations will be presented in this section.

The observed and calculated frequencies and force constants for the neutral TCNQ are given in Table VI. The numbering of the modes is that of Girlando and Pecile (116). The stretching force constants are in units of mdyne/^{o}A and bending force constants in mdyne ^{o}A/(radian)^{2}. The interaction stretching-bending force constants are given in mdyne/radian units. The fifth column in Table VII gives contribution of the force constants, defined in the columns one and two Table VI , to the energy of a particular mode. Only force

TABLE VI

CALCULATED FORCE CONSTANTS OF THE NEUTRAL, MONO-, DI- AND TRIANIONS OF TCNQ

Force Constants[a]					
Def.[b]	Bond[c]	$TCNQ^{o}$	$TCNQ^{\cdot-}$	$TCNQ^{-2}$	$TCNQ^{-3}$
K_1	C-H	5.05	4.983	4.92	4.85
K_2	$C-C^{R}$	5.46	5.83	5.98	6.309
K_3	$C=C^{R}$	7.50	7.06	6.92	6.447
K_4	$C=C^{W}$	6.90	5.82	5.41	5.225
K_5	$C-C^{W}$	5.35	5.68	5.92	6.045
K_6	C≡N	16.90	16.18	15.48	13.42
H_7	$C-C=C^{R}$	0.996			
H_8	(C-C-H) = (C=C-H)	0.335			
H_9	$C-C-C^{R}$	1.034			
H_{10}	$C-C=C^{R,W}$	0.564			
H_{11}	$C-C-C^{W}$	0.866			
H_{12}	$C-C=C^{W}$	0.924			
H_{13}	C-C≡N	0.758			
$F_{2,2}$	$C-C^{R}, C-C^{R}$	0.157			
$F_{2,3}$	$C-C^{R}, C=C^{R}$	0.608			

TABLE VI (continued)

Force Constants[a]					
Def.[b]	Bond[c]	$TCNQ^{o}$	$TCNQ^{-}$	$TCNQ^{-2}$	$TCNQ^{-3}$
$F_{2,4}$	$C\text{-}C^{R}, C{=}C^{W}$	1.29			
$F_{2,7}{=}F_{2,9}$	$C\text{-}C^{R}, C\text{-}C{=}C^{R}{=}C\text{-}C^{R}, C\text{-}C\text{-}C^{R}$	0.098			
$2F_{2,10}$	$C\text{-}C^{R}, (C\text{-}C{=}C^{R,W}C\text{-}C{=}C^{(R,W)'})$[d]	0.647			
$2F_{2,8}$	$C\text{-}C^{R}, (C\text{-}C\text{-}H - C{=}C\text{-}H)$	0.126			
$F_{3,7}$	$C{=}C^{R}, C\text{-}C{=}C^{R}$	0.090			
$2F_{3,8}$	$C{=}C^{R}, (C{=}C\text{-}H - C\text{-}C\text{-}H)$	0.317			
$F_{4,5}$	$C{=}C^{W}, C\text{-}C^{W}$	0.161			
$F_{4,11}{=}F_{4,12}$	$C{=}C^{W}, C\text{-}C{=}C^{R,W} = C{=}C^{W}, C\text{-}C{=}C^{W}$	0.242			
$F_{5,5}$	$C\text{-}C^{W}, C\text{-}C^{W}$	0.517			
$F_{5,12}$	$C\text{-}C^{W}, C\text{-}C{=}C^{W}$	0.197			
$F_{7,7}{=}F_{9,7}$	$C\text{-}C{=}C^{R}, C\text{-}C{=}C^{R} = C\text{-}C\text{-}C^{R}, C\text{-}C{=}C^{R}$	-0.045			

a: units: K in mdyne/^{o}A; H in mdyne-^{o}A/(radian)^{2}
F in mdyne/radian for stretching bending

b : K, H and F are the stretching, bending, stretching-bending and stretching-stretching interaction force constants.

c : R = ring, W = wing, R,W = ring and wing

d : (R.W) indicates ring and wing bending opposite to the $C\text{-}C^{R}$ stretching

TABLE VII

THE OBSERVED AND CALCULATED IN-PLANE VIBRATIONAL FREQUENCIES OF NEUTRAL TCNQ MOLECULE

Symmetry and Modes[a]		Frequency (cm^{-1}) Observed[a]	Calculated	Potential Energy Distribution (%)[b]
a_g	ν_1	3048.0	2051.9	$K_1(99)$
	ν_2	2229.0	2229.5	$K_6(87),K_5(11)$
	ν_3	1602.0	1614.2	$K_2(19,K_3(60),H_8(15)$
	ν_4	1454.0	1457.5	$K_4(79),K_5(13)$
	ν_5	1207.0	1208.3	$K_3(13),H_8(47),H_{13}(27)$
	ν_6	948.0	944.0	$K_2(44),K_5(16)$
	ν_7	715.0	703.6	$K_2(44),K_5(17),H_9(14)$
	ν_8	602.0	598.9	$k_5(29),H_{11}(20),H_8(26)$
	ν_9	334.0	322.1	$K_4(16),H_9(24),H_{13}(21)$
	ν_{10}	144.0	144.6	$H_{11}(23),H_{13}(56)$
b_{3g}	ν_{41}	3060.0	3051.8	$K_1(99)$
	ν_{42}	2223.0	2226.4	$K_6(85),K_5(15)$
	ν_{43}	1451.0	1446.2	$K_2(61),H_8(20)$
	ν_{44}	1328.0	1353.4	$K_2(22),K_5(19),H_8(20)$ $H_{12}(15),H_{13}(18)$
	ν_{45}	1187.0	1197.9	$K_5(50),H_8(15)$
	ν_{46}	609.0	615.5	$H_7(63)$
	ν_{47}	519.0	490.6	$K_5(18),H_{12}(23),H_{13}(42)$
	ν_{48}	---	353.9	$H_{10}(50),H_{13}(40)$
	ν_{49}	---	125.8	$H_{13}(32),H_{12}(30),H_{10}(40)$
b_{1u}	ν_{18}	3065.0	3054.5	$K_1(99)$
	ν_{19}	2228.0	2229.5	$K_6(87),K_5(11)$
	ν_{20}	1545.0	1547.2	$K_2(C16),H_8(17),H_{13}(15)$
	ν_{21}	1405.0	1392.1	$K_4(22),H_8(35),H_{13}(13)$
	ν_{22}	998.0	1001.9	$K_5(18),H_7(26),H_9(16)$
	ν_{23}	962.0	949.1	$K_2(60),H_7(17),H_8(19)$
	ν_{24}	600.0	599.8	$K_5(33),H_{13}(24),H_{11}(18)$

TABLE VII (continued)

Symmetry and Modes[a]		Frequency (cm^{-1}) Observed[a]	Frequency (cm^{-1}) Calculated	Potential Energy Distribtuion (%)[b]
	ν_{25}	549.0	529.9	$H_{13}(13),K_5(20),K_4(21)$
	ν_{26}	146.0	173.3	$H_{11}(24),H_{12}(13),H_{15}(62)$
b_{2u}	ν_{32}	3053.0	3049.9	$K_1(99)$
	ν_{33}	2228.0	2226.3	$K_6(85),K_5(15)$
	ν_{34}	1540.0	1535.2	$K_2(16),K_3(76),H_3(15)$
	ν_{35}	1354.0	1340.5	$K_2(54),K_9(14),K_{12}(14)$
	ν_{36}	---	1228.8	$K_5(42),H_8(24),H_{13}(14)$
	ν_{37}	1125.0	1135.9	$K_2(41),K_3(15),K_5(15)$
	ν_{38}	498.0	489.2	$K_5(16),H_{12}(28),H_{13}(15)$
	ν_{39}	---	296.1	$H_{13}(39),H_{12}(23),H_{10}(24)$
	ν_{40}	---	63.0	$H_{10}(75),H_{12}(23),H_{10}(24)$

[a] Reference 116

[b] For the definitions of K's and H's see Table VI

constants contributing more than 10% are given. It also serves the purpose of indicating the assignments of vibrational bands. Since the TCNQ molecule is a complicated molecule with 20 atoms and 20 bonds, many vibrational modes have contribution from more than one internal coordinates and there is extensive interaction between stretching-stretching, stretching-bending, and the bending-bending coordinates. The average error in the observed and calculated frequencies is less than 7 cm^{-1}.

As mentioned earlier the observed frequencies for the a_g symmetry modes of $TCNQ^{\cdot-}$ were taken as the average of the frequencies of the factor group component bands, observed in the IR and Raman spectra. The MVFF shown in Table VI, for the neutral molecule was taken as a starting point to calculate the observed frequency and the stretching force constants were adjusted until a best fit was obtained. The remaining force field was the same as for $TCNQ^{o}$. The results of calculation are given in Table VIII. The average error between the observed and calculated values is of the order of 5 cm^{-1}. Thus, by adjusting six force constants, twenty observed frequencies are reproduced to an acceptable accuracy.

A similar procedure was followed for the dianion with sixteen observed frequencies. The average error in the observed and calculated frequencies is 5 cm^{-1}. The results of the calculation are presented in the Table IX.

For the trianion there are fourteen observed frequencies for the inplane modes. Six stretching force constants of $TCNQ^{-2}$ MVFF were adjusted to reproduce these fourteen frequences. Average error in the observed and calculated frequencies is less than 6 cm^{-1}.

TABLE VIII

THE OBSERVED AND CALCULATED IN-PLANE VIBRATIONAL FREQUENCIES OF NaTCNQ: MONOANION RADICAL SALT

Symmetry and Modes[a]		Frequency (cm^{-1}) Observed	Frequency (cm^{-1}) Calculated	Potential Energy Distribution (%)[b]
a_g	ν_1	---	3028.6	$k_1(99)$
	ν_2	2193.0	2195.7	$K_6(86),K_5(13)$
	ν_3	1594.0	1595.6	$K_2(21),K_3(56),H_8(17)$
	ν_4	1368.0	1368.8	$K_4(77),K_5(13)$
	ν_5	1192.0	1202.3	$K_3(15),H_8(46),H_{13}(25)$
	ν_6	974.0	956.8	$K_2(46),K_5(18)$
	ν_7	726.0	719.8	$K_2(39),K_5(17),H_9(15)$
	ν_8	616.0	606.5	$K_5(28),H_{11}(21),H_8(26)$
	ν_9	338.0	319.5	$K_4(19),H_9(22),H_8(21)$
	ν_{10}	146.0	142.99	$H_{11}(22),H_{13}(56)$
b_{3g}	ν_{41}	---	3040.5	$K_1(98)$
	ν_{42}	---	2197.4	$K_6(83),K_5(13)$
	ν_{43}	---	1545.5	$K_2(65),H_8(19),H_{13}(13)$
	ν_{44}	---	1275.8	$K_5(55),H_{12}(18)$
	ν_{45}	---	1193.7	$K_2(28),K_4(20),H_8(41)$
	ν_{46}	---	617.5	$H_{13}(14),H_7(46)$
	ν_{47}	---	496.5	$K_5(18),H_{12}(26),H_{13}(42)$
	ν_{48}	---	352.3	$H_{10}(49),H_{13}(41)$
	ν_{49}	117.0	124.5	$H_{10}(39),H_{12}(32),H_{13}(31)$
b_{1u}	ν_{18}	3038.0	3032.3	$K_1(99)$
	ν_{19}	2197.0	2195.7	$K_6(86),K_5(13)$
	ν_{20}	1505.0	1510.4	$K_4(31),K_2(24),H_{13}(22)$
	ν_{21}	---	1356.4	$H_8(19),K_4(41)$
	ν_{22}	1008.0	1014.6	$K_5(18),H_7(23),H_9(16)$
	ν_{23}	954.0	959.6	$K_2(60),H_7(17),H_8(15)$
	ν_{24}	608.0	607.7	$K_5(33),H_{13}(24)$
	ν_{25}	521.0	523.9	$H_{13}(13),K_5(18)$

TABLE VIII (continued)

Symmetry and Modes[a]		Frequency (cm^{-1}) Observed	Frequency (cm^{-1}) Calculated	Potential Energy Distribution (%)[b]
	ν_{26}	---	173.0	$H_{11}(23),H_{13}(63)$
b_{2u}	ν_{32}	3020.0	3026.6	$K_1(99)$
	ν_{33}	---	2196.9	$K_6(83),K_5(17)$
	ν_{34}	---	1512.9	$K_2(24),K_3(72),H_8(16)$
	ν_{35}	1363.0	1365.6	$K_2(57),H_{12}(13)$
	ν_{36}	1225.0	1241.0	$K_5(48),H_8(18)$
	ν_{37}	---	1145.0	$K_2(28),K_3(21),H_8(20)$
	ν_{38}	---	492.3	$K_5(15),H_{12}(13),H_{13}(51)$
	ν_{39}	---	289.8	$H_{13}(39),H_{10}(24),H_{12}(24)$
	ν_{40}	---	63.0	$H_{10}(76),H_{12}(24)$

[a] Reference 116

[b] For the definitions of K's and H's see Table VI

TABLE IX

THE OBSERVED AND CALCULATED IN-PLANE VIBRATIONAL FREQUENCIES OF Na_2TCNQ: DIANION SALT

Symmetry and Modes[a]		Frequency (cm^{-1}) Observed	Frequency (cm^{-1}) Calculated	Potential Energy Distribution (%)[b]
a_g	ν_1	---	3010.5	$K_1(99)$
	ν_2	2150.0	2155.4	$K_5(15),K_6(84)$
	ν_3	1597.0	1590.9	$K_2(22),K_3(58),H_8(17)$
	ν_4	1328.0	1329.9	$K_4(75),K_5(15)$
	ν_5	1194.0	1201.0	$K_3(15),H_8(46),H_{13}(25)$
	ν_6	999.0	961.3	$K_2(46),K_3(16)$
	ν_7	731.0	725.0	$K_2(37),K_5(18),H_9(16)$
	ν_8	624.0	609.8	$K_5(26),H_{11}(22),H_{13}(27)$
	ν_9	---	317.1	$K_4(21),H_9(21),H_{13}(22)$
	ν_{10}	---	142.9	$H_{11}(22),H_{13}(56)$
b_{3g}	ν_{41}	---	3022.8	$K_1(98)$
	ν_{42}	---	2162.3	$K_5(21),K_6(80)$
	ν_{43}	1546.0	1557.7	$K_2(67),H_8(18),H_{13}(14)$
	ν_{44}	---	1289.0	$K_5(56),K_6(15),H_{12}(17)$
	ν_{45}	---	1200.0	$K_2(27),H_8(45),H_{13}(15)$
	ν_{46}	---	618.4	$H_7(64)$
	ν_{47}	---	498.6	$K_5(17),H_{12}(27),H_{13}(41)$
	ν_{48}	---	352.8	$H_{10}(49),H_{13}(42)$
	ν_{49}	---	124.7	$H_{10}(39),H_{13}(31),H_{13}(31)$
b_{1u}	ν_{18}	3014.0	3014.4	$K_1(99)$
	ν_{19}	---	2155.5	$K_5(15),K_6(84)$
	ν_{20}	1498.0	1499.5	$K_1(27),K_4(21),H_8(36),H_{13}(24)$
	ν_{21}	---	1334.6	$K_4(47),H_8(13)$
	ν_{22}	---	1018.56	$K_5(18),K_7(22)$
	ν_{23}	---	963.0	$K_2(60),H_7(17),H_8(15)$
	ν_{24}	606.0	611.4	$K_5(32),H_{13}(23)$
	ν_{25}	514.0	519.2	$K_4(32),K_5(15),H_{13}(13)$

TABLE IX (continued)

Symmetry and Modes[a]		Frequency (cm^{-1}) Observed	Frequency (cm^{-1}) Calculated	Potential Energy Distribution (%)[b]
	ν_{26}	---	173.0	$H_{11}(23), H_{13}(63)$
b_{2u}	ν_{32}	---	3008.5	$K_1(99)$
	ν_{33}	2164.0	2161.5	$K_5(21), K_6(79)$
	ν_{34}	1503.0	1510.2	$K_2(29), K_3(70), H_8(15)$
	ν_{35}	---	1377.4	$K_2(53), H_{11}(19), H_{12}(13)$
	ν_{36}	1238.0	1253.1	$K_4(32), K_5(48), H_8(17)$
	ν_{37}	1140.0	1148.6	$K_2(23), K_3(23), H_8(21)$
	ν_{38}	---	494.0	$K_5(14), H_{12}(31), H_{13}(51)$
	ν_{39}	---	290.3	$H_{10}(25), H_{12}(24), H_{13}(40)$
	ν_{40}	---	63.0	$H_{10}(74), H_{12}(24)$

[a] Reference 116

[b] For the definitions of K's and H's see Table VI.

The results and the adjusted force constants are given in Tables X and VI respectively.

As can be seen from Table VI the stretching force constants of TCNQ show a consistent trend of change with addition of each electron. For C=C bonds of the ring and wing as well for C≡N bonds, the force constants are decreasing with increasing negative charge on TCNQ. For the C-C bonds of the ring and wing, however, the force constants increase with an addition of each electron. Thus, for the trianion of TCNQ a picture emerges in which the force constants for $C{=}C^{R}$ and $C{-}C^{R}$ are almost equal, signifying a complete transition from the p-quinonoid structure to the benzenoid ring structure. The $C{=}C^{W}$ and $C{-}C^{W}$ force constant values indicate the progressive acquisition of the single bond and double character respectively with the addition of each electron. For the C-C single bonds of the wing to acquire double bond character and C≡N to become double bondlike requires extensive delocalization in the $C\lessdot^{C\equiv N}_{C\equiv N}$ part of $TCNQ^{-3}$. These force constants changes agree well with predictions made from the π-bond order changes estimated from the MO calculations (36) (61) (78). Detailed comparison between the calculated π-bond orders and the force constants of TCNQ and its anions will be made in a later part of this study.

Thus, these calculations support the tentative vibrational band assignments made in Table IV, for the anions of TCNQ. Agreement between the observed and calculated frequencies of the $TCNQ^{\cdot-}$ vibrational bands is better when COV vibronic interactions are taken into account. For the di- and trianions, though the agreement is quite good, the calculation does not answer questions raised in connection with their vibrational assignments. In this scheme strong Raman bands

TABLE X

THE OBSERVED AND CALCULATED IN-PLANE VIBRATIONAL FREQUENCIES OF Na_3TCNQ: TRIANION SALT

Symmetry and Modes[a]		Frequency (cm^{-1}) Observed	Frequency (cm^{-1}) Calculated	Potential Energy Distribution (%)[b]
a_g	ν_1	---	2991.5	$K_1(99)$
	ν_2	2033.0	2036.4	$K_2(18),K_6(80)$
	ν_3	1577.0	1568.9	$K_2(27),K_3(50),H_8(19),H_{13}(14)$
	ν_4	1312.0	1313.9	$K_4(72),K_5(14)$
	ν_5	1184.0	1194.9	$K_3(16),H_8(44),H_{13}(24)$
	ν_6	986.0	968.3	$K_2(47),K_3(22)$
	ν_7	737.0	731.4	$K_2(30),K_5(18),H_9(17)$
	ν_8	620.0	609.0	$K_5(26),H_{11}(22),H_{13}(27)$
	ν_9	---	315.0	$K_4(21),H_9(21),H_{13}(22)$
	ν_{10}	---	142.7	$H_{11}(22),H_{13}(56)$
b_{3g}	ν_{41}	---	3005.3	$K_1(98)$
	ν_{42}	---	2055.6	$K_5(28),K_6(73)$
	ν_{43}	1599.0	1595.5	$K_2(73),H_8(15)$
	ν_{44}	---	1281.3	$K_5(48),K_6(19),H_{12}(17)$
	ν_{45}	---	1207.5	$K_2(22),H_8(45)mH_{13}(16)$
	ν_{46}	---	620.5	$H_7(65)$
	ν_{47}	---	499.4	$K_5(16),H_{12}(27),H_{13}(41)$
	ν_{48}	---	352.8	$H_{10}(49),H_{13}(42)$
	ν_{49}	---	125.0	$H_{10}(38),H_{12}(32),H_{13}(31)$
b_{1u}	ν_{18}	2996.0	2996.5	$K_1(96)$
	ν_{19}	2035.0	2039.4	$K_5(18),K_6(80)$
	ν_{20}	---	1506.3	$K_2(32),K_4(17),H_8(36),H_{13}(24)$
	ν_{21}	1322.0	1325.6	$K_4(50)$
	ν_{22}	---	1018.4	$K_3(16),H_7(17),H_8(13),H_9(15)$
	ν_{23}	---	980.3	$K_2(52),H_7(21),H_8(15)$
	ν_{24}	---	610.4	$K_5(31),H_{11}(19),H_{13}(23)$
	ν_{25}	---	517.0	$K_4(34),K_5(15),H_{13}(13)$

TABLE X (continued)

Symmetry and Modes[a]		Frequency (cm^{-1}) Observed	Frequency (cm^{-1}) Calculated	Potential Energy Distribution (%)[b]
	ν_{26}	---	173.0	$H_{11}(23), H_{13}(63)$
b_{2u}	ν_{32}	---	2989.7	$K_1(99)$
	ν_{33}	---	2054.7	$K_5(27), K_6(74)$
	ν_{34}	1476.0	1490.4	$K_2(34), K_3(52)$
	ν_{35}	---	1392.1	$K_2(31), H_8(22), H_{13}(16)$
	ν_{36}	1245.0	1248.8	$K_4(47), H_8(15)$
	ν_{37}	1138.0	1142.9	$K_2(14), K_3(32), H_8(19)$
	ν_{38}	---	494.4	$K_5(14), H_{12}(31), H_{13}(51)$
	ν_{39}	---	290.1	$H_{10}(25), H_{12}(24), H_{13}(40)$
	ν_{40}	---	63.0	$H_{10}(73), H_{12}(24)$

[a] Reference 116

[b] For the definitions of K's and H's see Table VI.

at 1138 and 1478 cm^{-1} had to be assigned to b_u modes. The questions pertaining to such 'unreasonable assignments' will be discussed in Chapter V.

Vibrational Spectra of Nonstoichiometric TCNQ Salts

The response of the RR intensity pattern to the composition of the salt is potentially a more sensitive measure of the sample character than the frequencies of the vibrational and electronic bands (73) (110). Hence, it may be useful to explore the possible correlation between RR scattering intensity and a composition of the salt. Particularly, such a correlation might be of some use in better understanding the apparent erratic behavior of the electrical conductivity of many stoichiometric (6) and nonstoichiometric CT complexes.

Nonstoichiometric salts of sodium and TCNQ were prepared with composition in the range $0.0 \leq x \leq 3.0$ where the metal/organic ratio was increased in small steps. With each progressive increase in the value of x, the color of the thin film changed from coarse yellow (x=0) to green (0.1-0.7), turquoise (0.8-0.9), bright blue (1.0), dark blue (1.1-1.8), colorless (2.0) and golden yellow (2.1-3.0) (Table II). Since the nonstoichiometric salts in the composition range $0.0 \leq x \leq 1.0$ contain a mixture of $TCNQ^{o}$ and $TCNQ^{\cdot -}$, the RR intensity patterns of either molecule in this range did not show any significant changes with a change of composition. This may be because of a reluctance of the neutral molecule to form a solution with the monoanion radical. The following results for the nonstoichiometric salts in the composition range $1.0 \leq x \leq 3.0$, can be explained on the basis of the anions with different negative

charges forming ionic solutions. The nonstoichiometric salts in the composition range $0.0 \leq x \leq 1.0$ are mere mixtures of $TCNQ^{o}$ and $TCNQ^{-\cdot}$. The electronic spectra of either species seem to not be affected significantly, which is reflected in the apparently unaltered intensity patterns of their RR spectra. For the nonstoichiometric salts in the range $1.0 \leq x \leq 2.0$, the relative intensity changes in RR as well as IR spectra with a change in the value of x will be described. Different RR intensity patterns of nonstoichiometric salts in this range will be compared with the intensity patterns of 1:1 KTCNQ salts observed by Chi and Nixon (91) (Figure 2) at different laser excitation lines. However, use of Chi and Nixon's intensity patterns as reference is of limited value because of the possible presence of products due to the reaction with oxygen (76) (130). In the range $2.0 \leq x \leq 3.0$, the changing RR intensity patterns of $TCNQ^{-3}$ with a change in composition will be presented.

The usefulness of the correlation of RR intensity patterns with composition is restricted due to certain limitations: 1) As pointed out above, a lack of reference intensity patterns of the pure 1:1 or 1:3 salts of fixed composition at different excitation wavelengths, 2) the compositions of these salts are estimated from the intensities of the C≡N stretching IR bands of the TCNQ anions which may depend not only on the amount of the particular ion present in the sample, but also the orientation and the extent and nature of vibronic interactions, 3) the electronic spectra of the nonstoichiometric salts, often could not be recorded because of high optical densities ($\varepsilon \sim 4$ to 6) in the solid state. With these limitations, the value of the correlation is only to point out the trends of RR intensity changes with composition, rather than accurate measurements.

Range $1.0 \leq x \leq 2.0$

IR spectra of nonstoichiometric salts of NaTCNQ in this range are shown in Figure 10a, b, c, and d. The frequencies of the mono- and dianion bands do not change significantly with the change of composition. However, the intensities of certain monoanionic IR bands change consistently with an increasing value of x. The COV IR bands of $TCNQ^{\cdot -}$ at 723, 1186, 1326, 1343, 1578 and 2168 cm^{-1} become relatively stronger and stronger as the concentration of Na_2TCNQ increases in the sample. Such increases in the relative intensities of the COV IR bands was measured with respect to the 1226, 1363 and 1505 cm^{-1} nonvibronic, in-plane IR bands. Since the 1363 cm^{-1} in-plane band exclusively belongs to the monoanion without any dianion band in the nearby region, its intensity was used as a reference to measure the change in intensities of COV IR bands with composition. Particularly, in the $1.0 \leq x \leq 1.3$ range, the relative intensities of the COV IR bands of $TCNQ^{\cdot -}$ show remarkable increase (Figure 10a, b, c). Beyond a certain metal/organic ratio ($x \sim 1.3$), the relative intensities of COV and nonvibronic bands do not change significantly. In some of the nonstoichiometric salts, each of the 823 and 1226 cm^{-1} IR bands split into two components. These components can distinctly be observed at 816, 823, 1226, 1246 cm^{-1} or the x=1.38 and 1.55 values (Figures 10c and 10d). For the other nonstoichiometric salts in the composition range $1.2 \leq x \leq 1.75$, the 816 and 1246 cm^{-1} IR bands appear as shoulders (Figures 10a, b, c, and d). The 816 and 1246 cm^{-1} bands were not observed in either of the 1:1 or 2:1 sodium salts of TCNQ. Hence, the splitting of the 823 and 1226 cm^{-1} bands may be attributed to the ionic solution of the $TCNQ^{\cdot -}$ and $TCNQ^{-2}$.

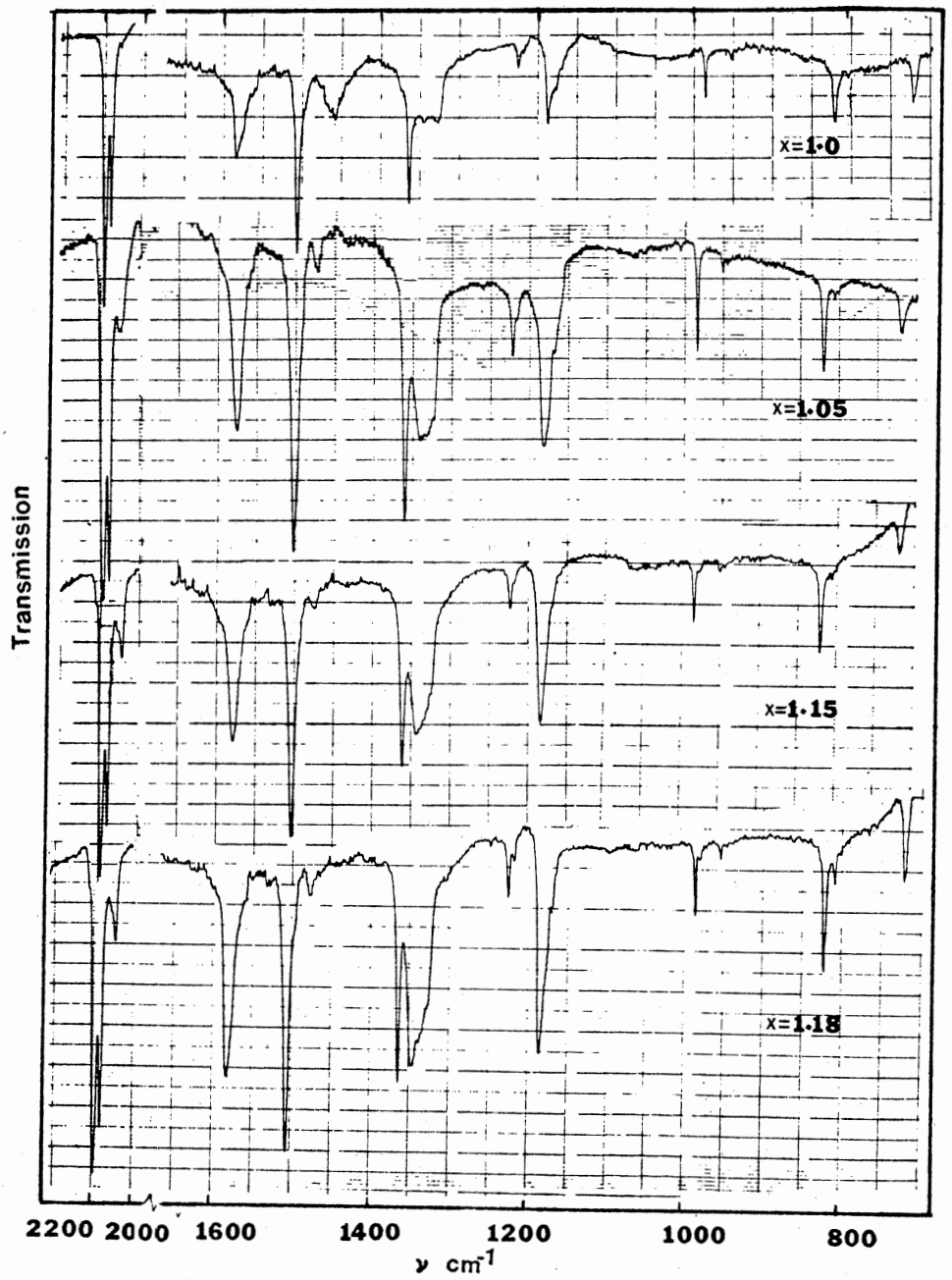

a) Range: $1.0 \leq x \leq 1.18$

Figure 10. IR spectra of Nonstoichiometric Salts with the Na/TCNQ Ratio between 1.0 and 2.0

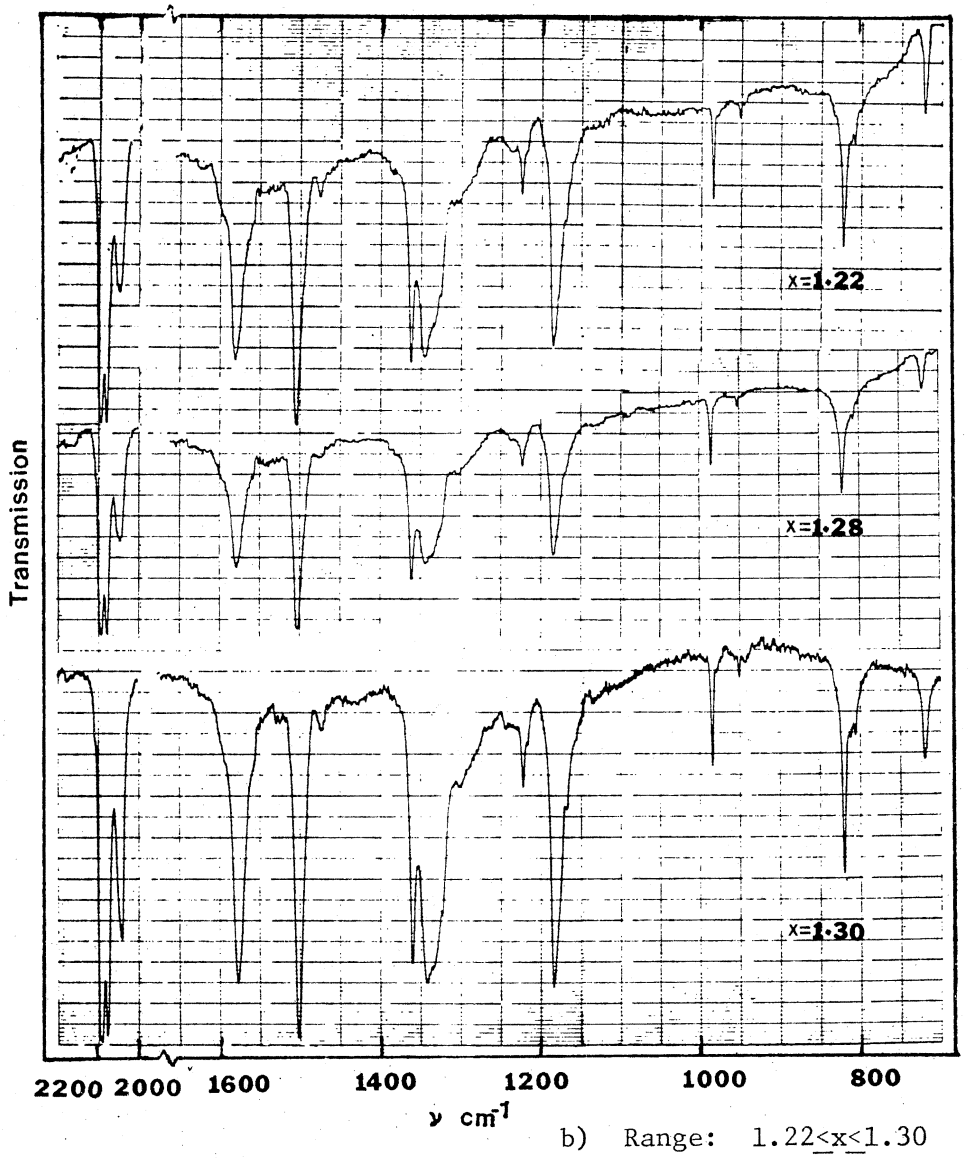

b) Range: $1.22 \leq x \leq 1.30$

Figure 10. (Continued)

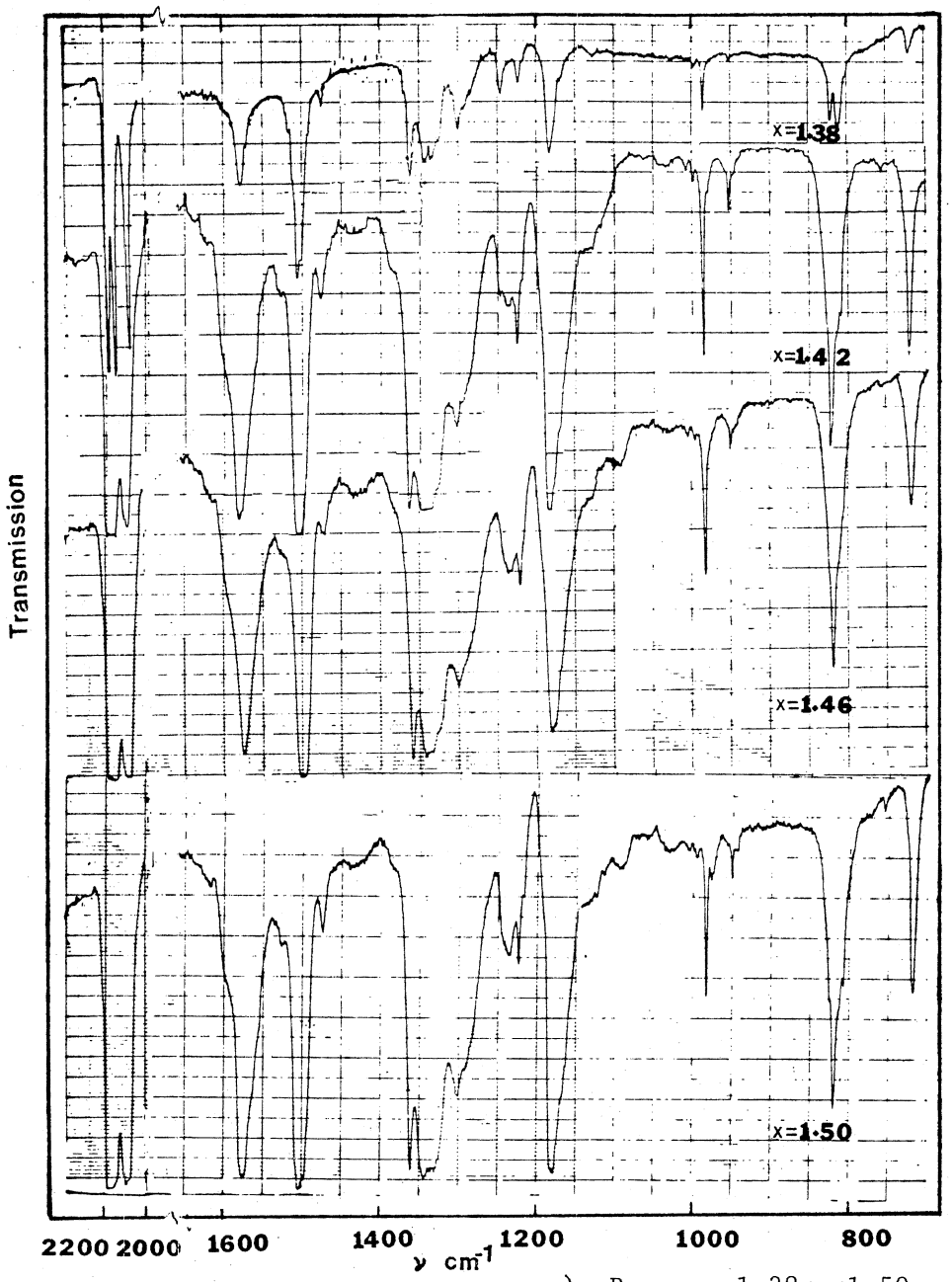

c) Range: $1.38 \leq x \leq 1.50$

Figure 10. (Continued)

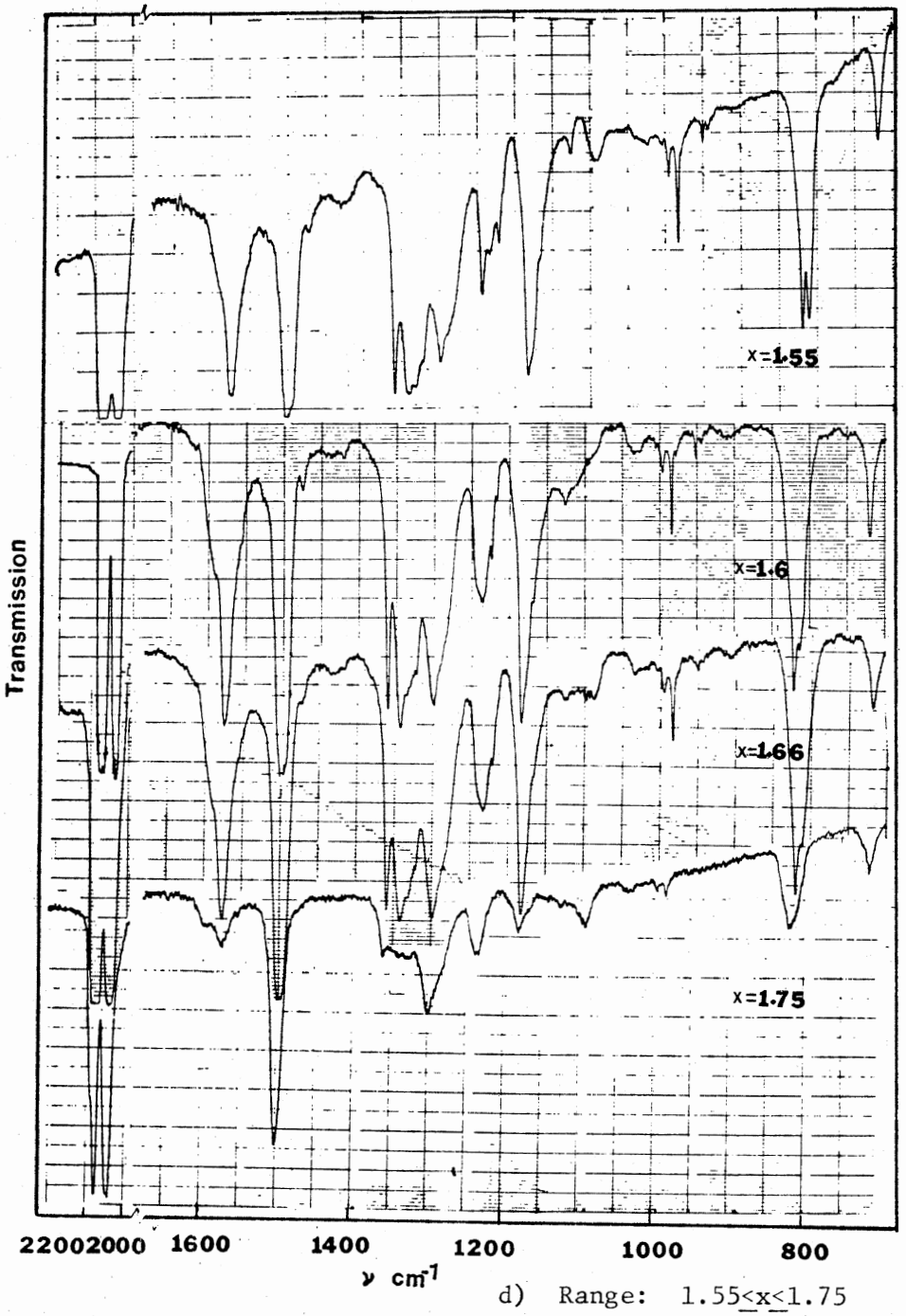

d) Range: $1.55 \leq x \leq 1.75$

Figure 10. (Continued)

The increase in the COV IR band intensities with increasing value of x in nonstoichiometric salts may be attributed to one of the following reasons: a) the increase in electron density available for electron exchange between components of the dimer, b) loss of planar-to-substrate orientation of NaTCNQ in the sample with increasing concentration of Na_2TCNQ. The intensities of $TCNQ^-$ RR bands are more sensitive to changes in the sample composition than the IR bands. The intensity patterns of the RR spectra in the $1.0 \leq x \leq 2.0$ composition range of nonstoichiometric salts, for the 4880°A and 5145°A laser excitation lines are presented in Figure 11a, b, c, and d and 12a, b, c, and d respectively. For the 1:1 MTCNQ salt, RR vibrational bands can be classified into two types. The 1207, 1396, 1610 and 2220 cm^{-1} Raman bands are most intense with the laser excitation lines of longer wavelengths (in the region of the 620mμ $^2B_{3u}(1) \leftarrow {}^2b_{2g}$ electronic band), at 5145°A, 5682 and 6471°A (Figure 2). These bands can be classified as A-type Raman bands. The intensity of these bands is resonantly enhanced when the laser excitation lines are in the region of a strongly allowed electronic absorption band. The intensity of other types of bands at 347, 620, 729, 967, 978, 1185, 1326, 1368 and 1583 cm^{-1} is resonantly enhanced when laser excitation lines, like 4880°A and 4579°A, are in the overlap region of the two electronic bands or in the region of weakly allowed electronic bands. These bands will be called non-A type Raman bands. The Raman bands at 1012, 1297, and 1635 cm^{-1} from Figure 2 will be ignored because of the possibility of their origin from α,α-$DCTC^-$. In the study of RR spectra of nonstoichiometric salts, the laser excitation line was kept at a fixed position and the composition of the sample was changed. For the 4880°A laser line with

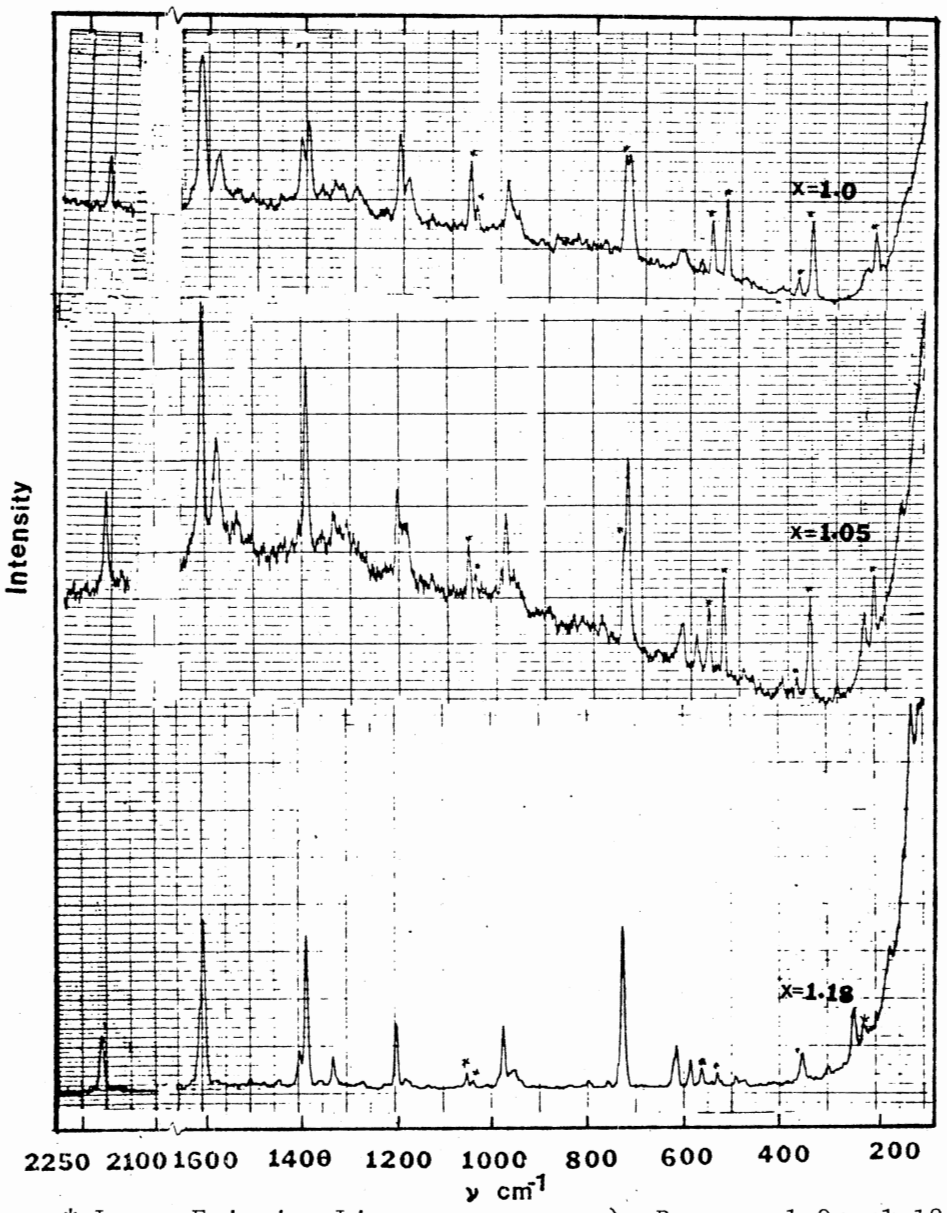

Figure 11. Raman Spectra of Nonstoichiometric Salts in a Range, $1.0 \leq Na/TCNQ \leq 2.0$, for the 4880°A Laser Excitation Line

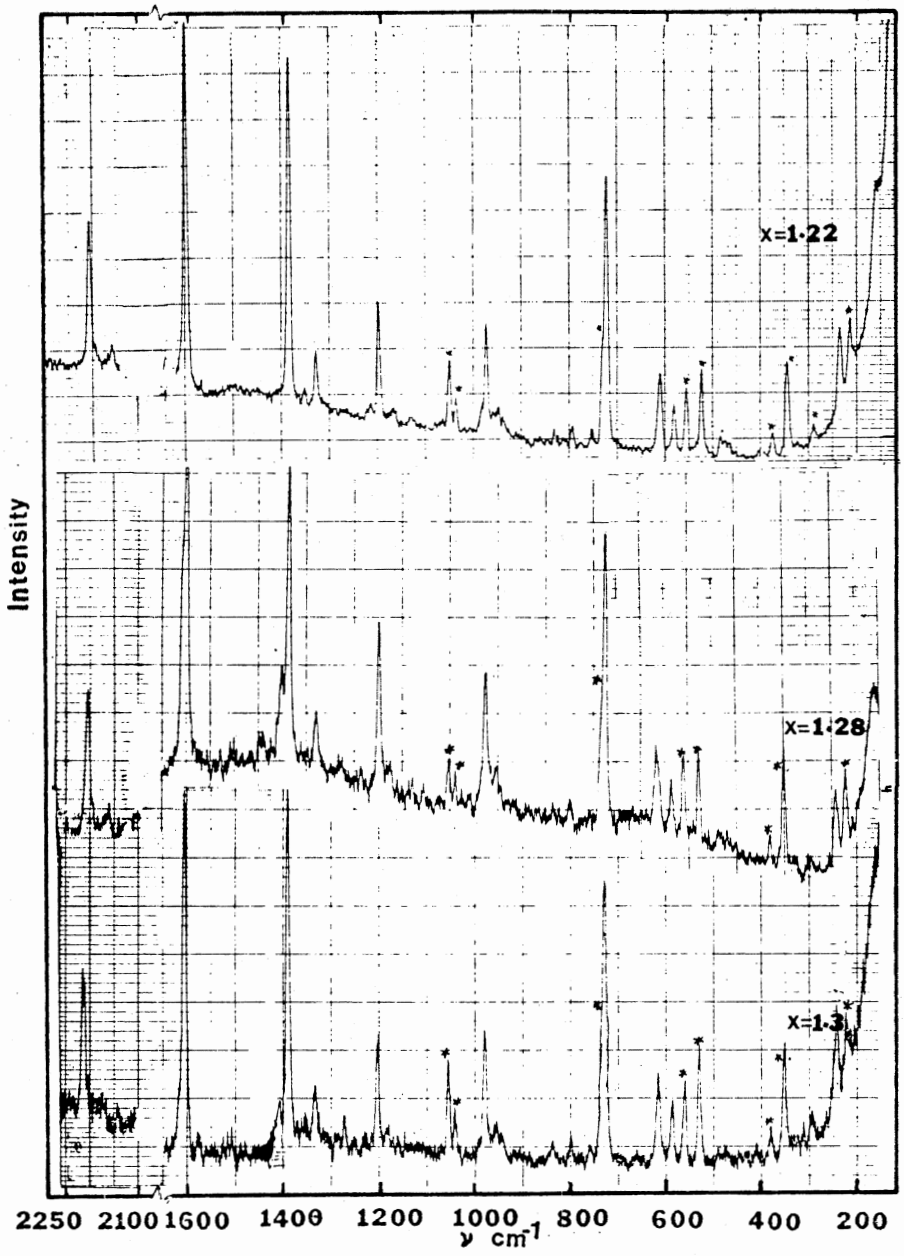

* Laser Emission Lines b) Range: $1.22 \leq x \leq 1.30$

Figure 11. (Continued)

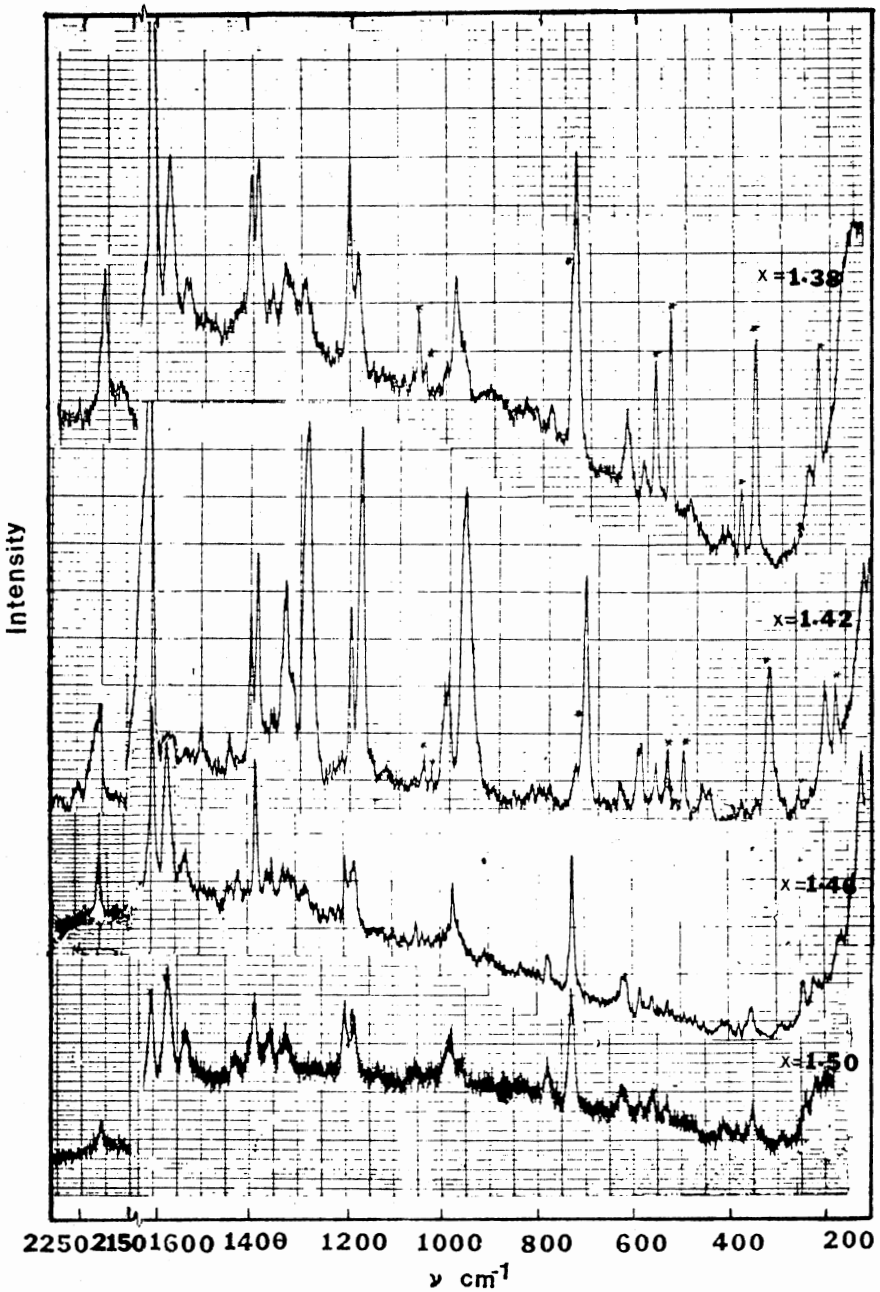

* Laser Emission Lines c) Range: $1.38 \leq x \leq 1.50$

Figure 11. (Continued)

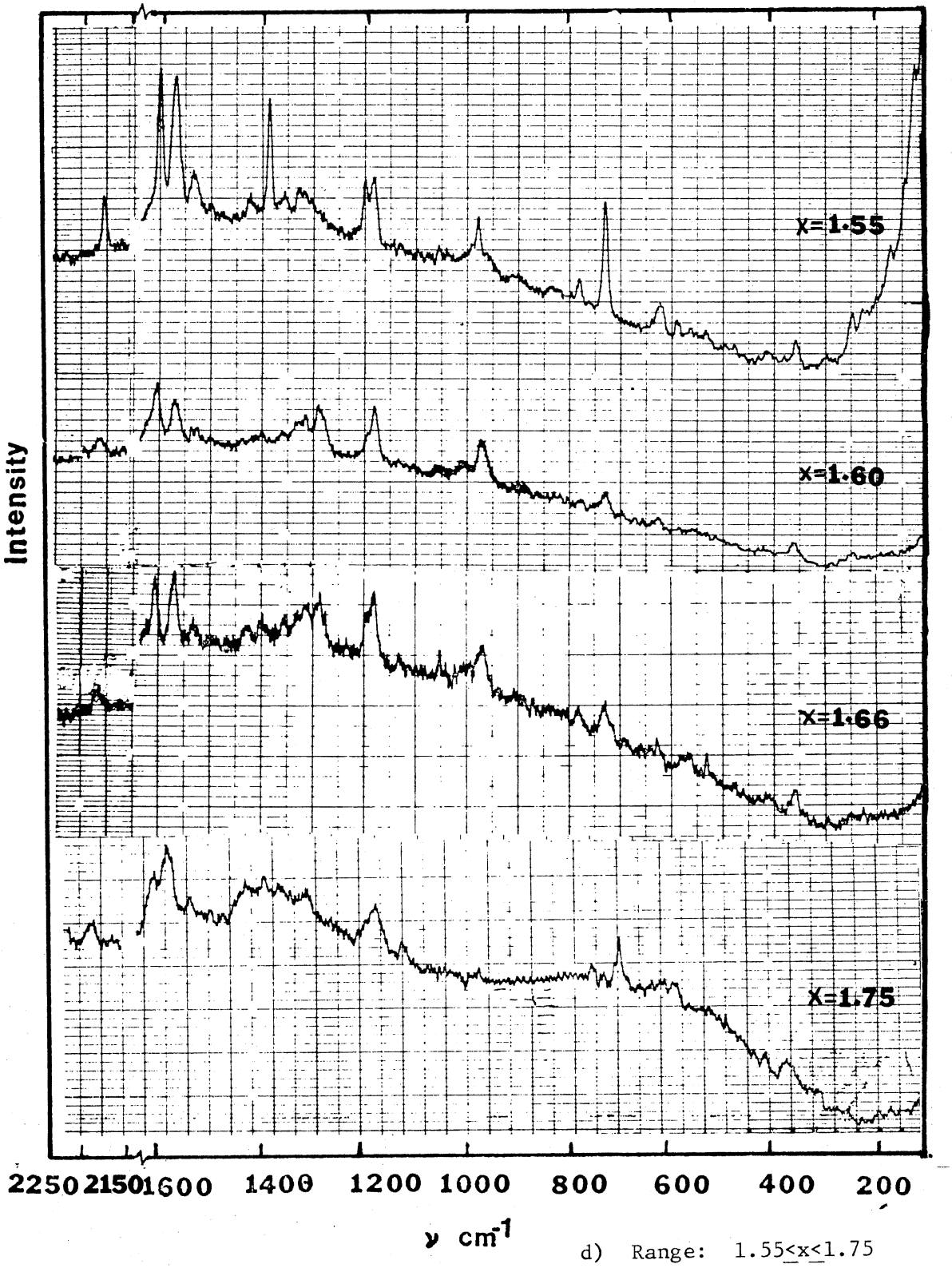

d) Range: $1.55 \leq x \leq 1.75$

Figure 11. (Continued)

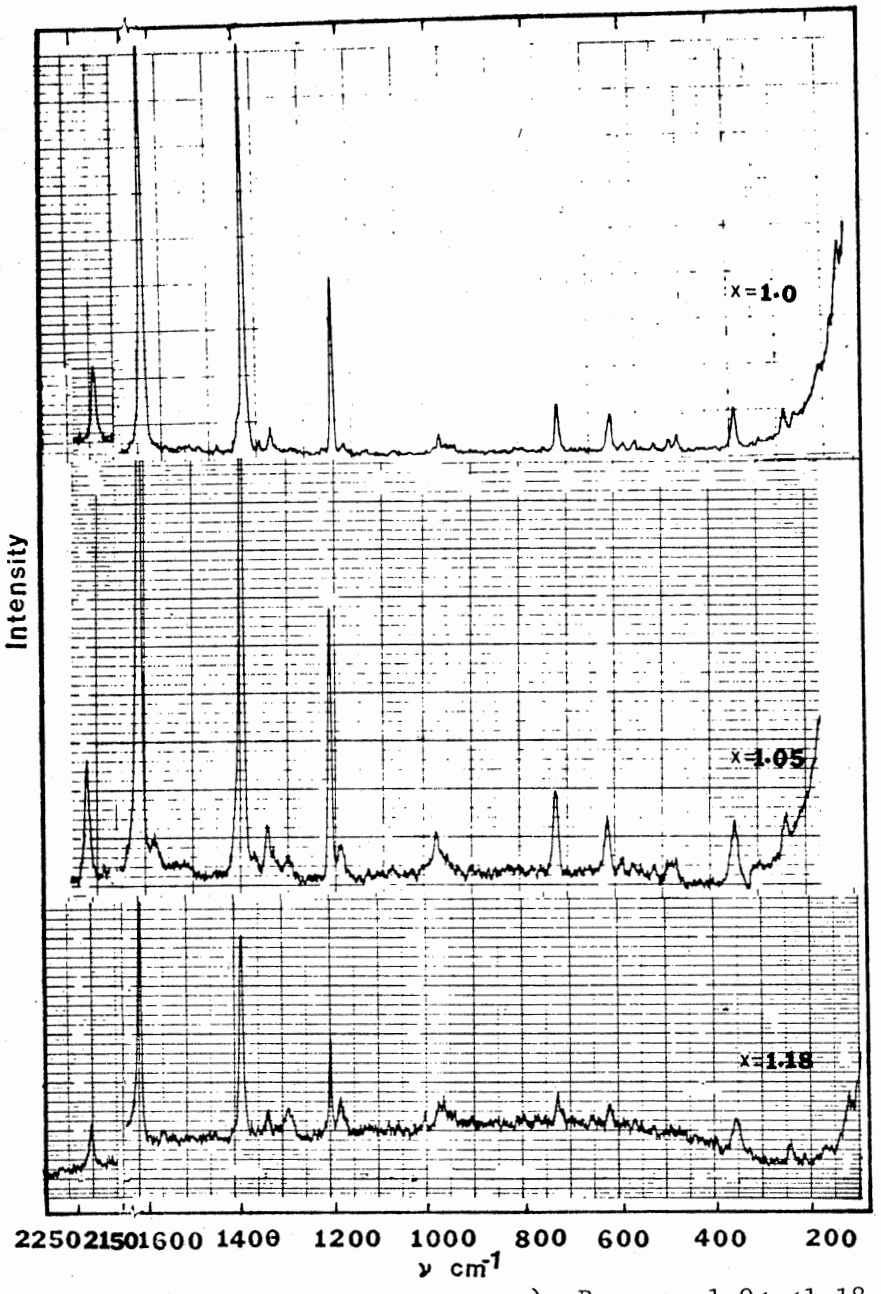

a) Range: $1.0 \leq x \leq 1.18$

Figure 12. Resonance Raman Spectra of Nonstoichiometric Salts in a Range $1.0 \leq Na \leq 2.0$ for the 5145°A Laser Excitation Line

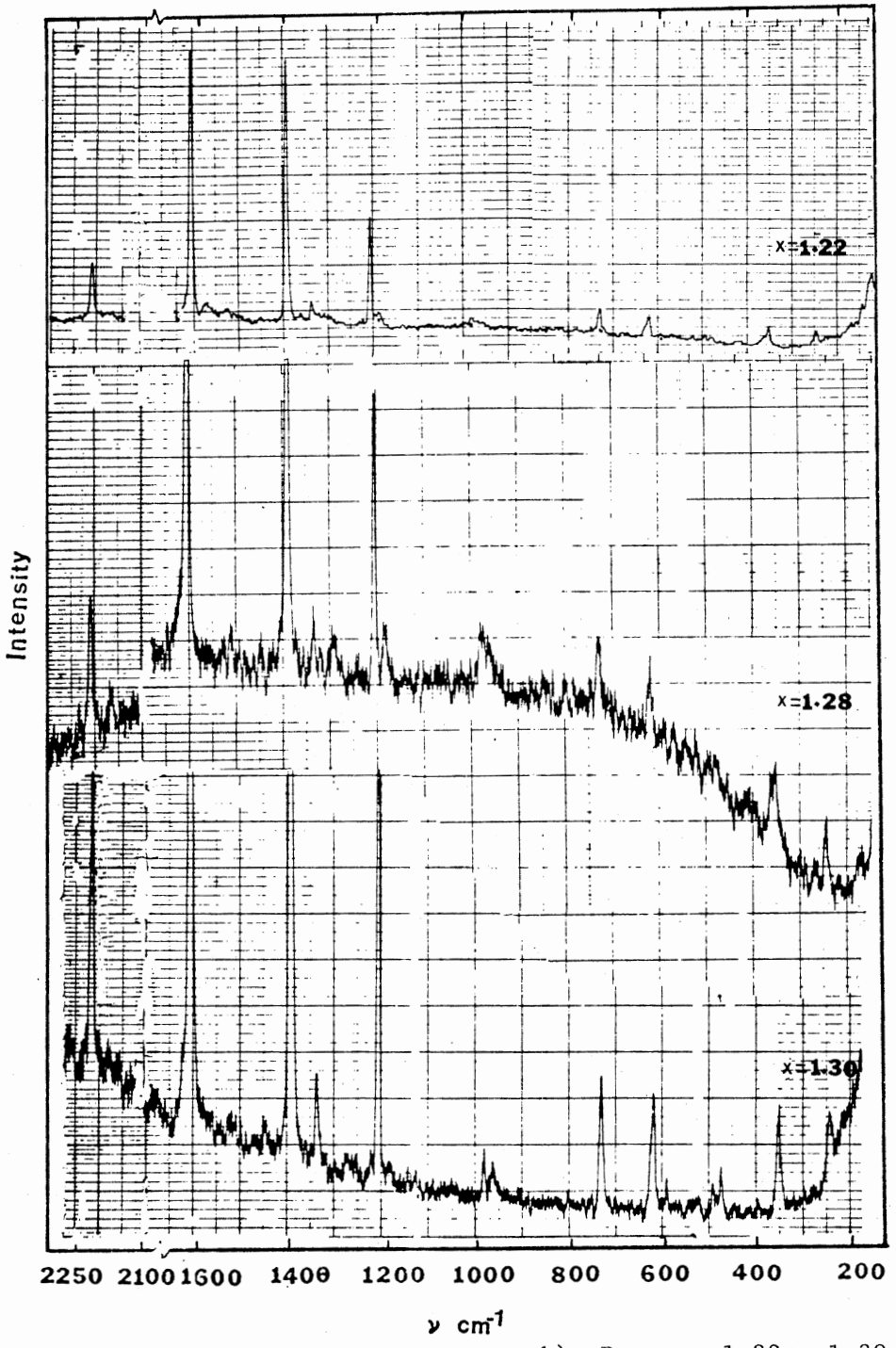

b) Range: $1.22 \leq x \leq 1.30$

Figure 12. (Continued)

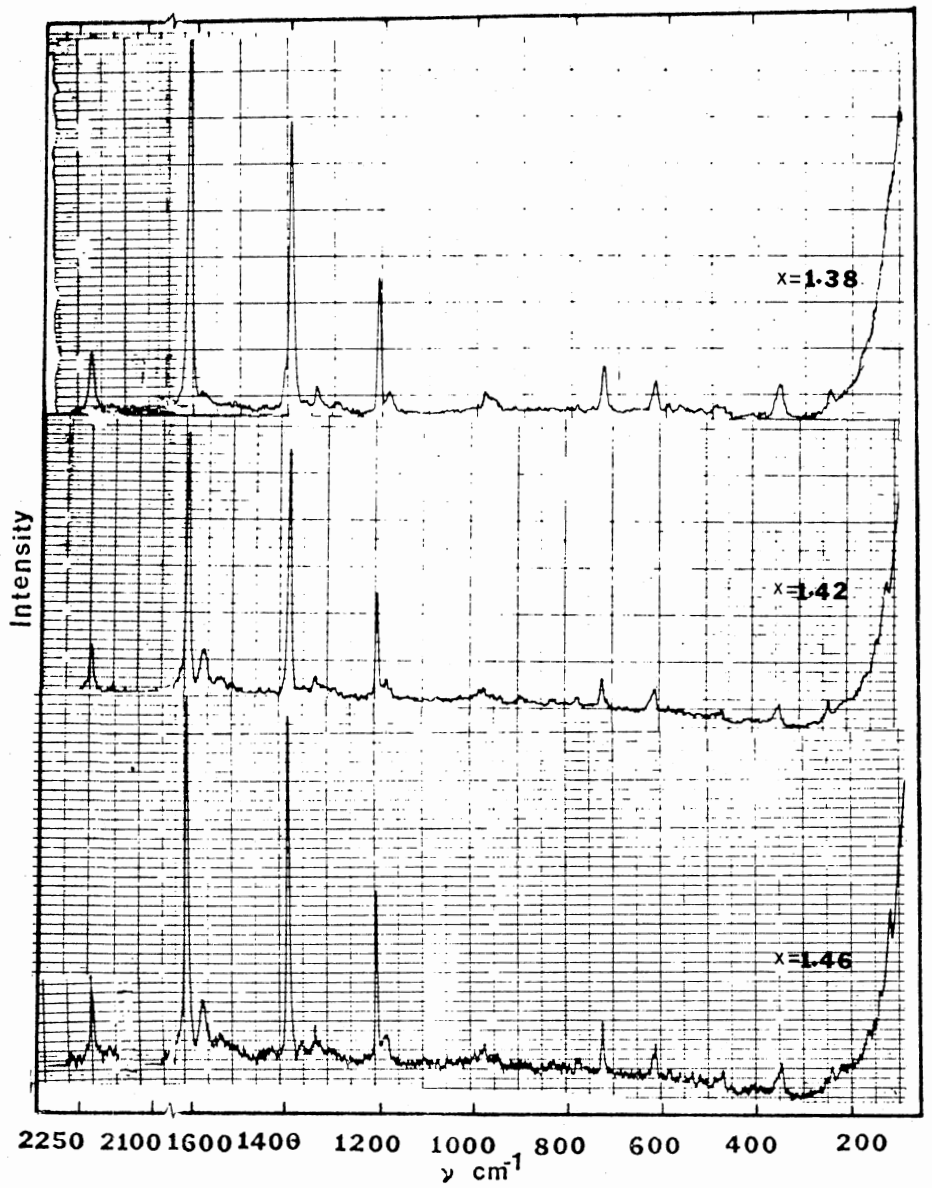

c) Range: $1.38 \leq x \leq 1.46$

Figure 12. (Continued)

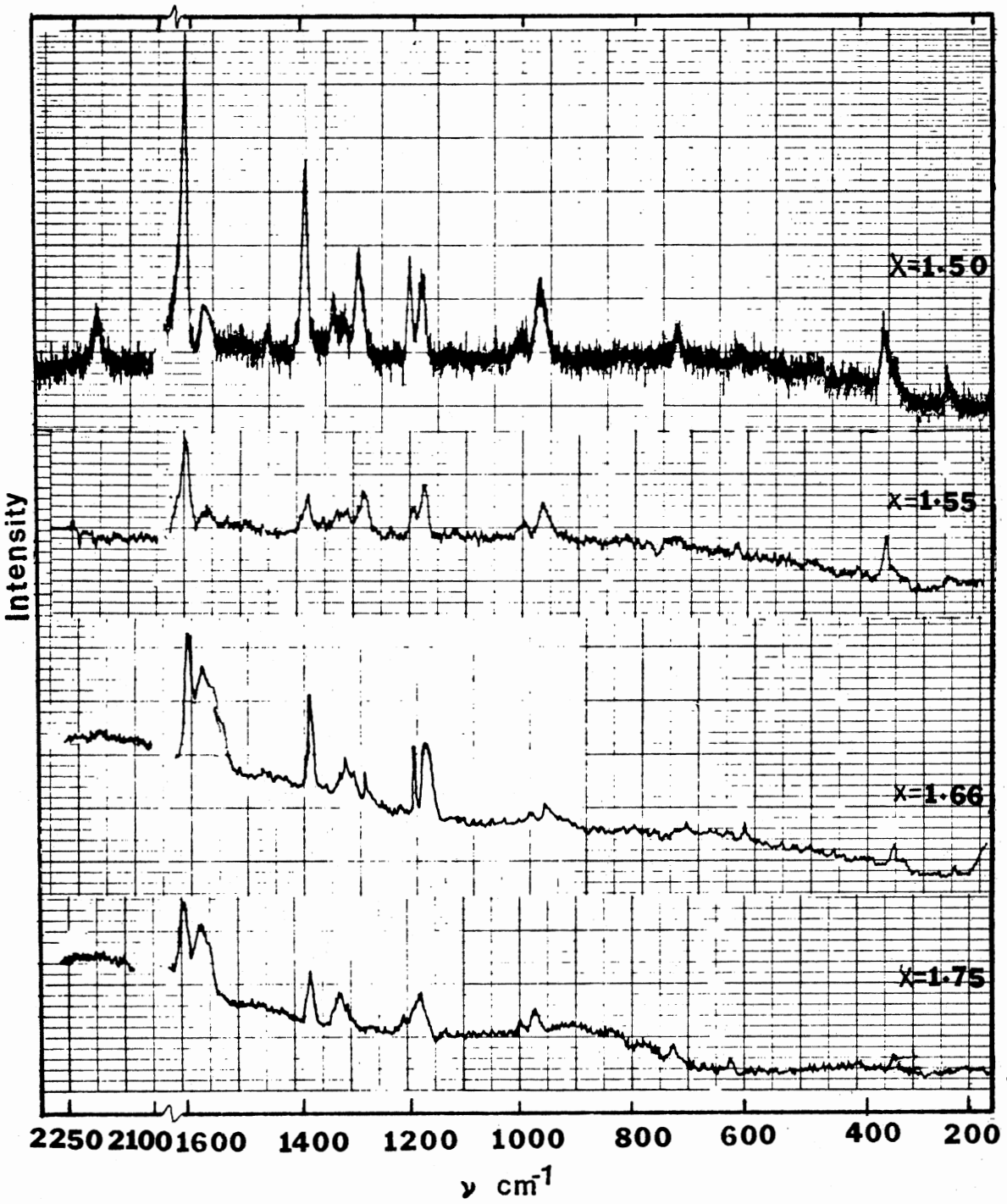

d) Range: $1.50 \leq x \leq 1.75$

Figure 12. (Continued)

x=1.0, intensity of the A-type RR bands is strongly enhanced and the non-A type bands are observed to be weak. With increasing value of x in the range $1.0 \leq x \leq 1.4$, the A-type band intensity enhancement is increased and non-A type bands become so weak to be almost undetectable. Particularly, the 1185 and 1583 cm^{-1} bands are indistinguishable from background noise in this range. With further increase of the metal/organic ratio in the range $1.4 < x < 1.75$, the intensity of non-A type bands is enhanced and a decrease in the enhancement of A-type Raman bands is observed. Similar, though less obvious behavior of A- and non-A type band intensities is observed for the 5145^{o}A laser excitation line, as shown in Figure 12a, b, c, and d. The non-A type bands appear to be very weak or completely undetectable at x=1.0 and in the range $1.0 \leq x \leq 1.45$. In the $1.45 \leq x \leq 1.75$ range non-A type band intensities are enhanced, though the extentof enhancement is less than that observed for the 4880^{o}A laser line.

Thus, the RR intensity patterns of nonstoichiometric salts in the $1.15 < x < 1.4$ composition range for the 4880^{o}A laser excitation line and $1.0 < x \leq 1.45$ for the 5145^{o}A line, appear to be similar to the patterns observed for 1:1 stoichiometric salt with 5682^{o}A and 6471^{o}A excitation lines (91) (131). The RR intensity patterns of nonstoichiometric salts in the composition range $1.4 \leq x \leq 1.75$ for the 4880^{o}A laser line and $1.45 \leq x \leq 1.75$ for the 5145^{o}A excitation line resemble that of the 1:1 stoichiometric salt at shorter wavelength laser excitation lines like 4579^{o}A and 4880^{o}A. Thus A-type Raman bands of $TCNQ^{-}$ are resonantly enhanced for the long wavelength (5682 and 6471^{o}A) laser excitation lines for the 1:1 stoichiometric salts and in the range $1.15 \leq x < 1.4$ for nonstoichiometric salts with the 4880^{o}A or 5145^{o}A laser excitation lines. The

non-A type Raman band intensity is enhanced by short wavelength laser excitation lines (4880°A and 4579°A) for the 1:1 salts and in the range $1.4 \leq x \leq 1.75$ of nonstoichiometric salts for 4880°A or 5145°A laser lines.

The changing intensity patterns in terms of A and non-A type Raman effect for the 1:1 stoichiometric salts and their correlation with the electronic spectrum has been discussed earlier. In the case of the stoichiometric salt the electronic spectrum is fixed by keeping the composition constant and the laser excitation lines are moved across the electronic spectrum. For the nonstoichiometric salts studied here the situation is reversed. For the nonstoichiometric salts, the laser excitation line is fixed and the electronic bands are moved with respect to the laser line by changing the composition. For the nonstoichiometric salts of composition in the $1.5 < x < 1.4$ range, the $TCNQ^{\cdot-}$ electronic band ($^2B_{3u}(1) \leftarrow {}^2B_{2g}$) is apparently shifted to low wavelength so that the 4880°A and 5145°A laser lines lie almost exclusively within its envelope. This situation is similar to the excitation of the 1:1 stoichiometric salt by the 5682°A and 6471°A laser lines. For the nonstoichiometric salts of composition in the range $1.4 \leq x \leq 1.75$, the electronic bands show bathochromic shifts and not only the 4880°A laser line but also the 5145°A line lie in the overlap region of the 365 mμ ($^2A_u(1) \leftarrow {}^2B_{2g}$ and $^2B_{3u}(2) \leftarrow {}^2B_{2g}$) and the 620 mμ ($^2B_{3u}(1) \leftarrow {}^2B_{2g}$) electronic absorption bands so that the intensity of the non-A type Raman bands is enhanced.

These changes in the RR intensity patterns can be explained in terms of shifts in the electronic bands of the monoanion radical salts. $TCNQ^{\cdot-}$ and $TCNQ^{-2}$ apparently form ionic solutions in the solid state which causes shifts in the electronic bands with respect to the

4880Å and 5145Å laser excitation lines. These shifts are reflected in the changing RR intensity patterns as described in the preceding paragraph.

Jeanmaire and VanDuyne (130) did not observe the non-A-type Raman bands in the solution RR spectrum of $TCNQ^{\cdot-}$ in acetonitrile. In the acetonitrile solution $TCNQ^{\cdot-}$ exists as a monomer (63). In the solid state RR spectrum however, non-A-type bands at 1186, 1339, 1578 cm^{-1} etc., are observed as described for the nonstoichiometric salts. Different RR intensity patterns in the solid state from that of the solution spectrum (130), can be attributed to the dimerization and crystal field effects. The 347, 620, 729 and 2220 cm^{-1} Raman bands in the solid state were observed at 336, 612, 725 and 2192 cm^{-1} respectively, in the acetonitrile solution (130). The frequencies of the a_g modes of $TCNQ^{\cdot-}$ in acetonitrile at 336, 612, 725, 1195, and 2193 cm^{-1} (130) can be compared with the average frequencies of the a_g factor group components at 338, 616, 726, 1192 and 2193 cm^{-1} in the solid state (Table VIII). Thus it can be said that in the monomer, $TCNQ^{\cdot-}$ factor group components "colapse" into a single Raman band.

To verify the effect of oxygen interaction on the RR spectra of $TCNQ^{\cdot-}$ in nonstoichiometric salts, some of these salts were deliberately exposed to dry oxygen and eventually the atmosphere. The color of the sample changed from dark blue to a pink-blue color. New Raman bands at 1635 and 2228 cm^{-1} appeared in the spectrum (figure 11c; x=1.42 and 12d; x=1.5). The intensities of the 980, 1012, 1188, 1295 and 1635 cm^{-1} bands increased tremendously. However, the Raman bands at 1339, 1368, 1578 and 2220 cm^{-1} disappeared completely or became weak. Chi and Nixon's (91) spectra show the presence of the 1635 and 2228 cm^{-1} bands

and the 1578 cm^{-1} band is absent (Figure 2). Thus, it appears that Jeanmaire and VanDuyne's (130) contention that α,α-$DCTC^-$ may be present in Chi and Nixon's spectra is correct. The IR spectra of the nonstoichiometric salts exposed to O_2, show IR bands at 835, 1396 and 1635 cm^{-1} along with the other $TCNQ^-$ bands. These bands can exclusively be assigned to α,α-$DCTC^-$. It is apparent that the RR intensity pattern changes with exposure to oxygen, compared with the unexposed 1:1 stoichiometric salts, as well as with a change in the composition of the nonstoichiometric salts.

For the nonstoichiometric salts in the range $1.75 \leq x \leq 2.0$ many IR and Raman bands of the mono- and dianion become indistinguishable and intensity of the monoanion bands is difficult to measure.

Range $2.0 < x < 3.0$

The IR and Raman Spectra of these nonstoichiometric salts are given in Figure 13a, b, c, d, 14a, b, c, d, e, and 15a, b, c, d, e. In this range, the changing intensity patterns of the RR spectra of $TCNQ^{-3}$ are presented in Figures 14a, b, c, d, e, and 15a, b, c, d, e. Since assignments of the electronic and vibrational bands has not been established for the trianion, the RR effect in the nonstoichiometric salts will not be described in terms of A and non-A type bands. However, if the 427 mμ electronic band is due to a single 'allowed' electronic transition then possibly all the RR bands of $TCNQ^{-3}$ may be described as of the A-type.

Unlike the $1.0 \leq x \leq 2.0$ range for which the electronic band shifts with a change in composition could not be observed because of very high optical density, the electronic spectra for some of the non-

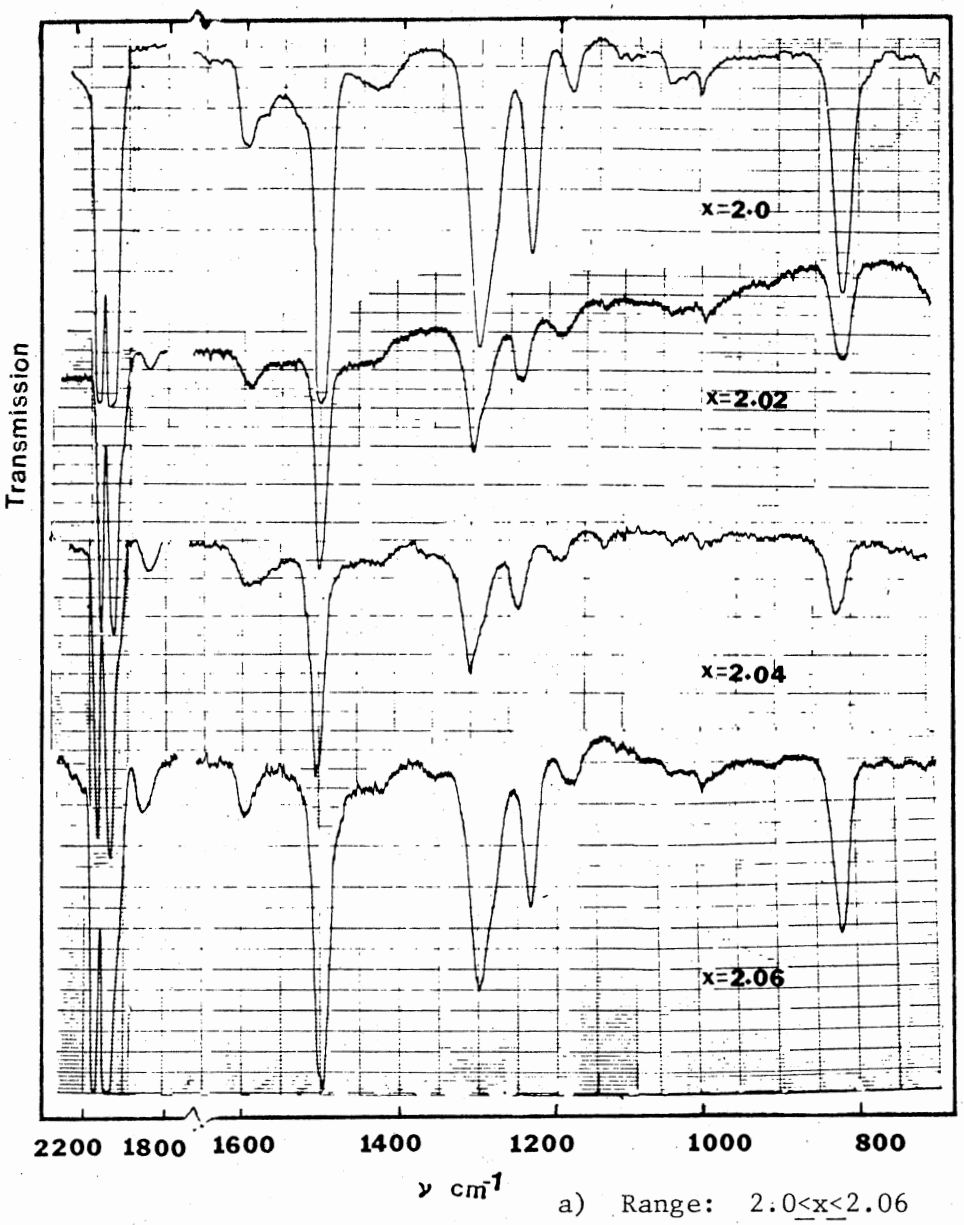

a) Range: $2.0 \leq x \leq 2.06$

Figure 13. IR Spectra of Nonstoichiometric Salts in a Range $2.0 \leq Na/TCNQ \leq 3.0$

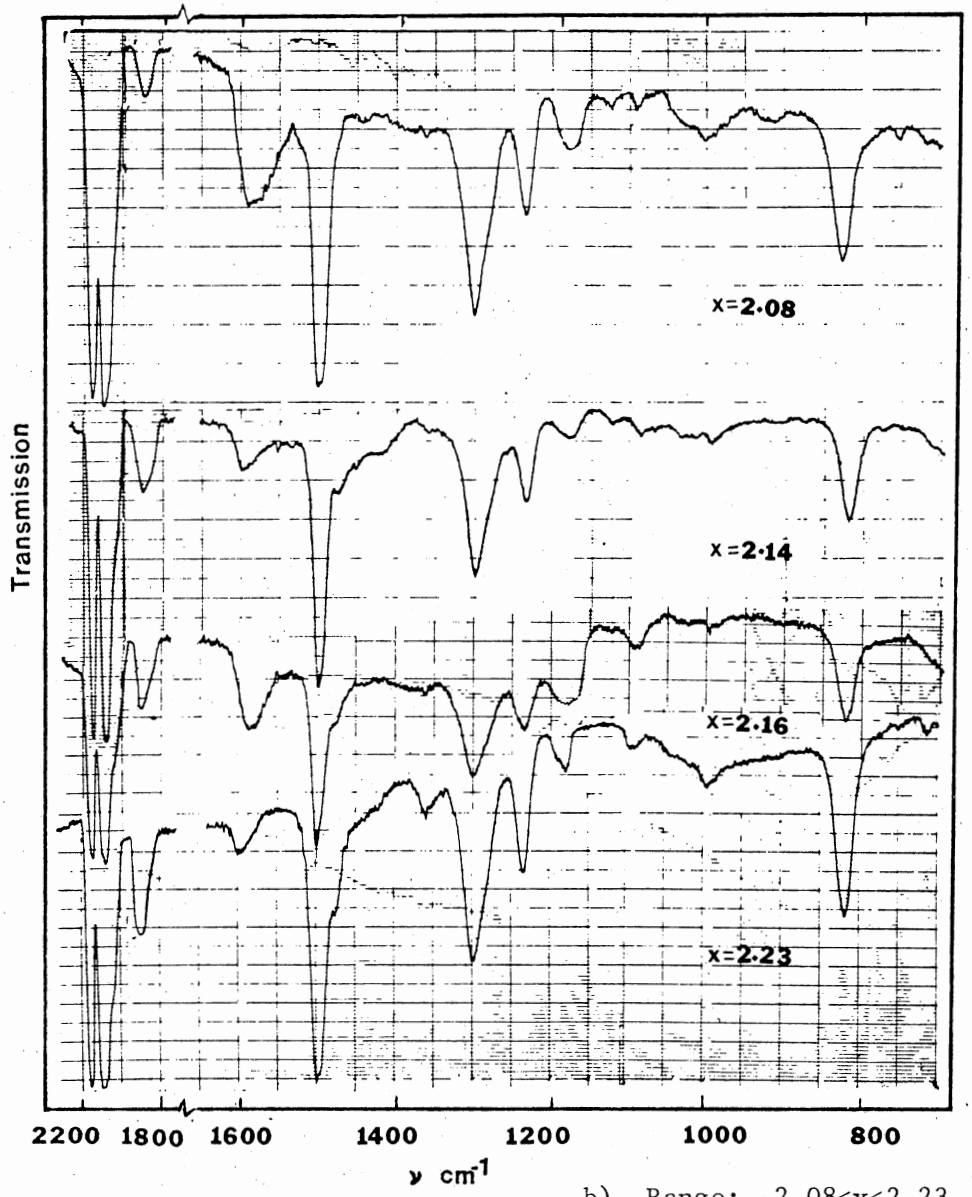

b) Range: $2.08 \leq x \leq 2.23$

Figure 13. (Continued)

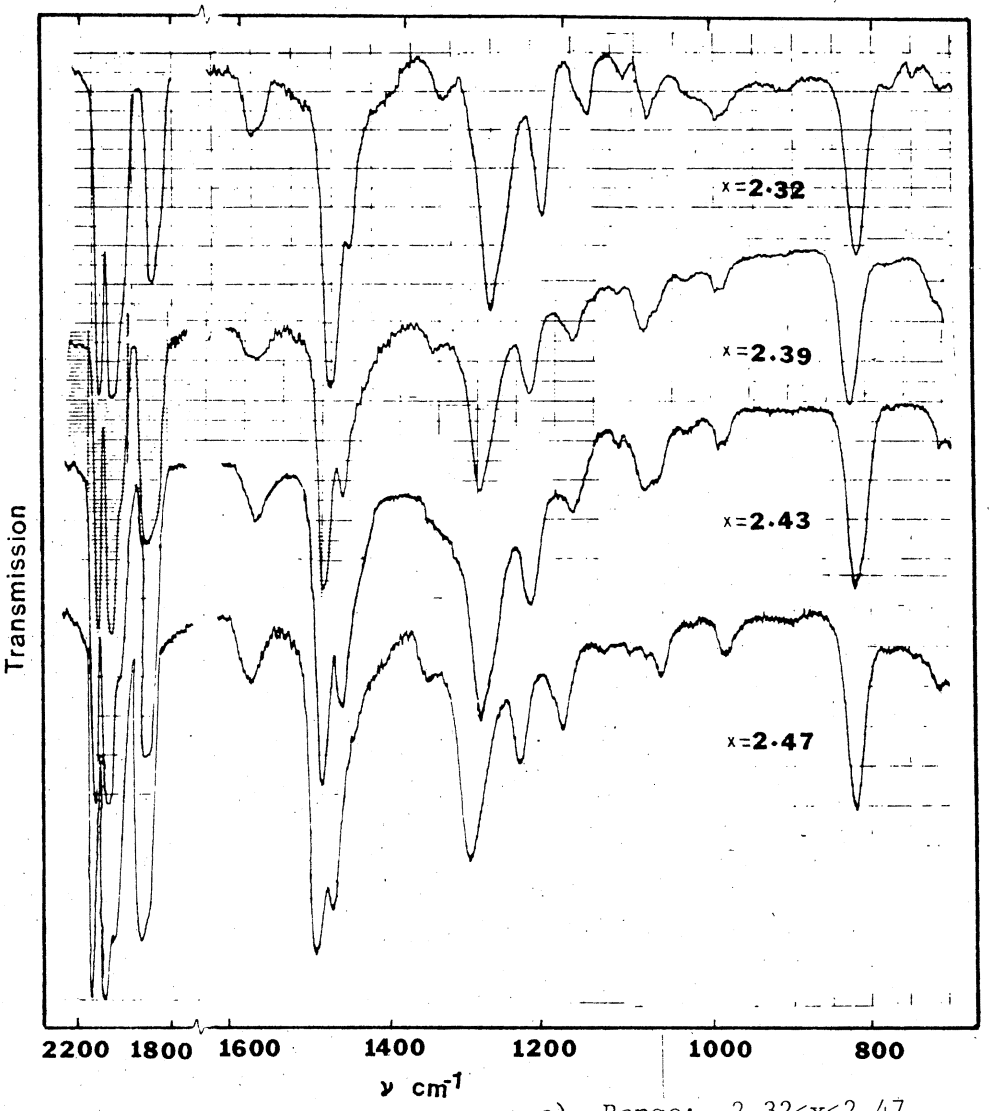

c) Range: $2.32 \leq x \leq 2.47$

Figure 13. (Continued)

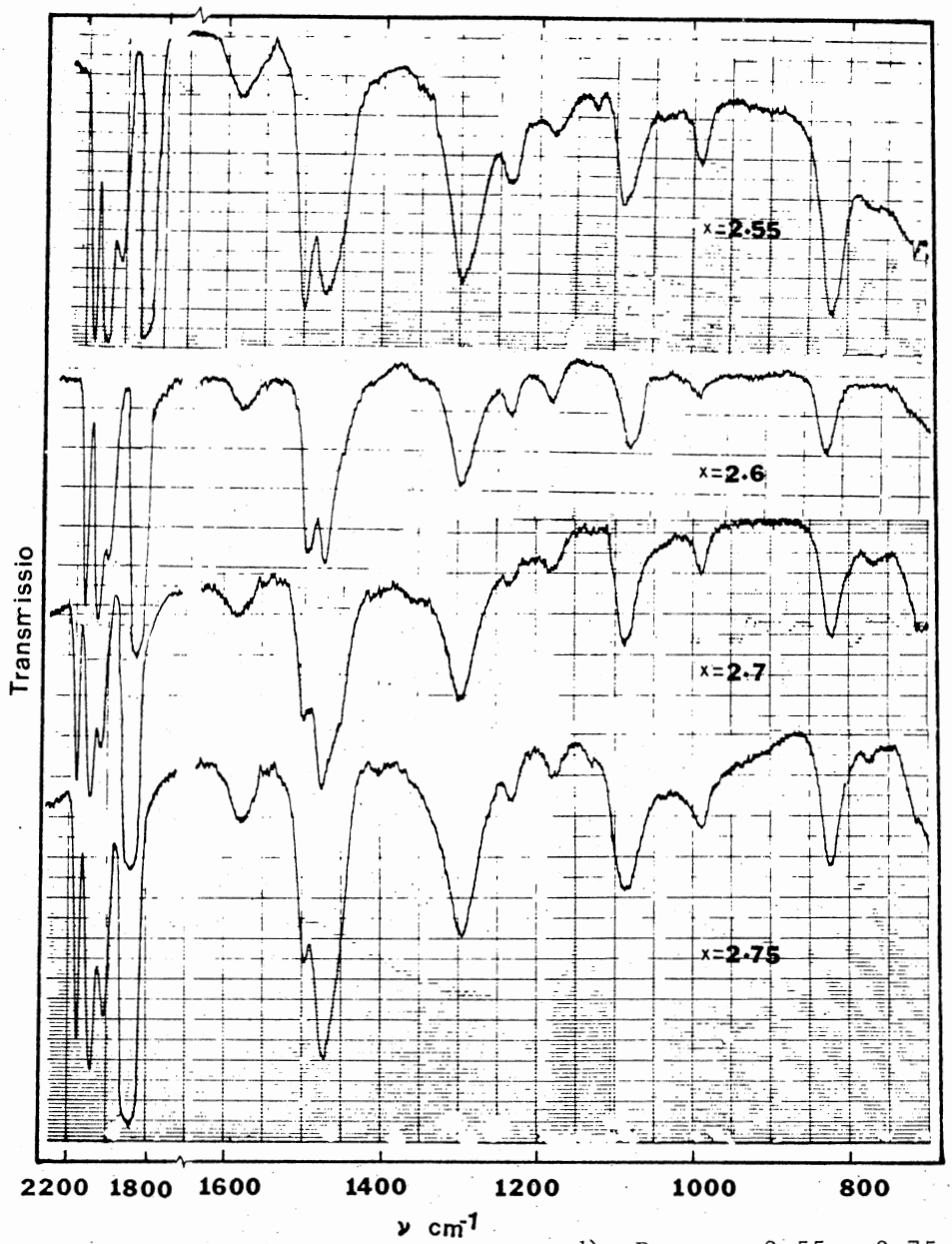

d) Range: $2.55 \leq x \leq 2.75$

Figure 13. (Continued)

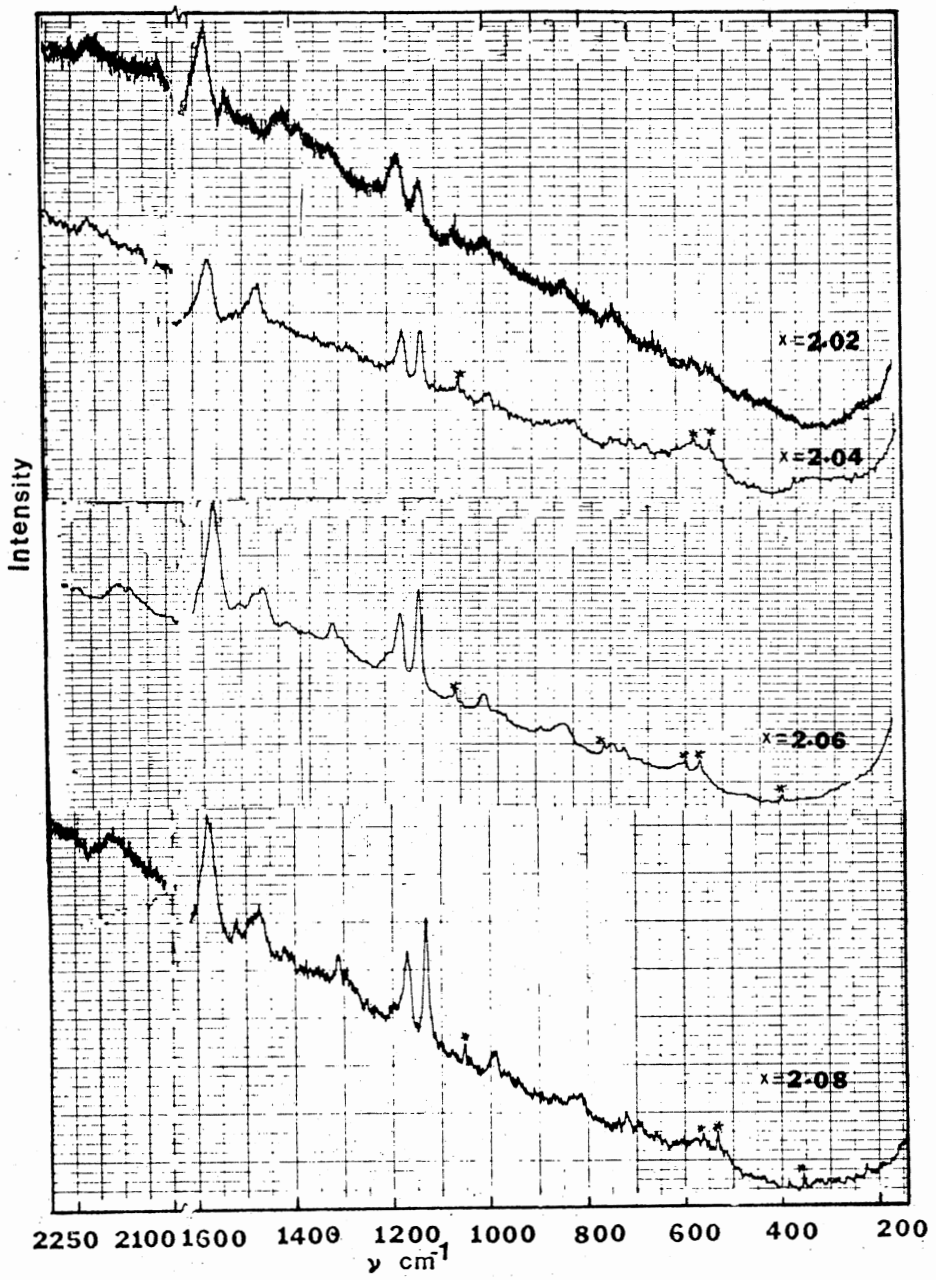

* Laser Emission Lines a) Range: $2.02 \leq x \leq 2.08$

Figure 14. Raman Spectra of Nonstoichiometric Salts in a Range, $2.0 \leq$ Na/TCNQ ≤ 3.0, for the 4880°A Laser Excitation Line

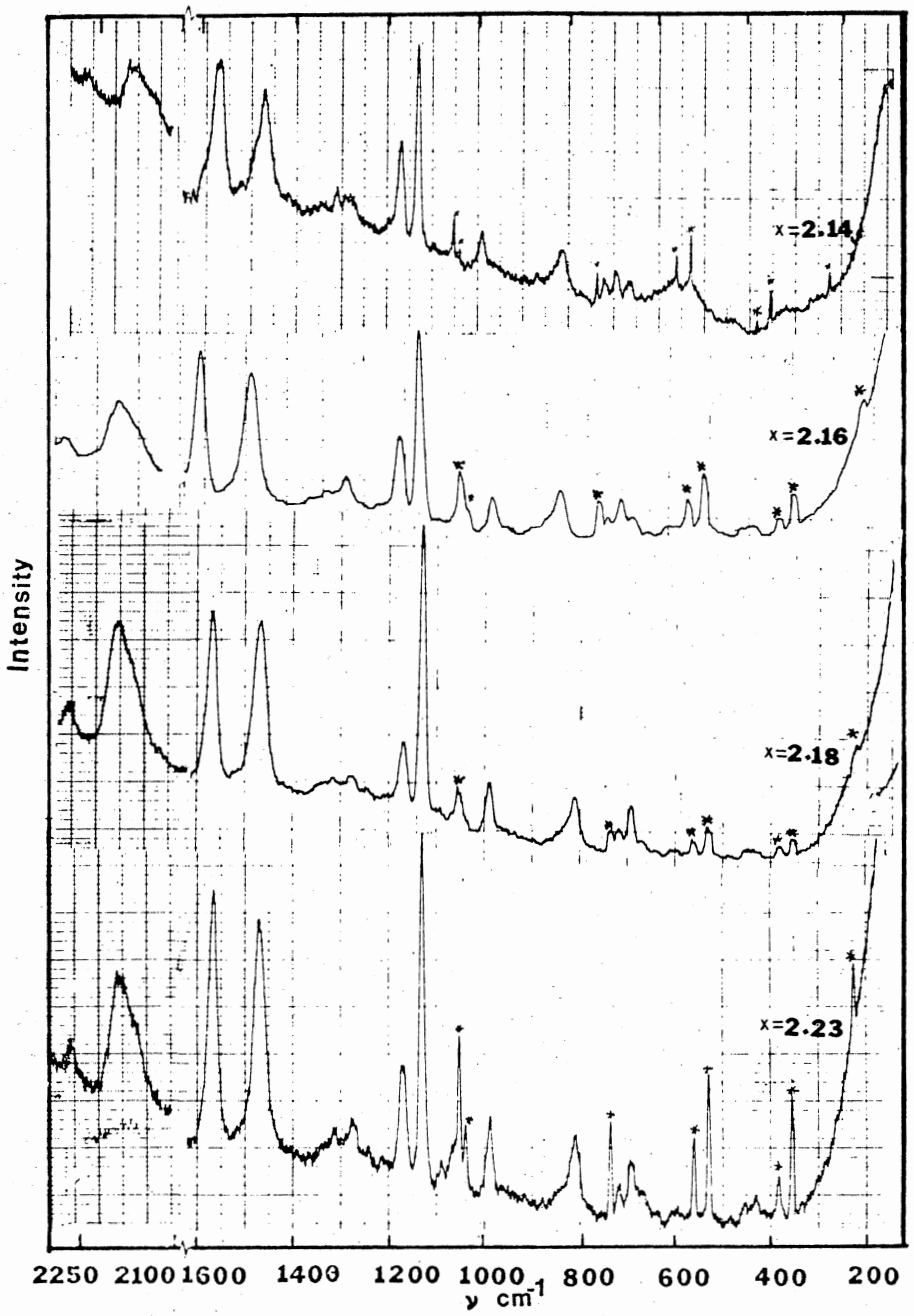

* Laser Emission Lines

b) Range: $2.14 \leq x \leq 2.23$

Figure 14. (Continued)

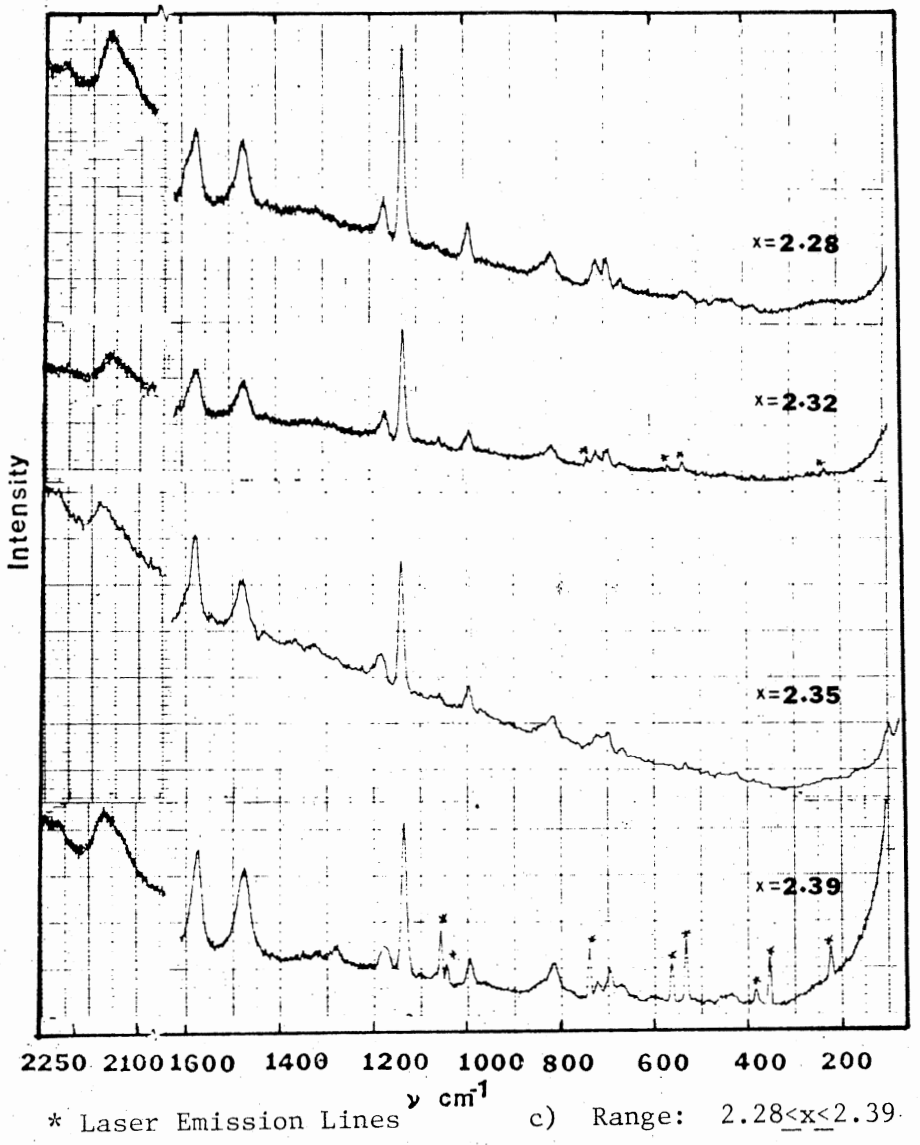

* Laser Emission Lines c) Range: $2.28 \leq x \leq 2.39$

Figure 14. (Continued)

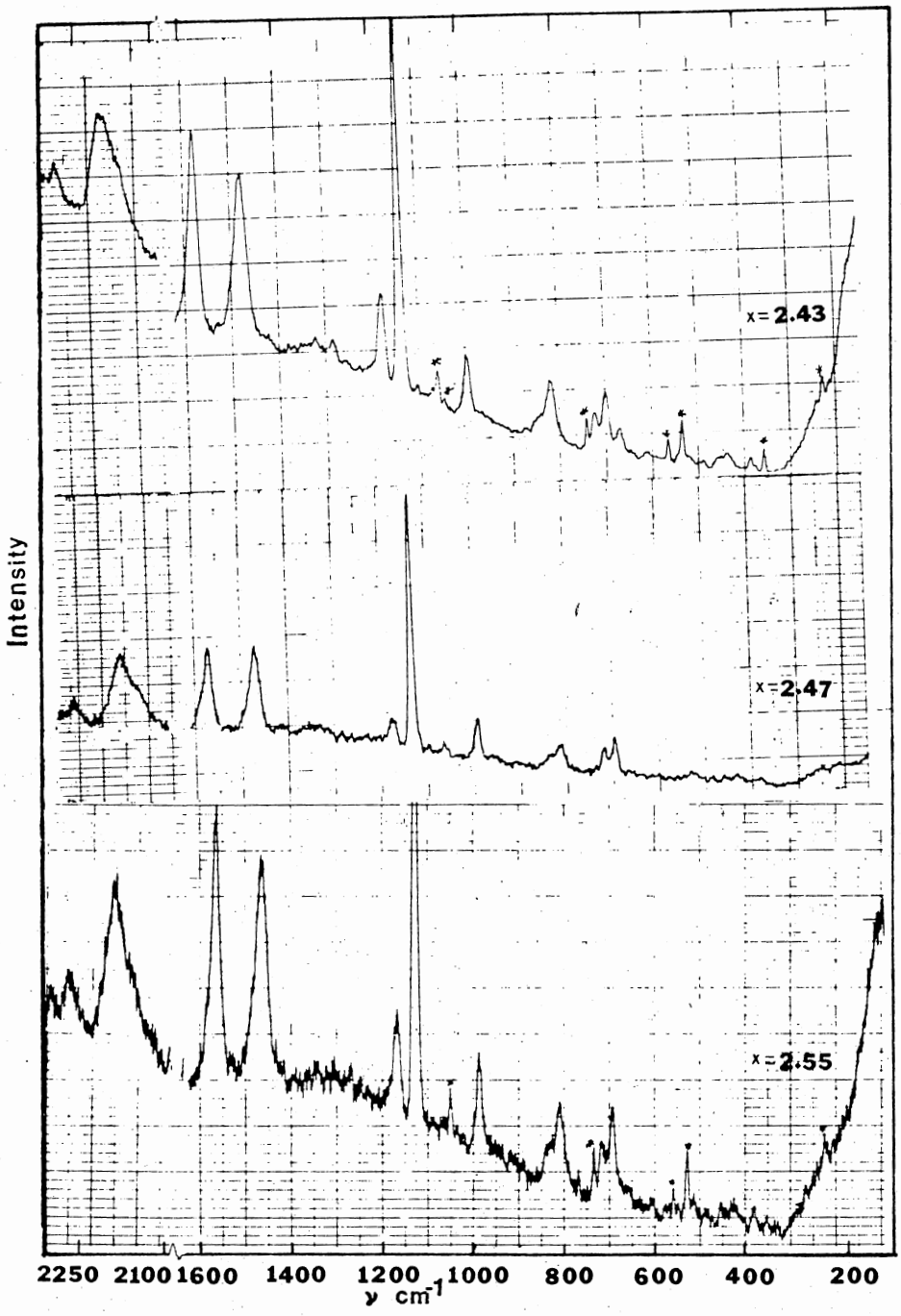

* Laser Emission Lines

d) Range: $2.43 \leq x \leq 2.55$

Figure 14. (Continued)

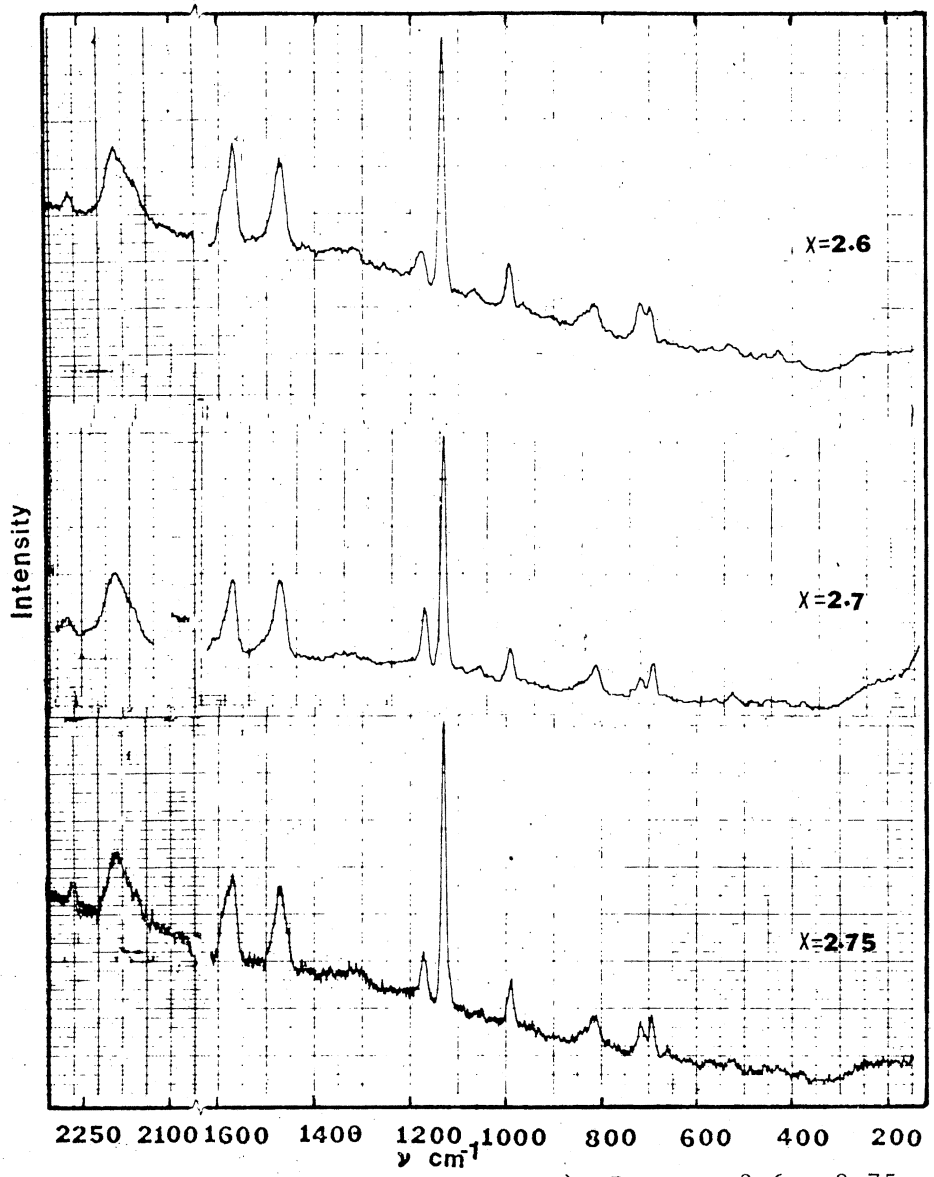

e) Range: $2.6 \leq x \leq 2.75$

Figure 14. (Continued)

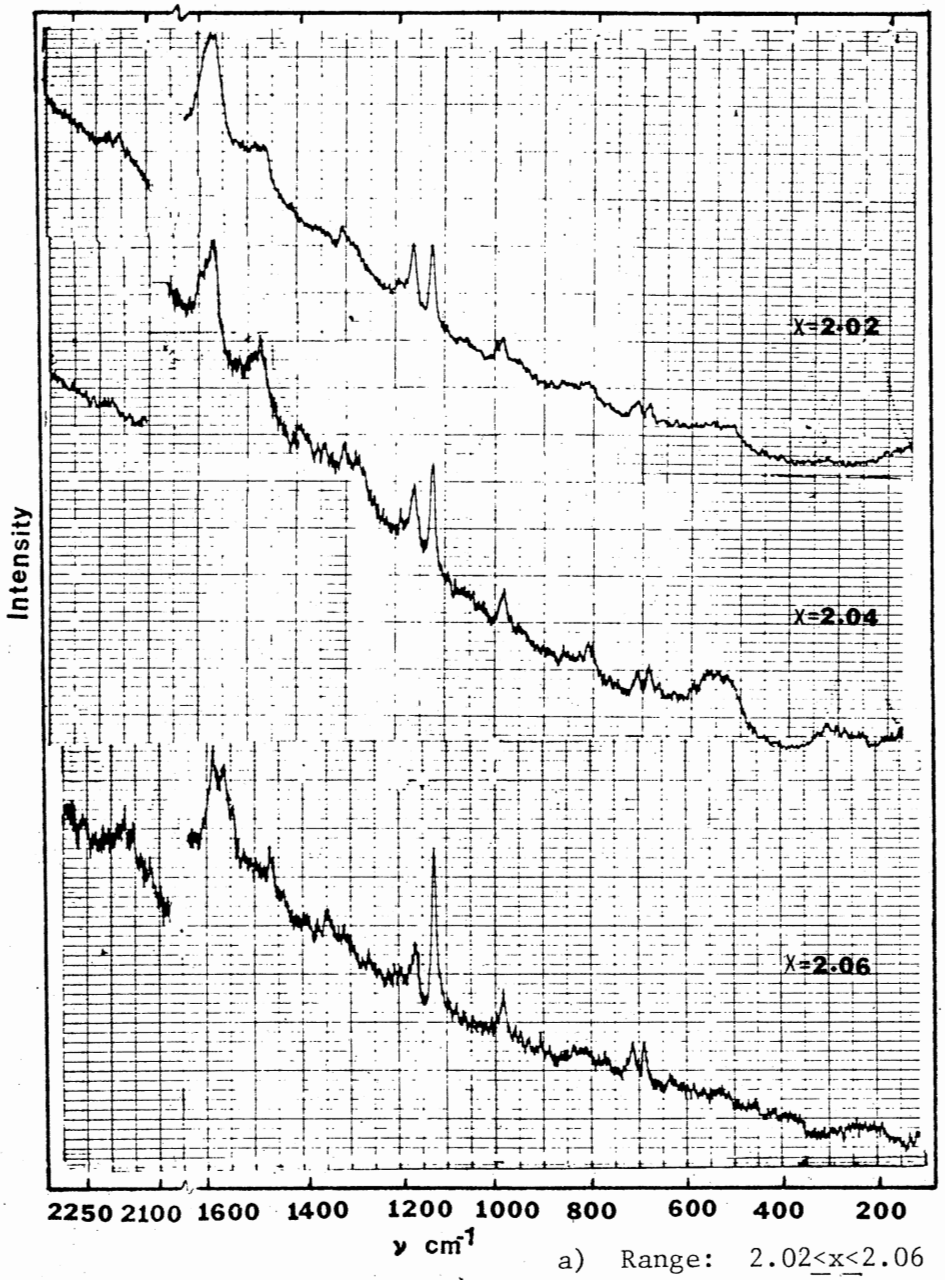

a) Range: $2.02 \leq x \leq 2.06$

Figure 15. Raman Spectra of Nonstoichiometric Salts in a Range, $2.0 \leq Na/TCNQ \leq 3.0$, for the 5145°A Laser Excitation Line

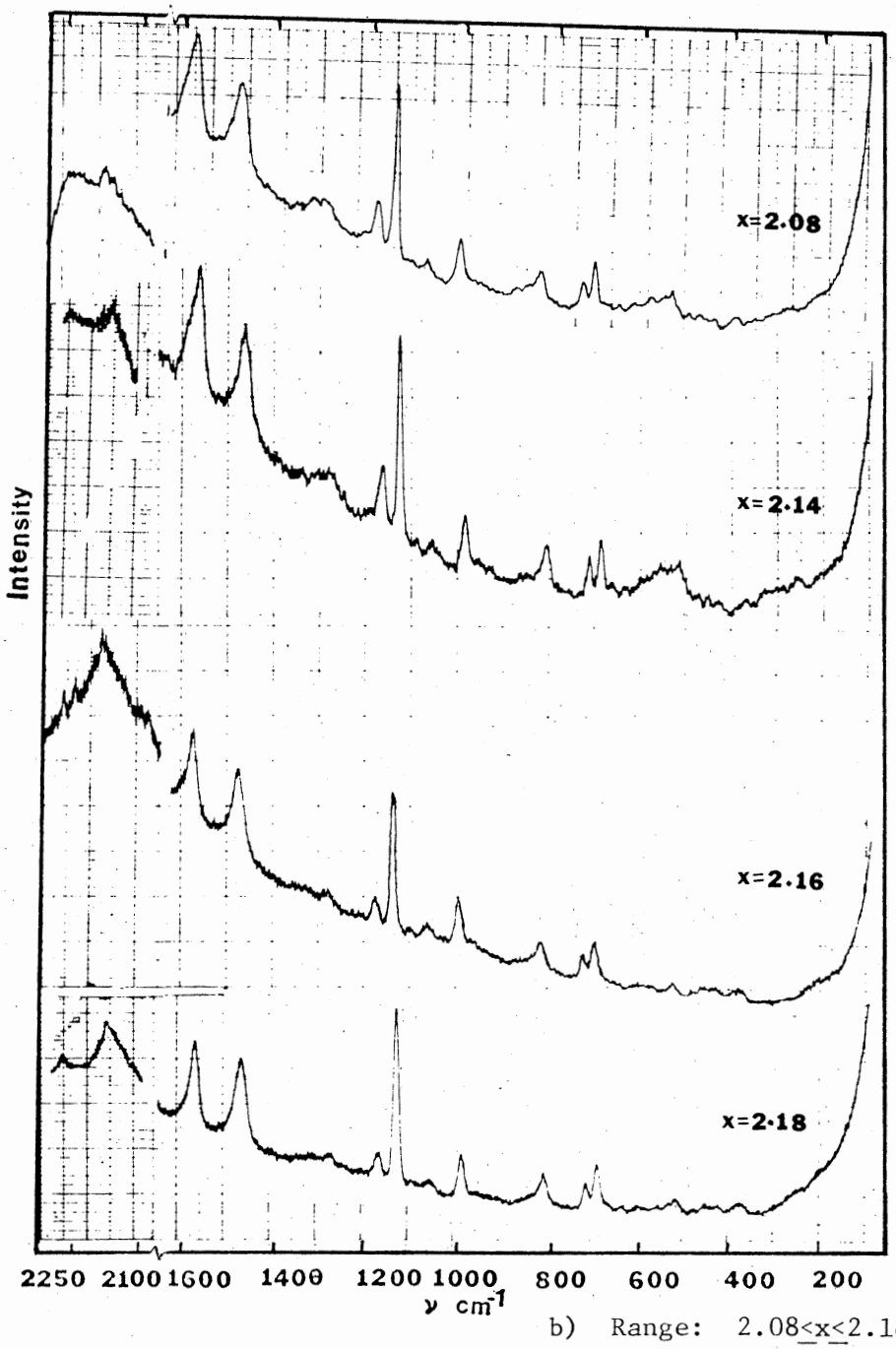

b) Range: $2.08 \leq x \leq 2.18$

Figure 15. (Continued)

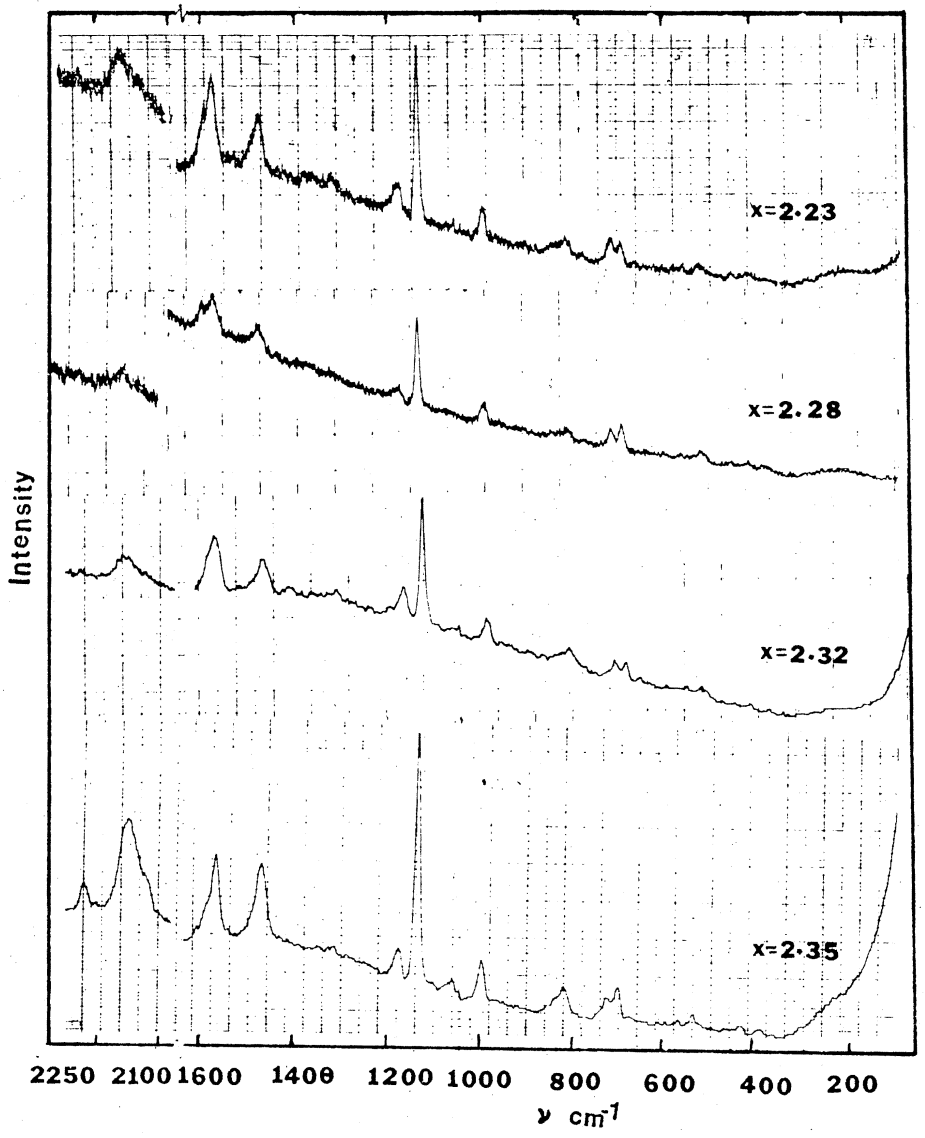

c) Range: $2.23 \leq x \leq 2.35$

Figure 15. (Continued)

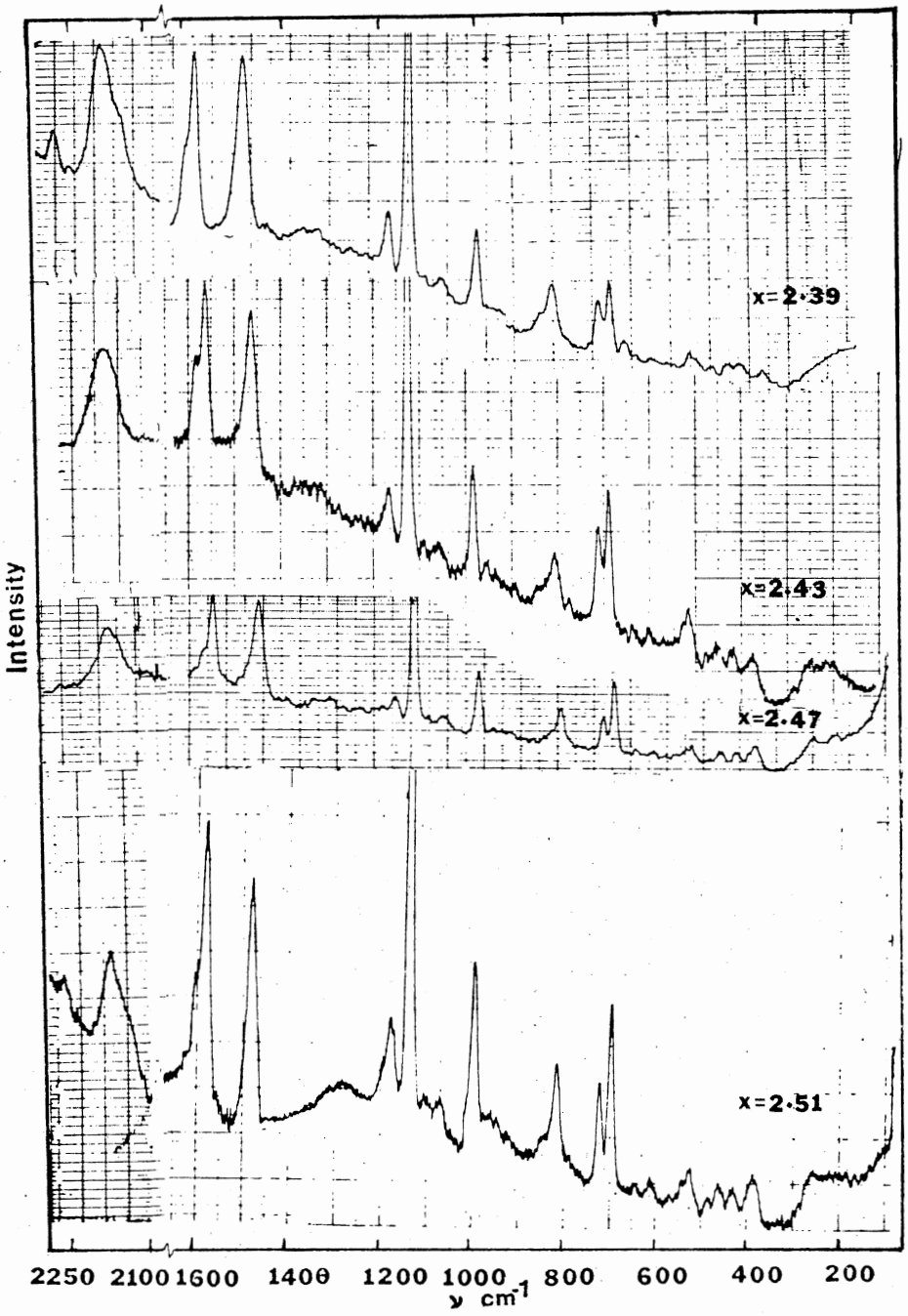

d) Range: $2.39 \leq x \leq 2.51$

Figure 15. (Continued)

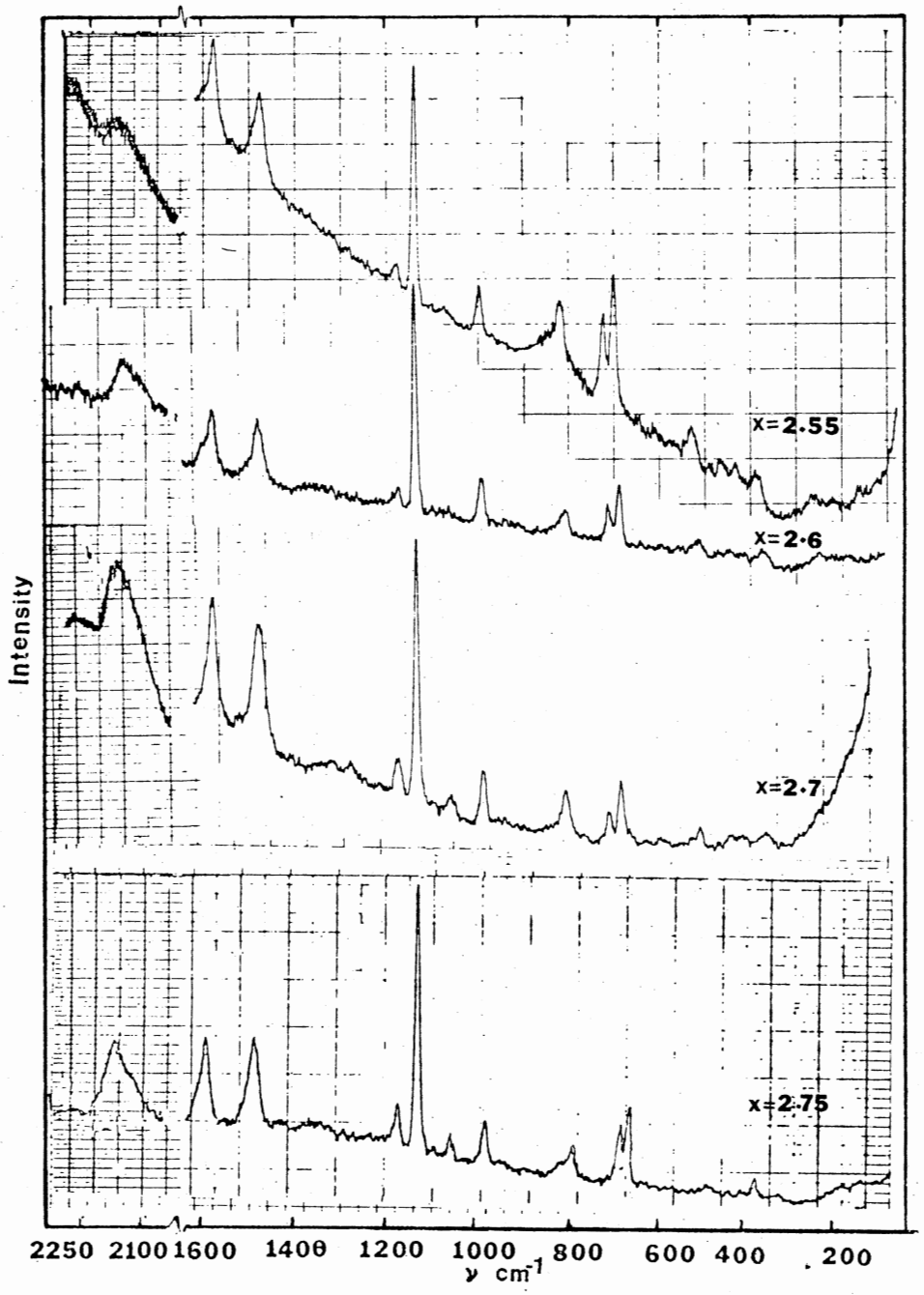

e) Range: $2.55 \leq x \leq 2.75$

Figure 15. (Continued)

stoichiometric salts in the $2.0 \leq x \leq 3.0$ range were recorded. One such spectrum is given in Figure 8. The intensity and frequency of the electronic bands for the nonstoichiometric $Na_{2.2}TCNQ$ are at different wavelengths from the Na_2TCNQ and Na_3TCNQ electronic bands. The nonstoichiometric salt shows electronic absorption bands at 190, 220, 252, 221, 330, and 430 mμ . Particularly, the 427 mμ electronic band of $TCNQ^{-3}$ seems to show some bathochromic shift when the $TCNQ^{-2}$ concentration is high in the nonstoichiometric salts.

In the IR spectra of nonstoichiometric salts in this range, the intensity of IR bands at 780, 1073, 1090, 1476 and 1901 cm^{-1} increases with increasing value of x (Figure 13a, b, c, d). The frequencies of the dianion and trianion bands do not show any significant change in the nonstoichiometric salts with a change in composition.

Since both the laser excitation lines at 4880°A and 5145°A lie within the 427 m electronic absorption band of $TCNQ^{-3}$ (Figure 8, inset part), the changes in intensity of the Raman bands with composition may be associated with shifts of this electronic band. The relative intensity of the 698, 722, 780, 820, 840, 842, 1138, 1476 and 2163 cm^{-1} RR bands with respect to the 1579 cm^{-1} band intensity increases with increasing value of x. The 1138 cm^{-1} band is most sensitive to the composition of the nonstoichiometric salts in this range. The intensity of the 1183 cm^{-1} band relative to the 1579 cm^{-1} band decreases with increasing concentration of $TCNQ^{-3}$ in the sample. Since this band is very close to the 1194 cm^{-1} band of the dianion some of the reduction in the intensity of the 1183 cm^{-1} band may be attributed

to the decrease in the concentration of $TCNQ^{-2}$. The maximum RR intensity enhancement of the 698, 722, 1138, 1476, and 2163 cm^{-1} bands was observed in the composition range $2.35<x<2.55$.

The movement of the electronic bands from the changing intensity patterns of the RR spectrum of $TCNQ^{-3}$, as in the case of NaTCNQ cannot be described for the lack of reference intensity patterns of the 3:1 stoichiometric salt at different excitation wavelengths. It seems that the 427 mμ band may have originated from asingle electronic transition in which case changing intensity pattern may be due to the bathochromic shift of this electronic band.

Interaction of TCNQ Anions with Oxygen

As mentioned earlier, the study of the reaction of oxygen with the anions of TCNQ was done for the following reasons, a) several spectroscopic results (80-83) attributed to the di- and trianions should be reexamined for the possibility of contamination by the oxygen reaction products, b) these oxygen reaction products themselves show interesting physical properties (138) (139), c) it is essential to distinguish the spectra of TCNQ anions from their reaction products.

NaTCNQ and Oxygen

Though electrical conductivity, energy of activation and the sign of the charge carrier changes when NaTCNQ reacts with oxygen (138) (139), little change in the electronic or vibrational spectra was observed. However, monoanion salts prepared by the solution method (19) (91) (113) may be contaminated by α,α-$DCTC^{-}$ (130). NaTCNQ prepared by co-condensation methods in vacuum, does not show any significant change in the spectra when exposed to dry oxygen.

Na_2TCNQ and Oxygen

The reaction product of $TCNQ^{-2}$ and oxygen in solution was identified (76) as α,α-$DCTC^-$. A possible reaction mechanism of a two step radical reaction of O_2 or π^2a cycloadditon has been suggested (76). In this study this reaction was reexamined in the solid state.

When Na_2TCNQ, a colorless salt was exposed to dry oxygen, the electronic spectrum observed for the reaction product is shown in Figure 16. The electronic absorption bands for the blood red colored reaction product were observed at 842, 760, 470, 420, 335, 275, 220 and 190 mμ (Table II and V). The electronic absorption bands for α,α-$DCTC^-$ prepared by reaction of TCNQ and $NaNO_2$ were observed to be at 480, 330 and 280 mμ (19). The O_2 decomposition products of $TCNQ^{-2}$ in solution show electronic bands at 477, 330 and 290 mμ (36) (76). The additional electronic bands observed in the reaction products of Na_2TCNQ in solid state may be attributed to the TCNQ monoanion formed by the reaction,

$$Na_2TCNQ+O_2 \rightarrow NaO_2+NaTCNQ$$

Thus, the O_2 reaction product of Na_2TCNQ may be a mixture of α,α-$DCTC^-$, NaO_2 and NaTCNQ. Another indication of the presence of NaTCNQ in the reaction product was observed in the vibrational spectrum. Also when the red colored reaction product was exposed to the atmosphere the color of the sample changed to dark blue. The electronic bands attributed to $perylene_3$ (TCNQ) (83) at 930, 470, 438 and 420 mμ indicate the presence of perylene, α,α-$DCTC^-$, perylene-TCNQ and neutral TCNQ.

When the reaction product of Na_2TCNQ and O_2 was dissolved in acetone several additional electronic bands were observed. The

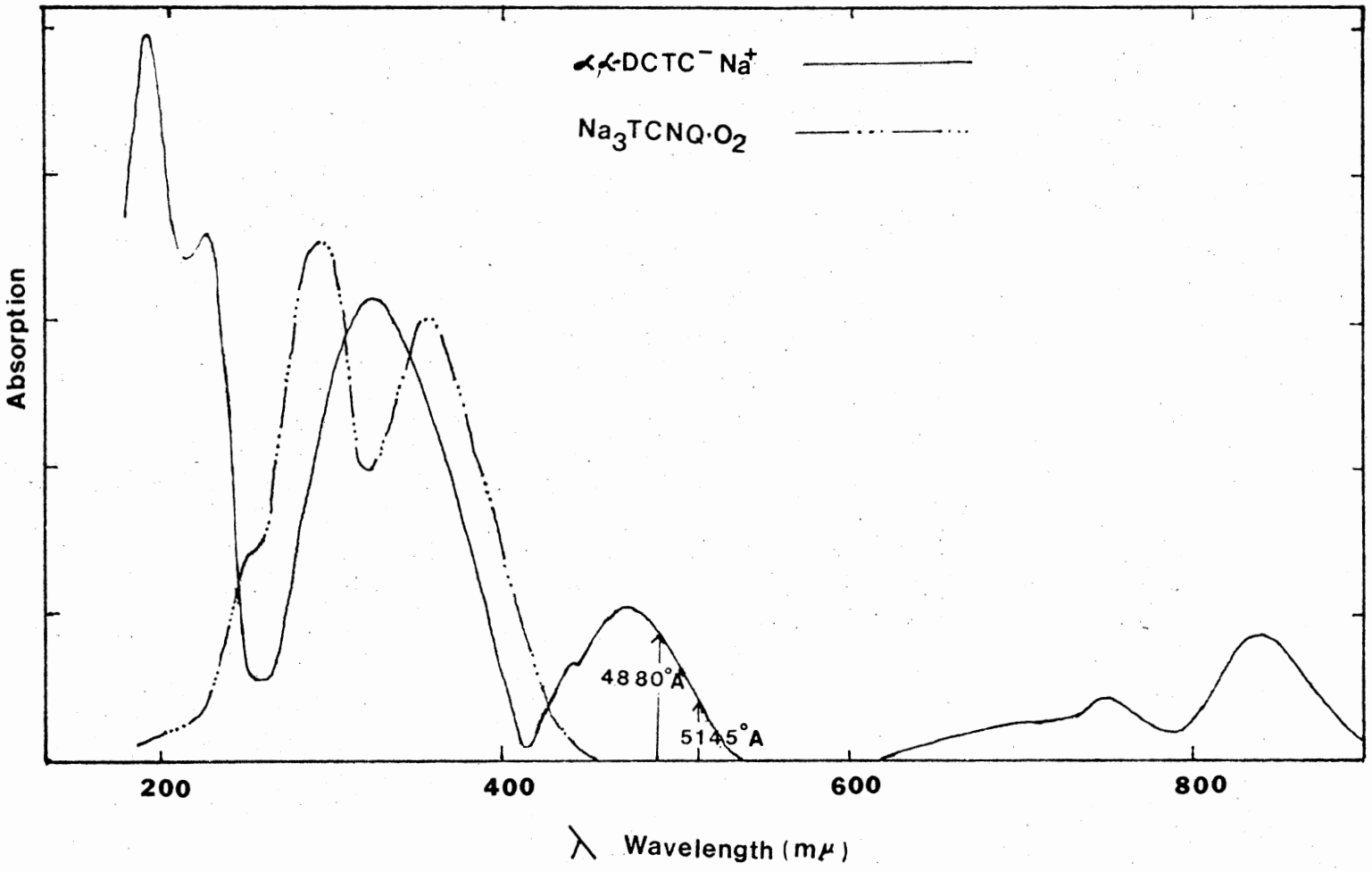

Figure 16. Electronic Spectra of α,α-$DCTC^-$(———) and $Na_3TCNQ \cdot O_2$ (—·—·—)

electronic bands for the acetone solution were observed at 845, 820, 760, 750, 725, 680, 665, 650, 640, 620, 610, 605, 550, 488, 477, 420, 335, 320, 317, 280, 228, 220, 208, 195, and 190 mμ. Such resolution of the electronic bands may possibly be a result of the solvent effects on the constituents of the reaction product, as well as their disintegration into some other product.

When the Na_2TCNQ reaction with dry oxygen was complete, IR and Raman spectra as shown in Figure 17 were observed. The IR bands at 835, 1590, 1635, 2150, 2180 and 2208 cm^{-1} can be identified with α,α-$DCTC^-$ (19) (76). Additional IR bands, not identified for $TCNQ^o$, $TCNQ^-$, $TCNQ^{-2}$ and α,α-$DCTC^-$, at 600, 656, 746, 778, 1295, 1396, 1463, 1558, and 2102 cm^{-1} were also observed in the spectrum (Figure 17) which may belong to α,α-$DCTC^-$ or other reaction products. Many IR bands at 615, 720, 983, 989, 1187, 1326, 1346, 1505, 1590 cm^{-1} may be attributed to both $TCNQ^-$ and α,α-$DCTC^-$. The 1527 and 2220 cm^{-1} IR bands may possibly result from the neutral TCNQ formed when both sodium atoms of Na_2TCNQ react with oxygen.

Raman spectra of the O_2 reaction products with the 4880°A and 5145°A laser excitation lines were observed to be almost identical in their intensity patterns. The Raman spectrum of α,α-$DCTC^-$ reported in the literature (76) resembles the spectrum given in Figure 17. The Raman bands of α,α-$DCTC^-$ in the solid state appear to be somewhat broader than those reported in solution. The similarity of the RR intensity patterns at 4880°A and 5145°A is not unexpected since both the laser excitation lines are in the absorption region of only one electronic band (470 mμ) of α,α-$DCTC^-$ (Figure 16). The Raman bands which can

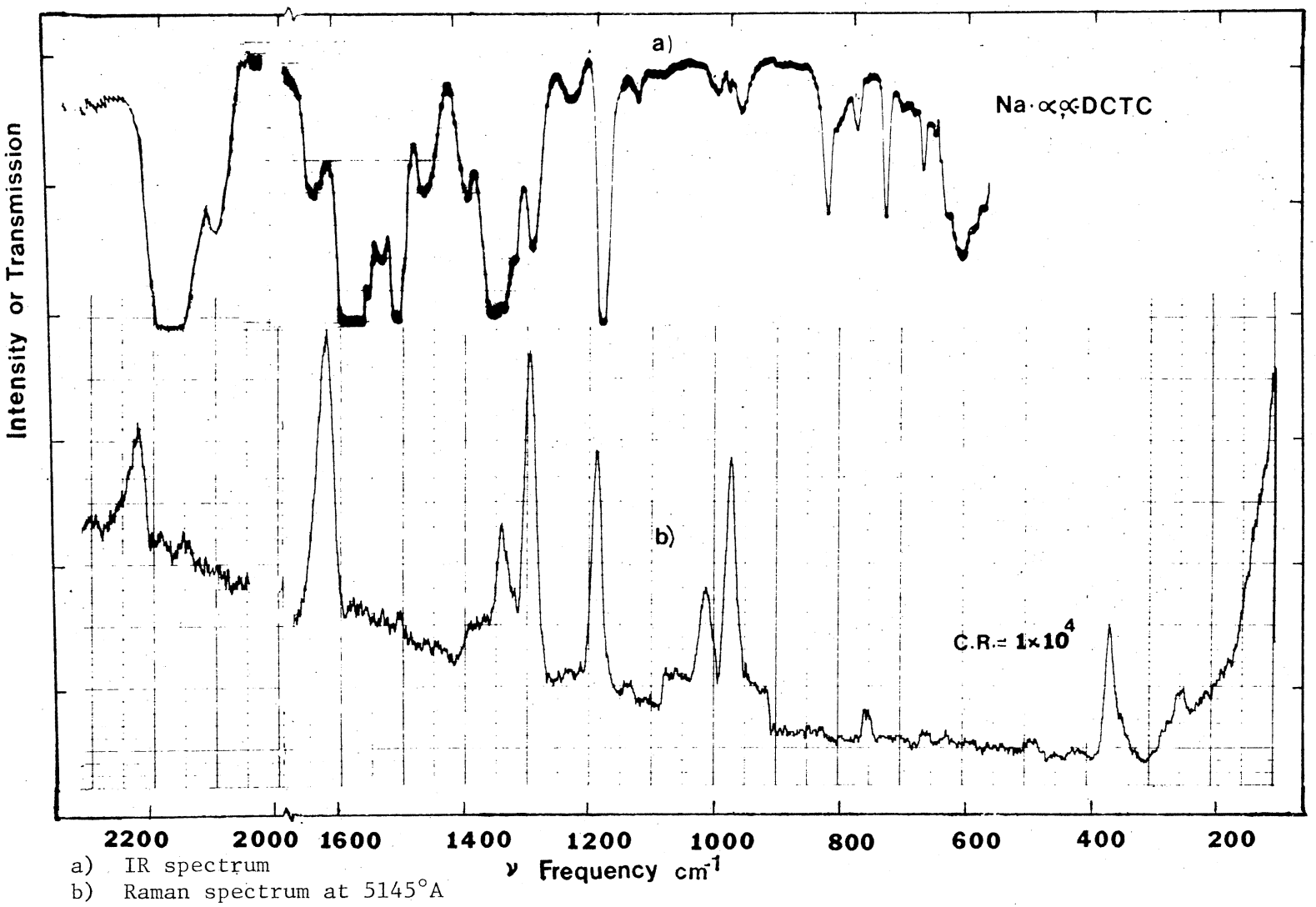

a) IR spectrum
b) Raman spectrum at 5145°A

Figure 17. IR and Raman Vibrational Spectra of α,α-DCTC$^-$

exclusively be identified with α,α-DCTC$^-$ were observed at 1638 and 2228 cm^{-1}. Other Raman bands at 356, 750, 983, 1188, 1346 and 1588 cm^{-1} are shifted from the corresponding $TCNQ^{\cdot-}$ monoanion Raman bands by a few wave numbers. New Raman bands at 1012, 1143, 1505 and 1635 cm^{-1} appeared in the spectrum because the center of symmetry of the TCNQ molecule is destroyed with the substitution of one of the C-C≡N groups by oxygen, so the mutual exclusion principle is no longer applicable. Even though many IR and electronic bands of $TCNQ^{o}$ and $TCNQ^{\cdot-}$ appeared in the reaction product, their Raman bands were not detected probably because of a larger concentration and stronger RR enhancement of α,α-DCTC$^-$ modes.

Tentative vibrational band assignments for the oxygen reaction products of Na_2TCNQ and Na_3TCNQ is given in Table XI. These assignments are made from analogy to those of the mono- and dianions. The 1635 cm^{-1} bands has been assigned to C=O by Melby et al. (19).

Another interesting RR spectrum for an interaction product of O_2 with the dianion was observed when limited amounts of oxygen were introduced into the vacuum reaction cell. In this case, two strong and very broad Raman bands (band width $\sim$130 cm^{-1}) were observed around 350 and 550 cm^{-1} (Figure 18). A change in the laser excitation line or composition (to some extent) did not alter the shape or position of these bands. These unusual Raman bands for the pinkish orange samples were observed only when the composition was in the vicinity of x=2.0 (x=1.9, 2.0 and 2.1, Figure 18). The other Raman bands in these samples were the same as for the mono-, di- and trianion salts. The IR bands for the corresponding samples were not

TABLE XI

THE OBSERVED VIBRATIONAL FREQUENCIES OF $Na_2TCNQ \cdot O_2$ α,α-DICYANO-P-TOLUOYL CYANIDE AND Na_3-$TCNQ \cdot O_2$

$Na_2TCNQ \cdot O_2$	α,α-DCTC$^-$			$Na_3TCNQ \cdot O_2$		
Raman (cm^{-1})	IR (cm^{-1})	Raman (cm^{-1})	Assignments*	IR (cm^{-1})	Raman (cm^{-1})	Assignments*
		250				
350		356	$\delta^R_{C-C-C,\ C-C\equiv N}$		350	$\delta^R_{C-C-C,\ C-C\equiv N}$
				496		
				550	550	
550				578		
	600					
	615		$\delta_{C-C\equiv N}$			
	656			650		
	720					
	746	750	$\nu^R_{C-C},\ \nu^W_{C-C}$		740	$\nu^W_{C-C},\ \nu^R_{C-C}$
	778			780		
	835		γ_{C-C-H}	821		γ_{C-C-H}
	965	965		999	999	
	983	983	ν^W_{C-C}			
	989					
	1012	1012		1024	1032	
				1090		
	1143	1143				
	1187	1188	δ_{C-C-H}	1192	1191	δ_{C-C-H}
	1246			1238		
	1295	1296	ν^R_{C-C}			
	1326	1326		1303	1301	
	1346	1346	$\nu^R_{C=C},\ \nu^R_{C=C}$		1346	$\nu^R_{C=C},\ \nu^W_{C=C}$
	1354					
	1396	1396	$\nu^W_{C=C}$	1396		
	1463					
	1505	1505	$\nu^R_{C=C}$	1503		$\nu^R_{C=C}$
	1537					
	1558		$\nu^R_{C=C}$			
	1590	1588		1594	1595	$\nu^R_{C=C}$
	1635	1638	$\nu_{C=O}$		1620	$\nu_{C=O}$
	2102					
	2152			2096	2096	
	2188		$\nu_{C\equiv N}$	2158	2196	$\nu_{C\equiv N}$
	2208	2228				

* ν = stretching
δ = in-plane bending
γ = out-of-plane bending
R = ring
W = wing

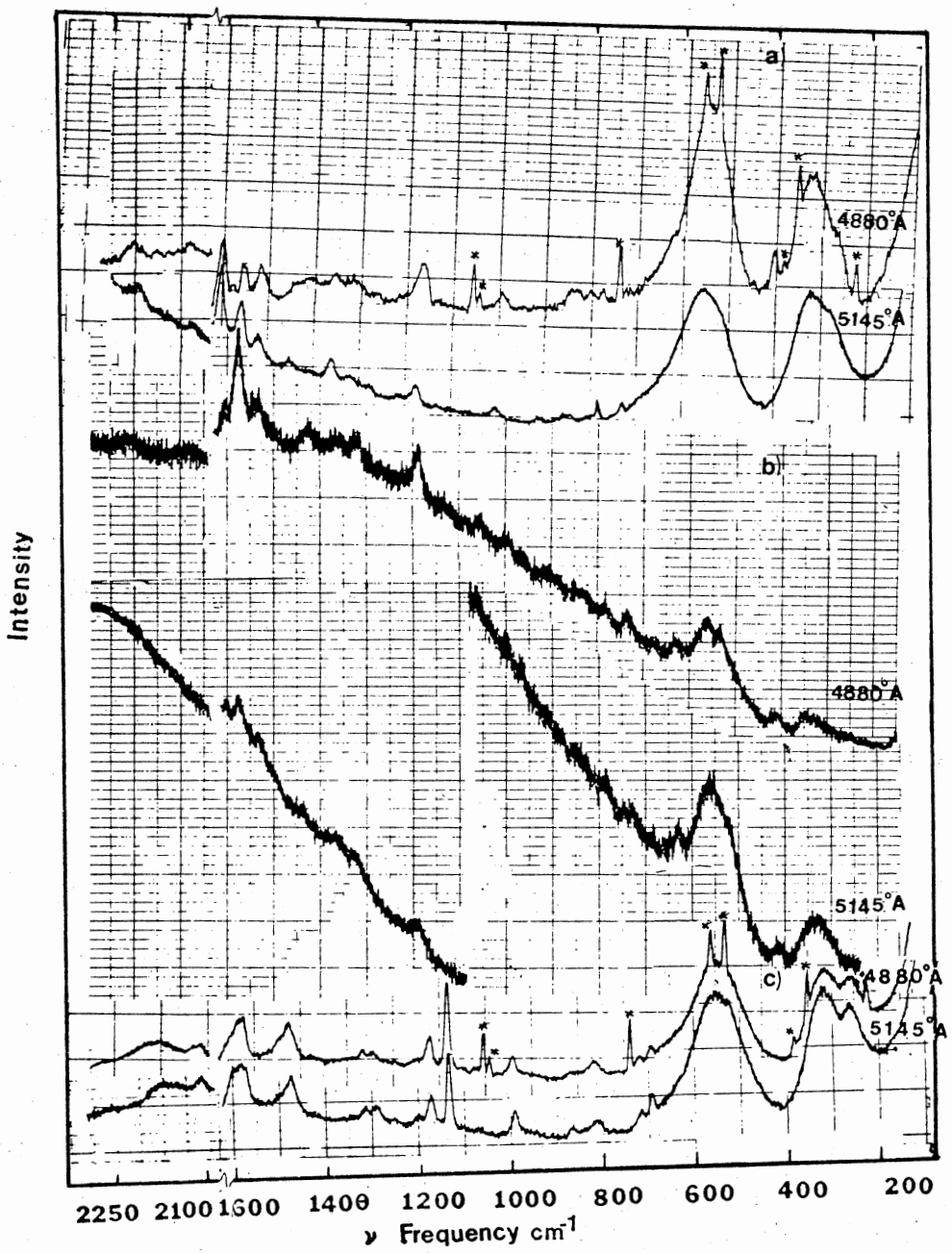

* Laser Emission Lines

Figure 18. Raman Spectra of a) $Na_{1.9}TCNQ \cdot O_2$, b) $Na_2TCNQ \cdot O_2$ and c) $Na_{2.1}TCNQ \cdot O_2$ at 4880°A and 5145°A

much different from salts of composition x=1.9, 2.0 and 2.1. The only difference noticed was the appearance of a weak band at 1396 cm^{-1} and the intensity of the 1187 cm^{-1} band was slightly higher than normal possibly due to some α,α-$DCTC^-$ impurity.

Now the question of the presence of α,α-$DCTC^-$ in the 1:1 MTCNQ and its contribution to the altered intensity patterns, with change in the excitation wavelengths (Figure 2), will be discussed. Chi and Nixon's spectra (91) show the Raman bands at 356, 1005, 1181, 1295, 1630 and 2214 cm^{-1} which may have originated from α,α-$DCTC^-$, present in the sample. Paticularly, the 1630 and 2214 cm^{-1} bands certainly point out such a possibility. However, as discussed earlier, some of the above mentioned α,α-$DCTC^-$ bands may be common with the monoanion of TCNQ. Since substituting one oxygen for the C-C≡N group only changes the bonding structure in that part of the molecule but not for the rest of the molecule, there may be some similarity in the bond strengths and bond structure between the two, to produce vibrational bands at almost the same frequency. The change in structure and symmetry of the whole molecule in α,α-$DCTC^-$ as compared with $TCNQ^{\cdot-}$ is reflected in, a) new coincident IR and Raman bands at 1143, 1296, 1396 and 1505 cm^{-1}, b) increased relative intensity of 983, 1012, 1187, 1295 1346, and 1588 cm^{-1} Raman bands and c) some of the vibrational Raman bands like 347, 620 and 729 cm^{-1} of $TCNQ^{\cdot-}$ are shifted to 356, 654 and 750 cm^{-1} in α,α-$DCTC^-$.

For the nonstoichiometric salts, the RR intensity pattern changes either by changing the excitation wavelength or composition of the salt should not be attributed only to the presence of α,α-$DCTC^-$. Appearance of the 1638 cm^{-1} Raman band and the 835 and 1635 cm^{-1} IR bands in the

vibrational spectra should indicate the presence of α,α-DCTC^{-}. The presence of the 1583 cm^{-1} Raman band and the absence of the above mentioned bands may signify the absence of α,α-DCTC^{-}, though some common vibrational bands appear in both cases, particularly, the 347, 729, 967, 974, 1184, 1326, 1339, 1583 and 2168 cm^{-1} Raman bands can be attributed to the TCNQ monoanion radical. The presence of the above mentioned bands in the Raman spectra of MTCNQ crystals should be expected. These bands were not observed by Jeanmaire and VanDuyne (130) for the Raman spectra of TCNQ$^{\cdot-}$ in acetonitrile solution. The absence of these bands may be attributed to the fact that in an acetonitrile solution, TCNQ$^{\cdot-}$ has been observed to be predominantly in the monomeric form (63). The shape and wavelengths of the TCNQ$^{\cdot-}$ monomer electronic bands in acetonitrile are different than those of the dimer in the solid state (46) (47) (63). Hence, different intensity patterns of the RR spectrum, at the 4579^{o}A and 6471^{o}A laser excitation lines in the solid state, may not be observed in the CH_3CN solution.

Na_3TCNQ and Oxygen

As described in the experimental part, TCNQ^{-3} reaction with dry oxygen is slower than that of TCNQ^{-2}. An oxygen reaction product of TCNQ^{-3} was characterized by a color (Table II), electronic spectrum (Figure 16) and the vibrational spectra (Figure 19). A complete disappearance of the 1476 and 1901 cm^{-1} IR bands and the 698, 722, 1138, 1476 and 2163 cm^{-1} Raman bands of TCNQ^{-3} was taken as an indication of completion of the reaction. When the reaction product thus obtained was exposed to the atmosphere, the IR and Raman spectra did not change significantly over a long period of time.

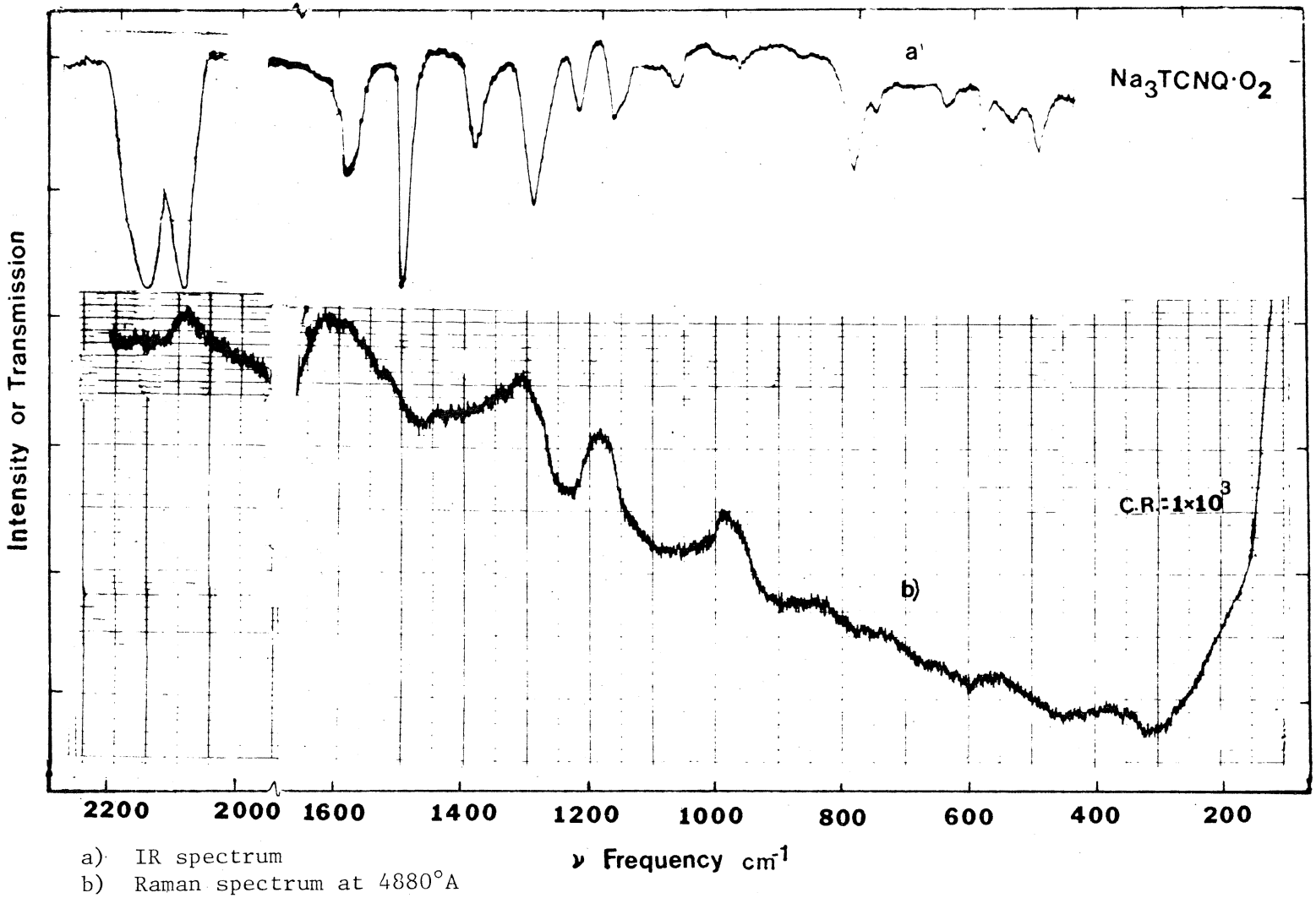

a) IR spectrum
b) Raman spectrum at 4880°A

Figure 19. IR and Raman Vibrational Spectra of $Na_3TCNQ \cdot O_2$

All the electronic bands of $Na_3TCNQ.O_2$ reaction products were observed to be in the uv region (Figure 16). Three electronic absorption bands at 352, 292, and 246 mμ of $Na_3TCNQ.O_2$ are at different wavelengths than the Na_2TCNQ electronic bands (Table 5). Since there is no electronic absorption in the region of the 4880°A and 5145°A laser lines the Raman spectrum is expected to be non resonant.

The IR and Raman spectra of the $Na_3TCNQ.O_2$ reaction product are almost identical to the Na_2TCNQ spectra (Figure 19). The band intensity and frequency of all IR and Raman features are the same as described for Na_2TCNQ. The only differences observed were extra IR bands at 1396 and 1620 cm^{-1} and a slightly higher intensity of the 1192 and 1594 cm^{-1} bands. The Raman bands of $Na_3TCNQ.O_2$ are broader as compared with the Na_2TCNQ bands. Weak broad bands at 350 and 550 cm^{-1} may be due to contamination with an oxygen complex of Na_2TCNQ described earlier. Higher intensity of the 1192 and 1594 cm^{-1} IR bands and presence of the 1396 cm^{-1} IR band as well as broadness of the Raman bands may be attributed to the α,α-$DCTC^-$ impurity. The vibrational band frequencies and their tentative assignments are listed in Table XI. The assignments are made on the basis of Na_2TCNQ band assignments.

No obvious explanation for the apparent relative stability of $TCNQ^{-3}$ towards oxygen or $Na_3TCNQ.O_2$ towards the atmosphere can be given. The possible reactions of Na_3TCNQ and O_2 may be given as

$$Na_3TCNQ+O_2 \rightarrow Na_2TCNQ+NaO_2$$

or

$$2Na_3TCNQ+O_2 \rightarrow 2NaO+2Na_2TCNQ$$

The oxide or peroxides of sodium may be forming a coating on the product sample thus slowing down the further reaction of O_2. Such a coating may also be responsible for the stability of $Na_3TCNQ.O_2$

towards the atmosphere. When $Na_3TCNQ.O_2$ was dissolved in acetone such coating is probably removed and a reaction of Na_3TCNQ and oxygen produces α,α-$DCTC^-$, giving the red color to the solution.

CHAPTER IV

RESULTS FOR SODIUM SALTS OF TCNE

The similarity between the physical and chemical properties of TCNE and TCNQ (1) (12) (13) as well as their monoanions, prompted the investigation of $TCNE^{-2}$ and $TCNE^{-3}$. Since TCNE is nothing but TCNQ minus the central ring, the comparison between their anions may help to understand the role of the central ring in stability, electrical conductivity and other physical properties of the TCNQ salts. Besides TCNE is a much simpler molecule, so the study of the nature and extent of vibronic interactions in the di- and trianions should be easier.

The vibrational spectra for the neutral TCNE (137) and its CT complexes (9) (10) (74) (109-111) have been studied extensively. The COV interaction has been shown to dominate the IR spectrum of TCNE monoanion radical (9) (75) (110). Since the results of the monoanion radical of TCNE will be used as reference in the vibrational band assignments of the di- and trianions, a brief survey is in order.

The IR bands of NaTCNE at 455, 463, 521, 530, 1385, 2188 and 2222 cm^{-1} and the Raman bands at 523, 530, 1380, 1430, 2188 and 2225 cm^{-1} were assigned to the a_g symmetry modes. The discrepancies between the IR and Raman frequencies of the bands assigned to the same a_g modes ($\sim$50 cm^{-1}) were attributed to factor group splittings (110). The only nonvibronic IR bands observed, were at 556 cm^{-1} (out-of-plane bending), 970 cm^{-1} (b_{1u}) and 1187 cm^{-1} (b_{2u}) (110). The intensity of the COV IR

bands was observed to be higher than that of the nonvibronic bands by an order of magnitude (75) (110).

Electronic Spectra: NaTCNE, Na_2TCNE and Na_3TCNE

The electronic band for the neutral TCNE which was observed at 265 mμ (34) (35) was assigned to the $^1B_{1u} \leftarrow {}^1A_g$ electronic transition (9) (Table XII). The electronic absorption bands of NaTCNE in the solid state were observed to be at 350 (3.54 eV) and 580 (2.14 eV) mμ. The $TCNE^{\cdot-}$ dimer electronic bands in MTHF solution were observed at 392 and 534 mμ (86). From the position of NaTCNE electronic bands it appears that $TCNE^{\cdot-}$ in the solid state, like $TCNQ^{\cdot-}$ may be in a dimer form. The observed electronic spectra for the anions of TCNE are shown in Figure 20.

For the colorless Na_2TCNE salts, the electronic absorption bands at 213 (5.82 eV) and 237 (5.23 eV) mμ were observed in the uv region. Since these electronic bands are far off from the 4880°A and 5145°A laser excitation lines, RR intensity enhancement of the dianion vibrational bands is not expected. Na_3TCNE, a yellow colored salt, shows four electronic absorption peaks at 210 (5.90 eV), 236 (5.25 eV), 265 (4.68 eV) and 365 (3.40 eV) mμ. Though the trianion salt is colored, the electronic absorption band at 365 mμ is somewhat away from the region of the 4880°A and 5145°A laser lines. Some electronic absorption activity seems to be near the laser lines, however, it is doubtful whether a RR spectrum of the trianion can be observed.

Since Na_3TCNE was contaminated by the dianion impurity, as well as some oxygen reaction products, the electronic and vibrational spectra should be interpreted with due caution.

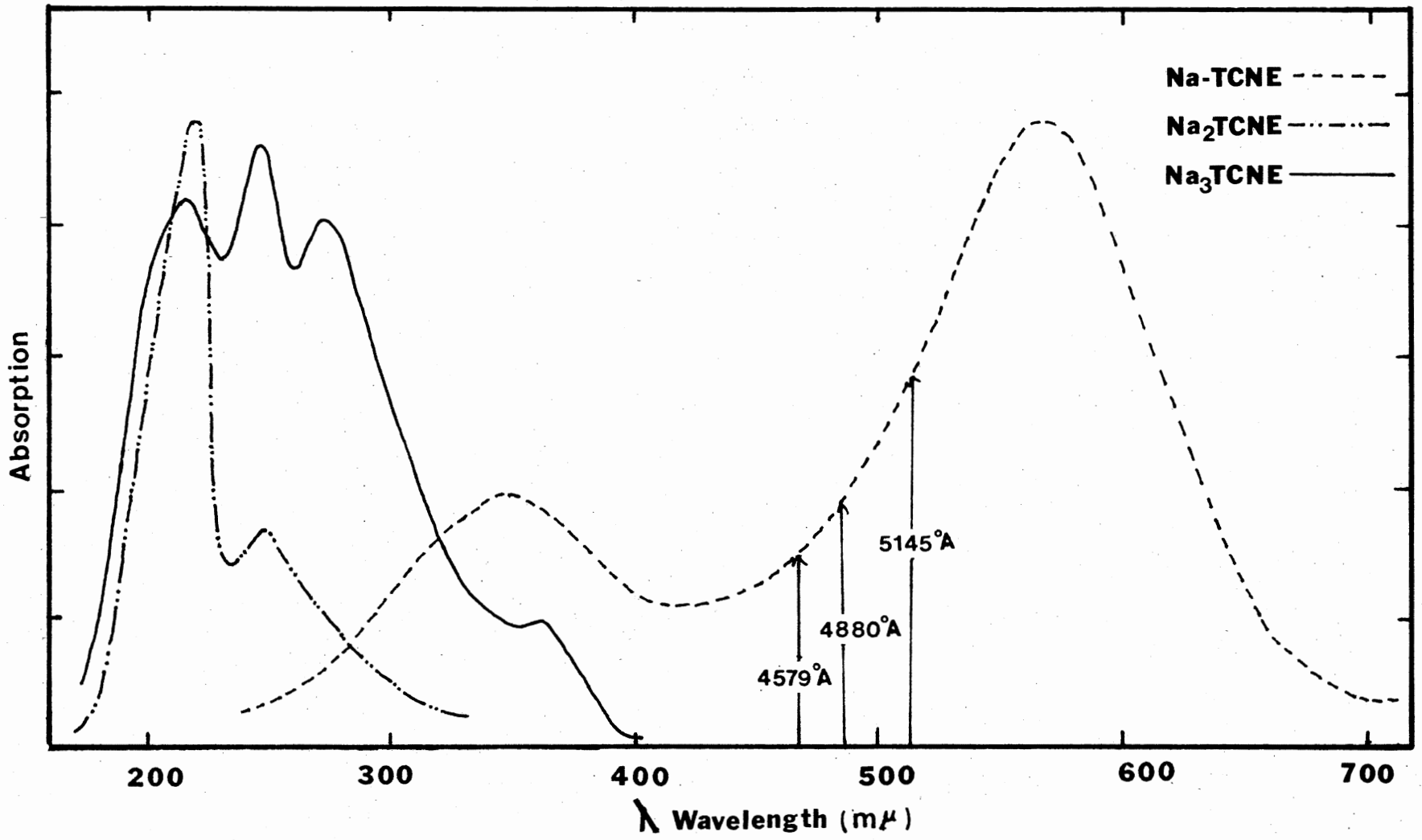

Figure 20. Electronic Spectra of NaTCNE, Na_2TCNE and Na_3TCNE in the Solid State

TABLE XII

THE OBSERVED AND CALCULATED ELECTRONIC BANDS OF TCNE, ITS SODIUM SALTS AND THE OXYGEN REACTION PRODUCTS

Compound	Observed Elect. Bands: Solid State (eV)	Observed Elect. Bands: Solution[c] (eV)	Calculated Elect. Bands[a] (eV)	Assignments[a]
TCNE (Neutral)	5.05[b]	5.06	5.136	$^1B_{1u} \leftarrow {}^1A_g$
Dimer	2.14	2.32		
NaTCNE	3.54	3.76		
or $TCNE^{\cdot-}$ Monomer		2.93	2.956	$^2B_{3g} \leftarrow {}^2B_{1u}$
Na_2TCNE or $TCNE^{-2}$	5.23 5.82			
Na_3TCNE	3.40 4.68 5.25 5.90			
$Na_2TCNE.O_2$	2.64			
$Na_3TCNE.O_2$	5.49 6.36			

[a] Reference 9

[b] Reference 85

[c] Reference 86

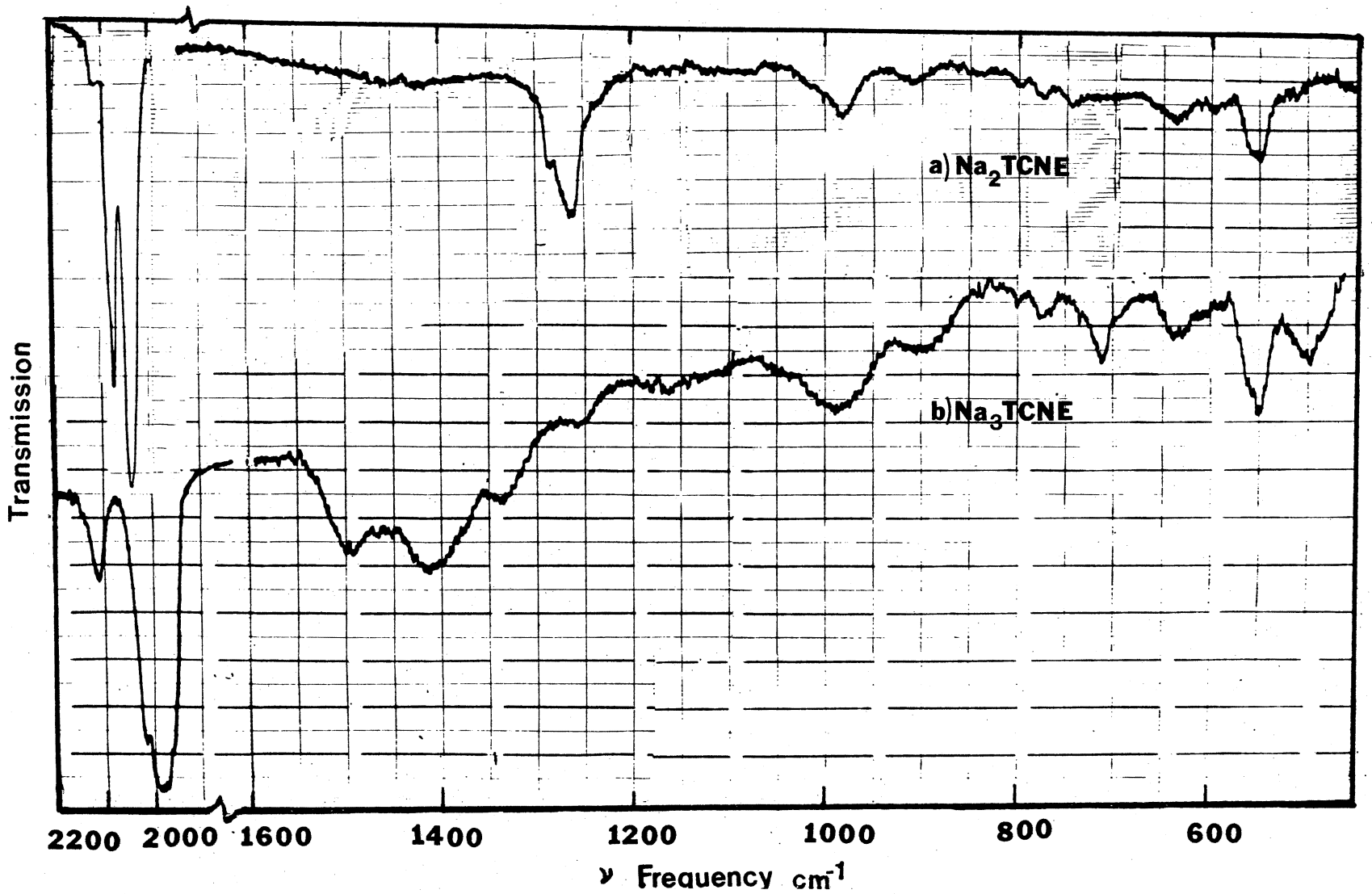

Figure 21. IR Spectra of a) Na_2TCNE and b) Na_3TCNE

Vibrational Spectra of Na_2TCNE

The IR spectrum of Na_2TCNE is shown in Figure 21. IR bands for the Na_2TCNE salt were observed at 418, 452, 546, 552, 558, 982, 1256, 1263, 1282, 1312, 2076 and 2146 cm^{-1}. Several additional IR bands in the region of 600-950 cm^{-1} were also observed in the spectrum of Na_2TCNE. However, these bands were also observed in the spectrum of Na_3TCNE and the oxygen reaction products of the di- and trianion so it is questionable whether these bands can be assigned to $TCNE^{-2}$. Some weak bands in the nonresonant Raman spectrum of the dianion were observed. Tentative assignments for the dianion vibrational bands are given in Table XIII. These assignments are made from an analogy to the neutral and monoanion vibrational spectra and the dianion is presumed to be of the D_{2h} molecular symmetry. The 546, 552, 1256, 1263, 1282, 1312, 2076 and 2146 cm^{-1} IR bands and the 549, 1265, and 2058 cm^{-1} bands are assigned to the a_g symmetry modes. Again as in the case of $TCNQ^{-2}$, there is uncertainty about the nature of the vibronic interactions which activate a_g modes in the IR spectrum. The intensity ratio (1256, 1263, 1282 cm^{-1})/2076 cm^{-1} for the dianion is quite less than that of the 1385/2188 cm^{-1} IR bands of $TCNE^{\cdot-}$. Thus relative intensity of the other a_g modes in the dianion IR spectrum is also reduced with respect to the monanion spectrum. Such intensity reduction may be attributed to the decreased extent of the vibronic interaction in $TCNE^{-2}$.

Other IR bands at 558 and 982 cm^{-1} are assigned to the ν_{23} (b_{3u}) and ν_{10} (b_{1u}) modes respectively. In the vibrational assignments, the convention for the vibrational mode numbers is adopted from Miller

TABLE XIII

THE OBSERVED VIBRATIONAL FREQUENCIES OF TCNE AND ITS ANIONS

TCNE Neutral[a]		NaTCNE[b]		Na_2TCNE		Na_3TCNE		
IR (cm^{-1})	Raman (cm^{-1})	IR (cm^{-1})	Raman (cm^{-1})	IR (cm^{-1})	Raman (cm^{-1})	IR (cm^{-1})	Raman (cm^{-1})	Assignments
119								$\nu_{18}\ ^{b}_{1u}$
	133							$\nu_{5}\ ^{a}_{g}$
		270	140		130			Libration mode
			160		156			
			170		178			
165								$\nu_{12}\ ^{b}_{1u}$
	250							$\nu_{22}\ ^{b}_{3g}$
	359							$\nu_{14}\ ^{b}_{2g}$
	416							$\nu_{8}\ ^{b}_{1g}$
428				418				$\nu_{24}\ ^{b}_{1u}$
443						432		$\nu_{17}\ ^{b}_{2u}$
	490	455		452				$\nu_{4}\ ^{a}_{g}$

TABLE XIII (continued)

TCNE Neutral[a]		Na_2TCNE[b]		Na_3TCNE			
IR (cm^{-1})	Raman (cm^{-1})	IR (cm^{-1})	Raman (cm^{-1})	IR (cm^{-1})	Raman (cm^{-1})	IR (cm^{-1})	Raman (cm^{-1})	Assignments
	510							ν_{21} b_{3g}
	535[b]	521	523	546	549	549	530	ν_3 a_g
		530	530	552		642	675	
554		556		558		558	560	ν_{23} b_{3u}
579								ν_{11} b_{1u}
	595							ν_{13} b_{2g}
				630				
	679							
				744		712		
				776		746		
				800		776		
				856		800		
				901		841		
						904		
958		970		982		995		ν_{10} b_{1u}
						1014	1020	
				[illegible]		1094		
						1172		

TABLE XIII (continued)

TCNE Neutral[a]		Na_2TCNE[b]		Na_3TCNE			
IR (cm^{-1})	Raman (cm^{-1})	IR (cm^{-1})	Raman (cm^{-1})	IR (cm^{-1})	Raman (cm^{-1})	IR (cm^{-1})	Raman (cm^{-1})	Assignments
1154		1187				1253		$\nu_{16}\ b_{2u}$
	1282							$\nu_{20}\ b_{3g}$
	1569	1385 1428[c]	1380 1430	1256 1263 1282 1312	1265	1346 1417 1498	1348 1456 1503	$\nu_2\ a_g$
	2235	2188 2222	2188 2225	2072 2086 2146	2068	1980 2032 2236	2062 2120 2160	$\nu_1\ a_g$
2230								$\nu_{15}\ b_{2u}$
	2247						2216	$\nu_{19}\ b_{3g}$
2263								$\nu_7\ b_{1u}$

[a] Reference 137

[b] Reference 110

[c] Observed in thick films of 1:1 stoichiometric salt

et al. (137). The strongest Raman bands at 130, 156 and 178 cm^{-1} are assigned to the librational modes in analogy to the $TCNE^{\cdot-}$ assignments (9) (110).

In the IR spectra of ZnTCNE and CdTCNE (10), vibrational bands at 985, 1260, 1305 and 2055 cm^{-1} have been observed. Other vibrational bands at 600, 690, 800, 925, 995 and 1155 cm^{-1} which may have originated from the oxygen reaction products have also been reported. IR activation of a_g symmetry modes of the dianion was attributed to the 'back-bonding' (10). The idea of back-bonding relates to the transfer of electron from TCNE anions to Zn^{+2} or Cd^{+2} cations. The vibronic interactions involved in the back-bonding may be responsible for the IR activation of a_g modes in the di- and trianions.

Vibrational Spectra of Na_3TCNE

The trianion alkali metal salt of TCNE, like Na_3TCNQ, is yellow colored. The IR spectrum of Na_3TCNE is shown in Figure 21. The vibrational bands of the trianion with tentative band assignments are listed in Table XIII. The 1980 cm^{-1} band was assigned to the C≡N stretching mode of $TCNE^{-3}$ (75). There are four IR bands in the 1250-1500 cm^{-1} region, probably originated from the C=C stretching modes. Only one of these IR bands at 1256 cm^{-1} appears in the dianion spectrum. This band is assigned to the trianion also, because with an increasing concentration of Na_3TCNE in the sample, no significant reduction in its relative intensity (as compared with the 2086 cm^{-1} band) was observed. The vibrational band assignments of the trianion are made under the same considerations as described for the dianion. Thus, the 549, 642, 1346, 1417, 1498, 1980 and 2032 cm^{-1} IR bands and the 530, 675, 1348,

1456, 1503, 2062, 2120 and 2160 cm^{-1} Raman bands are assigned to the a_g symmetry modes of $TCNE^{-3}$. The 558 cm^{-1} IR band and the 560 cm^{-1} Raman band are assigned to the out-of-plane b_{3u} mode. The activation of the out-of-plane b_u mode in the Raman spectrum seems to be analogous to that of the 822 cm^{-1} (b_{3u}) mode of $TCNQ^{-3}$. Assignments for other vibrational bands are shown in Table XIII.

Again as in the case of the dianion, IR bands in the 600-950 cm^{-1} region also appeared in the $TCNE^{-3}$ spectrum. The assignment of these bands will be discussed in the study of the oxygen reaction products. The C≡N stretching IR bands show bathochromic shifts of about 30, 84 and 110 cm^{-1}, with an addition of the first, second and third electron to TCNE respectively. These shifts are calculated from the average frequencies of the C≡N stretching IR bands of each anion. Again, as in the case of TCNQ, splitting between the C≡N stretching internal modes in the IR spectra, increases with the addition of each electron. The observed splitting values for the neutral, mono-, di- and trianion are 33, 37, 72 and 256 cm^{-1} respectively. The vibrational bands corresponding to the C=C stretch appear to show bathochromic shifts with the addition of the first and second electron. However, when a third electron is added, they shift to higher frequency with respect to the dianion bands. The bathochromic shifts of the C≡N bands signify a progressive weakening of the C≡N bonds. A sudden about face in the shifts to low frequency of the C=C stretching bands, with the addition of a third electron, indicates that the C=C bond in the trianion may be stronger than in the dianion.

The Raman spectrum of $TCNE^{-3}$ did not show very significant intensity enhancement due to the RR effect. This is not surprising, since the

365 mμ electronic absorption band is somewhat away from the region of the 4880°A and 5145°A laser excitation lines.

Incidentally, TCNE seems to accept a fourth electron also. The C≡N stretching IR band for the tetranion was observed at 1870 cm^{-1}. Since there are four C≡N bonds, the additional four electrons should be possible. Such tetranion band was not observed for TCNQ. Though both the TCNQ and TCNE molecules have four C≡N bonds, no reasonable explanation can be given for the difference in their behavior towards the fourth electron.

Force Constant Calculation For The TCNE Anions

The force constant calculation for TCNE and the monoanion radical based on a reasonable vibrational band assignment has been reported (110). The modified valence force field of the neutral and monoanion was used to calculate the force constants for the di- and trianion. The observed frequencies for the modes of $TCNE^{-2}$ and $TCNE^{-3}$ were taken as the average of the factor group component bands. The force constant and frequency calculation was done in the same way as for the TCNQ anions.

The C≡N stretching force constants decreased progressively with the addition of each electron and the C=C stretching force constant, as expected decreased progressively from the neutral to the dianion. However, the empiricaly calculated C=C force constant for the trianion is higher than for the dianion. The observed and calculated frequencies for neutral TCNE and its anions are compared in Table XIV. The force constants calculated and π-bond orders from MO calculation (84) are given in Table XV.

TABLE XIV

THE OBSERVED AND CALCULATED IN-PLANE VIBRATIONAL FREQUENCIES OF TCNE AND ITS ANIONS

Symmetry Species[+]		$TCNE^{o}$*		$TCNE^{-}$*		$TCNE^{-2}$		$TCNE^{-3}$	
		Obs. cm^{-1}	Calc. cm^{-1}	Obs. cm^{-1}	Calc. cm^{-1}	Obs. cm^{-1}	Calc. cm^{-1}	Obs. cm^{-1}	Calc. cm^{-1}
a_g	ν_1	2235	2235	2200	2201	2098	2099.1	2073	2074.2
	ν_2	1569	1569	1392	1392	1276	1281.6	1428	1424.1
	ν_3	535	558	532	565	549	568.1	575	585.6
	ν_4	490	489	464	466	452	440.3	--	475.2
	ν_5	130	133	--	132	--	131.1	--	132.0
b_{3g}	ν_{19}	2247	2257	--	2231	--	2142.0	--	2133.4
	ν_{20}	1282	1287	--	1308	--	1310.0	--	1346.8
	ν_{21}	510	482	--	454	--	452.6	--	455.1
	ν_{22}	254	245	--	246	--	245.7	--	247.0
b_{1u}	ν_9	2230	2231	--	2198	--	2097.6	--	2066.4
	ν_{10}	958	953	970	967	982	972.8	--	1003.1
	ν_{11}	579	558	--	563	--	565.4	--	575.8
	ν_{12}	165	182	--	181	--	181.2	--	181.4
b_{2u}	ν_{15}	2263	2253	--	2226	--	2134.9	--	2122.33
	ν_{16}	1155	1152	1187	1178	--	1185.1	1253	1233.0
	ν_{17}	443	440	--	440	--	438.3	432	438.6
	ν_{18}	119	81	--	81	--	80.6	--	80.6

*Reference 110

+Reference 137

TABLE XV

FORCE CONSTANTS AND π-BOND ORDERS[1] FOR TCNE AND ITS ANIONS

Force Constants		$TCNE^{o}$		$TCNE^{\cdot-}$		$TCNE^{-2}$		$TCNE^{-3}$	
			π-Bond		π-Bond		π-Bond		π-Bond
Def.	Bond	F.C.[2]	Order	F.C.[2]	Order	F.C.	Order	F.C.	Order[3]
K_1	C=C	6.59	0.76	4.54	0.58	3.35	0.42	4.76	0.58
K_2	C-C	5.32	0.35	5.68	0.46	5.95	0.56	6.8	0.76
K_3	C≡N	17.04	0.87	16.35	0.79	14.52	0.71	13.61	0.65
H_4	C-C=C	0.43							
H_5	C-C-C	0.96							
H_6	C-C≡N	0.38							
$F_{1,2}$	C=C,C-C	0.12							
$F_{2,6}$	C-C,C≡N	-0.06							

[1]Reference 84 [2]Reference 110 [3]Extrapolated from graph, Figure 26

F.C. = Force Constants; K: Stretching Force Constants in mdyne/^{o}A

H: Bending Force Constants in mdyne.^{o}A/(radian)^2

F: Stretching-Stretching Interaction Force Constants

Vibrational Spectra of Nonstoichiometric Salts of TCNE

The nonstoichiometric salts of NaTCNE in the $1.0 \leq x < 2.0$ and $2.0 < x \leq 3.0$ composition ranges were also studied. IR spectra of thick films (6-7μ) show COV IR band at 1428 cm^{-1} nearly coincident with the 1430 cm^{-1} Raman band (110). The relative intensity of the 1385 and 2188 cm^{-1} $TCNE^{\cdot-}$ IR bands with respect to the 970 and 1187 cm^{-1} bands increases with increasing metal/organic ratio in the $1.0 < x < 1.5$ range. The sensitivity of the 140, 160 and 170 cm^{-1} librational modes and the 523 and 1430 cm^{-1} vibrational bands has been described in the literature (110). The splitting between the librational modes increases with increasing value of x. The relative intensity of the 1430 and 2222 cm^{-1} Raman bands with respect to the 523 cm^{-1} band increases with the increasing value of x. Particularly, for x=1.5 the 1430 cm^{-1} band dominates all the Raman bands of NaTCNE, except the bands corresponding to the librational modes. For the 1:1 NaTCNE, the 1430 and 2188 cm^{-1} bands were observed to be resonant with the 4880°A and to some extent the 4579°A laser excitation line (9) (110). Thus parallel trends in changing intensity patterns of the RR spectrum of NaTCNE between the change of laser excitation lines from higher to lower wavelength and an increasing value of x were observed. Thus, a bathochromic shift of the electronic band of $TCNE^{\cdot-}$ with increasing value of x, similar to that observed for the nonstoichiometric salts of NaTCNQ, can be deduced.

In the IR spectra, the intensity and frequency of the 1263 and 2086 cm^{-1} bands of the dianion, seems to depend on the composition of the salt. In the $1.0 < x < 2.0$ composition range, three IR bands at 1263, 1282

and 1312 cm^{-1} were observed. The C≡N stretching band appeared at 2086 cm^{-1}. However, in the composition range $2.0<x<3.0$, only one IR band in the 1256 cm^{-1} region was observed. The C≡N stretching band appeared anywhere between 2046-2086 cm^{-1}, depending on the composition of the salt. The relative intensity of the 1263 cm^{-1} band with respect to the 2086 cm^{-1} band appears to be somewhat higher in the $1.0\leq x\leq 2.0$ range than in the $2.0\leq x\leq 3.0$ range. However, these observations were not checked by quantitative measurements for reasons mentioned in the experimental part.

Since neither of the di- or trianions of TCNE spectra are strongly Raman resonant, the changing intensity patterns with changing composition in the $2.0\leq x\leq 3.0$ range were not investigated. However, shifts of the electronic bands of $TCNE^{-3}$ with changing composition in this range were noted (Table II).

Interaction of the TCNE Anions With Oxygen

The vibrational spectra of $TCNE^{-2}$ and $TCNE^{-3}$, as mentioned earlier contain IR bands in the 600-950 cm^{-1} region which could not be assigned to any of their vibrational modes. To verify the possibility that these bands may have originated from the oxygen reaction products, the vibrational spectra of the $Na_2TCNE.O_2$ and $Na_3TCNE.O_2$ reaction products were examined. Such possibility was contemplated in the case of Zn and Cd salts of TCNE (10). When oxygen reacts with TCNE or its anions, the reaction products have been identified as pentacyanopropenide (PCP) and tricyanoethenolate (TCE^-) (151). In this section the observed vibrational spectra and vibrational frequency for the oxygen reaction products of NaTCNE, Na_2TCNE and Na_3TCNE will be reported.

NaTCNE and Oxygen

When the monanion salt samples were prepared under high vacuum ($\sim 10^{-5}$ torr) and that vacuum was maintained, no significant reaction of oxygen was observed. When such samples were exposed to dry oxygen, vibrational bands at 598, 626, 776, 1540 and 1625 cm^{-1} were observed. Changes in the frequencies of the C≡N stretching bands were also observed. When this oxygen reaction product was exposed to the atmosphere vibrational bands for the neutral TCNE and other unidentified reaction products were observed.

Na_2TCNE and Oxygen

When the dianion salt was exposed to dry oxygen, the colorless sample turned into a pink-red reaction product with an electronic absorption band at 470 mμ. The IR spectrum of the reaction product is shown in Figure 22. The vibrational IR bands at 520, 598, 626, 662, 692, 712, 746, 760, 776, 798, 812, 846, 876, 980, 1140, 1215, 1258, 1300, 1540, 1580, 1625, 2102, 2156, and 2216 cm^{-1} and Raman bands at 526, 600, 1370, 1540 and 2180 cm^{-1} were observed. The vibrational bands and tentative assignments are given in Table XVI. The spectrum in Figure 22 still shows some dianion bands at 550, 1256 and 2086 cm^{-1}. For very thin films, instead of the broad 1350-1650 cm^{-1} band (Figure 22), separate bands at 1540, 1578 and 1625 cm^{-1} were observed.

The vibrational bands in the region 600-950 cm^{-1}, apparently originate from $TCE^{\cdot-}$ and similar reaction products. Precise identification of the compounds and the modes corresponding to these bands is not possible with the information at hand.

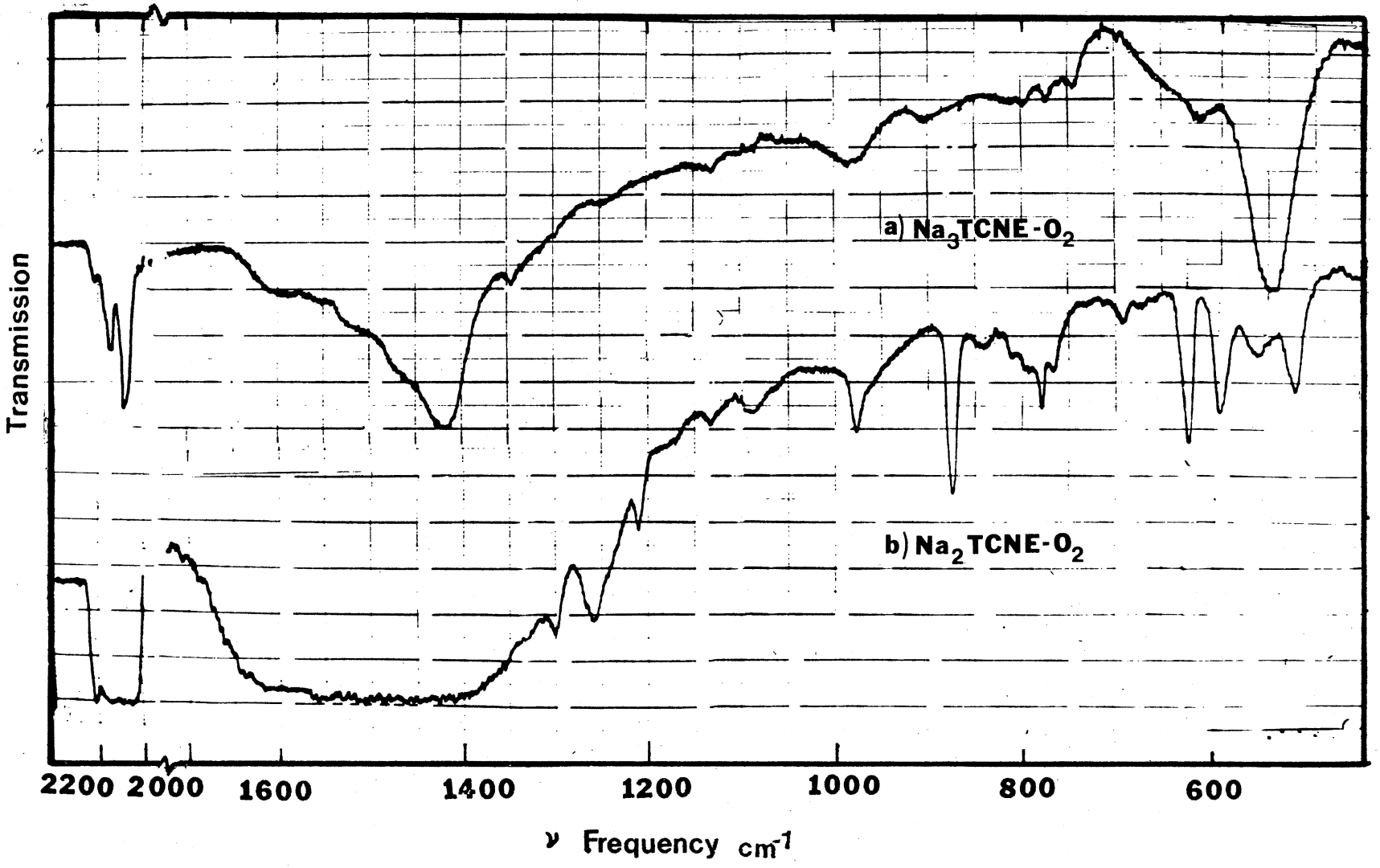

Figure 22. IR Spectra of a) $Na_3TCNE \cdot O_2$ and b) $Na_2TCNE \cdot O_2$

TABLE XVI

THE OBSERVED VIBRATIONAL FREQUENCIES OF $Na_2TCNE \cdot O_2$ AND $Na_3TCNE \cdot O_2$ REACTION PRODUCTS

$Na_2TCNE.O_2$			$Na_3TCNE.O_2$		
IR (cm^{-1})	Raman (cm^{-1})	Assignments*	IR (cm^{-1})	Raman (cm^{-1})	Assignments*
			440 458		$\delta_{C-C\equiv N}$
520	526	ν_{C-C}	549		ν_{C-C}
552		$TCNE^{-2}$			
598 626 662 692 712 746 760 776 798 812	600		620 794 800		
846		$\delta_{C-C=O}$	831 848		$\delta_{C-C=O}$
876					
980		ν_{C-C}	902 982		ν_{C-C}
1140 1215			1140		
1258		$TCNE^{-2}$			
1300 1380 1540 1580	1370 1565	$\nu_{C=C}$	1348 1430 1472 1540	1354 1427 	$\nu_{C=C}$
1625	1615	$\nu_{C=O}$	1610		$\nu_{C=O}$
2086		$TCNE^{-2}$			
2102 2156 2216	 2212	$\nu_{C\equiv N}$	2086 2158 2210	2062 2179 2220	$\nu_{C\equiv N}$

* ν = stretching mode

δ = bending mode

Na_3TCNE and Oxygen

The electronic spectrum for this stable reaction product shows two electronic bands at 195 and 226 mμ in the uv region. Like $Na_3TCNQ.O_2$, many IR bands of $Na_3TCNE.O_2$ appear to be at the same frequency as the $TCNE^{-2}$ bands. Thus, the 458, 549, 989, 2086, and 2158 cm^{-1} IR bands are very close to the similar dianion bands.

Again as in the case of TCNQ, these reaction products may contain $TCNE^{\cdot-}$ and $TCNE^{-2}$ in $Na_2TCNE.O_2$ and $Na_3TCNE.O_2$ respectively. Formation of the sodium peroxide coating on Na_2TCNE when Na_3TCNE reacts with oxygen may be one of the reasons for the apparent stability of the $Na_3TCNE.O_2$ reaction products.

CHAPTER V

DISCUSSION

Ionic Charge and Electronic States of TCNQ and TCNE

The electronic transitions of TCNQ and TCNE in their different ionic states show much similarity in their general behavior. With an addition of the first electron several LE and DE electronic bands in the IR, visible and uv region become active. In the monoanion radical salts of TCNQ and TCNE, there is an extensive dimerization in the solid state (e.g. monoclinic crystals of $TCNQ^{-}$). The charge oscillation vibronic interaction, as a result of electron exchange between the monoanion radicals of the dimer, profoundly affects their vibrational spectra. When a second electron is added, the dianions of TCNQ and TCNE formed are colorless with all electronic transitions in the uv region. Apparently, the extent of the vibronic interaction seems to be reduced in the dianion salts. The bathochromic shifts in the electronic bands of the monoanion with respect to the neutral molecule and the blue shifts of the dianion bands with respect to the monoanion bands seems to be the general rule for the π-electron acceptors (71) (72). The trianion salts of TCNQ and TCNE, however, show electronic transitions which are shifted to longer wavelengths with respect to the dianion electronic bands. In this section, the electronic states of the anions of TCNQ and TCNE will

be compared and their implication on the physical properties will be discussed.

The observed transition energies between the electronic states of the neutral, mono-, di- and trianions of TCNQ, as observed for their sodium salts are shown in Figure 23. The electronic transition energy for each anion depends on the crystal structure, the nature of the electron donor and the composition. As mentioned earlier, there is some correlation between the electrical conductivity and the energy of the excited DE states (4)(39). It is not certain whether the observed electronic bands of the di- and trianionic salts are of the DE or LE type, but they are presumed to be the LE electronic transitions. The results of the MO calculations for the dianion (58) (77) support such a presumption. On the basis of the electronic results obtained in this study, the di- and trianion salts are not expected to be better electrical conductors than the monoanion salt. Possibly, the trianion salt may show higher electrical conductivity than the dianion salt.

Since the electron density of the transferred electrons is concentrated mostly on the $C(CCN)_2$ wing part of the TCNQ molecule, particularly on the CN bond (57) (77) (78), a change in color with the addition of each electron may be associated with C≡N molecular orbitals. Since the di- and trianions of TCNQ and TCNE are colorless and yellow respectively, the C≡N bonds seem to play an important role in determining the color of the salt. It is also possible that the yellow color of the trianions of TCNQ and TCNE may have an origin in the so called back-bonding interactions (10).

The changes in the electronic states with the ionic charge on TCNE are similar to TCNQ, so the above discussion is also applicable to TCNE

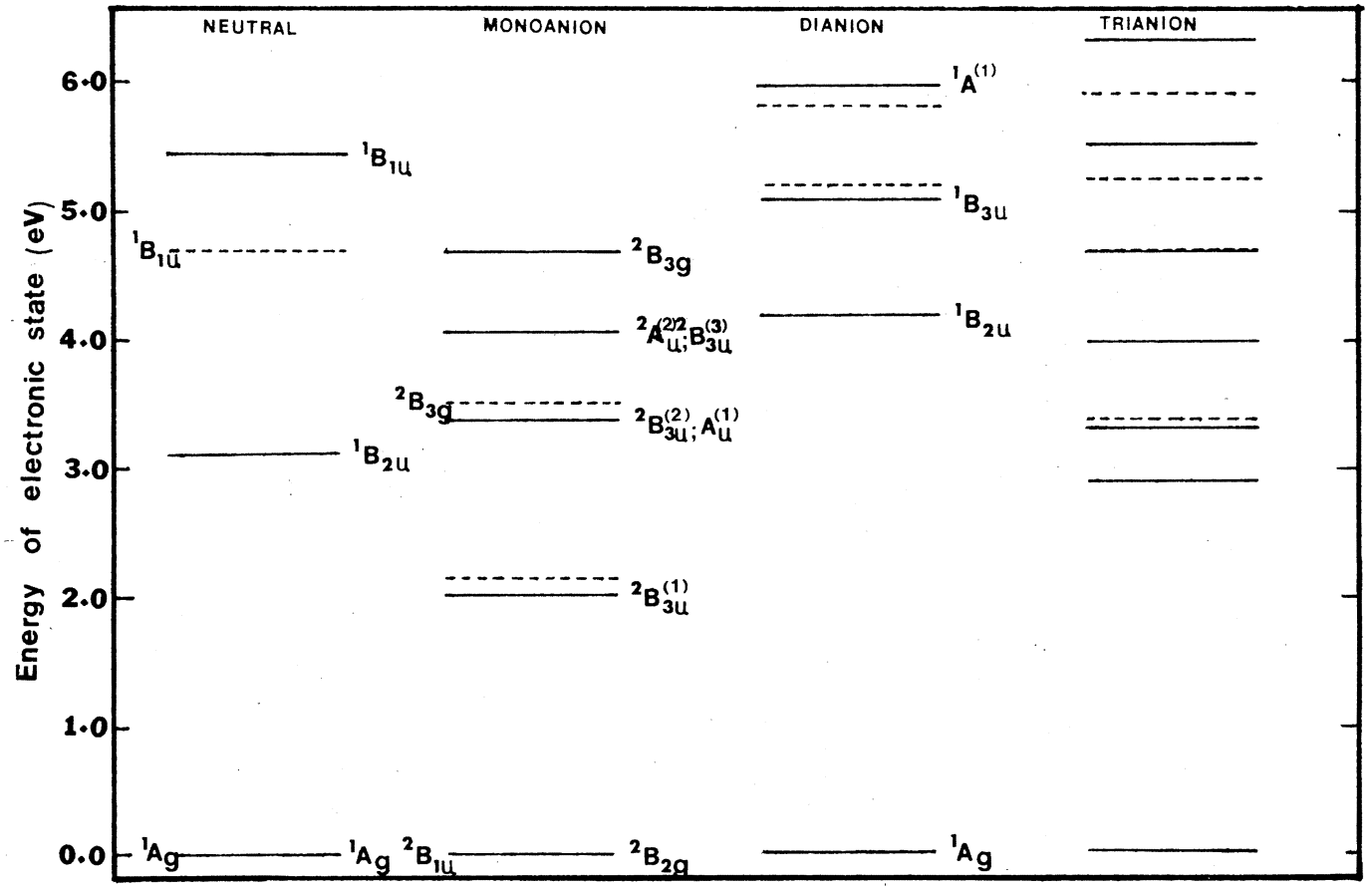

* Assignments on the Leftside are for the Electronic States of TCNE and its Anions and on the Rightside for Those of TCNQ and its Anions

Figure 23. Energy States of the Neutral, Mono-, Di- and Trianions of TNCQ(——) and TCNE (----)

salts. The electronic states of TCNE and its anions are also shown in Figure 23.

The central ring of TCNQ adds stability to its anions compared with the TCNE anions. The TCNE anions, particularly the di- and trianion were easily contaminated by some oxygen reaction products. Apparently, the central ring does not play an important role in determining the color of the di- and trianions.

π-Bond Orders, Overlap Populations and Force Constants

The strength of a bond, bond length, bond order, overlap population in the bond and bond force constant are interrelated to each other (9) (142-145). From the results of force constant calculations, it is evident that the C=C and the C≡N bonds of TCNQ and TCNE are weakened progressively with the addition of each electron. The C=C bonds become stronger and stronger as the negative charge on the molecules is increased. The trianion of TCNE seems to be an exception. The C=C force constant value for $TCNE^{-3}$ is higher than for the dianion. Changes in bond strengths should be reflected in the vibrational frequencies of the molecule and thus, the empirical force constants. In this section, the correlation between the force constants calculated from the normal coordinate analysis and π-bond orders as well as overlap populations from MO calculations will be discussed.

The values of the force constants, π-bond orders and overlap populations for the different bonds of TCNQ and its anions are listed in Table XVII. The plots of π-bond order vs. force constant and overlap population vs. force constant are shown in Figures 24 and 25, respectively. There is a nearly linear correlation between the π-bond orders

TABLE XVII

FORCE CONSTANTS, Π-BOND ORDERS AND OVERLAP POPULATIONS FOR TCNQ AND ITS ANIONS

Ionic Species	Bond	π-Bond Order			Overlap Population	Force Constants
		a	b	c	d	Mdyne/^{o}A
$TCNQ^{o}$	$C-C^{R}$	0.34658	0.287	0.29	0.75	5.46
	$C=C^{R}$	0.88874	0.922	0.92	1.14	7.50
	$C=C^{W}$	0.81176	0.859	0.85	0.76	6.90
	$C-C^{W}$	0.26854	0.247	0.25	0.28	5.35
	C≡N	0.95824	0.963	0.94	1.80	16.90
	C-H				0.72	5.05
$TCNQ^{-}$	$C-C^{R}$	0.48794	0.470	0.42	0.91	5.83
	$C=C^{R}$	0.77932	0.793	0.83	1.05	7.06
	$C=C^{W}$	0.59814	0.618	0.65	0.42	5.82
	$C-C^{W}$	0.35202	0.330	0.34	0.26	5.68
	C≡N	0.91668	0.925	0.89	1.90	16.18
	C-H				0.70	4.983
$TCNQ^{-2}$	$C-C^{R}$		0.610	0.57	1.06	5.98
	$C=C^{R}$		0.681	0.73	0.96	6.92
	$C=C^{W}$		0.361	0.42	0.12	5.41
	$C-C^{W}$		0.412	0.47	0.31	5.92
	C≡N		0.881	0.81	1.96	15.48
	C-H				0.67	4.92
$TCNQ^{-3}$	$C-C^{R}$			0.63*	1.18+	6.309
	$C=C^{R}$			0.64	0.87	6.447
	$C=C^{W}$			0.40	0.11	5.225
	$C-C^{W}$			0.485	0.34	6.045
	C≡N			0.67	2.18	13.42
	C-H				0.64	4.85

[a] Reference 116

[b] Reference 78

[c] Reference 36 except for $TCNQ^{-3}$

R = ring, W = wing

[d] Reference 77 except for $TCNQ^{-3}$

* Extrapolated values from the π-bond order vs K plots (Figure 24)

+ Extrapolated from the overlap population vs K plots (Figure 25)

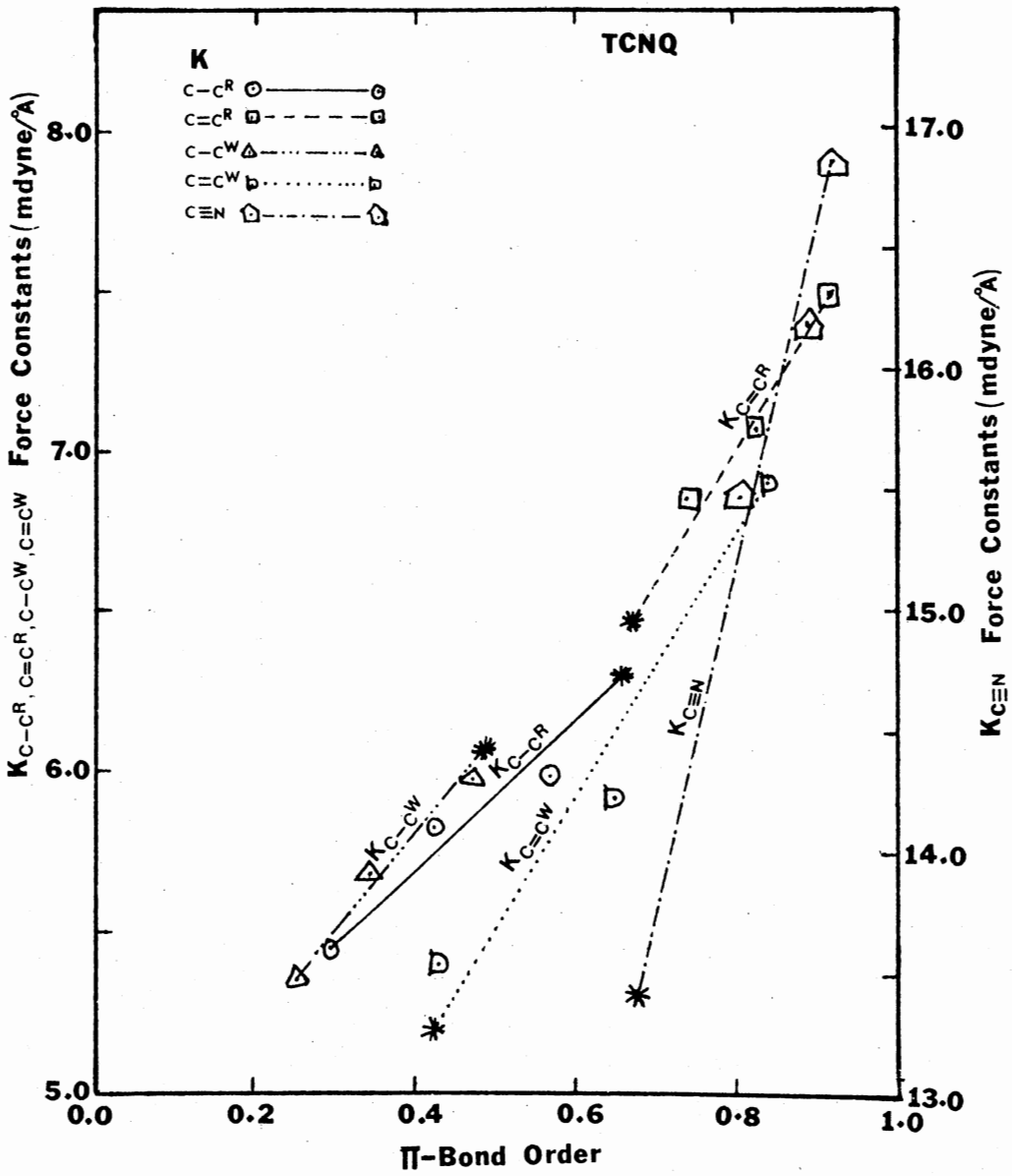

*For the Trianions Values are Extrapolated

Figure 24. Correlations Between the Π-Bond Orders and Force Constants of TCNQ and its Anions

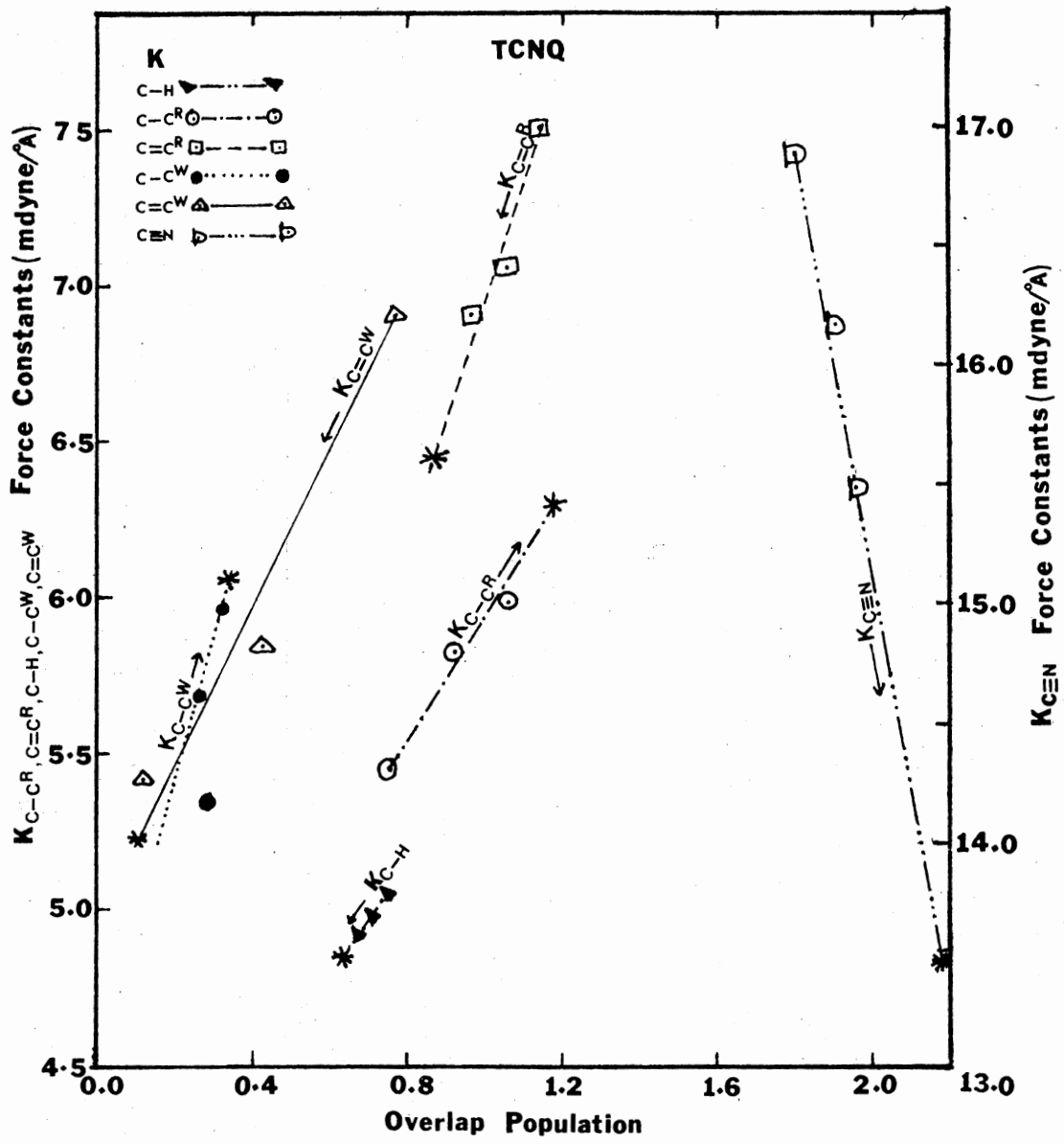

* For the Trianions Values are Extrapolated

Figure 25. Correlations Between the Overlap Populations (Ref. 56, 78) and Force Constants of TCNQ and its Anions

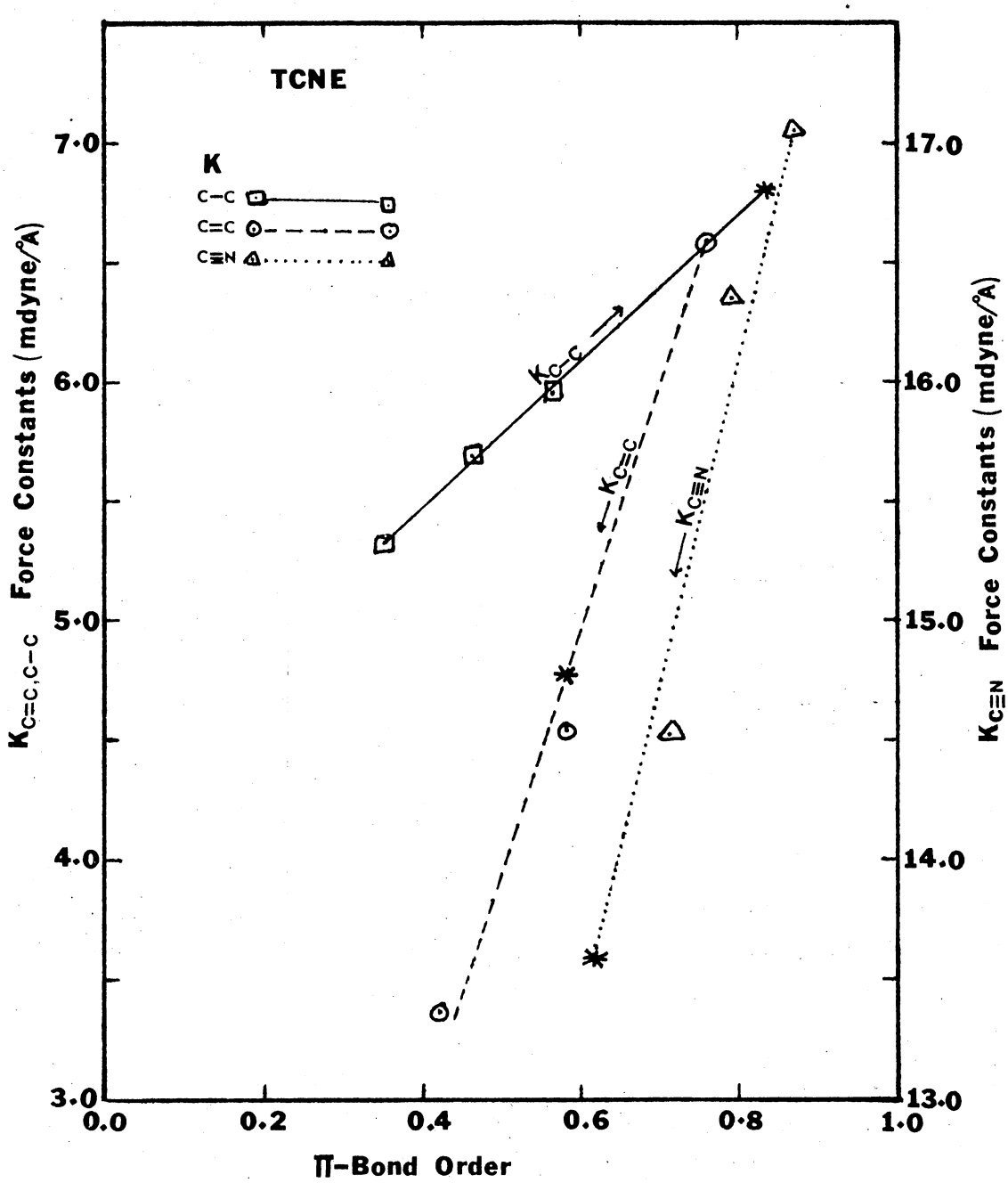

* For the Trianions Values are Extrapolated

Figure 26. Correlations Between the Force Constants and π-Bond Orders of TCNE and its Anions

and force constants (K) of the anions of TCNQ. π-bond orders for the $C\text{-}C^{R}$, $C{=}C^{R}$, $C{=}C^{W}$, $C\text{-}C^{W}$ and C≡N bonds of $TCNQ^{-3}$ are 0.63, 0.64, 0.40, 0.485 and 0.67 respectively. Similarly, the overlap populations in the trianion are estimated from extrapolation of the overlap population vs. force constant plots (Figure 25). The estimated values are listed in Table XVII.

Thus, in the trianion π-bond orders for the $C\text{-}C^{R}$ and $C{=}C^{R}$ bonds are almost equal, indicating a benzene-like structure of the TCNQ ring. The double bond-like nature of $C\text{-}C^{W}$ and a single bond character of $C{=}C^{W}$ in $TCNQ^{-3}$ also seems to be evident from the estimated π-bond orders. The trends in the overlap populations calculated in the neutral, mono- and dianion are necessarily in the trianion.

The force constants and π-bond orders for $TCNE^{o}$, $TCNE^{-}$ and $TCNE^{-2}$ are listed in Table XV. The correlations between the π-bond orders and force constants of TCNE and its anions are shown in Figure 26. The estimated values of the π-bond orders for $TCNE^{-3}$ from the extrapolation of the π-bond order vs. K plots are listed in Table XV. From the values of the π-bond orders, the C=C bond seems to be stronger in the trianion than in the dianion.

Since empirical calculation of force constants are based on certain presumptions mentioned earlier, the estimated π-bond orders for the trianions should be accepted with caution.

Vibrational Band Assignments, Vibronic Interactions and Band Intensities of the Stoichiometric Salts of TCNQ and TCNE

In determining vibrational band assignments, the symmetry of the

anion, an extent and nature of the vibronic interactions, crystal structure and the polarization of the vibrational band with respect to the crystal axes should be taken into consideration. For the neutral molecules of TCNQ and TCNE, reasonable vibrational assignments have been established (9) (115) (116) (137). For the monoanion radicals, the effects of vibronic interaction on the vibrational spectra have been discussed earlier. In this section the vibrational band assignments of the anions, probable nature of the vibronic interactions and their effect on the band intensities will be discussed.

Two types of vibronic interactions in the anions of TCNQ and TCNE are considered to be important in determining the vibrational spectroscopic pattern, a) Interactions originated from the electron exchange between the anions, b) Interactions involved in back-bonding (10) between the anion and the cation (or cations). In the monoanion radical salts, charge oscillation (or charge density wave) vibronic interaction arising out of the electron exchange between the anions of the dimer, seems to be a dominant factor in determining the intensities of the IR vibrational bands. Thus the 328, 618, 723, 967, 987, 1167, 1178, 1186, 1219, 1326, 1343, 1578 and 2167 cm^{-1} IR bands of NaTCNQ may be attributed to such vibronic interactions. Similarly, the 455, 463, 521, 530, 1385, 1428, 2188 and 2222 cm^{-1} IR bands of NaTCNE (110) may be considered to be the COV bands due to the vibronic interactions, arising out of electron exhange between the monoanion radicals of the $TCNE^{-\cdot}$ dimer. $TCNQ^{-\cdot}$ and $TCNE^{-\cdot}$ in the solid state indicate predominance of the dimer form. Thus the above mentioned IR bands and nearly coincident corresponding Raman bands are assigned to the a_g symmetry modes. The discrepancies in the frequencies of the vibrational bands assigned to the same mode are attributed to the factor group or T/L splitting. Thus for the ν_2, ν_3,

ν_4, ν_5, ν_6, ν_7, ν_8 and ν_9 a_g modes show factor group splitting values of about 54, 32, 83, 52, 20, 10, 2 and 19 cm^{-1} respectively. Thses COV IR bands are broad and intense, particularly at low temperature (-180°C) as compared with the novibronic bands. The back-bonding type of vibronic interactions in the monoanion radical salts, may also make some minor contribution to the intensity of the COV IR bands.

The most intense Raman bands of $TCNQ^{\cdot-}$ at 1207, 1396, 1610 and 2220 cm^{-1} do not have any nearly coincident COV IR bands. The intensity of these bands is resonantly enhanced when the laser excitation lines lie in the region of strongly allowed 620mμ electronic absorption bands (A-type RR effect (125)). Other Raman bands at 620, 729, 967, 1184, 1326, 1339, 1583, and 2168 cm^{-1} which are nearly coincident with the COV IR bands, are resonantly enhanced when laser excitation lines within the overlap region of two electronic bands or weakly allowed electronic bands are used (Non-A type RR effect (125)).

Other weak IR and Raman vibrational bands of low frequency that are nearly coincident but not assigned to the a_g modes have been mentioned earlier. Thus the 484, 496, 578 and 802 cm^{-1} IR bands and the corresponding Raman bands at 482, 494, 590 and 800 cm^{-1} respectively, are assigned to b_{1g} and b_{2g} symmetry modes (Table IV), belonging to the out-of-plane rotational symmetry species. Though a possibility of non-totally symmetric vibrational modes, with out-of-plane rotational character participating in COV interaction has been predicted (103), the only question is that whether so many vibrational modes can be activated in the IR spectra. The change in overlap of molecular wave functions of $TCNQ^{\cdot-}$ neighbors in the stack, due to mechanical motion with respect to each other can activate b_{1g} and b_{2g} modes in the IR spectrum. However, this effect has been predicted to be weak compared with that for the a_g

symmetry modes. Alternatively, the 496 cm^{-1} IR band can be assigned to the b_{2u} symmetry mode and the 494 cm^{-1} Raman band to the in-plane b_{3g} mode. A choice between these alternate assignments can be made on the basis of a polarization study of the vibrational spectra of single crystals of MTCNQ. Kuzamy and Stolz (131) studied the RR spectrum of single crystals of TTF-TCNQ. However, a final determination of the symmetry of modes of the 482, 494 and 800 cm^{-1} Raman bands is not available. The 572 and 800 cm^{-1} Raman bands were assigned to the b_{2g} symmetry modes (131).

The nonvibronic IR and Raman bands of $TCNQ^{\cdot-}$ are assigned from analogy to the neutral TCNQ vibrational bands. For still other vibrational bands, like the 243 cm^{-1} Raman band and the 1475 cm^{-1} IR band, no reasonable assignments can be provided.

No clear evidence for low energy DE electronic bands in the di- and trianion salts of TCNQ and TCNE was obtained during this study. In the monoanion salts, continously created and destroyed neutral and dianion sites, in the electron exchange: $2TCNQ^{\cdot-} \rightleftharpoons TCNQ^{-2} + TCNQ^{o}$, reaction act as a sink and source for the electron. The extent of such electron exchange in the dianion salts is not known. From the electronic spectra, it seems probable that the extent of such exchange and the vibronic interaction arising through it might be reduced.

However, for the dianion of TCNQ, the 999, 1195, 1303, 1598 and 2096 cm^{-1} IR bands and nearly coincident Raman bands at 999, 1196, 1301, 1594 and 2096 cm^{-1} respectively were observed (Figure 7). The coincidence of the vibrational bands can be attributed to two effects: In one scheme, one may presume that the dianion of TCNQ is no longer a planar molecule. Since $C{=}C^{W}$ acquires a nearly single bond character, the $(C{-}C{\equiv}N)_2$ wings may be able to rotate more freely (around $C{=}C^{W}$) than

in the neutral or monoanion TCNQ. The configuartions that the dianion may assume under such rotations of the two wings may not be centrosymmetric and the mutual exclusion principle may no longer be valid. Under such conditions, the a_g and b_g modes can become IR active and the b_u modes Raman active even though there is no extensive vibronic interaction. However, there is no evidence for such conformations with substantial deviation from the D_{2h} molecular symmetry. Such non-planar structures were shown to be energetically unstable by the MO calculations (77) (78). In another scheme, the dianion molecule is presumed to be essentially of D_{2h} symmetry. It may be possible that there is a considerable back-bonding interaction where the electrons from the π-bonding or π-antibonding molecular orbitals of the dianion may be back-transferred to the two cations. When the two cations are associated with one dianion, then the back-bonding interactions with two cations may be coupled with the stretching vibrations of the dianion. Such coupling may produce in-phase and out-of-phase electron oscillations between the dianion and the two cations. The charge oscillation vibronic interaction arising out of such back-bonding may activate totally symmetric a_g modes, as well as b_g modes with out-of-plane charcater, in the IR spectrum; even though the overall molecule is centrosymmetric. In addition, there may possibly be an insignificant contribution from the vibronic interaction arising out of electron exchange between the dianions.

The vibrational spectroscopic analysis of $TCNQ^{-2}$ and $TCNE^{-2}$ is based on the considerations of the second scheme. Thus of the two types of COV interactions, a back-bonding type may be predominant in the dianions, in contrast to the monoanion radicals, where the electron exchange between the anions seems to be predominant. Thus the earlier

mentioned IR and Raman vibrational bands can be assigned to the a_g symmetry modes. This scheme could also explain nearly coincident Raman and IR bands at 435, 500 and 578 cm^{-1}, which are assigned to the b_g modes containing out-of-plane rotational symmetry species. Similar considerations for the dianion of TCNE are used in the vibrational band assignments (Table XIII). Thus the 452, 546, 552, 1256, 1263, 1282, 1312, 2072, 2086 and 2146 cm^{-1} IR bands and the 549, 1265 and 2068 cm^{-1} Raman bands are assigned to the a_g symmetry modes of $TCNE^{-2}$. The 2146 cm^{-1} IR band can alternatively be assigned to the b_{2u} mode (ν_{15}) of $TCNE^{-2}$.

For the vibrational band assignments given in Table IV and XIII, for $TCNQ^{-2}$ and $TCNE^{-2}$ respectively, it seems that factor group or T/L splitting in the dianions has been reduced considerably as compared with the mono-anion. Thus for the ν_2, ν_3, ν_4, ν_5, and ν_6 $TCNQ^{-2}$ a_g modes, splittings are 100, 4, 51, 1 and 0 cm^{-1} respectively. Similarly for TCNE dianion splittings between the factor group components of COV a_g symmetry modes of $TCNE^{-2}$ should be noted (Table XIII).

The most interesting vibrational spectra were observed for the trianion salts of TCNQ and TCNE. In the case of the trianion, presuming 1:1 type association, there are three cations and three possible back-bonding interactions, adding some new factors in determining the shape and intensity pattern of the vibrational spectra. Thus the trianion IR bands at 483, 580, 604, 780, 819, 983, 1073, 1090, 1136, 1183, 1245, 1284, 1408, 1476 and 1577 cm^{-1} are nearly coincident with the 479, 582, 598, 782, 820, 989, 1071, 1088, 1138, 1186, 1247, 1284, 1408, 1476 and 1579 cm^{-1} Raman bands respectively. For the presumed D_{2h} symmetry and based on analogy to the neutral, mono- and dianion vibrational bands, not only the a_g and b_g modes have IR active factor group components, but

Raman bands at frequencies corresponding to the IR bands of b_u modes appeared in the $TCNQ^{-3}$ spectra. Particularly, the out-of-plane, IR band corresponding to the ν_{50} (b_{3u}) mode, at 822 cm^{-1} has a nearly coincident Raman band at 820 cm^{-1}. Similarly, the 1476 cm^{-1} IR band corresponding to the 1505 cm^{-1} b_{1u} or b_{2u} modes of the mono- or dianion has a nearly coincident Raman band at 1478 cm^{-1}. The most intense 1138 cm^{-1} Raman band of the trianion, under the vibrational assignment scheme given in Table IV, belongs to the b_{2u} (ν_{37}) mode which has a weak IR band at 1136 cm^{-1}.

The IR active a_g modes of the trianion may find explanation under the phenamena of coupling of three back-bonding electron exchange interactions with the three cations, through the vibrational modes, similar to the dianion case. However, a difficult question is how to explain the Raman activity of b_u modes ? It seems possible that a third back-bonding interaction may introduce an element of asymmetry so that the mutual exclusion principle may temporarily be violated. When three cations are nearer to the three C≡N bonds of TCNQ than the fourth, the electron density distribution of the added electrons as well as induced distortions may add some elements of asymmetry. Under these conditions, it may be possible that b_u modes become Raman active.

Another explanation for the IR active a_g and b_g modes and Raman active b_u modes may be that the $(C\text{-}C\equiv N)_2$ may be rotating around a largely single $C=C^W$ bond or that the $(C\text{-}C\equiv N)_2$ groups move out of the plane of the central ring. In such a case, the centrosymmetric character of $TCNQ^{-3}$ may have been changed so that the mutual exclusion principle could be violated. However, under such conditions, all the IR bands should have Raman counterparts and vice versa. The strong Raman bands at 672, 698, 722, 1599, 2162 and 2163 cm^{-1} are not observed in the IR spectrum of $TCNQ^{-3}$.

The low frequency Raman spectrum of $TCNQ^{-3}$ contains vibrational bands at 260, 420, 450, 560, 598, 672, 780, 840, 848, 1073 and 1088 cm^{-1}, for which corresponding Raman bands are not observed in the spectra of the mono- or dianions. Activation of such additional Raman bands may be attributed to the possible structural distortions of $TCNQ^{-3}$ induced by the three cations.

Similarly for the trianion of TCNE, the 420, 432, 549, 1346, 1417, 1498, 1980 and probably 2032 cm^{-1} IR bands can be assigned to the a_g symmetry modes, activated by the structural distortions or the coupling of three back-bonding interactions through the vibrational modes of $TCNE^{-3}$. Again as in the case of $TCNQ^{-3}$, the out-of-plane b_{3u} mode can be assigned to the 558 cm^{-1} IR and the 560 cm^{-1} Raman bands.

For the di- and trianions of TCNQ and TCNE, IR bands are broader (10-110 cm^{-1}) than for the monoanions. An increase in band width with the increase of the anionic charge may be attributed to the fluctuations in the charge density of the unpaired electrons, the effect of minor structural distortions on the vibrations, or the vibronic interactions induced by back bonding. Particularly, band widths of the C≡N stretching IR bands of $TCNQ^{-3}$ and $TCNE^{-3}$ are about 110 cm^{-1} (1901 cm^{-1} band) and 70 cm^{-1} (1980 cm^{-1} band) respectively. Such large band widths may have origin in the induced structural distortions.

The correlation between the force constants calculated for the vibrational assignments given in Table IV with π-bond orders obtained from MO calculations for TCNQ and its anions is quite good. However, for the di- and trianions certain observed spectroscopic results are difficult to explain. Particularly, assignments of the strong 1138 and 1476 cm^{-1} Raman bands seem unreasonable. Also, no vibrational band assignments are provided for the IR and Raman bands at about 1073, 1090,

and 1408 cm^{-1}. For these and other bands, alternate assignments are listed in Table XVIII. Inequivalent forces for any two back bondings of the three may be one explanation for a large distortion splitting (up to 263 cm^{-1}). An attempt was made to calculate a MVFF which could reproduce the average frequencies of the a_g modes shown in Table XVIII. But such an attempt was not much successful. Though some of the observed frequencies were reproduced, overall agreement between the observed and calculated values was poor when the adjustment of only stretching force constants was made. The vibrational assignments of $TCNE^{-2}$ and $TCNE^{-3}$ (Table XIII) are of alternate type with large distortion splittings for the a_g modes (up to 152 cm^{-1}).

Vibrational Band Intensities and Vibronic Interaction in the Nonstoichiometric Salts of TCNQ and TCNE

Composition is one of the important factors which affects the spectroscopic and physical properties of the radical anion salts. The change in the intensities at the vibrational bands and shifts in the electronic bands with composition were discussed in Chapter III. In this section some correlations between intensity changes of the IR and Raman bands with composition will be discussed.

The intensity of the COV IR bands of $TCNQ^{\cdot-}$ was shown to be dependent on the temperature of the sample. The intensity of the vibronic IR bands at 325, 620, 723, 987, 1183, 1355, 1578 and 2187 cm^{-1} was observed to increase tremendously, as compared with non vibronic bands at 1363 or 2197 cm^{-1}, when the sample was cooled to the liquid nitrogen temperature. Such increase was associated with an increased extent of dimerzation and the vibronic interaction.

TABLE XVIII

ALTERNATE VIBRATIONAL BAND ASSIGNMENTS FOR $TCNQ^{-2}$ AND $TCNQ^{-3}$

$TCNQ^{-2}$				$TCNQ^{-3}$			
IR cm^{-1}	Raman cm^{-1}	Average cm^{-1}	Assignments*	IR cm^{-1}	Raman cm^{-1}	Average cm^{-1}	Assignments*
					91	91	
					102	102	
					210	210	ν_{53} b_{3u}
					260	260	ν_{31} b_{3g}
	355	355	ν_9 a_g		306 381	343	ν_9 a_g
435	435	435	ν_{16} b_{1g}		420 450	435	ν_{16} b_{1g}
500	500	500	ν_{30} b_{2g}	483	479	481	ν_{30} b_{2g}
514		514	ν_{25} b_{1u}				
	526	526	ν_{47} b_{3g}		523	523	ν_{47} b_{3g}
558		558					
578	578	578	ν_{29} b_{2g}	580	560 582	574	ν_{29} b_{2g}
606							
623	640	623	ν_8 a_g	604 628	598 642 672	629	ν_8 a_g
715	745	730	ν_7 a_g	 780	698 722 780	745	ν_7 a_g
822		822	ν_{50} b_{3u}	812 819 822	820 840 848	827	ν_{50} b_{3u}
999 1046	999 1052	1024	ν_6 a_g	983 1073 1090	989 1071 1088	1051	ν_6 a_g
1127 1140 1195	1196	1164	ν_5 a_g	1136 1183 1245	1138 1186 1247	1189	ν_5 a_g

TABLE XVIII (continued)

$TCNQ^{-2}$				$TCNQ^{-3}$			
IR cm^{-1}	Raman cm^{-1}	Average cm^{-1}	Assignment*	IR cm^{-1}	Raman cm^{-1}	Average cm^{-1}	Assignments*
1238		1238	ν_{36} b_{2u}				
1303	1301			1284	1284		
	1326	1358	ν_4 a_g		1318	1350	ν_4 a_g
1353	1354			1408	1410		
1435	1436						
1498		1498	ν_{20} b_{1u} or				
1503		1503	ν_{34} b_{2u}				
	1546	1546	ν_{43} b_{3g}				
1598	1594	1596	ν_3 a_g	1476	1478	1528	ν_3 a_g
				1577	1579		
					1599	1599	ν_{43} b_{3g}
2096	2096	2146		1901	1943		
2196	2196		ν_2 a_g		2126		ν_2 a_g
					2163	2033	
2164		2164	ν_{19} b_{1u}				
3010		3010	ν_{32} b_{2u}				
3014		3014	ν_{18} b_{1u}	2994		2994	ν_{18} b_{1u}

*Numbering of symmetry modes from Reference 116

Intensity enchancement for the COV IR bands was also observed with an increase of the metal/organic ratio in the salt. To compare the intensities of COV bands with those of nonvibronic bands, their intensity ratios at different compositions are plotted in Figure 27. The 1363 cm^{-1} nonvibronic IR band (ν_{35} b_{2u}) is used to monitor changes in intensities of the vibronic IR bands. Plots of I_{COV}/I_{1363} vs. x for the typical COV IR bands of $TCNQ^{\cdot-}$ at 1186, 1326, 1343 and 1578 cm^{-1} are shown in Figure 27. The intensities of the COV IR bands at x=1.0 are considerably less than that of the 1363 cm^{-1} band ($I_{COV}/I_{1363} \sim 0.5$). With an increasing value of x, the intensity ratio increases rapidly within the composition range $1.0 \leq x \leq 1.3$. The relative intensities of the 1186 and 1578 cm^{-1} bands are higher as compared with the 1363 cm^{-1} band at about $x \sim 1.3$. All the COV bands attained maximum intensity enchancement possible at this composition of the nonstochiometric salts. In the salts of the composition in the $1.5 \leq x \leq 2.0$ range, the intensity of the COV bands remained higher than that of the 1363 cm^{-1} band. One explanation for the intensity changes may be provided in terms of a loss of orientation of the TCNQ anion with respect to the substrate surface. For x=1.0, $TCNQ^{\cdot-}$ molecular planes tend to orient parallel to the substrate surface. With an increasing concentration Na_2TCNQ in the thin film deposits, there may be increasing tendency of $TCNQ^{\cdot-}$ towards random orientations. Once a maximum disorder is attained (at $x \sim 1.5$), further increase in the intensity ratio, I_{COV}/I_{1363} also stopped. Such a comparison for the IR bands of nonstoichiometric salts in the $2.0 \leq x \leq 3.0$ composition range is not possible, because polarizations of the di- and trianion bands with respect to the TCNQ molecular plane is not known. Also, orientations of $TCNQ^{-2}$ and $TCNQ^{-3}$ molecules with respect to the substrate surface and nature of vibronic interaction is not known. More detailed study of

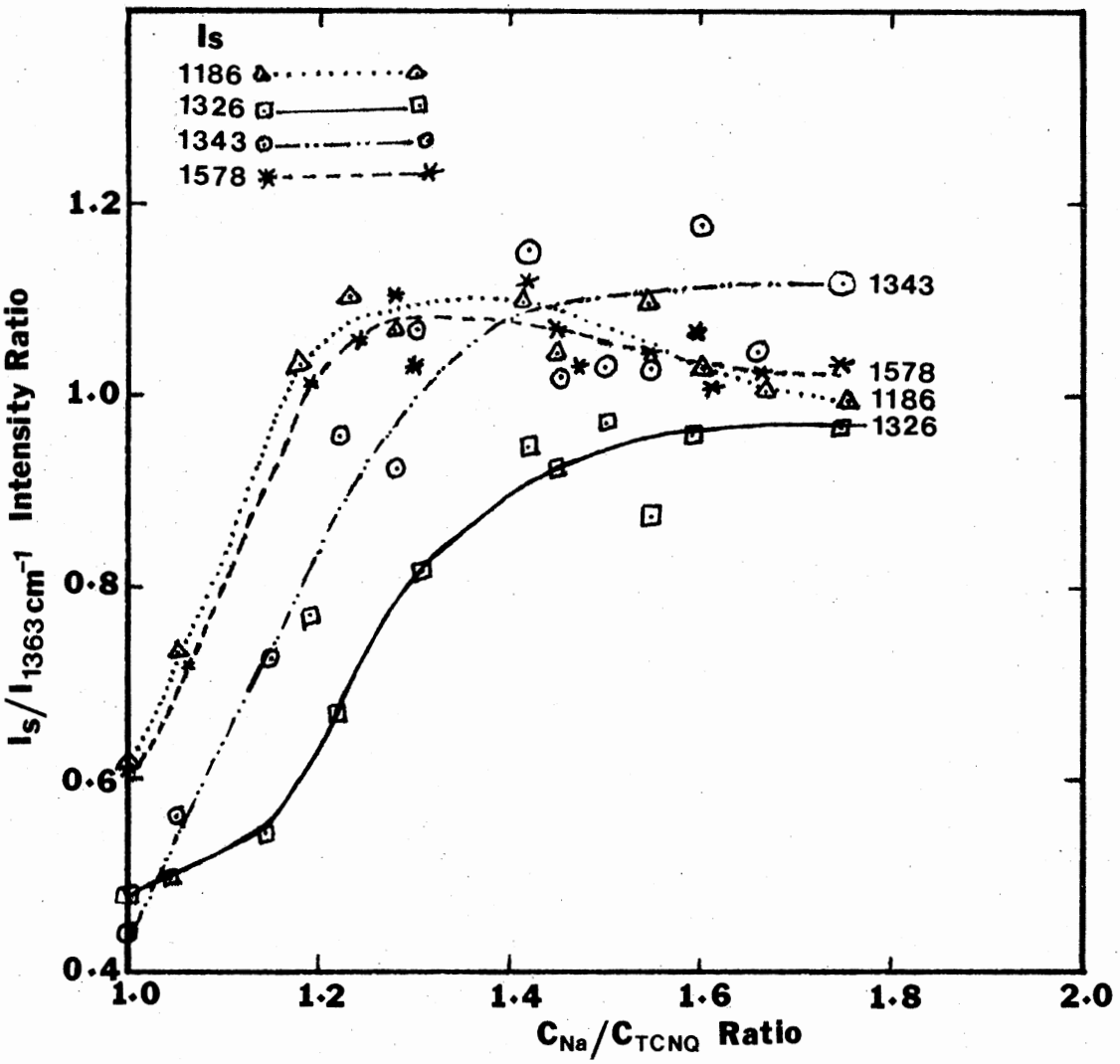

Figure 27. Variations in Intensity Ratios of the Charge Oscillation Vibronic IR Bands with Respect to the Nonvibronic (1363 cm^{-1}) IR Bands of the TCNQ Monoanion Radical with a Change in the Composition of Nonstoichiometric Salts

these factors than possible within the scope of this study is required to distinguish between the vibronic and non vibronic bands. A similar situation prevails for the anions of TCNE.

The intensity changes of the $TCNQ^{\cdot-}$ Raman bands with a change of excitation line wavelength were expressed in terms of Resonance Raman excitation curves (RREC) (130). The intensity of the Raman vibrational bands of $TCNQ^{\cdot-}$ in CH_3CN solution for different excitation wavelengths were compared with standard Raman bands of the solvent. The intensity ratios, $I_{TCNQ^{\cdot-}}/I_{CH_3CN}$ were plotted against the excitation wavelength to construct RRECs for the Raman bands of $TCNQ^{\cdot-}$. For the nonstoichiometric salts, relative intensity changes of the RR bands of $TCNQ^{\cdot-}$ for the $4880^{\circ}A$ and $5145^{\circ}A$ laser lines can be correlated with the composition. The intensities of the 1207, 1396, 1610 and 2220 cm^{-1} Raman bands are enhanced in the composition range $1.1 \leq x \leq 1.45$. Other $TCNQ^{\cdot-}$ Raman bands at 987, 1184, 1326, 1339 and 1583 cm^{-1} are resonantly enhanced in the range $1.45 \leq x \leq 1.75$. To measure the relative intensity changes, one of the $TCNQ^{\cdot-}$ Raman bands (1610 cm^{-1}) is chosen as a standard. Thus the peak intensity ratio of any RR band (I_s) and the 1610 cm^{-1} band are plotted against the metal/organic ratio (x) of the nonstoichiometric salt. The Resonance Raman composition curve (RRCC) constructed in this way for the $4880^{\circ}A$ and $5145^{\circ}A$ laser lines are shown in Figure 28. A change in I_s/I_{1610} depends on two factors: a) a change in the intensity of the Raman band (i.e. the numerator I_s) and b) a change in the intensity of the 1610 cm^{-1} Raman line (i.e. the denominator I_{1610}). The shapes of the curves thus obtained for the A-type Raman lines are different than those of the non-A-type. Since for the composition range $1.0 \leq x \leq 2.0$ I_{1610} is assumed to be 1.0 (i.e. a line parallel to the Na/TCNQ axis), RRCCs for the A-type bands are almost parallel to the 1610 cm^{-1} line. For the non-A type lines,

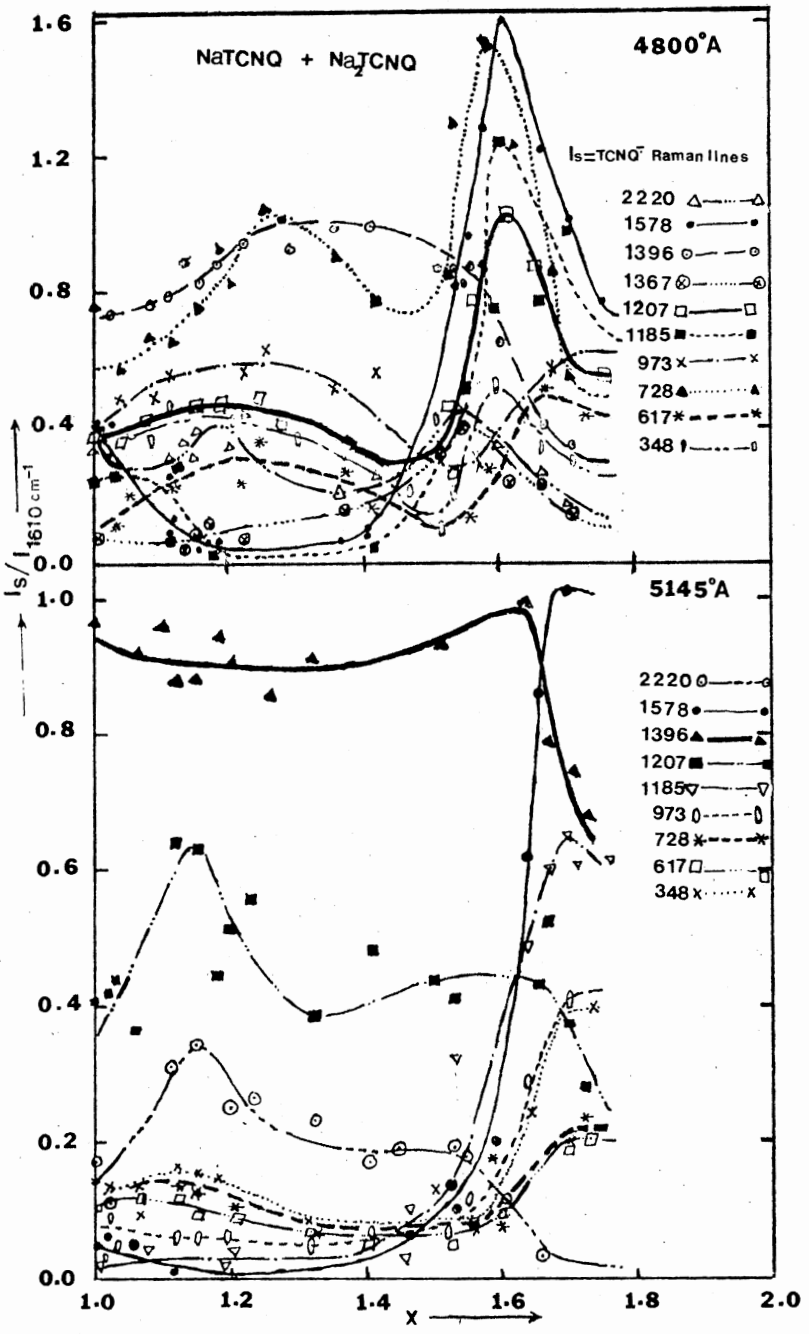

Figure 28. Resonance Raman Composition Curves for $TCNQ^-$ Bands, for the 4880°A and 5145°A Laser Excitation Lines in a Range: $1.0 \leq x \leq 1.75$

I_s/I_{1610} ratio increases in the range $1.45 \leq x \leq 1.6$. This may be due to the enhancement of the intensities of the non-A type bands and/or decrease in the intensity of the 1610 cm^{-1} line. The intensities of all the Raman bands in the range $1.6 \leq x \leq 1.75$ decrease as shown in Figure 28.

These RRCCs can be interpreted in terms of the electronic band movements. Chi and Nixon's RR spectra of KTCNQ at fixed composition (1:1) for the different excitation wavelengths are used as a reference (Figure 2). Though as discussed earlier, these RR intensity patterns are not for the pure monoanion salts, but contain some oxygen reaction products like α,α-DCTC$^-$. In spite of such limitations, Chi and Nixon's spectra can be used as a general reference since many TCNQ$^-$ and α,α-DCTC$^-$ RR bands appear to have almost the same frequency. Thus the RR intensity patterns of KTCNQ at the 5682 and 6471^{o}A appear to be similar to those of nonstoichiometric salts of compositions in the range $1.0 \leq x \leq 1.45$ for the 5145^{o}A laser line. Similar patterns are also observed for the 4880^{o}A laser line in the composition range $1.15 \leq x \leq 1.4$. Hence the positions of the 4880^{o}A and 5145^{o} laser lines with respect to the electronic spectrum of nonstoichiometric salts, in the range $1.15 \leq x \leq 1.4$, may be similar to those of the 5682^{o}A and 6471^{o}A laser lines for the 1:1 KTCNQ salts. Similarly, the 4880^{o}A and 5145^{o}A laser lines should be in the similar part of the electronic spectrum of the monostoichiometric salts ($1.45 \leq x \leq 1.6$) as the 4579^{o}A and 4880^{o}A laser lines for the 1:1 KTCNQ salt to display similar RR intensity patterns. Thus in the case of Chi and Nixon's RR spectra, the laser excitation lines are moved across the electronic spectrum of KTCNQ. In the case of the nonstoichiometric salts, the electronic bands are shifted with respect to the laser lines by changing the composition. Thus in the $1.0 \leq x \leq 1.3$ composition range,

the 365 and 620 mμ electronic bands may have been shifted towards the blue side of the spectrum. In the $1.3 \leq x \leq 1.6$ range, the bathochromic shifts of the electronic bands can be deduced from the changing RR intensity patterns. The shifts in the electronic bands of $TCNQ^{\cdot-}$, with a changing composition of the nonstoichiometric salts in the composition range $1.0 \leq x \leq 1.75$, are shown in Figure 29.

The reason for such electronic shifts may be that these nonstoichiometric salts are not mere mixtures of $TCNQ^{\cdot-}$ and $TCNQ^{-2}$, but are ionic solutions. At low concentrations of the dianion in the sample, the electronic bands of the monoanion which may be taken as a solvent show blue shifts. At higher concentrations of $TCNQ^{-2}$, the roles of the solute and solvent are reversed and the RR intensity patterns changed as if the electronic bands of the monoanion solute shifted to longer wavelengths. Though the actual shifts of the electronic bands could not be observed for reasons mentioned earlier, such bathochromic shifts in the electronic bands of 5,6-benzoquinoline have been observed when the composition of its nonstoichiometric salts with bromine was change (152). Shifts in the electronic bands of $TCNQ^{-2}$ and $TCNQ^{-3}$ in the nonstoichiometric salts have been noted earlier. For the nonstoichiometric salts of TCNE, in a composition range $2.0 \leq Na/TCNE \leq 3.0$, shifts in the electronic bands were also observed (Table II). Due to the shifts in the electronic bands of $TCNQ^{-3}$ in a composition range $2.0 \leq x \leq 3.0$, the changing RR intensity patterns were observed. RRCCs for the RR bands of $TCNQ^{-3}$ with the 1579 cm^{-1} line as a standard are constructed for the 4880°A and 5145°A laser excitation lines (Figure 30). The most intense 1138 cm^{-1} Raman band appears to be very sensitive to the composition of the salt. The maximum intensity enhancement for the 1138 cm^{-1} band was observed in the

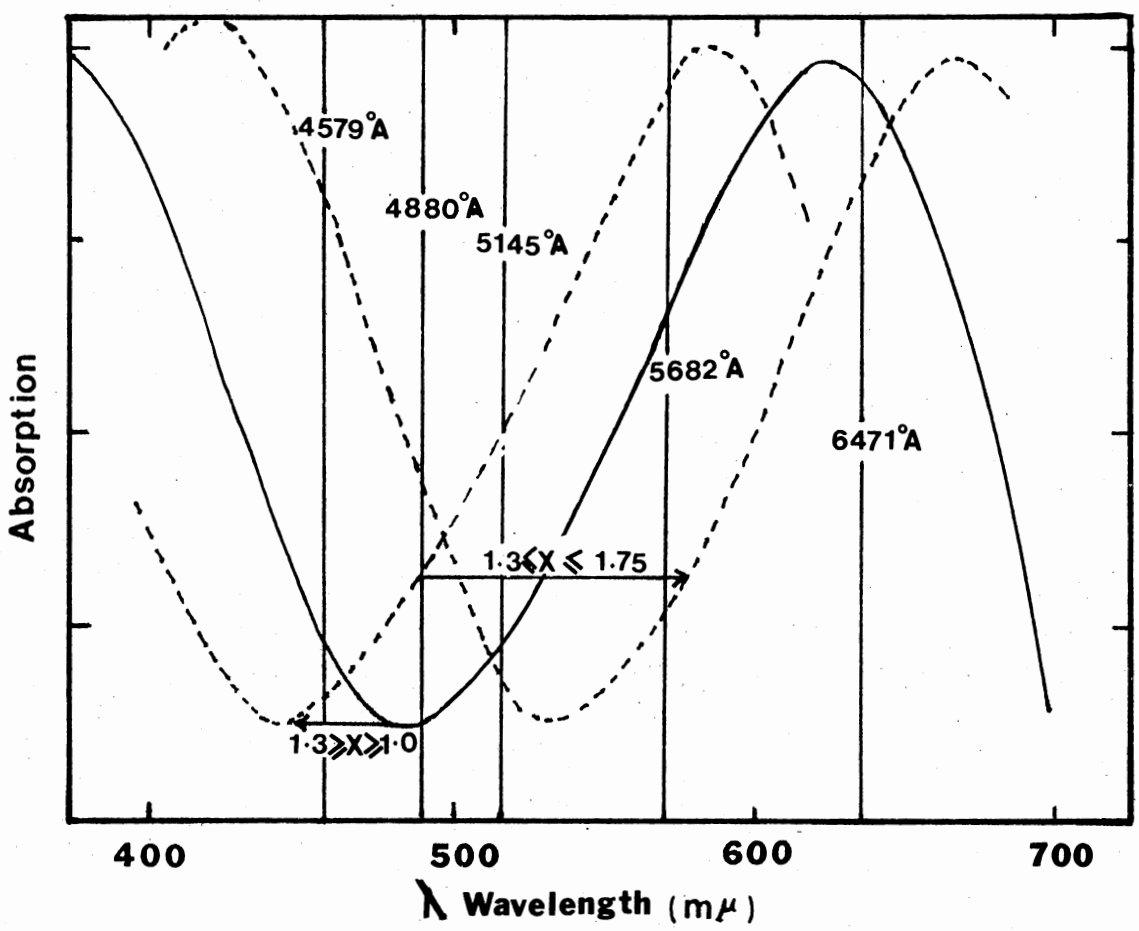

Figure 29. Shifts in the Electronic Bands of NaTCNQ with a Change in the Composition of the Nonstoichimetric Salts in a Range $1.0 \leq x \leq 2.0$, Deduced from the Changing Intensity Patterns of the Resonance Raman Spectra of $TCNQ^{-}$

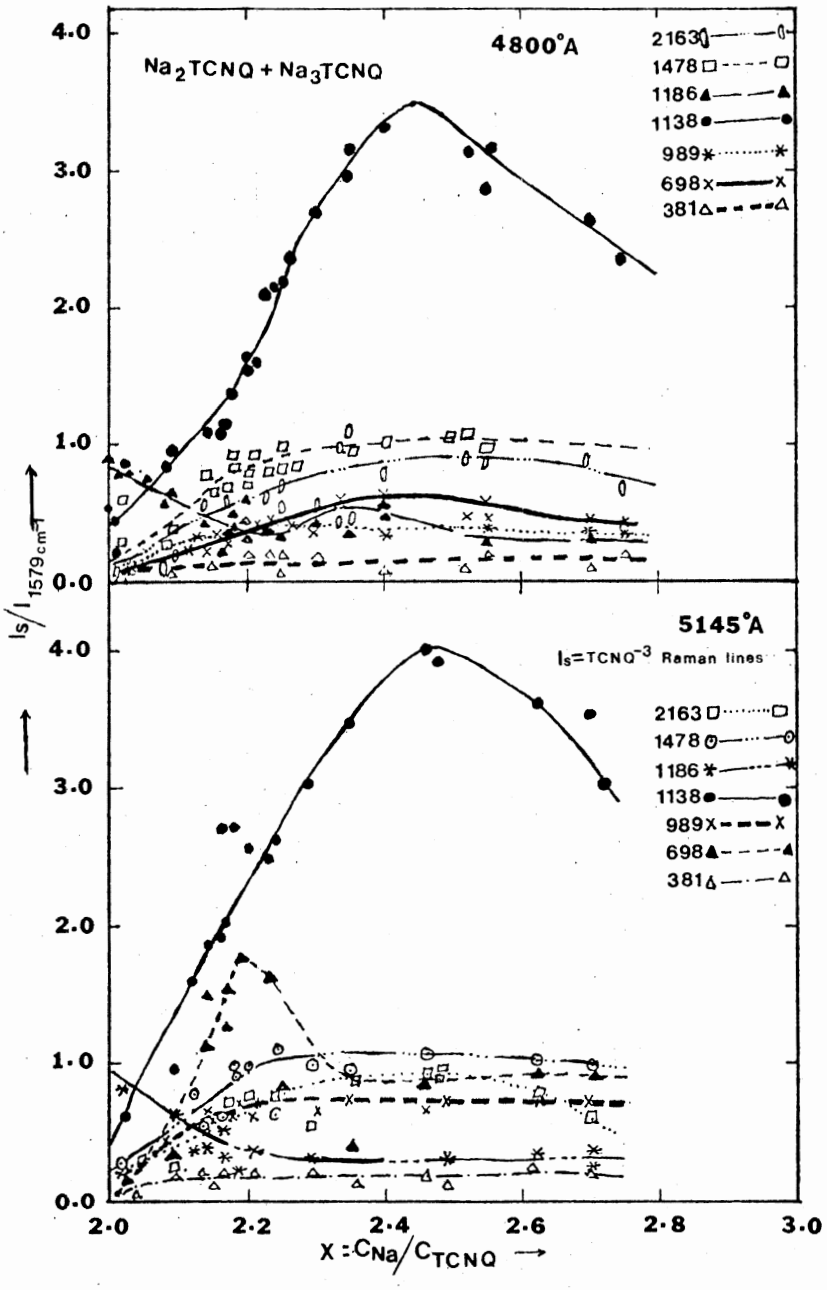

Figure 30. Resonance Raman Composition Curves for the $TCNQ^{-3}$ Bands, for the 4880°A and 5145°A Laser Excitation Lines, in a Composition Range $2.0 \leq Na/TCNQ \leq 3.0$

composition range $2.4 \leq x \leq 2.7$. Other Raman bands except the 698 cm^{-1} band do not show very high sensitivity towards composition change in the $2.2 \leq x \leq 2.75$ range. Again the changing RR intensity patterns of $TCNQ^{-3}$ with composition can be explained in terms of shifts of the 427mμ electronic band. Such shifts may be a result of solution formation between the di- and trianions of TCNQ.

For the TCNE salts, the 1420 and 2220 cm^{-1} Raman bands of $TCNE^{\cdot-}$ were observed to be sensitive to the composition in the range $1.0 \leq$ Na/TCNE ≤ 2.0 (9). The resonance intensity enhancement of the 1420 and the 2220 cm^{-1} Raman bands with respect to the other bands at Na/TCNE ~ 1.5 can be explained in terms of bathochromic shifts of the monoanionic electronic bands. The RR bands of $TCNE^{-3}$ were observed to be very weak, hence the Raman spectra of the nonstoichiometric salts in a range $2.0 \leq x \leq 3.0$ were not investigated.

Frequency Shifts and Factor Group Splitting for the Anions of TCNQ and TCNE

The changes in the bond strengths and force constants with the addition of each electron to TCNQ and TCNE were discussed earlier. In this section, the effect of the ionic charge on the electron acceptor, especially the frequencies of their symmetry modes will be examined. Since there are some questions about the vibrational band assignments of $TCNQ^{-2}$ and $TCNQ^{-3}$, the frequency shifts with an addition of each electron will be given for both the assignments given in Table IV and Table XVIII. Each of the TCNQ vibrational modes except those corresponding to the C≡N and C-H stretching vibrations are contributed by more than one internal coordinates. Hence no obvious correlation between the frequency shifts and bond strengths in the anions can be established. The

C≡N stretching vibrational bands, however, give some idea about the extent of the effect of an addition of each electron. For example, in the case of TCNQ, the bathochromic shifts increase with an addition of each successive electrons (Table XIX). Thus the C≡N stretching a_g mode shifts to lower frequency by about 36, 43 and 117 cm^{-1} in the mono-, di- and trianion with respect to the neutral TCNQ. Similarly, for the C≡N stretching a_g mode of TCNE, the shifts are 35, 103 and 26 cm^{-1}, for the addition of first, second and third electrons (Table XX). The shifts for other symmetry modes are listed in Tables XIX and XX.

As discussed earlier, the vibronic interactions in the anion salts of TCNQ and TCNE activate the a_g symmetry modes in the IR spectra. A contribution of vibronic interaction from the electron exchange between the monoanion radicals may be the dominant factor in the IR activation of a_g modes. For the di- and trianions IR activity of a_g modes may possibly be due to the vibronic interaction originated from the back-bonding and some distortion effects. The factor group and distortion splitting between the IR and Raman bands corresponding to the factor group components of the a_g modes vary with an ionic charge on TCNQ or TCNE. The possible values of the factor group/distortion splitting based on the vibrational band assignments given in Tables IV, XIII and XVIII are listed in Table XXI. Values of the factor group/distortion splitting for the anions appear to be dependent on the ionic charge. The values of the factor splitting for some of the a_g symmetry modes, in the di- and trianions of TCNQ are less for the assignments given in Table IV and more for those given in Table XVIII as compared with $TCNQ^{\cdot-}$. For the anions of TCNE, factor group splitting values are given in Table XXI. Until the vibrational band assignments are established on a more

TABLE XIX

FREQUENCY SHIFTS WITH AN ADDITION OF EACH ELECTRON TO TCNQ

Symmetry Species		Δ_0^1 (cm^{-1})	Δ_1^2 Assign. I (cm^{-1})	Δ_1^2 Assign. II (cm^{-1})	Δ_2^3 Assign. I (cm^{-1})	Δ_2^3 Assign II (cm^{-1})
a_g	ν_1	-23	-18		-19	
	ν_2	-36	-43	-47	-117	-117
	ν_3	- 8	+ 3	+ 2	-20	-68
	ν_4	-86	-40	-10	-12	- 8
	ν_5	-15	- 2	-28	- 8	+25
	ν_6	+26	+25	+50	-13	-27
	ν_7	+15	+ 6		+ 6	+15
b_{3g}	ν_{41}	-11	-18		-14	
	ν_{42}	-29	-35		-107	
	ν_{43}	+75	+20	+20	+53	+53
	ν_{44}	-26	- 2		+14	
	ν_{45}	+ 4	+ 7		+ 7	
b_{1u}	ν_{18}	-27	-24	-24	-18	-18
	ν_{19}	-31	-41		-116	
	ν_{20}	-40	- 7		-18	
	ν_{21}	-36	-32		- 9	
	ν_{22}	+10	+ 4		+ 4	
b_{2u}	ν_{32}	-23	-18	-18	-19	-19
	ν_{33}	-29	-35	-35	-112	-112
	ν_{34}	-30	- 2		-27	
	ν_{35}	+ 9	+14		+15	
	ν_{36}	- 2	+12	+12	+ 7	+ 7
b_{2g}	ν_{29}	- 9	- 6	- 6	+ 3	+ 3
	ν_{30}	--	+11	+11	-19	-19
b_{3u}	ν_{50}	-36	- 4	- 4	+ 8	+ 8

$\Delta_0^1 = \nu_{TCNQ^-} - \nu_{TCNQ^0}$

$\Delta_1^2 = \nu_{TCNQ^{-2}} - \nu_{TCNQ^-}$

$\Delta_2^3 = \nu_{TCNQ^{-3}} - \nu_{TCNQ^{-2}}$

Assign. I = assignments given in Table IV
Assign. II = assignments given in Table XVIII

TABLE XX

FREQUENCY SHIFTS WITH AN ADDITION OF EACH ELECTRON TO TCNQ

Symmetry Species		$\Delta^1_\circ$ (cm^{-1})	Δ^2_1 (cm^{-1})	Δ^3_2 (cm^{-1})
a_g	ν_1	- 35	-103	- 26
	ν_2	-177	-116	-152
	ν_3	- 3	+ 17	- 9
	ν_4	- 26	- 12	- 26
b_{3g}	ν_{19}	- 26	+ 11	- 9
	ν_{20}	+ 21	+ 2	+ 37
b_{1u}	ν_9	- 33		- 30
	ν_{10}	+ 12	+ 12	+ 10
b_{2u}	ν_{15}	- 27	- 92	- 12
	ν_{16}	+ 32	- 1	+ 68
b_{3u}	ν_{23}	+ 2	+ 2	+ 1

$\Delta^1_\circ = \nu_{TCNE^{\cdot -}} - \nu_{TCNE^\circ}$ (Ref. 110)

$\Delta^2_1 = \nu_{TCNE^{-2}} - \nu_{TCNE^{\cdot -}}$

$\Delta^3_2 = \nu_{TCNE^{-3}} - \nu_{TCNE^{-2}}$

reasonable basis, the choice between the two values and any conclusions drawn from these values are open to discussion.

Much of the added electron density in the anion salts of TCNQ and TCNE is apparently concentrated on the $(C\text{-}C\equiv N)_2$ part of the molecule (57) (77) and particularly C≡N bonds. The vibrational bands of TCNQ, TCNE and their anions in the 1900-2300 cm^{-1} frequency region are assigned to the C≡N stretching vibrations. The splitting between the internal modes of C≡N stretching vibrations, in addition to the π-bond order and force constant changes, may be helpful in understanding the effects of added electrons on the C≡N bond. The C≡N stretching internal mode splitting for the TCNQ molecule increases from 6 cm^{-1} for the neutral to 54 cm^{-1} for the monoanion, 100 cm^{-1} for the dianion and 262 cm^{-1} for the trianion (Table XXI). Similarly, the C≡N internal mode splittings for the neutral, mono-, di- and trianions of TCNE are 35, 37, 76 and 256 cm^{-1} respectively (Table XXI).

Such large splitting values indicate increasing unequality of the C≡N stretching internal modes. For example, an increase from 6 cm^{-1} to 54 cm^{-1} when the first electron is added to TCNQ may be attributed to the effect of unequal distance of different C≡N bonds from the sodium cation. The distance between Na^+ and N atoms of different C≡N bonds in the monoclinic crystals of NaTCNQ varies between 3.384°A and 3.686°A (21). This means that the four C≡N bonds of TCNQ may not be affected equally by the charge transfer from the electron donor to the acceptor. Even larger splittings of the di- and trianionic C≡N bonds induced by the sodium cations.

A correlation between the C≡N internal mode splittings ($\Delta\nu$ internal) and the negative charge on TCNQ and TCNE are shown in Figure 31. There is a nearly linear correlation between $\Delta\nu_{C\equiv N}^{int.}$ and ionic charge for the

TABLE XXI

THE CHANGES IN THE SPLITTINGS OF THE C≡N STRETCHING INTERNAL MODES AND THE FACTOR COMPONENTS WITH ADDITION OF EACH ELECTRON TO TCNQ AND TCNE

Anion and Type of Splitting	Symmetry Species	Monoanion (cm^{-1})	Dianion		Trianion	
			Assign. I (cm^{-1})	Assign. II (cm^{-1})	Assign. I (cm^{-1})	Assign. II (cm^{-1})
	a_g ν_2	54	100	100	262	262
TCNQ anions	ν_3	32	4	4	2	103
Factor Group	ν_4	83	53	135	32	136
Splitting	ν_5	52	2	69	1	111
	ν_6	20	0	53	6	105
	ν_7	10	40	40	24	82
	ν_8	2	17	34	44	74
	ν_9	18				
	b_{2g} ν_{29}	12	0	0	2	2
	ν_{30}	14	0	0	4	4
TCNE Anions	a_g ν_1	37	76		256	
Factor Group	ν_2	50	56		155	
Splitting	ν_3	9	6		19	
	ν_4	8			12	
Splitting between the Internal C≡N Stretching Modes of TCNQ Anions*	a_g ν_2 b_{3g} ν_{42} b_{1u} ν_{19} b_{2u} ν_{33}	54	100	100	262	262
Splitting between the Internal C≡N Stretching Modes of TCNE Anions*	a_g ν_1 b_{3g} ν_{19} b_{1u} ν_9 b_{2u} ν_{16}	37	76		256	

*Splitting between the C≡N stretching vibrational bands e.g. for $TCNQ^o$, 6 cm^{-1} (reference 116) and for $TCNE^o$, 35 cm^{-1} (reference 9).

Assign. I and Assign. II refer to the assignments given in Table IV and XVIII respectively for the TCNQ anions and in Table XIII for the TCNE anions.

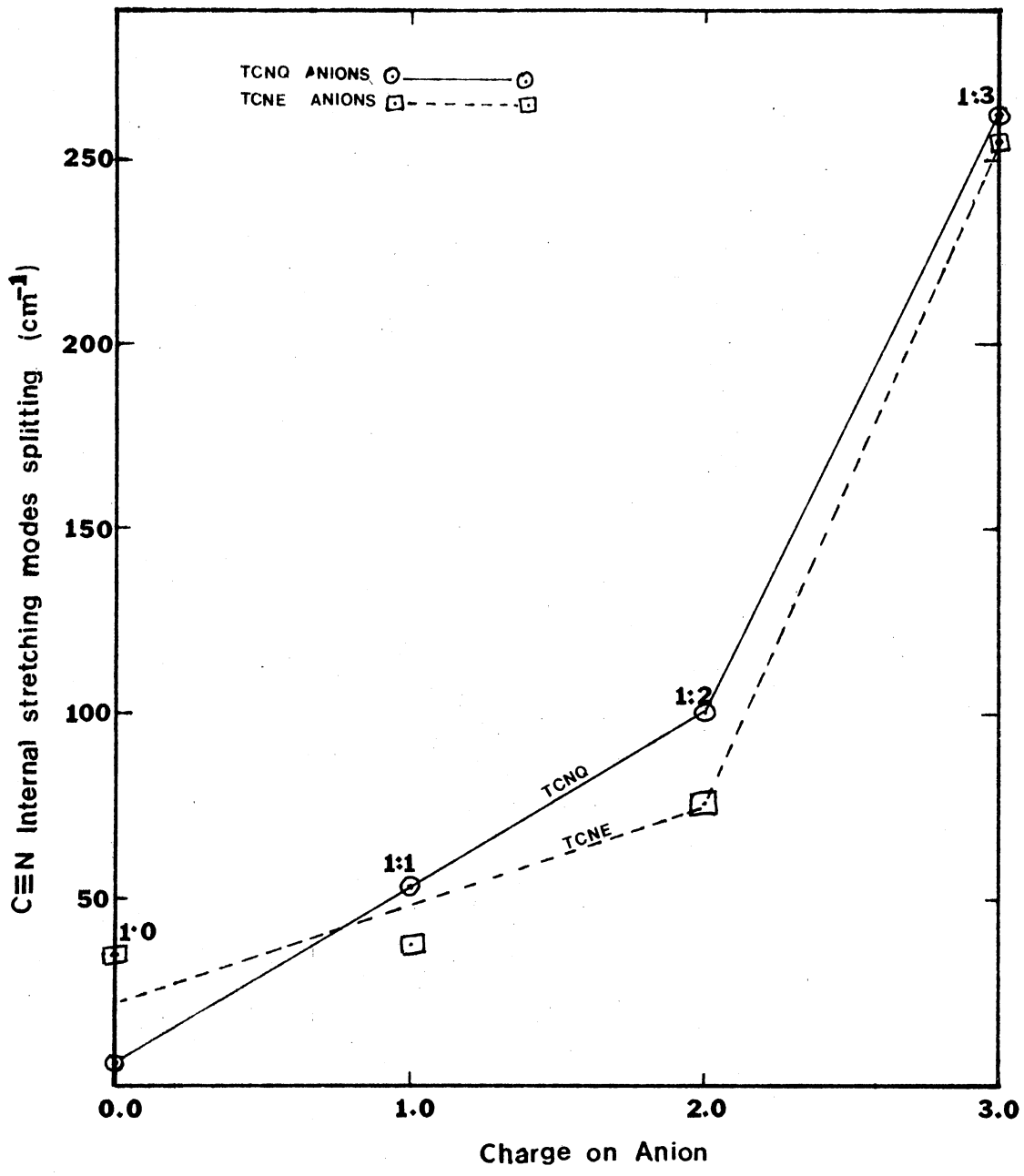

Figure 31. Correlations Between Splitting of the Vibrational Bands of the Internal Modes of the C≡N Stretching and Ionic Charge on TCNQ and TCNE

neutral, mono- and dianions. For the trianions, however, there is a tremendous increase in the internal mode splitting.

Possible orientations of the sodium cations with respect to $TCNQ^{-2}$ are shown in Figure 32. No crystallographic data is available to choose between these orientations, but intuitively, arrangement (a) where Na cations are farthest apart might be the most favored and (b) where Na cations are very close might be the least favorable. Arrangement of the Na cations with respect to the trianion of TCNQ is also shown in Figure 32.

Effect of Ionic Charge on the Nature of Interactions Between the TCNQ and TCNE Anions and Oxygen

The di- and trianions of TCNQ and TCNE act as electron donors and oxygen as an electron acceptor. When the di- and trianion salts interact with oxygen, there is competition between sodium and TCNQ or TCNE anions to form peroxides or oxygen complexes. Only dianions seem to undergo a chemical reaction with oxygen to form α,α-$DCTC^{-}$ or tricyanoethenolate. Apparent stability of the trianions and their oxygen reaction products is unexpectedly surprising. A similarity between spectroscopic and other physical properties of TCNQ and TCNE anions appears to be extended even to the ways they react with oxygen.

When the metal to organic ratio is about 2.0, reaction of oxygen with $TCNQ^{-2}$ produces two broad bands at 350 and 550 cm^{-1} in the Raman spectrum. Though it is tempting to assign these bands to the O_2 complex of the dianion, however, no other evidence like 1090 cm^{-1} O_2^{-} vibrational band (154) was observed. This oxygen reaction product was observed to be unstable and further exposure to O_2 leads to the formation of α,α-$DCTC^{-}$.

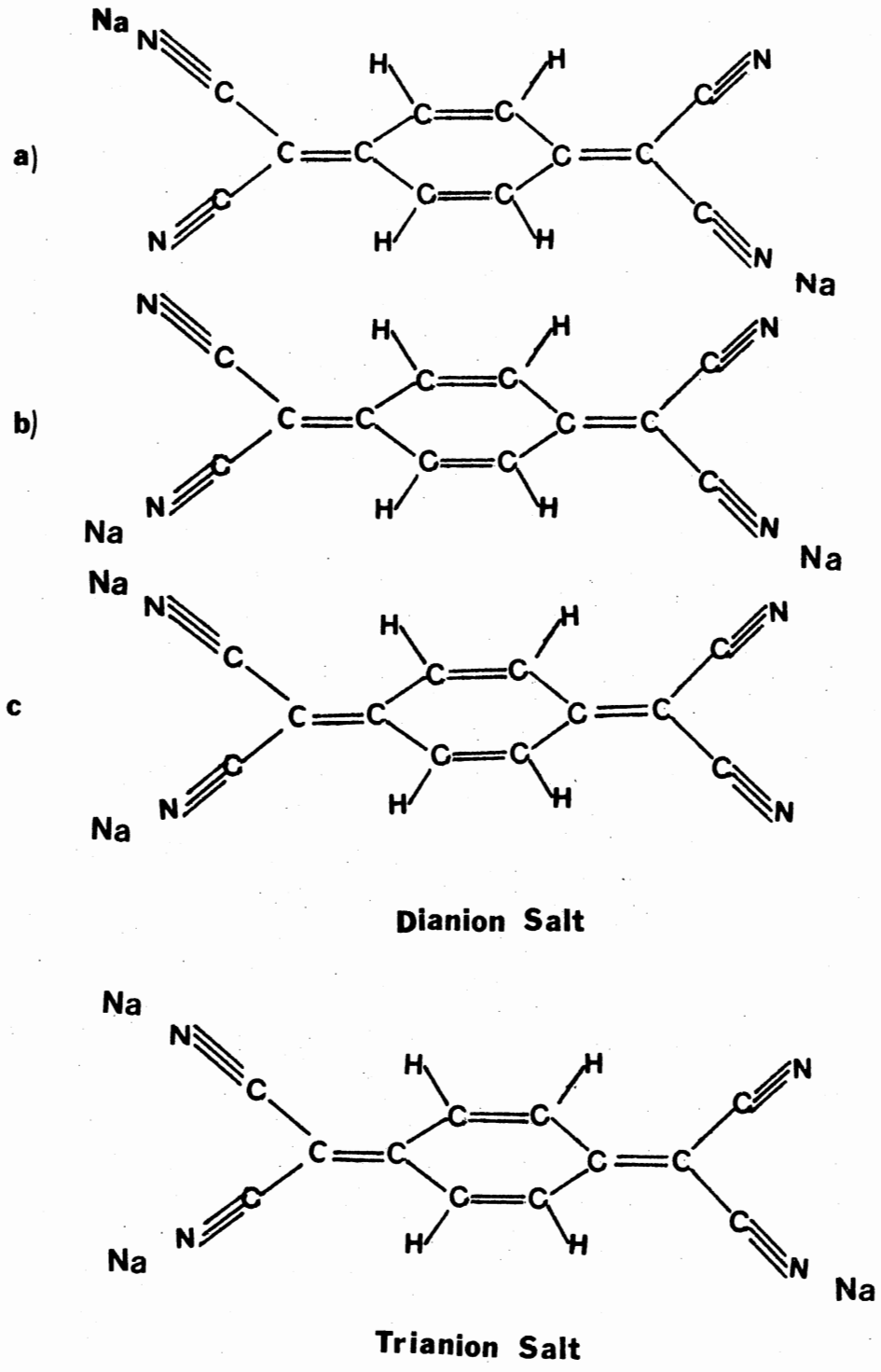

Figure 32. Possible Orientations of Sodium Cations with Respect to TCNQ in the Na_2TCNQ and Na_3TCNQ Salts

CHAPTER VI

SUMMARY AND CONCLUSIONS

In this study, the mono-, di- and trianion salts of TCNQ and TCNE were prepared. These salts were characterized by their electronic, IR and Raman vibrational spectra. The effect of an extent and nature of vibronic interaction on the vibrational spectra of each anion were examined for the vibrational band assignments. Based on these assignments, normal coordinate analysis was done and the force constants were calculated. These empirical force constants were correlated with the Π-bond orders obtained from the published MO calculations. Alternate vibrational band assignments for the di- and trianions of TCNQ has also been suggested. Effects of composition change on the vibrational band intensities and the energy of electronic transitions in nonstoichiometric salts were investigated. The nature and extent of the reactions of TCNQ and TCNE anions with oxygen were examined. The reaction products were characterized by their electronic and vibrational spectra.

The anion salts were prepared by co-condensation of the sodium and organic vapors in vacuum. The thin films of the salts thus prepared at room temperature were deposited on the appropriate substrates for the spectroscopic sampling. The electronic and vibrational spectra measured at the room temperature as well as liquid nitrogen temperature. The monoanion radical salts of TCNQ and TCNE were blue and violet colored thin films respectively. The di- and trianions of TCNQ and TCNE were

colorless and yellow colored respectively. The C≡N stretching IR bands, characteristic of each anion shifted to low frequency with an addition of each electron to TCNQ and TCNE. The oxygen reaction products were prepared by exposing anion salts to dry oxygen. This reaction progress arrested at various stages and examined the reaction products at each stage to monitor the course of the reaction.

For the monoclinic polycrystalline thin films of NaTCNQ, four distinct electronic absorption bands were observed at 260, 305, 368 and 620 mμ. The monoanion radicals in the monoclinic crystal structure have been observed to be in the dimer form. The charge oscillation vibronic interaction, as a result of electron exchange between the monoanion radicals activates a_g symmetry modes in the IR spectrum. Thus the 328, 618, 723, 967, 987, 1167, 1178, 1185, 1219, 1326, 1339, 1578 and 2168 cm^{-1} IR bands were assigned to the a_g vibrational modes of $TCNQ^{\cdot-}$. The vibrational bands nearly coincident with the above mentioned COV IR bands and the corresponding Raman bands at 482, 494, 590 and 800 cm^{-1} were assigned to the b_{1g} and b_{2g} symmetry modes attributed to the charge oscillation vibronic interaction as a result of variations in the overlap of neighboring $TCNQ^{\cdot-}$ wave functions due to the mechanical motion. Normal coordinate analysis and force constant calculations based on these vibrational band assignments reporduced the observed frequencies satisfactorily. The discrepanices between the IR and Raman frequencies were attributed to the factor group splittings. The values of the factor group splittings were in the range of 2-83 cm^{-1}. A large splitting between the internal modes of the C≡N stretching vibrations of the monanion radical (54 cm^{-1}) as compared with the neutral molecule (6 cm^{-1}) was attributed to the unequivalent effect of charge transfer on the four

C≡N groups. X-ray crystallographic study revealed that the distance between the C≡N bonds from sodium is not same.

Similarly, COV interaction originated from the electron exchange between the TCNE monoanion radicals components of the dimer, activates the a_g vibrational modes in the IR spectrum as observed by Hinkel and Develin (110). The electronic absorption bands were observed at 2.14 and 3.54 eV., indicating the dimer nature of the salt. The factor group splittings (110) for the a_g symmetry modes and the internal mode splitting for the C≡N stretching vibrations of $TCNE^{\cdot-}$ were observed to be in the range 9-50 cm^{-1}.

The electronic absorption peaks for the colorless Na_2TCNQ salt were observed at 205, 240 and 295 mμ in the uv region. All these electronic transitions correspond to the LE electronic bands of $TCNQ^{-2}$. The low energy electronic bands in the visible and IR region which may conceivably be indentified with the charge transfer interactions, were not detected. The IR bands at 623, 715, 999, 1195, 1303, 1598 and 2096 cm^{-1} and a nearly coincident Raman bands were assigned to the a_g vibrational modes of $TCNQ^{-2}$. Such an apparent violation of the mutual exclusion principle under the presumed D_{2h} molecular symmetry of $TCNQ^{-2}$, may be due to some vibronic interaction. One of the possible origins of such vibronic interaction may be back-bonding between the two sodium cation and $TCNQ^{-2}$. The coupling between the two back bonding interactions and stretching vibrations of the dianion may give rise to the COV type vibronic interaction, which may be responsible for IR activation of the a_g symmetry modes. The 500 and 578 cm^{-1} IR and Raman bands of $TCNQ^{-2}$ may be assigned to the b_{2g} mode (with out-of-plane rotational character).

Two alternative vibrational band assignments are suggested for the dianion of TCNQ. In the first case, factor group/distortion splitting

is less than that of the monoanion and in another case, the values are higher. The splittings between the internal stretching modes of C≡N bonds are higher than in the monoanion ($\sim$100 cm^{-1}). Possible orientations of the sodium cations with respect to $TCNQ^{-2}$ are suggested.

Similar observations were made for the colorless salt of Na_2TCNE. The electronic absorption bands were observed at 213 and 237mμ in the uv region. The 452, 546, 552, 1256, 1263, 1282, 1312, 2072, 2086, and 2146 cm^{-1} IR bands and the 549, 1268, 2068 cm^{-1} Raman bands were assigned to the a_g symmetry modes of $TCNE^{-2}$. The nature of vibronic interaction was presumed to be similar to that of $TCNQ^{-2}$. Factor group/distortion splitting between the C≡N stretching internal modes, the orientation of sodium cations with respect to $TCNE^{-2}$ may be similar to that of Na_2TCNQ.

For the golden yellow colored Na_3TCNQ, the electronic absorption peaks at 195, 234, 265, 310, 370 and 427mμ were observed in the visible and uv region. The strong resonant Raman spectra of $TCNQ^{-3}$ were observed for the laser excitation lines at 4880°A and 5145°A. The IR bands at 628, 983, 1183, 1284, 1577 and 1901 cm^{-1} and the nearly coincident Raman bands were assigned to the a_g symmetry modes. Again as in the case of the dianion, IR activation of the a_g modes was attributed to the vibronic interaction, as a result of coupling between the three back-bonding interactions and the stretching vibrational modes of $TCNQ^{-3}$. Interestingly, some of the out-of-plane and in-plane b_u symmetry modes became Raman active in $TCNQ^{-3}$. A possible explanation may lie in the elements of asymmetry (or distortions) introduced by three non-linear back-bonding interactions. Factor group and internal modes of the C≡N stretching splitting values for $TCNQ^{-3}$ were observed to be larger

($\sim$262 cm^{-1}) than the mono- and dianion salts. Possible arrangements of the three sodium cations with respect to $TCNQ^{-3}$ has been suggested.

In the vibrational band assignments considered above, very strong RR bands at 1138 and 1476 cm^{-1} were assigned to the b_u modes. Some other vibrational bands could not be assigned to the symmetry modes of $TCNQ^{-3}$. Alternative vibrational assignments were suggested. Under this scheme, very large factor group splitting values were observed.

The electronic transitions for Na_3TCNE were observed to be at 210, 236, 265, and 365 mμ in the uv region. Presuming the structure and vibronic interactions of Na_3TCNE similar to Na_3TCNQ, the 549, 642, 1346, 1417, 1498, 1980 and 2160 cm^{-1} Raman bands and the 530, 675, 1348, 1456, 1503, 2062, 2120 and 2160 cm^{-1} Raman bands were assigned to the factor group components of the a_g symmetry modes. The out-of-plane b_{3u} mode (ν_{23}) like $TCNQ^{-3}$ case, appears to be activated in Raman spectrum at 560 cm^{-1}. The splittings between the factor group components and the internal modes of C≡N stretching were observed to be enormously large ($\sim$256 cm^{-1}).

In the monoanion radical salts, band widths of the COV IR bands are larger than the nonvibronic bands. The IR bands of the TCNQ and TCNE were satisfactorily reproduced from the normal coordinate analyses. The force constants calculated for the neutral and anions show a nearly linear correlation with the Π-bond orders. The shifts in the vibrational frequencies of the TCNQ symmetry modes with the addition of each electron were noted. The vibrational bands corresponding to the ν_1, ν_2, ν_3, ν_4, ν_5 (all a_g) ν_{41}, ν_{42}, ν_{44} (b_{3g}) ν_{18}, ν_{19}, ν_{20}, ν_{21} (b_{1u}), ν_{32}, ν_{34} (b_{2u}) and ν_{15} (b_{17}) were shifted to low frequency side consistently with the addition of each electron to TCNQ. The ν_{43} (b_{3g}) mode shows consistent hypsochromic shifts with the addition of each electron. Other symmetry

modes show nonconsistent trends in their shifts as the neutral TCNQ is converted to the mono-, di- and trianion. Similarly, C≡N stretching modes of TCNE show consistent bathochromic shifts with the addition of the first two electrons and the trend appears to be reversed when the third electron is added.

The effect of a change in composition on the vibrational band intensities were observed in the nonstoichiometric salts. An increase in the intensity of the COV IR bands of $TCNQ^{\cdot-}$, with a change in composition in the $1.0 \leq Na/TCNQ \leq 1.3$ range, may be attributed to the loss of orientation of the monoanion radicals with respect to the substrate surface. The changing intensity patterns of RR spectra with change in composition of the nonstoichiometric salts were correlated with shifts of the electronic bands. The shifts of the electronic bands may be attributed to the formation of ionic solutions between the different anions of TCNQ. The Resonance Raman composition curves were constructed to correlate the relative intensity changes of the vibrational bands to the composition of the nonstoichiometric salts. Similar changes of intensity patterns of the RR spectra of NaTCNE in the $1.0 \leq Na/TCNE \leq 2.0$ composition range were noted.

The anionic charge on TCNQ and TCNE was observed to have an effect on the nature of their reaction with oxygen and that of the reaction products. Particularly, the dianion salts were observed to react with oxygen spontaneously. $TCNQ^{-2}$ and oxygen reaction produced αα-$DCTC^{-}$ which was characterized by the electronic and vibrational spectra. $TCNE^{-2}$ reaction with oxygen results in the formation of tricyanoethenolate.

The reaction of the trianion salts of TCNQ and TCNE with oxygen were observed to be slower than those of the dianion salts. The reaction products of Na_3TCNQ and oxygen appeared to be very stable. The

electronic absorption bands were observed to be at 250, 242, and 352 μ in the uv region. The intensity pattern and the vibrational band frequencies of the $Na_3TCNQ.O_2$ reaction product and Na_2TCNQ appeared to be almost identical. A possible reaction $Na_3TCNQ + O_2 \rightarrow NaO_2 + Na_2TCNQ$ may explain the similarity between the vibrational spectra of the $Na_3TCNQ.O_2$ reaction product and Na_2TCNQ. The stability of $Na_3TCNQ.O_2$ may be attributed to the formation of a NaO_2 coating on the thin film and thus preventing further reaction with oxygen.

A SELECTED BIBLIOGRAPHY

(1) F. Gutman and L. E. Lyons, Organic Semiconductors, Wiley Interscience, New York, N. Y., 1967.

(2) a) S. A. Berger, Spectrochim Acta, 23A, 2213, 1967.
b) L. E. Lyons and L. D. Palmer, Aust. J. Chem., 29, 1919, 1976.
c) E. C. M. Chen and W. E. Wentworth, J. Chem. Phys., 63, 3183, 1975.

(3) R. M. Metzger, J. Chem. Phys., 63, 5090, 1975.

(4) a) Roy Foster, 'Organic Charge Transfer Complexes', Academic Press, New York, N. Y., 1969.
b) J. Rose, 'Molecular Complexes', Pergamon Press, London, 1957.

(5) H. Kuroda, T. Amano, I. Ikemoto and H. Akamatu, J. Am. Chem. Soc., 89, 6056, 1967.

(6) a) D. J. Dahm, P. Horn, G. R. Johnson, M. G. Miles and J. D. Wilson, J. Cryst. Mol. Struct., 5, 27, 1975.
b) G. R. Anderson, J. Am. Chem. Soc., 92, 3552, 1970.

(7) R. S. Mulliken, J. Chim. Phys., 61, 20, 1964.

(8) a) R. G. Kepler, J. Chem. Phys., 39, 3528, 1963.
b) P. S. Flandrois and E. D. Chasseu, Acta Cryst., B33, 2744, 1977.

(9) Jerald J. Hinkel, A Theoretical and Experimental Study of Vibronic Interactions in the Radical Anion of Tetracyanoethylene, Ph.D. Thesis, Oklahoma State University, Stillwater, Okla., 1974.

(10) Jesse C. Moore, Studies of Some Anion Radicals of Tetracyanoethylene by Infra-red Spectroscopy, M.S. Thesis, Oklahoma State University, Stillwater, Okla., 1968.

(11) a) A. J. Epstein, S. Etemad, A. F. Garito and A. J. Heeger, Phys. Rev., B5, 952, 1972.
b) R. P. Shibaeva and L. O. Atovmyan, Zh. Strukt. Khim., 13, 546, 1972.

(12) R. E. Merrifield and W. D. Phillips, J. Am. Chem. Soc., 80, 2778, 1958.

(13) M. A. Komoryansky and A. C. Wohl, J. Phys. Chem., 79, 695, 1975.

(14) W. D. Phillips, J. C. Bowell and S. I. Weissman, J. Chem. Phys., 83, 626, 1960.

(15) G. Turrell, Infra red and Raman Spectra of Crystals, Academic Press, New York, N. Y., 1972.

(16) D. Steele, Theory of Vibrational Spectroscopy, W. B. Saunders Co., Philadelphia, Pa., 1971.

(17) E. B. Wilson, J. C. Decius and R. C. Cross, Molecular Vibrations, McGraw-Hill Book Company, Inc., New York, N. Y., 1955.

(18) L. R. Melby, R. J. Harder, W. R. Hertler, W. Mahler, R. E. Benson and W. E. Mochel, J. Am. Chem. Soc., 84, 3374, 1962.

(19) W. R. Hertler, H. D. Hertzler, D. S. Acker and R. E. Benson, J. Am. Chem. Soc., 84, 3387, 1962.

(20) W. J. Siemons, P. E. Bierstedt and R. G. Kepler, J. Chem. Phys., 39, 3523, 1963.

(21) a) M. Konno and Y. Saita, Acta. Cryst., B30, 1294, 1974; B31, 2007, 1975.
b) H. Teraruchi, N. Sakamoto and I. Shirotani, J. Chem. Phys., 64, 437, 1976.

(22) a) G. R. Anderson and C. J. Fritchie Jr., Second National Meeting, Society for Applied Spectroscopy, San Diego, 14-18, Oct. 1963, Paper III.
b) M. Konno, T. Ishii and Y. Saito, Acta Cryst., B33, 763, 1977.

(23) E. T. Maas Jr., Mat. Res. Bull., 9, 815, 1974.

(24) A. Hoekestra, T. Spolder and A. Vos, Acta Cryst., B28, 14, 1972.

(25) N. Sakai, I. Shirotani and S. Minomura, Bull. Chem. Soc. Japan, 45, 3314, 3321, 1972.

(26) C. J. Fritchie Jr. and Paul Arthur Jr., Acta. Cryst., 21, 139, 1966.

(27) a) Y. Oahasi and T. Sakata, Bull. Chem. Soc. Japan, 46, 3330, 1973.
b) I. Shirotani, N. Sakai, I. Inokuchi and S. Minomura, Bull. Chem. Soc. Japan, 42, 2087, 1969.

(28) G. P. Saakyan, R. P. Shibaeva and L. O. Atovmyan, Sov. Phys. Doklady, 17, 113, 1973.

(29) J. Ferraris, D. O. Cowan, V. V. Walatkka Jr. and J. H. Perlstein, J. Am. Chem. Soc., 95, 949, 1973.

(30) a) D. B. Tanner, C. S. Jacobson, A. F. Garito and A. J. Heeger, Phys. Rev. Lett., 32, 1301, 1974.
b) D. Jerome, W. Muller and M. Weger, Le Journ. De Phys. Lett., 35, L-77, 1974.
c) J. R. Cooper, D. Jerome, M. Weger and S. Etemad, ibid, 36, L-219, 1975.

(31) D. B. Chestnut and W. D. Phillips, J. Chem. Phys., 35, 1002, 1961.

(32) a) J. G. Vegter, J. Kommandeur and P. A. Feedars, Phys. Rev., B7, 2929, 1973.
b) J. G. Vegter, T. Hibma and J. Kommandeur, Chem. Phys. Lett., 3, 427, 1969.

(33) M. Nepras and R. Zahradnik, Colln. Czech. Chem. Commun. (Engl.) 29, 1545, 1964.

(34) R. Buckers and A. Szent-Györgyi, Recl. Trav. Chim. Pays. Bas. Belg., 81, 255, 1962.

(35) N. O. Lipari, P. Nielsen, J. J. Ritsko, A. J. Epstein and D. J. Sandman, Phys. Rev., B14, 2229, 1976.

(36) H. T. Jonkman and J. Kommandeur, Chem. Phys. Lett., 15, 496, 1972.

(37) S. Hiroma, H. Kuroda, and H. Akamatu, Bull. Chem. Soc. Japan, 43, 3626, 1970.

(38) a) T. Kondow and T. Sakata, Phys. Status Solidi, 6A, 551, 1971.
b) T. Kondow, S. Siratori and H. Inokuchi, J. Phys. Soc. Japan, 21, 824, 1966; 23, 98, 1967.

(39) a) H. Kuroda, K. Yoshihara and H. Akamatu, Bull. Chem. Soc. Japan, 35, 1604, 1962.
b) H. Kuroda, M. Kobayashi, M. Kinoshita and S. Takemoto, J. Chem. Phys., 36, 357. 1962.
C. H. Akamatu and H. Kuroda, J. Chem. Phys., 39, 3364, 1963.

(40) L. B. Coleman, C. R. Fincher Jr., A. F. Gorito, and A. J. Heeger, Phys. Status Solidi, B75, 239, 1976.

(41) J. E. Eldridge, Solid State Comm., 19, 607, 1976.

(42) T. O. Poehler, A. N. Bloch, J. P. Ferraris and D. O. Cowan, Soid State Comm., 15, 337, 1974.

(43) Y. Iida, Bull. Chem. Soc. Japan, 42, 71, 637, 1969.

(44) J. G. Vegter and J. Kommandeur, Phys. Rev., B9, 5150, 1974.

(45) A. A. Bright, A. F. Garito and A. J. Heeger, Solid State Comm., 13, 943, 1973.

(46) R. M. Vlasova, A. I. Gutman, L. D. Rosenshtein and A. F. Kartenko, Phys. Status Solidi, 47B, 435, 1970.

(47) R. M. Vlasova, A. I. Gutman, M. L. Freidin, A. A. Berlin, V. V. Kuzina, A. I. Sherle, M. I. Cherkashin and A. N. Chigir, Izv. Akad. Nauk. SSSR, Ser. Khim (8), 1822, 1971.

(48) M. Ratner, J. R. Sabin and E. E. Ball, Mol. Phys., 20, 1177, 1973.

(49) D. B. Chestnut and R. W. Mosley, Theor. Chim, Acta (Berl.), 13, 230, 1969.

(50) Z. G. Soos and D. J. Klein, J. Chem. Phys., 55, 3284, 1971.

(51) Y. Matsunaga and T. Tanaka, Bull. Chem. Soc. Japan, 49, 2713, 1976.

(52) F. Cavallone and E. Clementi, J. Chem. Phys., 63, 4304, 1975.

(53) J. Tanaka, M. Tanaka, T. Kawai, T. Takabe and O. Maki, Bull. Chem. Soc. Japan, 49, 2538, 1976.

(54) A. Brau, P. Brüesch, J. P. Farges, W. Hinz and D. Kuse, Phys. Status Solidi, B62, 615, 1974.

(55) J. B. Torance, B. A. Scott and F. B. Kaufman, Solid State Comm., 17, 1369, 1975.

(56) H. T. Jonkman, G. A. Van der Velde and W. C. Newport, Chem. Phys. Lett. 25, 62, 1974.

(57) J. Ladik, A. Karpfen, G. Stollhoff and P. Fulde, Chem. Phys., 7, 267, 1975.

(58) A. Biber and J. J. Andre', Chem. Phys., 5, 166, 1974.

(59) E. Menefee and Y. H. Pao. J. Chem. Phys., 36, 3472, 1962.

(60) S. Hiroma, H. Kuroda and H. Akamatu, Bull. Chem. Soc. Japan, 44, 9, 1971.

(61) D. A. Lowitz, J. Chem. Phys., 46, 4698, 1967.

(62) W. T. Wozniak, G. Despasquali and M. V. Klein, Chem. Phys. Lett., 40, 93, 1976.

(63) R. H. Boyd and W. D. Phillips, J. Chem. Phys., 43, 1, 1965.

(64) A. Yamagishi, Y. Iida and M. Fujimoto, Bull, Chem. Soc. Japan, 45, 3482, 1972.

(65) T. Sakata, A. Nakane and H. Tsubomura, Bull. Chem. Soc. Japan, 48, 3391, 1973.

(66) G. R. Anderson and R. L. McNeely, Symposium on Molecular Structure and Spectroscopy, Ohio State University, Columbus, Ohio, June 1963, Paper R5.

(67) A. J. Belinsky, J. F. Carolan and L. Weiler, Solid State Comm., 19, 1965, 1976.

(68) R. Bozio, A. Girlando, I. Zanan and C. Pecile, 5th International Conf. on Raman Spectroscopu Proc. (ed. E.D. Schmid), 5, 562, 1976.

(69) Y. Matsunaga, J. Chem. Phys., 42, 1982, 1965; 41, 3453, 1964.

(70) M. Hoshino, K. Kimura and M. Imamura, Chem. Phys. Lett., 20, 193, 1973.

(71) a) P. C. Li, Spectroscopic Properties and Resistivities of Some Alkali Metal-Arene Charge Transfer Complexes, Ph.D. Thesis, Oklahoma State University, Stillwater, Okla., 1973.
B) C. L. Dodson and J. F. Graham, J. Phys. Chem., 77, 2903, 1973.

(72) a) P. Balk, S. De Bruijn and G. J. Hoijtink, J. Mol. Phys., 1, 151, 1958.
b) G. J. Hoijtink, ibid, 2, 85, 1959.
c) G. J. Hoijtink and P. J. Zandstra, ibid, 3, 371, 1960.
d) G. J. Hoijtink, N. H. Velthorst and P. J. Zandstra, ibid, 3, 533, 1960.

(73) P. C. Li, J. Paul Devlin and H. A. Pohl. J. Phys. Chem., 76, 1006, 1972.

(74) a) B. Hall and J. Paul Devlin, J. Phys. Chem., 71, 465, 1967.
b) B. Mosyn'ska and A. Tramer, J. Chem. Phys., 46, 820, 1967.
c) M. Saheik and H. Yamada, Spectrochim Acta, 32A, 1425, 1976.

(75) J. C. Moore, D. Smith, Y. Youhne and J. Paul Devlin, J. Phys. Chem., 75, 325, 1971.

(76) M. R. Suchanski and R. P. VanDuyne, J. Am. Chem. Soc., 98, 250, 1976.

(77) H. Johnsen, Int. J. Quant. Chem., 9, 459, 1975.

(78) R. C. Holden, Aust. J. Chem., 28, 2333, 1975.

(79) R. N. Compton and C. D. Cooper, J. Chem. Phys., 66, 4325, 1977.

(80) A. R. Siedle, J. Am. Chem. Soc., 97, 5931, 1975.

(81) S. G. Clarkson, B. C. Lane, and F. Basalo, Inorg. Chem., 11, 662, 1972.

(82) M. E. Peover, Trans. Faraday Soc., 60, 417, 1964.

(83) K. D. Truong and A. D. Bandrauk, Chem. Phys. Lett., 44, 232, 1976.

(84) B. R. Penfold and W. N. Lipscomb, Acta Cryst., 14, 589, 1961.

(85) a) J. Helper, W. D. Classon and H. B. Gray, Theor. Chim. Acta (Berl.), 4, 174, 1966.
b) J. Prochrow and A. Tramer, Bull. De L'Acad. Polon, Des. Sci. Series des Sci. Astron. et Phys., 12, 429, 1964.

(86) a) M. Itoh, J. Am. Chem. Soc., 92, 886, 1970.
b) O. W. Webster, W. Mahler and R. E. Benson, J. Am. Chem. Soc., 84, 3678, 1962.

(87) L. M. Fraus, J. E. Moore and R. E. Bruns, Chem. Phys. Lett., 21, 357, 1973.

(88) I. Heller and F. B. Kaufman, J. Am. Chem. Soc., 98, 1464, 1976.

(89) G. R. Anderson and J. Paul Devlin, J. Phys. Chem., 79, 1110, 1975.

(90) R. Bozio and C. Pecile, J. Chem. Phys., 67, 3864, 1977.

(91) C. Chi and E. R. Nixon, Spectrochim. Acta, A31, 1739, 1975.

(92) a) G. Herzberg and E. Teller, Z. Physik. Chem., B21, 410, 1933.
b) G. Herzberg, The Spectra and Structure of Free Radicals, pp 140-153, Cornell University Press, Ithacca, N.Y., 1971.

(93) a) A. D. Liehr, Z. Naturforsch, 13a, 311, 429, 596, 1958; 16a, 641, 1960.
b) W. E. Donath, J. Chem. Phys., 41, 626, 1964; 42, 118, 1964.

(94) a) W. D. Jones and W. J. Simpson, J. Chem. Phys., 32, 1747, 1960.
b) W. D. Jones, J. Mol. Spectr., 10, 131, 1963.

(95) T. L. Brown, J. Chem. Phys., 43, 2780, 1965.

(96) C. J. Balhausen and R. E. Hansen, Ann. Rev. Phys. Chem., 23, 15, 1972.

(97) A. A. Delyukov and G. V. Klimusheva, Opt. Spectrosc. (Engl.), 35, 648, 1973.

(98) I. P. Terenetskaya, Opt. Spectrosc. (Engl.), 36, 300, 1974.

(99) W. D. Hobey and A. D. Mclachlan, J. Chem. Phys., 33, 1695, 1960.

(100) R. L. Fulton and M. Gouterman, J. Chem. Phys., 35, 1069, 1961, 41, 2280, 1964.

(101) M. G. Kaplunov, T. P. Panova and Yu G. Borod'ko , Phys. Status Solidi, B13, K-67, 1972.

(102) H. A. John and E. Teller, Proc. Roy. Soc. (London), A161, 22, 1937.

(103) a) E. E. Ferguson and F. A. Matsen, J. Chem. Phys., 29, 105, 1958.
b) E. E. Ferguson and F. A. Matsen, J. Am. Chem. Soc., 82, 3268, 1960.
c) E. E. Ferguson, J. Chim. Phys., 61, 257, 1964.

(104) M. J. Rice, Phys. Rev., 37, 36, 1976.

(105) a) J. Tang and A. C. Albrecht, Raman Spectroscopy (Ed. S. A. Szymanski), Vol. II, Chapter 2, Plenum Press, London, 1970.
b) A. C. Albrecht and M. C. Hutley, J. Chem. Phys., 55, 4438, 1971.
c) A. Anderson, The Raman Effect, Vol. I, Marcel Dekker Inc., New York, N. Y., 1971.

(106) E. E. Ferguson and I, Y. Chang, J. Chem. Phys., 34, 628, 1961.

(107) M. W. Hanna and D. E. Williams, J. Am. Chem. Soc., 90, 5358, 1968.

(108) H. B. Friedrich and W. B. Person, J. Chem. Phys., 44, 2161, 1968.

(109) J. Stanley, D. Smith, B. Latimer and J. Paul Devlin, J. Phys. Chem., 70, 2011, 1966.

(110) J. J. Hinkel and J. Paul Devlin, J. Chem. Phys., 58, 4750, 1973.

(111) D. L. Jeanmaire, M. R. Suchanski and R. P. Van Duyne, J. Am. Chem. Soc. 97, 1699, 1975.

(112) R. M. Martin and T. C. Damen, Phys. Rev. Lett., 26, 86, 1971.

(113) a) R. Bozio, A. Girlando and C. Pecile, Chem. Comm., 87, 1974; Chem. Phys., 25, 409, 1974.
b) A. Girlando, L. Morrelli and C. Pecile, Chem. Phys., 22, 553, 1973.

(114) R. Bozio, A. Girlando and C. Pecile, J. Chem. Soc., Faraday Trans. II, 71, 1237, 1975.

(115) T. Takenaka, Spectrochim. Acta, A27, 1735, 1971.

(116) A. Girlando and C. Pecile, Spectrochim. Acta, A29, 1859, 1973.

(117) T. B. Friedman and E. R. Nixon, (Unpublished) Vibrational Spectroscopic Study of Neutral TCNQ Single Crystals, 1973.

(118) M. J. Rice, L. Pietrononero and P. Brüesch, Solid State Comm., 21, 757, 1977.

(119) M. J. Rice, C. B. Duke and N. O. Lipari, Solid State Comm., 17, 1089, 1975.

(120) P. A. Lee, T. M. Rice and P. W. Anderson, Solid State Comm., 14, 703, 1974.

(121) M. J. Rice, N. O. Lipari and D. Strässler, Phys. Rev. Lett., 39, 1359, 1977.

(122) M. Mingardi and W. Siebrand, Chem. Phys. Lett., 23, 1, 1973; J. Chem. Phys., 62, 1074, 1975.

(123) a) M. Jacon, M. Berjot and L. Bernard, C. R. Acad. Sci. (Paris), 273B, 395, 1971; Opt. Comm., 4, 117, 146, 1971.
b) D. Van Lebeke, M. Jacon, M. Berjot and L. Bernard, J. Raman Spectr., 2, 219, 1974.

(124) W. Holzer, W. F. Murphy and H. J. Bernstein, J. Chem. Phys., 52, 399, 1970.

(125) H. Shinoda, Bull. Chem. Soc. Japan, 48, 1777, 1975.

(126) F. A. Savin, Opt. Spektrosk. (Russ.), 19, 555, 743, 1965; 20, 549, 1966.

(127) R. J. Gillespie and M. J. Morton, J. Mol. Spectrosc., 30, 178, 1969.

(128) O. S. Mortensen, J. Mol. Spectrosc., 89, 48, 1971.

(129) W. Kiefer and H. J. Bernstein, Mol. Phys., 23, 835, 1972.

(130) D. L. Jeanmaire and R. D. Van Duyne, J. Am. Chem. Soc., 98, 4029, 4034, 1976.

(131) H. Kuzmany and H. J. Stolz, J. Phys. (Sol. State Phys.), 10C, 2241, 1977.

(132) K. H. Michaellian, K. E. Rieckhoff and E. M. Vogt, Chem. Phys. Lett., 45, 250, 1977.

(133) P. W. Jensen, Chem. Phys. Lett., 39, 138, 1976.

(134) M. G. Kaplunov, T. P. Panova, E. B. Yagubskii and Yu G. Borod'ko, zh. Strukt Khim., 13, 440, 1972.

(135) E. Ahron-Shalom, M. Weger, I. Agranat and E. Wiener-Avnear, Solid State Comm., 23, 53, 1977.

(136) Z. Iqbal, C. W. Christoe and D. K. Dawson, J. Chem. Phys., 63, 4485, 1975.

(137) a) A. Rosenberg and J. Paul Devlin, Spectrochim. Acta, 21, 1613, 1965.

b) F. A. Miller, O. Sala, P. Devlin, J. Overend, E. Lippert, W. Luder, H. Moser and J. Varchmin, Spectrochim Acta, 20, 1233, 1964.
c) T. Takenaka and S. Hayashi, Bull. Chem. Soc. Japan, 37, 1216, 1964.

(138) R. M. Vlasova, T. I. Brishaeva and A. A. Berlin, Izv. Akad Nauk SSSR. Ser. Khim (3), 659, 1968.

(139) T. Sakata, T. Okai and H. Tsubomura Bull. Chem. Soc. Japan, 48, 2207, 1975.

(140) J. L. Pack and A. V. Phelps, J. Chem. Phys., 44, 1870, 1966.

(141) C. A. Coulson, Proc. Roy. Soc. (London), A169, 413, 1939.

(142) W. Gordy, J. Chem. Phys., 14, 305, 1946.

(143) R. M. Badger, J. Chem. Phys., 2, 128, 1934; 3, 710, 1935.

(144) D. H. Eargle Jr., J. Chem. Soc. (B), 1556, 1970.

(145) Jesse C. Moore, I. A. Theoretical Investigation of the Distor-Distortions of NO_3 Ion in $LiNO_3.nH_2O$; II. An Experimental Investigation of Glassy Metal-Ammonia Solution, Ph.D. Thesis Kansas State University, Manhatten, Kansas, 1977.

(146) J. Howard Stanley, Spectroscopic Studies of Selected Radical Anion Derivatives of Tetracyanoethylene , M. S. Thesis, Oklahoma State University, Stillwater, Okla., 1966.

(147) R. E. Long, R. A. Sparks and K. N. Trueblood, Acta Cryst., B18, 932, 1965.

(148) J. Overend and J. R. Scherer, J. Chem. Phys., 32, 1289, 1296, 1720, 1960.

(149) J. R. Scherer, Spectrochim. Acta, 20, 345, 1964.

(150) a) J. Tanaka, Bull. Chem. Soc. Japan, 36, 1237, 1963.
b) J. Tanaka, T. Kishi and M. Tanaka, Bull. Chem. Soc. Japan, 47, 2376, 1976.

(151) C. Looney and J. Downing, J. Am. Chem. Soc., 80, 2840, 1958.

(152) W. Slough and A. R. Ubbelohde, J. Chem. Soc., 911, 1957.

VITA

Murlidhar Sadashiv Khatkale

Candidate for the Degree of

Doctor of Philosophy

Thesis: SPECTROSCOPIC STUDIES OF THE STOICHIOMETRIC AND NONSTOICHIOMETRIC SODIUM SALTS OF TCNQ AND TCNE

Major Field: Chemistry

Biographical:

Personal Data: Born in Akola (Wasud), Sholapur, India, June 1, 1943, the son of Sadashiv and Yashoda Khatkale.

Education: Graduated from S. S. Ligade High School, Akola (Wasud), India, in June 1961; received the Bachelor of Science degree from the University of Poona, India, with majors in chemistry, physics and mathematics, in June, 1965; completed Scientific Officer's training course at Bhabha Atomic Research Center, Trombay, Bombay, India, in July 1968; received Master of Science degree from the University of Poona, India, with a major in physical chemistry in June, 1972; received Master of Science degree from the University of Rochester, Rochester, New York, with a major in theoretical chemistry in January, 1974; completed requirements for the Doctor of Philosophy degree at Oklahoma State University, July, 1978.

Professional Experience: Scientific officer, Bhabha Atomic Research Center, Trombay, Bombay, India, 1968-1972; Graduate teaching assistant, University of Rochester, Rochester, New York, 1972-1973; Graduate teaching assistant, Oklahoma State University, 1974-1976; National Science Foundation Reserach Fellow, 1974-1978.

Membership in Honorary and Profession Societies: Member of Phi Lambda Upsilon, Honorary Chemical Society, Member of the American Chemical Society.